



UNIVERSITÀ
DEGLI STUDI
DI PADOVA

Università degli Studi di Padova

Dipartimento di Scienze Biomediche Sperimentali

SCUOLA DI DOTTORATO DI RICERCA IN BIOSCIENZE

INDIRIZZO DI NEUROBIOLOGIA

CICLO XXIV

Ca²⁺ HOMEOSTASIS IN FAMILIAL ALZHEIMER'S DISEASE: A VIEW FROM INTRACELLULAR Ca²⁺ STORES

Direttore della Scuola : Ch.mo Prof. Giuseppe ZANOTTI

Coordinatore d'indirizzo: Ch.mo Prof. Daniela PIETROBON

Supervisore :Ch.mo Prof. Cristina FASOLATO

Dottorando: Maulilio John KIPANYULA

31st December 2011

DEDICATION

To my parents Mr. John Kipanyula and Mrs Theresia Kipanyula

and

My beloved wife Mrs Tumaini Wapilila-Kipanyula

ACKNOWLEDGEMENTS

This work was carried out at the Department of Experimental Biomedical Sciences, Biosciences and Biotechnology PhD School, University of Padua, Italy and was funded by a CARIPARO PhD fellowship for international students (cycle XXIV). I heartily acknowledge the financial support that enabled me pursue the studies. With deep appreciation, I would like to express my sincere and special thanks to the Department of Experimental Biomedical Sciences for providing excellent working facilities and enabling working environment, which were central to my success. I am grateful to my employer Sokoine University of Agriculture (SUA) in Tanzania for granting a study leave that enabled me to focus more efficiently on my studies.

I express my sincere and heartfelt gratitude to Prof. Tullio Pozzan, the group leader, for giving me the opportunity to work in his Laboratory and for his interest, positive attitude, and constructive criticism towards my work throughout my three-year stay. Indeed the three-year stay in his Laboratory was very rewarding.

I am deeply grateful to my supervisor Prof. Cristina Fasolato for her inspiring, encouragement, tireless guidance, enthusiasm, constructive and timely comments and friendly support from the initial to the final stage of my project. Her friendly, never failing enthusiasm and a close constant supervision is highly appreciated. I would like to express my sincere appreciation to Prof. Paola Pizzo for her tireless support, guidance, fruitful discussions, and encouragements and inspiring collaboration.

My special thanks are extended to Dr Enrico Zampese, for his collaboration, unlimited guidance, and technical support. I wish to express my appreciation to Dr. Cristian Lazzari and Dr. Laura Contreras, for their tireless cooperation and assistance in carrying out molecular biology work they were always available for consultation. I wish to express my gratitude to all present and former members of the laboratory for creating a special and stimulating working atmosphere. Especially, I am much indebted to Dr Lucia Brunello, Dr. Ilaria Drago, Dr. Valentina Lissandron, Dr. Paulo Magalhães, Paola Capitano, Riccardo Filadi, and Andrea Wong for providing me the inspiring and

optimistic atmosphere in the laboratory. The technical assistance from Giovanni Ronconi and Mario Santato is gratefully acknowledged.

I would like to express my appreciation to Profs. Giuseppe Zanotti and Daniela Pietrobon (the School Director and Coordinator of the Neurobiology programme) who enabled smooth running of my studies. My special thanks are extended to colleagues in the Neurobiology programme: Elisa Bianchini, Michele Sessolo and Andrea Urbani for their fruitful discussions, comments, encouragements and their inspiring collaboration. I wish to express my gratitude to all members of the Department of Veterinary Anatomy (SUA) in Tanzania for their support and encouragement while I was away for my studies.

I wish to express my special thanks to the following families that made my social life in Italy meaningful: Mr and Mrs Wapalila, Mr Melkizedecky Mlyapatali and Mr. Majhidy Zakaria Mhessa. My colleagues and friends in Tanzania in particular Dr. Camilus Sanga, Dr. Fredy T. Kilima, Dr. Solomon Nong'ona, and Mr. Fredy Kipanyula provided appreciable support to my family while I was away.

My gratitude and special love to my wife Tumaini and our son John for their love, prayers, support, sacrifice, and patience during the entire period of my studies. My beloved parents and relatives are gratefully thanked for their sacrifices, encouragement, prayers, and enthusiastic support.

Above all, I am very thankful to my God

Maulilio John Kipanyula

Padua, 31st December 2011.

TABLE OF CONTENTS

ABBREVIATIONS	vii
SUMMARY	xi
SOMMARIO	xv
GENERAL INTRODUCTION	1
1.1 Background	1
1.2 Alzheimer’s disease: An overview	5
<i>1.2.1 Clinical manifestation of AD</i>	6
<i>1.2.2 Types of AD and risk factors</i>	7
<i>1.2.3 Gross features of AD</i>	11
<i>1.2.4 Neuropathological features of AD</i>	11
1.3 γ-secretases	18
1.4 Presenilins	22
<i>1.4.1 The structure of presenilins</i>	24
<i>1.4.2 Biological functions of presenilin</i>	25
1.5 Calcium homeostasis: An overview	28
<i>1.5.1 Intracellular Ca^{2+} homeostasis</i>	30
<i>1.5.2 Calcium influx</i>	30
1.5.2.1 Voltage –Operated Ca^{2+} Channels.....	31
1.5.2.2 Ligand-Gated Ca^{2+} Channels	31
1.5.3.1 Endoplasmic reticulum	37
1.5.3.2 Other intracellular Ca^{2+} stores.....	44
<i>1.5.4 The sarco/endoplasmic reticulum Ca^{2+} ATPase pump</i>	45
<i>1.5.5 Organization of the intracellular Ca^{2+} signal</i>	45
<i>1.5.6 Regulation of intracellular Ca^{2+} dynamics</i>	47
1.6 Neuronal Ca^{2+} signalling and homeostasis	48
1.7 Presenilins and intracellular Ca^{2+}homeostasis in AD	51
1.8 The soluble Aβ42 oligomers and AD	55
<i>1.8.1 The Aβ oligomers and neuronal Ca^{2+} dysregulation</i>	58
<i>1.8.2 Role of Ca^{2+} in learning and memory</i>	59

1.9 Ca²⁺ measurements in living cells.....	60
1.9.1 Synthetic Ca ²⁺ probes	61
1.9.2 Protein based Ca ²⁺ probes	62
1.10 Fura-2 measurement of cytosolic free Ca²⁺ in living cells.....	65
AIMS OF THE PROJECT.....	68
MATERIALS AND METHODS.....	70
RESULTS.....	79
Result I.....	79
4.1 Ca²⁺ Homeostasis in Primary Cortical Neuronal Cultures from Tg Mice....	79
4.1.1 Ca ²⁺ release induced by IP ₃ -generating agonists in cells transiently transfected with the FAD linked PS2-N141I mutant	79
4.1.2 Expression levels of PS2 in wt and tg mice.....	82
4.1.3 Ca ²⁺ release induced by IP ₃ -generating agonists is reduced in neurons from tg mice carrying PS2-N141I.	84
4.1.4 The total intracellular store Ca ²⁺ content assayed by ionomycin is reduced in cortical neurons from tg mice	90
4.1.5 Ca ²⁺ release from the ryanodine-sensitive intracellular Ca ²⁺ stores is increased in neurons from both tg mice	92
4.1.6 PS2-N141I does not alter SERCA-2B and IP ₃ R protein levels but upregulates RyR protein levels in the tg neurons	94
4.1.7 Intracellular store Ca ²⁺ leak is increased in tg neurons.....	97
4.1.8 Do primary cultures of cortical neurons from tg mice produce enough Aβ ₄₂ to affect Ca ²⁺ homeostasis?	99
4.1.9 Tg neurons have higher synchronous Ca ²⁺ oscillations induced by picrotoxin 100	
4.1.10 In the tg neurons reduction in ER Ca ²⁺ content does not affect the sensitivity to ER mediated death stimuli	106
Result II.....	108
4.2 Functional effects of synthetic Aβ₄₂ oligomers on Ca²⁺ homeostasis.....	108
4.2.1 Ca ²⁺ release induced by IP ₃ -generating agonists is reduced in mouse cortical neurons treated with Aβ ₄₂ oligomers	108
4.2.2 Ca ²⁺ release induced by IP ₃ -generating agonists is reduced in cell lines treated with Aβ ₄₂ oligomers.....	113

4.2.3 *The total intracellular store Ca^{2+} content is not affected in cells treated with $A\beta_{42}$ oligomers.*..... 114

4.2.4 *Ca^{2+} release from the ryanodine-sensitive intracellular Ca^{2+} stores is increased in cells treated with $A\beta_{42}$ oligomers*..... 117

DISCUSSION..... **119**

CONCLUSIONS..... **134**

PERSPECTIVES AND FURTHER STUDIES..... **136**

REFERENCES **138**

APPENDIX **167**

ABBREVIATIONS

A β : Amyloid β peptide

AD: Alzheimer's Disease

Aeq: Aequorin

AICD: APP IntraCellular Domain

Aph-1: Antherior Pharynx-defective 1

APP: Amyloid Precursor Protein

APP^{swe}: APP swedish

BAPTA: 1,2-bis(o-aminophenoxy)ethane-N,N,N',N'-tetraacetic acid

Bk: Bradikinin

Ca²⁺: calcium

[Ca²⁺]: Ca²⁺ concentration

[Ca²⁺]_{cyt}: cytosolic Ca²⁺ concentration

[Ca²⁺]_{ER}: ER Ca²⁺ concentration

CaM: calmodulin

CCE: Capacitative Ca²⁺ Entry

CCH: Carbachol

CFP: Cyan Fluorescent Protein

CICR: Ca²⁺-Induced-Ca²⁺-Release

CPA: cyclopiazonic acid

CRAC: Ca²⁺-Release Activated Ca²⁺

CM: Conditioned medium

CTF: C-terminal fragment

DAG: diacylglycerol

DHPG: (RS)-3, 5-dihydroxyphenylglycine

DIV: day in vitro

EGTA: glycol-bis (2-aminoethylether)-*N, N, N', N'*-tetraacetic acid

ER: Endoplasmic Reticulum

FAD: Familial Alzheimer's disease

FL: full length

FRET: Fluorescence Resonance Energy Transfer

GFP: Green Fluorescent Protein

GPCR: G-protein-coupled Receptor

HFIP: 1, 1, 1, 3, 3, 3-hexafluoro-2-isopropanol

IP₃: inositol-1, 4, 5-trisphosphate

IP₃R: IP₃ receptor

KCl: Potassium Chloride

MAM: Mitochondria-Associated-Membrane

MEFs: mouse embryonic fibroblasts

MEM: Minimum Essential Medium

mKRB: modified Krebs–Ringer buffer

MW: molecular weight

NCT: Nicastrin

NCX: Na⁺/Ca²⁺ exchanger

NTF: N-terminal fragment

PEN-2: Presenilin Enhancer-2

PHF: Paired Helical Filament

PIP₂: phosphatidylinositol-4,5-bisphosphate

PLC β: Phospholipase-C β

PM: plasma membrane

PMCA: Plasma-Membrane Ca²⁺-ATPase

PS1: Presenilin-1

PS2: Presenilin-2

RFP: Red Fluorescent Protein

ROCC: Receptor-Operated Ca²⁺ Channel

RTK: Receptor-Tyrosin-Kinase

RyR: Ryanodine Receptor

SERCA: Sarco/Endoplasmatic Ca²⁺-ATPase

SMOCC: Second-Messenger-Operated Ca²⁺ Channel

SOCC: Store-Operated Ca²⁺ Channel

SOCE: Store-Operated Ca²⁺ entry

STIM: STromal Interaction Molecule

Tg : transgenic

TM : transmembrane

TMD: trans-membrane domain

TRIS: 1, 1, 1-tris(hydroxymethyl)-methanamine

TRP: transient receptor potential

TUNEL: terminal dUTP nick end labelling

VOCC: Voltage-Operated Ca²⁺ Channel

WT: wild type

YFP: Yellow Fluorescent Protein

SUMMARY

The role of neuronal Ca^{2+} dysregulation in aging and several neurological disorders including Alzheimer's disease (AD) has been underscored and extensively studied in recent years. Neurons utilize Ca^{2+} signalling to control a variety of functions, including membrane excitability, neurotransmitter release, gene expression, cellular growth, differentiation, free radical species formation and cell death. Mutations in presenilin (PS) 1 and 2 linked to Familial Alzheimer's disease (FAD) have been causally implicated in neurodegeneration and eventually neuronal cell death by amyloid toxicity and perturbation of cellular Ca^{2+} homeostasis. Although PSs play other physiological functions, they primarily represent the catalytic core of the multiprotein γ -secretase complex required for toxic β -amyloid ($\text{A}\beta$) peptide production (in particular $\text{A}\beta_{42}$), which is a key factor in AD pathogenesis. Indeed FAD-linked PS1 and PS2 mutations have been associated with altered $\text{A}\beta$ peptide generation, resulting in increased ratios between $\text{A}\beta_{42}$ and $\text{A}\beta_{40}$ peptides.

A large body of evidence, accumulated for many years since PSs were discovered more than a decade ago, has established a strong link between FAD-linked PS mutants and dysregulation of intracellular Ca^{2+} homeostasis. Interestingly, both exaggerated (Ca^{2+} overload) and reduced cytosolic Ca^{2+} release have been reported and attributed to different FAD-linked PS mutants. Previously work, carried out with organelle specific Ca^{2+} probes in the laboratory where this study was conducted, demonstrated that FAD-linked PS2, but not PS1, mutants strongly reduce the Ca^{2+} content of intracellular stores. The observed reduction in endoplasmic reticulum (ER) steady state Ca^{2+} level, as result of expressing FAD-linked PS2 mutants, is due to both inhibition of ER Ca^{2+} pumps (SERCAs) and increase of ER Ca^{2+} leak through Ca^{2+} release channels. The analyses of the functional effects of the PS2 were carried out in different cell lines transiently over-expressing FAD-linked PS2 mutants. The transient expression of mutated proteins or stably expressing cell clones are the most commonly used approaches to start defining the molecular mechanism of disease-associated

proteins. Both approaches however are subjected to criticisms: in the first case, the level of overexpression is usually very high; secondly, the specificity of each clone (and/or adaptation phenomena to the over-expressed protein) may lead to erroneous interpretations.

In the work described here, we took advantage of two available lines of transgenic (tg) mice expressing a mutant PS2 alone or together with a mutant amyloid precursor protein (APP) - both linked to FAD - in order to investigate its effects on Ca^{2+} homeostasis in a physiological environment more relevant to the pathology under study. We particularly focused our attention on Ca^{2+} dysregulation in cortical neurons from tg mice either single homozygous for human PS2-N141I or double homozygous for human PS2-N141I and human APP swedish mutations. The C57BL/6J mice were used as suitable controls, having the tg mice the same background; Ca^{2+} measurements were carried by the fura-2/AM technique.

This study highlights the role of PS2-N141I in modulating Ca^{2+} homeostasis in primary cultures of cortical neurons at 10-12 days in vitro. We have demonstrated that, irrespective of the presence of mutant APP, the PS2-N141I, at a low expression level, altered the Ca^{2+} dynamics of intracellular stores. In these neurons, the total Ca^{2+} content of intracellular stores is partially depleted, as demonstrated by reduced Ca^{2+} release upon stimulation with a Ca^{2+} ionophore such as ionomycin. Consequently, the tg neurons have reduced Ca^{2+} release in response to inositol (1,4,5)-trisphosphate (IP_3)-generating agonists. Conversely, measurements of Ca^{2+} release via ryanodine receptors (RyRs) revealed a novel and unexpected finding in PS2 mutant tg mice i.e. increased Ca^{2+} release in response to caffeine. Consistently, upregulation of RyR2 and no significant change in the level of SERCA-2 and IP_3 Rs were found in both tg mice.

Neuronal excitability has a strong link to intracellular Ca^{2+} dynamics. To study the effect of PS2-N141I on this type of Ca^{2+} excitability, we examined the synchronous neuronal activity induced by picrotoxin (a GABA receptor inhibitor). The tg neurons had significantly elevated number of picrotoxin-evoked Ca^{2+} spikes that required extracellular Ca^{2+} influx but not Ca^{2+} release from intracellular stores. Interestingly,

while Ca^{2+} dysregulation appeared to be similar qualitatively and quantitatively in both single and double tg mouse models, the total amount of brain A β 42 and A β 40 peptides, as assayed by ELISA, as well as their ratios were strikingly different between the two tg lines. Altogether these results strongly suggest that in neurons of tg mice, the expression of mutant APP and/or A β levels have no primary effect on the store Ca^{2+} content at this early stage (at two weeks) and provide evidence that the quite similar effects on Ca^{2+} dynamics observed in both tg mice are due to the mutant PS2.

As far as partially depleted ER Ca^{2+} stores are concerned, the pathophysiological relevance and implication in FAD have never been investigated in depth. It is not known whether the reduction in ER Ca^{2+} content can either worsen or delay the disease, or even be neutral. Indeed, the apoptotic assay (TUNEL), carried out in primary neuronal cultures, excludes an increased toxicity linked to the PS2 mutant when the apoptotic stimulus was coupled to ER Ca^{2+} release.

To conclude our data suggest that the PS2-N141I FAD mutant causes a functional defect in ER Ca^{2+} entry/exit pathways. We have also shown that both tg neurons express very low levels of the mutant protein but show a Ca^{2+} dysregulation similar quantitatively and qualitatively to that previously reported in cell lines upon transient over-expression of the same mutant protein.

Finally, results presented in this work suggest that although Ca^{2+} dysregulation is an early event in FAD, it does not affect vulnerability to cytotoxic stimuli at this early stage.

The second part of this study focused on the role of A β 42 oligomers in cellular Ca^{2+} dynamics. The soluble oligomeric forms rather than monomeric or deposited A β 42 peptides have recently been associated with neuropathology in AD. For this purpose neurons from wt mice and neuronal cell lines were briefly treated (5-60min) with synthetic A β 42 oligomers (or monomers), at sub-micromolar concentrations, before measurement of ER Ca^{2+} release. A β 42 oligomers but not monomers reduced Ca^{2+} release in response to IP_3 -generating agonists in wt neurons but did not affect the total

Ca²⁺ content as monitored by ionomycin. Conversely, Aβ42 oligomers increased the Ca²⁺ release induced by caffeine. It is likely that Aβ42 oligomers exert their effect on the activation pathway from IP₃-generating agonists to IP₃Rs. The mechanisms through which Aβ42 deranges intracellular Ca²⁺ homeostasis require further investigation.

Nonetheless, it is conceivable that in addition to Aβ42 oligomers, also intracellular Ca²⁺ stores could become likely therapeutic targets in FAD and AD in general.

SOMMARIO

Negli ultimi anni il ruolo dell'alterazione del segnale Ca^{2+} nell'invecchiamento cerebrale e nei disordini neurologici, inclusa la malattia di Alzheimer (AD), è stato ampiamente studiato e ne è stata messa in luce l'importanza. I neuroni utilizzano il segnale Ca^{2+} per controllare una grande varietà di funzioni che vanno dall'eccitabilità di membrana al rilascio di neurotrasmettitore, all'espressione genica, alla crescita e differenziazione, alla formazione di specie radicali e alla morte cellulare. Mutazioni in presenilina (PS) 1 and 2 associate alle forme familiari della malattia di Alzheimer (FAD) sono considerate responsabili della neurodegenerazione e infine della morte neuronale causata sia dalle forme tossiche della amiloide-beta ($\text{A}\beta$) che dalla perturbazione dell'omeostasi cellulare del Ca^{2+} . Sebbene le PSs abbiano diverse funzioni fisiologiche, esse principalmente costituiscono il nucleo catalitico del complesso multi-proteico dotato di attività γ -secretasica richiesto per la produzione dei peptidi $\text{A}\beta$, in particolare di $\text{A}\beta_{42}$, il fattore chiave nella patogenesi dell'AD. Le mutazioni in PS1 e PS2 associate a FAD infatti modificano i livelli di peptidi $\text{A}\beta$ causando un aumento del rapporto tra $\text{A}\beta_{42}$ e $\text{A}\beta_{40}$.

Negli ultimi dieci anni, con la scoperta del ruolo delle PSs, sono state accumulate diverse evidenze sperimentali che suggeriscono un ruolo diretto delle PS mutate, associate a FAD, nell'alterazione dell'omeostasi intracellulare del Ca^{2+} . È interessante notare che tali lavori riportano sia un aumento, cui corrisponde il cosiddetto "Ca²⁺ overload", che una riduzione del rilascio citosolico di Ca^{2+} , entrambi gli effetti attribuiti a diverse mutazioni in PS associate a FAD. Studi precedenti, effettuati nel laboratorio in cui è stata avviata questa tesi, con biosensori del Ca^{2+} specifici per gli organuli intracellulari hanno dimostrato che i mutanti in PS2 (ma non quelli in PS1) associati a FAD, riducono fortemente il contenuto totale di Ca^{2+} dei depositi intracellulari. La riduzione dei livelli di Ca^{2+} nel reticolo endoplasmatico (RE), causata dall'espressione delle PS2 mutate, è dovuta sia all'inibizione della pompe del Ca^{2+}

presenti nel RE (SERCAs), sia all'aumento della perdita passiva di Ca^{2+} attraverso i canali di rilascio presenti nel RE.

Inizialmente lo studio degli effetti delle forme mutate della PS2, associate a FAD, è stato in gran parte effettuato in diverse linee cellulari che esprimono la proteina in modo transitorio. L'espressione transiente di proteine mutate o l'impiego di cloni che le esprimono stabilmente sono gli approcci più comunemente impiegati per definire i meccanismi molecolari di proteine associate a malattie. Entrambe le metodologie presentano criticità: nel primo caso, il livello di espressione è di solito molto alto; nel secondo caso la specificità di ciascun clone (e/o l'adattamento conseguente alla sovra-espressione) può dar luogo ad interpretazioni errate.

In questo lavoro ci siamo avvalsi di due linee di topi transgenici (tg) che esprimono una PS2 mutata, sia da sola che in associazione con una forma mutata della proteina precursore dell'amiloide (APP) (entrambe comunque associate a FAD), al fine di studiarne l'effetto sull'omeostasi del Ca^{2+} , in un ambiente fisiologico più rilevante per la patologia in oggetto. In particolare abbiamo centrato l'attenzione sull'alterazione dell'omeostasi del Ca^{2+} in neuroni corticali ottenuti da topi tg omozigoti per la sola PS2-N141I umana o doppi omozigoti per la stessa proteina e per l'APP umana con mutazione *swedish*. Come controllo sono stati considerati topi C57BL/6J (wt), essendo questo il ceppo di riferimento dei topi tg; le misure del segnale Ca^{2+} sono state eseguite con la tecnica del fura-2/AM.

Questo studio mette in luce il ruolo della PS2-N141I nella modulazione dell'omeostasi del Ca^{2+} in colture primarie di neuroni corticali a 10-12 giorni in vitro. Abbiamo dimostrato che, indipendentemente dalla presenza della forma mutata dell'APP, la PS2-N141I, a bassi livelli di espressione, altera le dinamiche del Ca^{2+} che dipendono dai depositi intracellulari. In questi neuroni, il contenuto totale di Ca^{2+} all'interno dei depositi è diminuito, come si ricava dalla riduzione del rilascio di Ca^{2+} dopo stimolazione con uno ionoforo del Ca^{2+} come la ionomicina. Di conseguenza, i neuroni tg presentano una riduzione del rilascio di Ca^{2+} anche in risposta ad agonisti associati alla produzione di IP_3 . Al contrario, un dato del tutto nuovo è emerso nei topi

esprimenti la PS2 mutata: studiando il rilascio di Ca^{2+} mediato dai recettori sensibili alla rianodina (RyRs) si è osservato un aumento significativo del rilascio di Ca^{2+} in risposta alla caffeina. In maniera consistente, nei topi tg si è osservato un aumento dei livelli del RyR2 tuttavia in assenza di variazioni dei livelli della pompa del Ca^{2+} SERCA-2 e dei recettori dell' IP_3 (IP_3Rs).

L'eccitabilità neuronale dipende strettamente dalle dinamiche del Ca^{2+} intracellulare. Per studiare l'effetto della PS2-N141I su questo parametro, abbiamo studiato l'attività neuronale sincrona indotta da picrotossina (un inibitore del recettore del GABA). I neuroni tg presentano un aumento significativo del numero di picchi di Ca^{2+} indotti dalla picrotossina. Tali picchi richiedono ingresso di Ca^{2+} extracellulare ma non rilascio di Ca^{2+} dai depositi intracellulari. E' interessante notare che mentre l'alterazione del segnale Ca^{2+} è simile, in termini qualitativi e quantitativi, tra topi singoli e doppi tg, la quantità totale dei peptidi $\text{A}\beta_{42}$ e $\text{A}\beta_{40}$, misurata via ELISA, così come i loro rapporti sono profondamente differenti tra le due linee tg. Nell'insieme questi dati suggeriscono che, nei neuroni dei topi tg, l'espressione della forma mutata dell'APP e/o i livelli di $\text{A}\beta$ non hanno effetti primari sul contenuto di Ca^{2+} dei depositi intracellulari in una fase precoce (a due settimane) e, inoltre, favoriscono l'idea che gli effetti sulle dinamiche del Ca^{2+} , così simili nelle due linee di topi tg, dipendono dalla forma mutata della PS2.

Per quanto riguarda la deplezione dei depositi intracellulari del Ca^{2+} , non è mai stata approfondita in dettaglio la rilevanza pato-fisiologica e l'implicazione nelle forme FAD. Non è noto se la riduzione del contenuto di Ca^{2+} nel RE può peggiorare o ritardare la malattia, o addirittura essere neutrale. Di fatto, il saggio di apoptosi (TUNEL), eseguito in colture primarie di neuroni, esclude un aumento della tossicità associata alla forma mutata della PS2 in questa fase precoce, quando lo stimolo apoptotico viene associato al rilascio di Ca^{2+} dal RE.

Per concludere, i nostri dati suggeriscono che la PS2-N141I, associata a FAD, causa un difetto funzionale delle vie di ingresso e di uscita del Ca^{2+} dal RE. Abbiamo inoltre dimostrato che i neuroni tg, pur esprimendo livelli molto bassi di PS2 mutata,

l'alterazione del segnale Ca^{2+} è simile, qualitativamente e quantitativamente, a quella osservata in precedenza in linee cellulari che sovra-esprimono, in modo transiente, la proteina ad alti livelli.

Infine, i risultati presentati in questo lavoro suggeriscono che sebbene l'alterazione del segnale Ca^{2+} sia un evento precoce nelle forme FAD, non influisce sulla vulnerabilità a stimoli citotossici nei primi giorni di sviluppo.

La seconda parte di questo studio ha analizzato il ruolo degli oligomeri di A β 42 sulle dinamiche cellulari del Ca^{2+} . Le forme oligomeriche solubili di A β 42, piuttosto che quelle monomeriche o precipitate, sono state associate recentemente alle forme di neuropatologiche associate ad AD. A questo proposito, colture primarie di neuroni da topi wt o linee cellulari neuronali sono state trattate brevemente (5-60min) con oligomeri (o monomeri) del peptide sintetico A β 42, a concentrazioni sub-micromolari, prima della misurazione del rilascio di Ca^{2+} dal RE. Gli oligomeri, ma non i monomeri, di A β 42 riducono il rilascio di Ca^{2+} in risposta ad agonisti che producono IP_3 ma non influiscono sul contenuto totale di Ca^{2+} , così come appare dalla risposta alla ionomicina. Al contrario, gli oligomeri di A β 42 aumentano il rilascio di Ca^{2+} indotto dalla caffeina. E' probabile che gli oligomeri di A β 42 esercitino il loro effetto sulla via di attivazione e produzione dell' IP_3 . Il meccanismo attraverso il quale gli oligomeri di A β 42 destabilizzano l'omeostasi intracellulare del Ca^{2+} richiede ulteriori approfondimenti.

Ciononostante è verosimile che oltre agli oligomeri di A β 42, anche i livelli di Ca^{2+} nei depositi intracellulari diventino possibili bersagli terapeutici nelle forme familiari e sporadiche della malattia di Alzheimer.

GENERAL INTRODUCTION

1.1 Background

The role of calcium (Ca^{2+}) during the onset and progression of Alzheimer's disease (AD), the most common form of neurodegenerative diseases has been extensively investigated for over 20 years since Ca^{2+} hypothesis of AD was formulated (Khachaturian, 1994; Toescu and Vreugdenhil, 2010). Although over 90% of the AD cases are sporadic, about 5% are linked to mutations in three genes: Amyloid Precursor Protein (APP), Presenilin (PS) 1 and 2 (PS1 and PS2) and run in families, hence the name Familial Alzheimer's disease (FAD) (LaFerla, 2002; Sisodia and St George-Hyslop, 2002).

The Ca^{2+} hypothesis of AD formulated by Khachaturian in 1982, and later on revised in 1989 to accommodate other aspects of brain aging and AD has made a substantial contribution towards understanding of the role of Ca^{2+} in AD (reviewed in Toescu and Vreugdenhil, 2010). Formulation of this hypothesis marked the beginning of extensive investigation on the role of Ca^{2+} dysregulation in AD and more so in FAD. Furthermore, cloning of the APP gene in 1980s (Lemaire et al., 1989) and later on the discovery of PS1 and PS2 in 1990s and their association with Ca^{2+} and early onset AD (Goate et al., 1991; Rogaev et al., 1995; Sherrington et al., 1995) were important milestones in understanding the physiopathology of AD.

AD accounts for 60-70% of all dementia cases reported worldwide. About 5-10% of the population over the age of 65 has dementia and out of these cases, a large proportion has AD (Grand et al., 2011). More than 35 million people suffer AD worldwide and cases are projected to quadruple by 2050 (Brookmeyer et al., 2007; Querfurth and LaFerla, 2010). There are two major and popular hypotheses that best explains the aetiology and pathogenesis of AD: the "amyloid hypothesis" and the " Ca^{2+} hypothesis", which integrate each other and have driven the research in this field.

Both hypotheses acknowledge that the 4 KDa β -amyloid ($A\beta$) peptides and particularly, the longer 42 amino acid residue form ($A\beta_{42}$) and aggregation prone species, play a causative role in AD. The amyloid hypothesis suggests that accumulation of $A\beta_{42}$ or increased ratio of $A\beta_{42}/A\beta_{40}$ is the primary cause of AD (Hardy and Higgin, 1992; Hardy, 2009). The Ca^{2+} hypothesis, on the other hand, describes Ca^{2+} dysregulation, caused directly by PSs or indirectly by $A\beta$ toxicity, as an important co-factor for the onset and progression of the disease (reviewed in Berridge, 2010) (figure 1). Indeed the pathophysiology of sporadic AD and FAD starts early enough during the preclinical stage, thus making it difficult for timely diagnosis and therapeutic intervention. Ca^{2+} dysregulation also appears to set in early enough even before the clinical signs of the disease are evident (Giacomello et al., 2005).

Following the discovery and cloning of APP and PS genes, rigorous genetic studies led to the identification of a dozen of mutations in genes coding for APP, PS1, and PS2 proteins. These mutations are strongly associated with FAD. Indeed, a large number of mutations in genes coding for PS1 (*PSEN1*) on chromosome 14, PS2 (*PSEN2*) on chromosome 1 and for APP (*APP*) on chromosome 21 have been reported. So far, there are about 197 PS1, 25 PS2 and 39 APP point mutations described. The majority of these are responsible for FAD in different families, leading to amyloid accumulation and/or increased $A\beta_{42}/A\beta_{40}$ ratio in the brain, which is crucial for the pathogenesis of AD (Scheuner et al., 1996; Tomita et al., 1997; Jankowsky et al., 2003). For regularly updated list of all mutations in APP, PS1 and PS2 genes refer: (<http://www.molgen.ua.ac.be/ADMutations>).

Whereas the direct role of FAD-linked APP mutations in perturbing Ca^{2+} homeostasis has not been demonstrated (Stieren et al., 2010) that of PS mutations has been widely documented, albeit with profound differences between PS1 and PS2 (Zampese et al. 2009; Supnet and Bezprozvanny 2011). Interestingly, both sporadic AD and FAD present similar clinical and pathological features.

Neuronal Ca^{2+} signalling utilizes both extracellular and intracellular Ca^{2+} pools. Each Ca^{2+} signalling event is interpreted in terms of spatial-temporal pattern in order to

generate adequate outputs (Carafoli, 2002; Saris and Carafoli, 2005). Because of its involvement in a wide range of processes, tight regulation of Ca^{2+} homeostasis is mandatory. Certainly, disturbances in Ca^{2+} homeostasis have been associated with different neurological diseases such as Parkinson, Huntington, Amyotrophic lateral sclerosis (ALS), and AD (Verkhatsky, 2005).

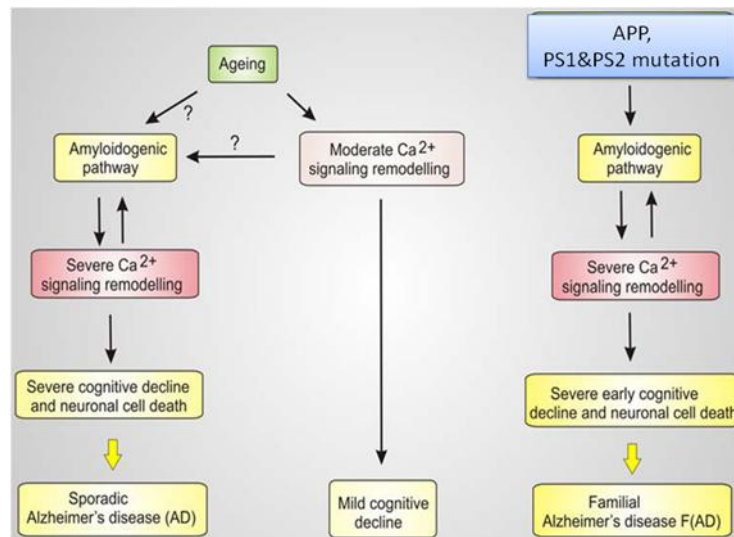


Figure 1: A scheme showing Ca^{2+} signalling remodeling and Alzheimer's disease (AD). A reciprocal interaction between amyloid metabolism and Ca^{2+} signalling may result in a profound remodeling of the Ca^{2+} signalling system, which leads to the severe cognitive decline, and neuronal cell death that characterizes both sporadic AD and FAD. Adapted and modified from (Berridge, 2010).

Although there are contradictory data on how PSs perturb intracellular Ca^{2+} homeostasis, PS1 mutations, which cause a more aggressive form of FAD, have been associated with Ca^{2+} overload. This notion is supported by different studies reporting increased ER Ca^{2+} release in the cytosolic compartment upon stimulation by IP_3 -generating agonists of cells expressing FAD linked PS1 mutations (Leissring et al., 1999; LaFerla 2002; Stutzmann et al., 2004; Thinakaran and Sisodia, 2006). The

elevated Ca^{2+} release was attributed to abnormal increase in the ER Ca^{2+} content, thus leading to the formulation of the “ Ca^{2+} overload” hypothesis (LaFerla 2002). Novel findings, mainly based on the biophysical properties of PS as Ca^{2+} permeable channels in both artificial membranes and over-expressing cell lines, pursued the idea that endogenous PSs, in the form of holoproteins, work as ER Ca^{2+} leak channel. FAD linked mutants, behave as defective channels thus increasing the store Ca^{2+} content (Tu et al. 2006; Bezprozvanny and Mattson, 2008; Nelson et al, 2011). However, direct measurements of the ER Ca^{2+} content with synthetic or genetically encoded Ca^{2+} probes not only failed to confirm the Ca^{2+} overload of intracellular stores, but also probed a reduction instead of an increase of the store Ca^{2+} content. Both findings, i.e. unaltered or even reduced ER Ca^{2+} content were better explained by exaggerated Ca^{2+} release through increased open probability of IP_3R and RyR Ca^{2+} release channels and/or inhibition of SERCA pump activity (Giacomello et al. 2005; Zatti et al. 2006; Fedrizzi et al. 2008; Cheung et al. 2008; Brunello et al. 2009).

Notwithstanding, recent studies both in vivo and in vitro have suggested that PS mutations perturb intracellular Ca^{2+} homeostasis in a way that sensitizes neurons to apoptosis and excitotoxicity and hence neurodegeneration in AD (Bezprozvanny and Mattson, 2008). An open question would be why should there be divergent consequences and outcome of PSs in different experimental models. A possible explanation might rely on the fact that the majority of the studies supporting the Ca^{2+} overload hypothesis focused on PS1 mutants are based primarily on cytosolic Ca^{2+} measurements. Further complexity also emerged by shifting the focus from PS1 to PS2 mutations, employing ER-targeted Ca^{2+} probes (Zampese et al. 2009). Indeed multiple and divergent roles for PS1 and PS2 are now emerging and they will be discussed below (Zampese et al. 2011).

In the study described here, we took advantage of two available lines of tg mice expressing a FAD linked mutant PS2 alone or together with mutant APP, in order to investigate in a more physiological and relevant environment the effects of PS2 on Ca^{2+} homeostasis. We particularly focused our attention on Ca^{2+} dysregulation in cortical

neurons from the tg line PS2.30H homozygous for human PS2-N141I and from the tg line B6.152H double homozygous for human PS2-N141I and human APP swedish (APP^{swe}) mutations K670N, M671L both in the background strain C57BL/6J (Richards et al., 2003; Page et al., 2008; Ozmen et al., 2009). By employing classical Ca²⁺ imaging techniques on primary neuronal cultures, we demonstrate that, both single and double tg mice show altered Ca²⁺ dynamics that are consistent with previous findings described in human FAD fibroblasts and cell lines over-expressing FAD-linked PS2 mutants.

The second part of this study focused on the role of A β 42 oligomers in cellular Ca²⁺ dynamics. Recent evidence from both correlation and functional studies suggest that soluble oligomeric forms rather than monomeric or deposited A β 42 peptides are associated with neuropathology in AD and define the onset of dementia (Walsh and Selkoe, 2007). Data obtained from mouse models and even in human disease, have suggested a strong correlation between the level of A β oligomers and functional impairment as compared to either A β plaque deposition or total A β monomer concentration. Although the underlying mechanism of A β 42 oligomer toxicity and also of the even more toxic species A β 43 (Saito et al. 2011) remains controversial, they appear to cause also Ca²⁺ dysregulation (Demuro et al., 2005; Du et al., 2008; Sanz-Blasco et al., 2008) and consequently, synaptic dysfunction and impaired memory function. In this study, we also investigated the role of soluble A β 42 oligomers in AD and their effect on intracellular Ca²⁺ homeostasis.

1.2 Alzheimer's disease: An overview

Alois Alzheimer, a German psychiatrist and neuropathologist described AD for the first time in 1906 and therefore named after him (Weber, 1997). AD is the most common form of neurodegenerative diseases and accounts for 60-70% of all dementia cases reported worldwide with substantial socio-economic impacts (Brookmeyer et al., 2007). To date it is estimated that there are more than 35 million people suffering from AD worldwide and such cases are projected to quadruple by 2050 (Brookmeyer et al.,

2007; Querfurth and LaFerla, 2010; Grand et al., 2011). The prevalence of AD is high in people over 60 years of age, although the less-prevalent early-onset FAD can occur much earlier. The duration of illness varies considerably from patient to patient and ranges from two to 20 years, although the survival time for patients with Alzheimer's disease is limited between 3 to 4 years (reviewed in Mayeux, 2003).

1.2.1 Clinical manifestation of AD

The clinical features of AD vary according to the stage and progression of its pathology. Progressive memory loss is one of the first signs noted in AD patients. Patients with memory problems may have a condition called amnesic mild cognitive impairment (MCI) (Frank and Petersen, 2008; Petersen, 2009; Ladeira et al., 2009; Grand et al., 2011). Such individuals with MCI usually have remarkable memory problems than normal people of the same age, however, the severity of the symptoms are not as those individuals with severe AD (Morris, 2005; 2006; Rozzini et al., 2007; Petersen, 2009; Sperling et al., 2011; Albert et al., 2011). MCI forms a transition from normal aging individual and demented person. These patients convert to early AD, characterized by: mild cognitive impairment problems that can include getting lost, trouble handling money and paying bills, repeating questions, taking longer to complete normal and simple daily tasks, poor judgment, mood swings, personality changes, and neuro-psychiatric disturbances that seriously interfere with daily life undertakings (Förstl and Kurz, 1999; Selkoe, 2001; Morris, 2005). The changes in personality are a reflection of AD pathological process occurring in the brain related to the neurodegenerative process. However, this stage patients can still live alone without any assistance from relatives or caregivers. Diagnosis of patients with mild AD sometimes get complicated by the fact that these patients tend to avoid difficult tasks and challenges in so doing they downplay or dissimulate their cognitive impairment (Sperling et al., 2011).

Furthermore, during early stages of AD, some patients may show significant deficits in learning and memory and cognitive decline becomes more obvious. In such

patients symptoms prompting AD diagnosis at this stage include: Forgetting details about current events (e.g. autobiographical memory), losing self-awareness, change in sleep/awake patterns, difficulty reading or writing, deficit in abstract thinking and reasoning, poor judgment and loss of ability to recognize danger, loss of language skills. Other symptoms include: loss of personality including withdrawing from social contacts, having hallucinations, arguments, striking out, violent behaviour, delusions, depression, agitation, difficulty doing basic tasks such as preparing meals, choosing proper clothing and driving (Addis and Tippett, 2004; Wilson et al., 2010; Grand et al., 2011).

As symptoms become severe, the patient become completely dependent upon caregivers, language skills are completely compromised and reduced to simple phrases or even single words and complete loss of speech (Förstl and Kurz et al., 1999; Petersen, 2009). Other symptoms that may occur at terminal stage of AD include incontinence and swallowing problems. Some patients develop neurological signs towards the terminal stage. Death occurs due to external factor such as exhaustion, infection of pressure ulcers or pneumonia followed by myocardial infarction and septicaemia (Förstl and Kurz et al., 1999).

At postmortem, the most frequently encountered pathological lesions in the brain include reduced brain mass, deposits of extracellular A β peptides in diffuse plaques and in plaques containing elements of degenerating neurons, usually referred to as neuritic plaques (Hardy and Higgins, 1992; Duyckaerts et al., 2009). Furthermore, intracellular changes include deposits of abnormally hyperphosphorylated tau, a microtubule assembly protein, in the form of neurofibrillary tangles (Goedert and Spillantini, 2006; Selkoe, 2001).

1.2.2 Types of AD and risk factors

Genetic studies have characterized two main types of AD namely, early-onset (FAD) and late-onset (sporadic AD). Sporadic AD is the more common of the two, accounting for over 90-95% of all cases (reviewed in Brookmeyer et al., 2007; Grand et

al., 2011). Sporadic AD affects both men and women; although most cases of occur in people over the age of 65 years. Patients who have this form of AD may or may not have a family history of the disease. Different risk factors determine the susceptibility to sporadic AD, which include:

Advancing age: The incidence of AD increases with age. Epidemiological studies have estimated that for people over the age of 65, AD represents the eighth leading cause of death (Hoyert and Rosenberg 1997, reviewed in Mayeur, 2003). The prevalence, or proportion, of individuals surviving with clinically diagnosed AD also varies dramatically with age. For example, under age 65, the disease is rare with exception of early onset FAD, but it increases dramatically at age above 85 where 10% to 40% of the age group has AD (Farlow, 1998; Mayeur, 2003; Dartigues, 2011).

Down syndrome: Individuals with Down syndrome develop a clinical syndrome of dementia that has almost identical clinical and neuropathologic characteristics of AD. Indeed the neuropathological hallmark lesions (tangles and plaques) of AD are present in the brains of all adults with Down syndrome as early as at age of 40 years, which suggests a shared genetic susceptibility to Down syndrome and AD (Masters et al., 1984; Temple et al., 2001; Temple and Konstantareas, 2005). Interestingly, these characteristic tangles and plaques do not necessarily mean that all individuals with Down syndrome will develop AD dementia. However, the clinical and behavioral symptoms of AD are present in approximately 50-70% of individuals with Down syndrome by the time they reach 60 years of age (Temple et al., 2001; Devenny et al., 2000). Two-to five folds increase in the risk of AD is associated with a family history of Down's syndrome (Schupf et al., 2001).

Traumatic head injury: Traumatic head injury increases the risk of AD (Plassman et al. 2000; Guo et al. 2000). A severe head injury appears to increase the risk of developing AD; however, it also depends on the frequency and severity of the injuries. Such head injury may also hasten the onset of AD symptoms especially in people who already have risk factors for AD (Mayeux, 2003). For example, people who

have head injury and carry one form of the apolipoprotein E (APOE- ϵ 4) gene are at higher risk of developing AD (Horsburgh et al. 2000). Although a severe head injury may slightly increase the risk of developing AD, it is important to note that not all people who sustain severe head injury develop AD. The mechanism through which traumatic head injury increases the risk to AD is not well understood, but it has been speculated that A β peptides deposition follows closed head injury in humans and rodents (Horsburgh et al. 2000, Jellinger et al. 2001, Uryu et al., 2002).

Allelic variants: People with an allelic variant of APOE- ϵ 4 gene are at higher risk for developing AD with onset usually after age 65 years. A single APOE- ϵ 4 allele increases the risk of disease by two fold. Homozygous configuration causes as high as up to fivefold increase in risk (Myers et al., 1996; Mayeux, 2003; Lovati et al., 2010). About 20% of all AD cases occur due to APOE- ϵ 4, making it a single most important risk factor for the disease (Slooter et al. 1998; Lovati et al., 2010). APOE play a physiological role to mediate neuronal protection, repair and remodeling and the clearance of A β (St George-Hyslop, 2000). How APOE- ϵ 4 genes and AD interact remains unclear. It is likely to be due to the pivotal role of APOE- ϵ 4 genes in lipid and cholesterol storage, transport and metabolism.

Gender: AD is more prevalent among women (Mayeux, 2003; De Deyn et al., 2011). This is often associated with the fact that women typically live longer as compared to men (Hebert et al., 2001; Bonsignore et al., 2002; Rigby and Dorling, 2007) and therefore will reach the age at which one is likely have AD. Although there are no concrete data to support this hypothesis, there is also the possibility that women and men respond to the same risk factor differently. For example, there is little evidence to suggest that the ApoE4 genotype is more prevalent in women than in men (Martinez et al., 1998).

Environmental factors: Different studies indicate that pre-exposure to several environmental factors may increase chances for individuals to develop AD (Mayeur, 2003; Casserly and Topol, 2004). Therefore correctly and timely identification of such

environmental risk factors would somehow help to reduce the prevalence of AD. Several environmental factors and life style predispose people to AD. For example, a diet high in fat and cholesterol may elevate the risk to AD. Furthermore, factors such as education appear to lower the risk of cognitive decline. Research suggests that the more years of formal education one has, the less likely to develop Alzheimer's (Cobb et al., 1995; Schmand et al., 1997; Letenneur et al., 1999; Caamaño-Isorna et al., 2005). Longer education can modify the neural connectivity and plasticity leading to a denser network of synapses, the nerve-fiber connections that enable neurons to communicate with one another (Takeuchi et al., 2010). This may create a kind of neural reserve that enables people to compensate longer for the early brain changes associated with AD.

Furthermore, increased exposure to certain substances, such as aluminium, may make a person more susceptible to AD (Ferreira et al., 2008). Although there are contradictory studies regarding this issue, experimental evidence indicates that mice treated with aluminium have reduced brain mass (Tanino et al., 2000), as well as increased formation of neurofibrillary tangles and A β plaques, which are the pathological hallmark of AD (Campbell et al., 2000; Kawahara et al., 2001; Ferreira et al., 2008). Other behavioural and personal habits like smoking and excessive alcohol consumption may also increase the risk to AD.

Conversely, FAD is less common form of AD than the sporadic form; characterized by early onset usually affecting people aged 30-60 years old. Usually inherited as autosomal dominant and clearly passed from one generation to the next. FAD accounts for about 4-5% of total AD cases (Rogaev et al., 1995; Sherrington et al., 1995). As it was earlier mentioned, mutations in the genes coding for PS1, PS2 and APP are the major cause of FAD. These mutations lead to increased production of A β 42 and hence early onset AD (Borchelt et al., 1996; Maruyama et al., 1996; Tomita et al., 1997; Scheuner et al., 1996; Tanzi and Bertram, 2005). PS1 mutations account for the majority of FAD cases (81%) and considered to cause the relatively more aggressive phenotype of the disease than PS2 and APP gene mutations, which account for only 6% and 14% of all FAD cases respectively (Cruts et al., 1998; Jayadev et al., 2010).

The clinical and neuropathological features of FAD closely resemble those of sporadic AD. Extensive neuron loss in the cerebral cortex and hippocampus accompanied by massive deposition of amyloid plaques (extracellular) and neurofibrillary tangles (NFTs) (intracellular) in affected brain regions are the most presenting pathological features of both sporadic AD and FAD (see details below).

1.2.3 Gross features of AD

Before the development of the modern brain imaging tools and techniques like magnetic resonance imaging (MRI), postmortem examination was the only reliable mean to reveal both gross brain and histopathological lesions. Thanks to development of these techniques, it is now possible to establish regional volume and thickness measurements in the brain of live AD patients (Hof et al., 1997; Perl, 2010; Tunnard et al., 2011). However most of the grossly apparent features of the brain of AD patients are non-specific thus, are not diagnostic (Perl, 2010). Brain specimens obtained from most cases of AD show a modest degree of cerebral cortical atrophy due to extensive neuron loss (Hof et al., 1997; Morrison and Hof, 1997) as shown in (figure 2A, B). Atrophy however, tends to spare primary motor, sensory, and visual areas (McEvoy et al., 2009). In addition to cortical atrophy in AD, there is also significant atrophy of the hippocampus, with an associated loss of brain tissue that generally leads to a symmetrical selective dilatation of the adjacent temporal horn of the lateral ventricle (Perl, 2010).

1.2.4 Neuropathological features of AD

The accumulation of protein aggregates in the brain of AD patients is the major histopathological hallmark. The aggregates consist of intracellular, neurofibrillary tangles and extracellular deposits of A β 42 (Hardy and Selkoe, 2002; Tanzi and Bertram, 2005). Both amyloid plaques and neurofibrillary tangles are clearly visible by

microscopy in brains sections from AD patients (Goedert and Spillantini, 2006; Selkoe, 2001) and are used as cardinal microscopic lesions and requirement for AD diagnosis (figure 2C, D).

Although many older individuals develop to some extent amyloid plaques and neurofibrillary tangles because of the aging process, in the contrary the brains of AD patients have extraordinary large numbers of both in specific brain regions. In AD patient these histopathological lesions are diffuse and especially abundant in designated areas such as within the cerebral cortex, hippocampus and amygdala leading to progressive and extensive neuronal loss and cortical atrophy (Wenk, 2003; Price et al., 2009; Perl, 2010; Nelson et al., 2009; 2011; Abner et al., 2011). These lesions may occur, although to a lesser extent in the medial nucleus of the thalamus, dorsal tegmentum, locus ceruleus paramedian reticular area and the lateral hypothalamic nuclei (Haroutunian et al., 1998; Wenk, 2003; Nelson et al., 2010; Prohovnik et al., 2006). Consequently, this loss in brain tissue results in gross atrophy as described above (figure 2A, B), leading to reduced total brain size and mass as the patient progresses from MCI to AD.

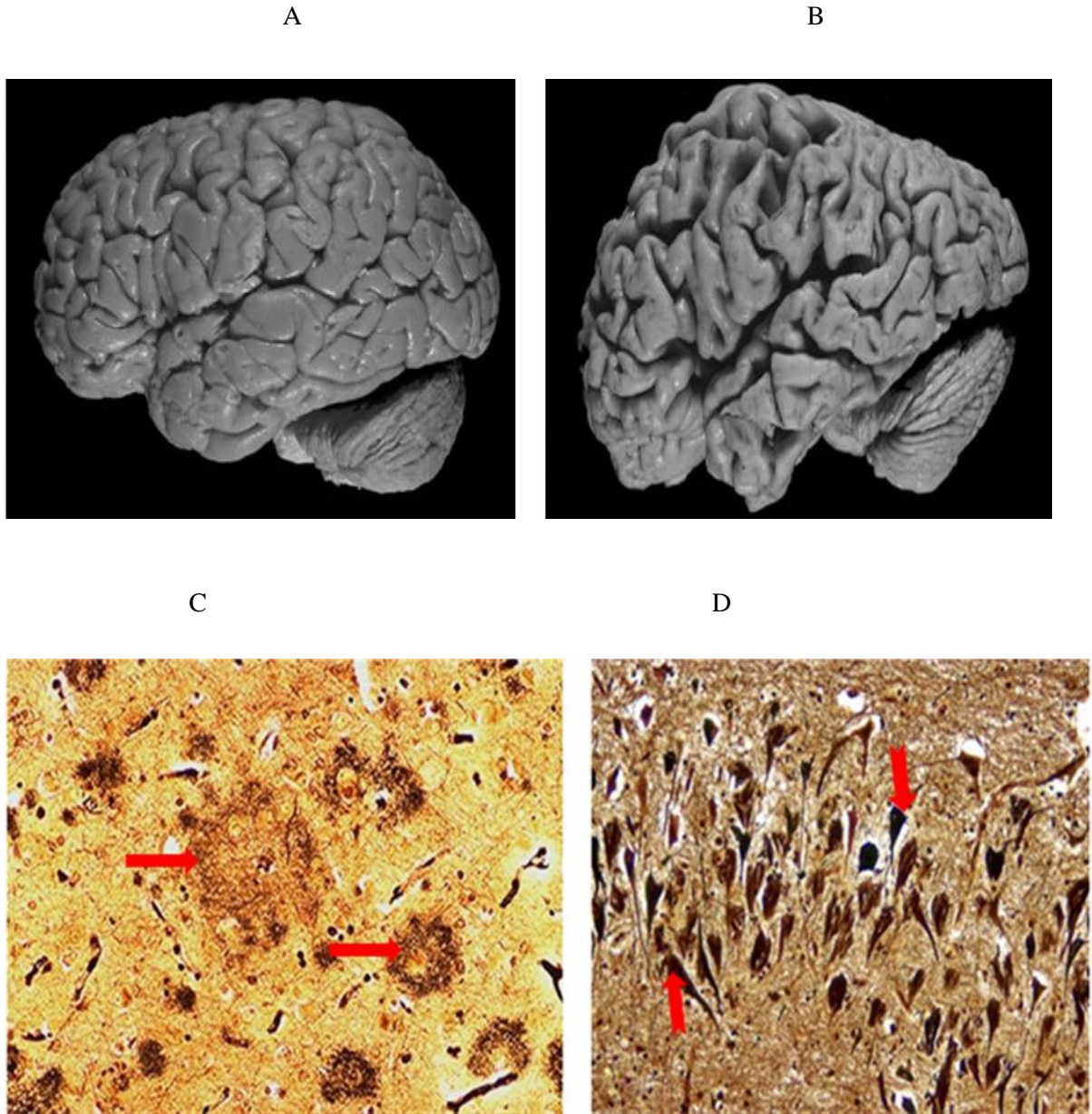


Figure 2: *The gross and histopathological hallmark of AD.* Normal brain (A), Brain from AD patient (B), amyloid plaque (C, arrow) and Dark black neurofibrillary tangle (D, notched arrow); C and D are both stained with Bielschowsky silver stain. Adopted and modified from (<http://www.neuropathologyweb.org/chapter9/chapter9bAD.html>).

Neurofibrillary tangles occur as intracellular aggregates of large bundles of abnormal filaments with paired helical morphology (paired helical filaments – PHFs) composed of hyper-phosphorylated tau protein (Goedert and Spillantini, 2006; Selkoe,

2001; Querfurth and LaFerla, 2010). Tau is a microtubule-associated protein in neurons and plays a pivotal function in microtubules dynamics and axonal transport with its functions tightly regulated by phosphorylation (Johnson and Stoothoff, 2004). Hyperphosphorylated tau proteins lacks affinity for microtubules and results in the transformation of normal adult tau into PHF-tau proteins that clump together to form neurofibrillary tangles, causing microtubules to collapse (Singer et al., 2006; Querfurth and LaFerla, 2010).

Amyloid plaques are dense, mostly insoluble extracellular deposits of A β 42 peptide and cellular material outside and around neurons. The A β peptides are generated as natural products after a sequential cleavage of APP. Full-length APP is a type I transmembrane (TM) glycoprotein with a large extracellular N-terminal domain and a short cytosolic C-terminal domain. APP belongs to a protein family that includes APP-like protein 1 (APLP1) and 2 (APLP2) in mammals (Wasco et al., 1992; Coulson et al., 2000; Walsh et al., 2007). There are three major isoforms of APP in human brain: APP₆₉₅, APP₇₅₁, and APP₇₇₀, which differ in the amino acid length of the protein (Zhang et al., 2011; Selkoe, 1998). In terms of regional localization, APP₆₉₅ is restricted to the central nervous system (CNS) particularly in neurons, where as APP₇₅₁ and APP₇₇₀ are widely expressed in both the CNS and peripheral tissues (Rohan de Silva et al., 1997). The amyloid plaque forms mainly from the APP₆₉₅ isoform, found in higher concentration in the brain as compared to other isoforms and preferentially cleaved by β -secretase to generate A β 42 peptide (Belyaev et al., 2010; Zhang et al., 2011).

Being TM protein, APP is synthesized in the ER and subsequently transported through the Golgi apparatus to the trans-Golgi-network (TGN) where highest concentration of APP is found in neurons at steady state (Zhang et al, 2011). From the TGN, APP is normally transported in secretory vesicles to reach the cell surface for further processing by a group of enzymes called α -, β -, and γ -secretases and two other recently reported members, ϵ and ζ -secretases (Price et al.,1992; Sastre et al., 2001; Weidemann et al., 2002; Thinakaran and Koo, 2008). The amyloidogenic (A β

producing) and the non-amyloidogenic pathway (figure 2) form the major APP processing steps.

The cleavage of APP, by α -secretase initiates non-amyloidogenic APP processing pathway. The α -secretase is primarily a membrane bound endoprotease thus cleaves APP at the plasma membrane (Zhang et al., 2011). The cleavage by α -secretase within the A β domain liberates a large sAPP α ectodomain leaving behind the C-terminal fragment, C83. The γ -secretase then cleaves C83, forming extracellular p3 and the amyloid intracellular domain (AICD) (see also figure 3). The biologic role of p3 fragment remains unresolved.

Interestingly several members of ADAM (a disintegrin and metalloprotease) family, have also been reported to mediate α -secretase activities. Particularly ADAM 9, ADAM 10, ADAM 17, and ADAMS 19 can proteolytically cleave APP suggesting that they are likely to be constitutive partners of α -secretases at cell surface (Buxbaum et al., 1998; Fahrenholz et al. 2000; Asai et al. 2003; Seals and Courtneidge, 2003; Colciaghi et al., 2004; Tanabe et al. 2006). However, most of them may have functional redundancy in APP processing.

Conversely, the beta site APP-cleaving enzyme 1 (BACE-1), initiate the amyloidogenic APP processing by β -secretase (Vassar, 2004). Cleavage by β -secretase release sAPP β ectodomain leaving behind C-terminal fragment, C99. Then γ -secretases further cleaved C99 fragment liberating A β and AICD (see also figure 2). This cleavage occurs within the cell membrane and the process is also known as regulated intramembranous proteolysis (De Strooper and Annaert, 2010).

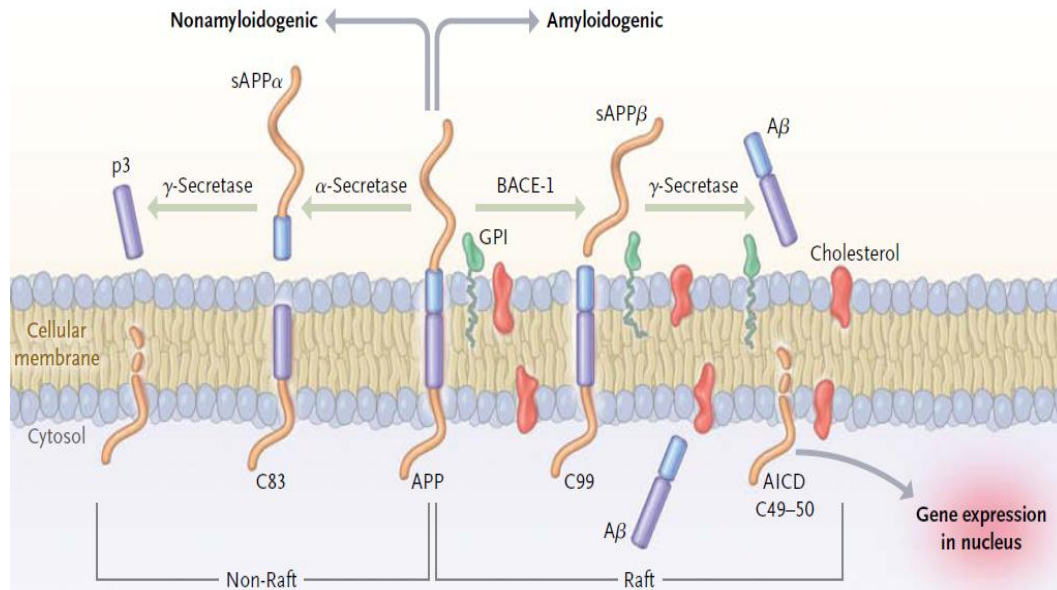


Figure 3: *Amyloidogenic and non-amyloidogenic processing of APP:* In non-amyloidogenic pathway, the α -secretase initially cleaves APP, to release sAPP α , leaving behind an intramembranous stub, C83. The C83 undergoes further cleavage by γ -secretase, liberating extracellular p3 and AICD. In the amyloidogenic processing, the initial processing of APP is performed by β -secretase (BACE-1), releasing a shortened sAPP β and intramembranous stub, the C99. The C99 undergoes cleavage by γ -secretase, generating A β and AICD. Adapted and modified from (Querfurth and LaFerla, 2010).

The sAPP α and sAPP β are secreted fragments of APP, which seem to exhibit different cellular functions (Furukawa et al., 1996; Mattson, 1997; Nikolaev et al., 2009; Chasseigneaux et al., 2011). The physiological roles of both sAPP α and sAPP β are still emerging. Some of the functions of sAPP α include: regulation of neural stem cell proliferation during embryonic developmental, protection against neuronal excitotoxicity, promotion of neuronal survival, plasticity (enhances LTP), neurite outgrowth, synaptogenesis, and cell adhesion (Furukawa et al., 1996; Mattson, 1997; Gakhar-Koppole et al., 2008; Chow et al., 2010). The sAPP β also function as a death receptor ligand to mediate axonal pruning and neuronal death (Nikolaev et al., 2009; Chow et al., 2010).

The AICD is a short tail (about 50 amino acids long) peptide, released into the cytoplasm after successive sequential cleavages by α -, β -, and γ -secretases. AICD targeted to the nucleus, where it regulates transcription of several neuronal genes including A β -degrading enzymes, neprilysin (Belyaev et al., 2010). Although the γ -secretase cleavage produces a number of A β species (36-43 amino acid residues in length), A β 40 and A β 42 are the most common and prevalent. The A β 40 is the more abundant of the two, but A β 42 is more prone to self-aggregation and is thus associated with AD. Most recent studies have also suggested that the A β 43 species, which is even less abundant than A β 42, plays an important role in AD and might substantially contribute to the neurotoxicity and formation of amyloid plaques (Chow et al., 2010; Saito et al., 2011).

In particular, Saito and colleagues (2011) used PS1-R278I knock-in mice to study the role of A β 43 in AD. The PS1-R278I mutant generates larger amount of A β 43. The authors elegantly demonstrated that crossing APP tg mice (APP23 mice carrying the human APP isoform 751 transgene harboring the Swedish mutation (K651N M652L) with PS1-R278I mice resulted in elevated A β 43 generation. These mice showed impaired short-term memory and accelerated A β -pathology, which accompanied accumulation of A β 43 in plaque cores similar in biochemical composition to those observed in the brains of affected AD patients. Furthermore, A β 43 showed a higher tendency to aggregate and was even more neurotoxic than A β 42. Indeed this study opens a new avenue for further investigation on the possible role of longer A β species in AD. A number of longer A β species, including A β 43, A β 45, A β 48, A β 49 and A β 50, occur in the brains of individuals with Alzheimer's disease (Miravalle et al., 2005; Saito et al., 2011). Interestingly, similar A β species have also been found in tg mice that over-express APP carrying FAD-linked mutations (Van Vickle et al., 2007), further suggesting that probably the role of the longer A β species may have been underestimated.

1. 3 γ -secretases

The γ -secretase complex is a multi-subunit internal protease that cleaves within the membrane-spanning domain of a variety of membrane-associated fragments derived from type I integral membrane proteins. It is a key enzyme for the generation of A β 42 peptide, associate with AD (Steiner et al., 2008). Although the most well-known and characterized substrate of γ -secretase is APP as described above, the enzyme is also critical in the intramembranous processing of the Notch (Zhao et al., 2007, Lleó, 2008; Chow et al., 2010). The composition of the γ -secretase complex has not yet been fully characterized. However, it has been suggested that the catalytic part minimally is constituted by four individual proteins: PSs, nicastrin (NCT), anterior pharynx-defective 1 (APH-1), and presenilin enhancer 2 (PEN-2) (Kimberly et al., 2003; Lee et al., 2004; Yamasaki et al., 2006; Kaether et al., 2006) see also (figure 4A, B).

Modification of the proteins in the γ -secretase complex occurs by proteolysis throughout trafficking, assembly, and maturation of the complex. Of note, during assembly and maturation of the complex, PS is endoproteolyzed into two active subunits; amino- and carboxyl- terminal fragments (N- and C-terminal fragments, also abbreviated as NTF and CTF, respectively (Borchelt et al, 1998; Ahn et al., 2010). The full-length PS proteins contain nine TM regions and undergo endoproteolytic cleavage within the cytoplasmic loop between the sixth and seventh TM region, to generate NTF and CTF (Thinakaran et al. 1996) (figure 4A). Both fragments are stable and remain associated to each other to form a functional PS heterodimer in the membrane and represent the active form of PS, whereas full-length PS is rapidly degraded. Each of the two fragments contributes one aspartate to the active site of an aspartyl protease constituting the biologically active form of the γ -secretase complex. Endoproteolysis of PS is therefore a necessity for the activation step of the γ -secretase complex.

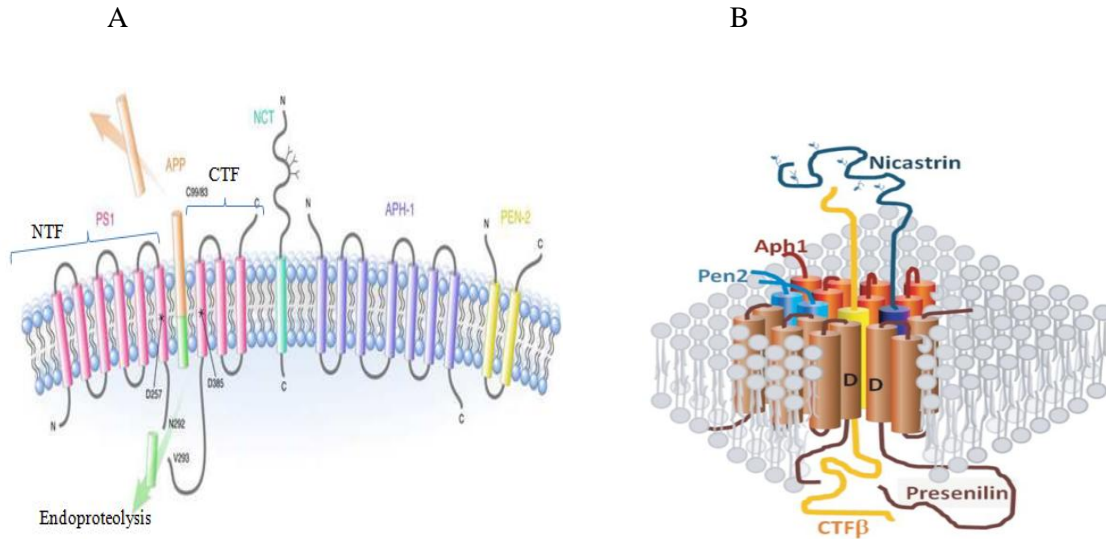


Figure 4: *Topology of the γ -secretase complex.* (A), the four major components [presenilin (PS), nicastrin (NCT), anterior pharynx-defective 1 (APH-1), and presenilin enhancer 2 (PEN-2)] are indicated. Adapted and modified from (Li et al., 2009). (B), γ -secretase sub-units assembly (from Xu, 2009).

NCT is a 130-kDa type I integral membrane protein with a large and highly glycosylated ectodomain (Yu et al., 2000; Chen et al., 2003; Fluhner et al., 2011). Its role in the γ -secretase complex is to serve as a scaffold for assembly of the γ -secretase complex by facilitating proper assembly of the γ -secretase complexes within the ER and their intracellular trafficking. Furthermore, it is required for initial recognition of the γ -secretase substrates and acting as a regulator (rate limiting step) in the recognition and proteolysis of substrates (Shirotani et al., 2004; De Strooper, 2005; Shah et al., 2005; Zhang et al., 2005; Zhao et al., 2010).

PEN-2 on the other hand, displays a hairpin-like structure with two transmembrane domains (TMD) with both termini being located at first facing the lumen of the ER and later on the extracellular environment (Francis et al., 2002; Hasegawa et al., 2004). It consists of 101 amino acid residues and usually found associated with the γ -secretase complexes via binding of a transmembrane domain of PS and, among other possible roles; it confers stability to the complexes especially after PS endoproteolytic

cleavage to generate NTF/CTF fragments (Steiner et al., 2002; 2008; Luo et al., 2003). To demonstrate further the role of PEN-2 in the γ -secretase complex, indeed genetic studies have revealed that PEN-2 knockouts have identical phenotype to PS and APH-1 knockouts in *C. Elegans* model (Prokop et al., 2004; Watanabe et al., 2005).

APH-1 another component of the γ -secretase complex, encodes a unique protein whose topology consists of a seven TM spanning structure with a predicted molecular weight of ~29kDa (Francis et al., 2002; Steiner et al., 2008). In humans, there are two APH-1 genes (APH-1a and APH-1b). The APH-1a further consists of APH-1a long and short form (APH-1aL or APH-1aS) splice variants (Lee et al., 2004; Shirotani et al., 2004; Fortna et al., 2004). Three APH-1 genes occur in mice; APH-1a, APH-1b, and APH-1 c. APH-1aL and APH-1aS are two isoforms generated as alternative splicing of APH-1a, and therefore four distinct APH-1 isoforms are present in mice (Ma et al., 2004). The role of APH-1 in the γ -secretase complexes is highly attributed to its ability to form a complex with NCT that precedes association with PS. As such, the APH-1/NCT complex is responsible for enabling the stabilization and integration of PS and initiating assembly of premature components of the γ -secretase.

PS, NCT, APH-1, and PEN-2 individually or in partnership with other cofactors, regulate each other's assembly, maturation, and γ -secretase activity. Indeed, ablation or simply reduction of one or the other, result into reciprocal effects. For example Steiner et al (2002), demonstrated that ablation of the expression of NCT in mammalian cells, results in a loss of PEN-2 stability and reciprocally, whereas, reduction of cellular PEN-2 interferes with maturation of NCT and PS stability. Apart from the four principal components of the γ -secretase complex, there are several other additional γ -secretase components. However, these other components play just modulatory role for γ -secretase activity. They include CD147 and TMP21/p23; these are TM glycoprotein, which interact with all four essential γ -secretase components (Zhou et al., 2005; Vetrivel et al., 2007; Pardossi-Piquard et al., 2009).

The γ -secretase complex cleaves multiple substrates with essential roles from development to neurodegeneration, and its aberrant processing underlies a variety of

human disorders including AD. The γ -secretase is responsible for the cleavage and processing of over 66, type I integral membrane proteins (Steiner et al., 2008; McCarthy et al., 2009). Biologically and clinically important γ -secretase substrates include APP (Haass, 2004; Thinakaran and Koo, 2008; Wolfe, 2009), ErbB4 (Ni et al., 2001), neuregulin (Bao et al., 2003), and Notch (De Strooper et al., 1999).

APP and notch are the most extensively studied substrates proteins of the γ -secretase complex. As previously mentioned, substrate recognition occurs by NCT ectodomain binding to the N-terminus of the target, passed via a poorly understood mechanism between the two PS fragments (Yu et al., 2000; Chen et al., 2001). With respect to APP processing, the γ -secretase complexes can cleave APP in any of the multiple sites to generate peptides of different size ranging from 39 to 43 amino acids long (Zhang et al., 2011) also (figure 3). A β 40 is the most common isoform, while A β 42 is the most susceptible to conformational changes and self aggregation leading to amyloid fibrillogenesis and eventually aggregate formation, one of the key pathological hallmarks of AD (Thinakaran and Koo, 2008). Interestingly, mutations in APP, PS1, and PS2 have been strongly associated with changes in A β 42/A β 40 ratio by shifting the balance towards increased A β 42 production in FAD (Borchelt et al, 1996; Scheuner et al, 1996).

For notch processing, the initial proteolytic cleavage by members of the ADAM family precedes cleavage by γ -secretase (Tousseyn et al., 2009). The notch is a type I TM protein and is part of an evolutionarily conserved signalling pathway involved in numerous cell fate decisions through local cell–cell interactions in invertebrates and vertebrates. Notch undergo consecutive cleavages at site-2 (S2) and site-3 (S3) (Mumm and Kopan, 2000). ADAM-mediated cleavage of notch represents the first step in regulated intramembrane proteolysis of the receptor, leading to activation of the notch pathway.

Members of ADAMs cleave the notch protein at S2, just outside the membrane. As result of this initial cleavage the extracellular portion of notch is liberated, which continues to interact with notch ligands. The ligand plus notch extracellular domain is

then endocytosed by the ligand-expressing cell. Following ectodomain shedding by ADAM, the remaining intramembraneous part of notch protein undergoes strictly PS dependent γ -secretase constitutive intramembraneous cleavage at S3 (figure 5). This cleavage is similar to the PS-dependent cleavage of the β APP and releases the intracellular domain of the notch protein (NICD) that translocates to the nucleus, where it is involved in target gene transcription (Mumm and Kopan, 2000).

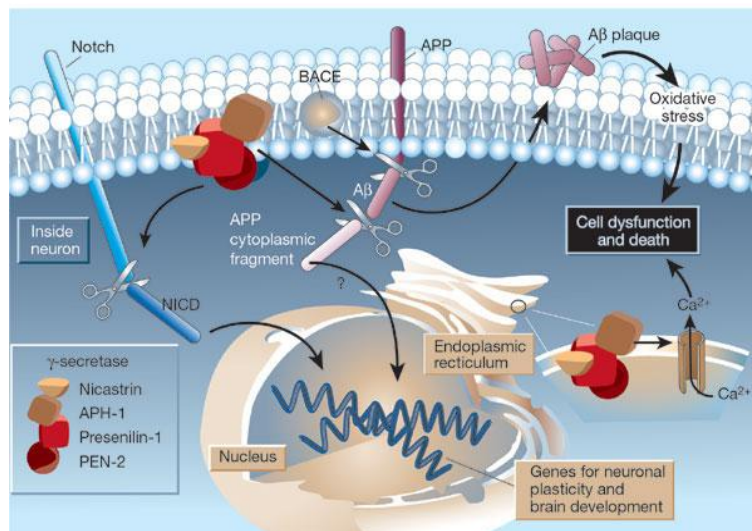


Figure 5: *Functions of the multiprotein γ -secretase.* PS1, NCT, APH-1, and PEN-2 form a functional γ -secretase, located in the plasma membrane and ER of neurons. The γ -secretase complex cleaves notch (left) to generate a fragment (NICD) that moves to the nucleus and regulates the expression of genes involved in brain development and adult neuronal plasticity. The complex also generates A β 42-peptide (A β 42; centre). This involves an initial cleavage of APP by an enzyme called BACE (or β -secretase). Adapted and modified from (Mattson, 2003).

1.4 Presenilins

PSs are the catalytic core of the multiprotein γ -secretase. Both PS1 and PS2 are integral membrane proteins involved in the production of A β protein. The proteins are highly homologous, polytopic membrane proteins described for the first time about 15 years ago through standard positional cloning strategies aimed at identifying the genetic

basis of FAD (Small and Gandy, 2006). There are two PS genes *PSEN1* and *PSEN2*, which encode for PS1 and PS2 respectively. Both genes are highly conserved between species, with little differences between rat and human PSs (Rogaev et al., 1995; St George-Hyslop, 2000). PSs are widely expressed in mammalian tissues (Lee et al., 1996). Their mRNAs are at similar levels in most tissues, with minor exceptions for example, in the brain. Neurons express the highest levels of PS1 and PS2 mRNAs in comparison to levels in glial cells (Sherrington et al., 1995; Lee et al., 1996). At subcellular levels, PSs are abundantly localized in the nuclear envelope (Kimura et al., 2001), ER (Annaert et al., 1999) and the mitochondria and mitochondria associated membranes (Ankarcrona et al., 2002; Area-Gomez et al., 2009). The presenilins are also enriched in the Golgi complex, TGN, and endo-exocytic vesicles (Annaert et al., 1999; Siman and Velji, 2003), endosomes (Vetrivel et al., 2004), and lysosomes (Pasternak et al., 2003); kinetochores and centrosomes (Li et al., 1997) and only a small fraction being present in the plasma membrane (Vetrivel et al., 2006). The broad cellular and subcellular distribution suggests multiple PS-dependent functions in different tissues.

PSs are synthesized as inactive holoproteins of about 50-150 kDa. However, under physiological conditions PSs undergo endoproteolytic cleavage in an alpha helical region of one of the cytoplasmic loops to produce a large NTF (~27- to 30-kDa) and a smaller CTF (~16- to 20-kDa CTF) (Ward et al., 1996; Wakabayashi and De Strooper, 2008). The NTF and CTF non-covalently bound together, form part of the functional protein. PSs have two critical aspartyl residues, which form the catalytic sites, each located on one of these non-covalently bound fragments. The fact that PS1 and PS2 share some structural similarities, suggests that these molecules play highly related functional roles. Conversely the highly variable hydrophilic regions at the N-terminal “head” and the central “loop” domains (figure 6) are likely to mediate cell- or PS-specific functions via differential interaction(s) with other ligands (Wakabayashi and De Strooper, 2008).

1.4.1 The structure of presenilins

Although it is more than a decade since PSs were discovered (Rogaev et al., 1995; Sherrington et al., 1995), yet the transmembrane topology is still debatable. PS is an integral membrane protein consisting of six to nine trans-membrane domains (TMD) structure. However, most recent experimental approaches have favoured the 9-TMD structure as the most popular and widely accepted model (Laudon et al. 2005; Spasic et al., 2006). The 9-TMD topology consists of the N-terminus oriented towards the cytosol, the C-terminus towards the extracellular space and the tenth hydrophobic domain in a cytosolic loop between TMD6 and TMD7 (also see figure 6). There is a significant degree of homology (67%) between PS1 and PS2, and up to 95% conservation in some of the TMDs (McCarthy et al., 2009).

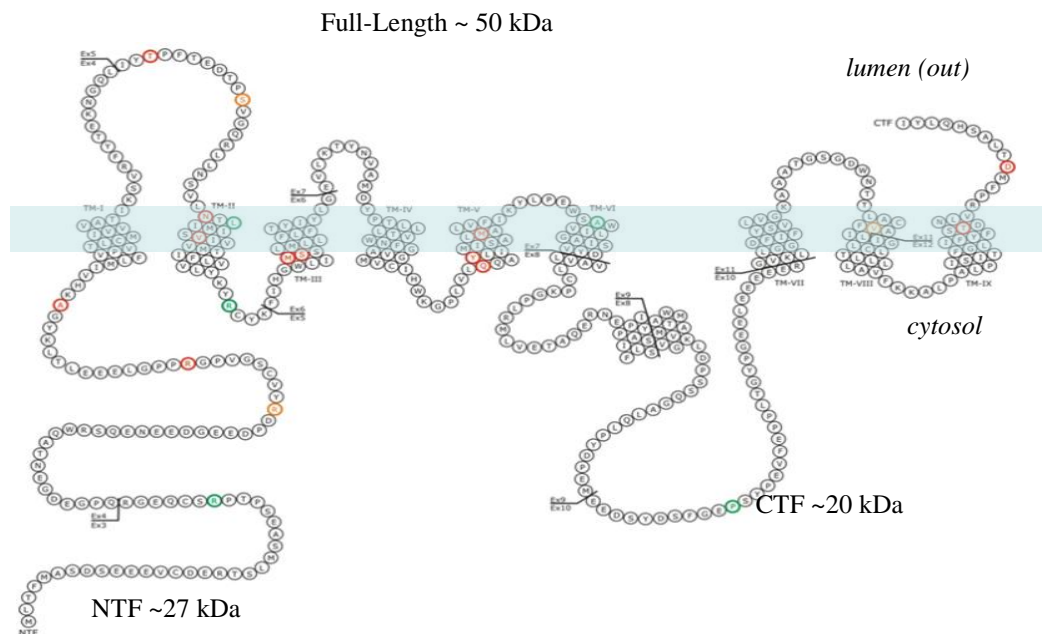


Figure 6: Schematic representation of the 9 TMD topology of PS2. CTF, carboxyl-terminal fragment; NTF, amino-terminal fragment. The coloured circles indicate some of the PS2 mutation sites. Red: pathogenic, orange: pathogenic nature unclear, green: not pathogenic. Adapted and modified from (<http://www.molgen.ua.ac.be/ADMutations>).

1.4.2 Biological functions of presenilin

Both PS1 and PS2 form catalytic core of the γ -secretase and have undergone extensive investigation in recent years. There are studies suggesting that both PS1 and PS2 have overlapping substrate preferences perhaps derived from their 67% identity (Lai et al., 2003; McCarthy et al., 2009). PS/ γ -secretase cleaves with remarkable relaxed sequence specificity the TMD of many proteins. Their role in APP and notch processing among others is well established. Interestingly, despite the accumulated body of evidence that PSs are the catalytic core of the γ -secretase, yet only a small fraction (14%) of PS (Lai et al., 2003; Koo and Kopan, 2004) is engaged in active form of the γ -secretase complexes and the rest interact with other proteins.

Despite the fact that both PS1 and/or PS2 are essential for the γ -secretase mediated cleavage of APP and notch, considerably different phenotypes of the PS1-deficient or PS2-deficient mice have been reported suggesting that these proteins may have distinct roles during the developmental process (Mastrangelo et al., 2005). For example, the PS1-deficient mice exhibit severe developmental defects and perinatal lethality (Davis et al., 1998; Shen et al., 1997; 2007); whereas the PS2-deficient mice are viable and fertile and develop normally although they progressively show, only mild, pulmonary fibrosis and hemorrhage with increasing age (Herreman et al., 1999). These findings support the notion that beyond γ -secretase activity and generation of A β , both PS1 and PS2 play important role in other biological functions through their interaction with other proteins (McCarthy et al., 2009; Wakabayashi and De Strooper, 2008).

A substantial number of studies have implicated PSs in different γ -secretase-independent functions. In addition to binding to the γ -secretase complex partners, PS1 and PS2 can autonomously interact with numerous intracellular proteins in the regulation of a diversity of cellular and tissue homeostatic processes (McCarthy et al., 2009). However, the major challenge for these studies has always been lack of sufficient evidence demonstrating loss of such functions in a PS genetic knockout model and its rescue upon expression of a catalytic active PS in the same model. This would be the best way to prove that a certain function of PS is independent of γ -secretase complex

activities. Beyond their role in the γ -secretase complex activities, recent reports have suggested that PS are involved in: intracellular Ca^{2+} homeostasis, intracellular protein trafficking and transport regulation, β -catenin and wnt signalling, cell adhesion and cytoskeletal stabilization and modulation of apoptosis (Hass et al., 2009; De Strooper and Annaert, 2010; Bezprozvanny and Mattson 2008).

PSs interact with β -catenin. The β -catenin is a cytosolic protein and a major component of adherens cell junctions, linking the actin cytoskeleton to members of the cadherin family of transmembrane cell-cell adhesion receptors (Chen and Schubert, 2002). PS1 is a negative regulator of the Wnt/ β -catenin signalling pathway mediating the degradation of β -catenin (Raurell et al., 2008). In different cell lines and neuronal cultures as well as in the brain tissues, PS1 forms complexes with the N- and E-cadherins and the α - and β -catenins at the cell surface, to constitute the adherens junctions (reviewed in De Strooper and Annaert, 2010). The E-cadherin plays role as the linchpin for the interaction, by binding PS1 and β -catenin. How PS is involved in the turnover β -catenins is still debatable, however, PS stimulates the phosphorylation, ubiquitination, and degradation of β -catenins. PS acts as a scaffold to the β -catenin thus facilitating their phosphorylation by kinases such PKA and GSK-3, a process that regulates their turn-over (Kang et al., 2002, Wakabayashi and De Strooper, 2008; De Strooper and Annaert, 2010). Furthermore, this pathway runs in parallel with Wnt-signalling that also controls phosphorylation and turnover of β -catenin. Interestingly, loss of presenilins/ β -catenin interaction is an important factor in the development of skin cancer observed in presenilin knockout mice (Kang et al., 2002). Evidence that associates this phenotype with reduced β -catenin turnover is now emerging.

Furthermore, PSs play role in regulating protein trafficking in both γ -secretase dependent and independent manner (reviewed in De Strooper and Annaert, 2010). PSs interact with several vesicle transport proteins such as syntaxins, independently of the γ -secretase complex (Suga et al., 2004). Members of the mammalian syntaxin family are involved in the intracellular trafficking of vesicles in the ER–Golgi vesicular transport system. In this context, PSs play important role in the trafficking of different proteins by

regulating the turnover of autophagic vacuoles (Nixon and Yang, 2011; Neely et al., 2011). For example PS1 has been reported to interact and modulate the trafficking of surface proteins such as intercellular adhesion molecule 5 (ICAM5) or telencephalin (TLN), epidermal growth factor receptor (EGFR) and $\beta 1$ integrins to affect the maturation of autophagic vacuoles. Indeed, there are reports suggesting that abnormal accumulation and missorting of ICAM5 or TLN, EGFR, and $\beta 1$ integrins occur as result of PS deficiency in PS1 knockout cells (Esselens et al., 2004).

Most recent, Neely et al (2011) further demonstrated the role of PSs in autophagy. The authors used PS1, and PS2 knockout cells and PS siRNAs to investigate the effects of reduced PS levels on autophagy. By this approach, they found increased levels of LC3-II a common marker for mature autophagosomes, and decreased levels of phospho-mTOR (normally a key inhibitor of autophagy activation). The Authors therefore concluded that in the absence of both PS1 and PS2, autophagy activity appears elevated further suggesting that PSs play an important role in regulating autophagosomal-lysosomal protein degradation; in a γ -secretase independent manner.

PSs play role in apoptotic cell death (Vito et al., 1996); however, their role of in apoptosis is still emerging. Recent reports suggest that some of FAD linked mutations appear to enhance apoptosis (Hass et al., 2009). Although the mechanism governing the involvement of PSs in apoptosis is still vague, emerging evidence suggests that they also modulate apoptosis through their interactions with mitochondrial associated proteins. For example, FAD linked PS2 mutants increase mitochondria-ER interaction, a phenomenon that favours increased mitochondrial Ca^{2+} uptake (Zampese et al., 2011) that may in turn enhance Ca^{2+} induced mitochondrial toxicity leading to apoptotic cell death. Further details on the role of PSs in intracellular Ca^{2+} homeostasis is dealt with in later sections.

1.5 Calcium homeostasis: An overview

The calcium ion “Ca²⁺” is a universal signal molecule essential for a range of life processes (Berridge et al., 2000). Ca²⁺ plays a major role in cell physiology (Pozzan et al., 1994). It is a key element for the bone structure and is involved in many extracellular and intracellular signalling processes, normal blood clotting, and together with Na⁺ and K⁺, it functions to maintain the TM potential that is necessary for normal cellular function (Flynn, 2003). Furthermore, Ca²⁺ regulates numerous physiological processes as an intracellular second messenger (Toescu and Vreugdenhil, 2010).

Experimental evidence both in vivo and in vitro indicate that Ca²⁺ is essential and regulates an array of cellular processes such as secretion, muscle contraction, embryonic development, immunity, apoptosis, metabolism, fertilization, proliferation and differentiation, gene transcription, brain function, chemical senses and light transduction (Berridge et al., 2003), also summarized in figure 7. The universality and enormous versatility of Ca²⁺ attributes to its capability to use extensive molecular repertoire with other signalling components. Through the inherent and highly conserved capability to interact with other molecules, Ca²⁺ mediate signals maintained and/or varied through the crosstalk made with other signalling pathways (Rizzuto and Pozzan, 2006). Through different mechanisms Ca²⁺ is therefore essential for the propagation of both life and death signalling pathway that are usually defined by precise cytosolic Ca²⁺ dynamics.

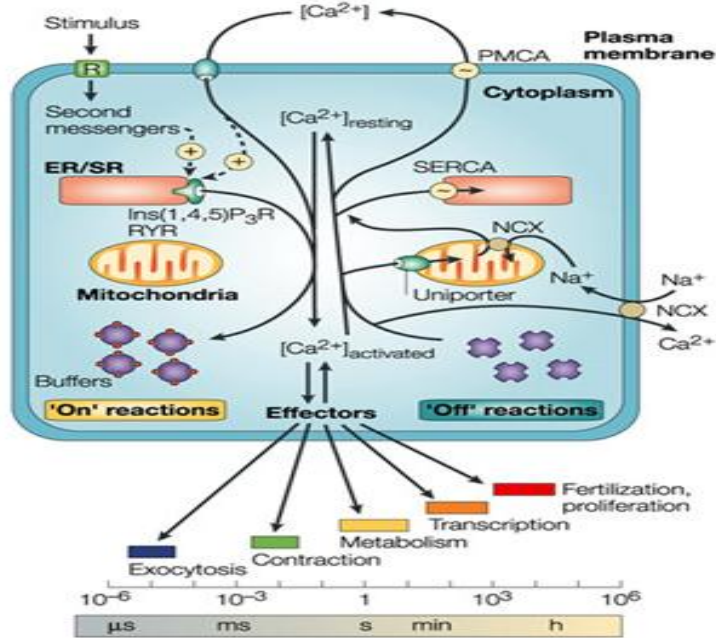


Figure 7: A scheme to summarize Ca^{2+} homeostasis in a single cell. Extracellular Ca^{2+} enters the cell through plasma membrane Ca^{2+} channels and leaves the cell using Ca^{2+} pumps and $\text{Na}^+/\text{Ca}^{2+}$ exchangers. The ER, which is the major intracellular store accumulates large amount of Ca^{2+} by means of SERCA pumps and releases it by IP₃Rs and RyRs. The cytosolic Ca^{2+} rise activates different cell signalling processes vital for different cellular processes including fertilization, transcription, metabolism, contraction, and exocytosis. Adopted and modified from (Berridge et al., 2003).

Interestingly, healthy cells can maintain a large Ca^{2+} concentration ($[\text{Ca}^{2+}]$) gradient between the extracellular and intracellular milieu. With a normal extracellular $[\text{Ca}^{2+}]$ in the 1-3 mM range, the cytosolic free $[\text{Ca}^{2+}]$ is variable among different cells, being generally in the sub-micromolar range between 0.1 to 0.2 μM in the resting state (Pietrobon et al., 1990; Berridge et al., 2000; Rizzuto and Pozzan, 2006; Gleichmann and Mattson, 2011). The $[\text{Ca}^{2+}]$ gradient between extracellular and cytosolic milieu occurs due to the action of plasma membrane Ca^{2+} -ATPases (PMCA) and $\text{Na}^+/\text{Ca}^{2+}$ exchangers (detailed account provided later). The long-term steady cytosolic free Ca^{2+}

concentration ($[Ca^{2+}]_{cyt}$) is therefore determined exclusively by the equilibrium between the rates of the influx and efflux mechanisms (figure 7).

1.5.1 Intracellular Ca^{2+} homeostasis

The cytosolic Ca^{2+} signals originate from two potential sources; opening of a single or a small group of Ca^{2+} channels located on plasma membrane allowing Ca^{2+} entry from the extracellular compartment and release from the intracellular Ca^{2+} stores (Cross et al., 2010; Berridge et al., 2003; Toescu and Vreugdenhil, 2010). Activation of both Ca^{2+} sources depend on external signals arriving at the cell surface and engaging plasma membrane receptors to initiate cell-signalling pathways. Among others, a rise in $[Ca^{2+}]_{cyt}$ is one of the results (LaFerla et al., 2002).

1.5.2 Calcium influx

A group of different Ca^{2+} channels particularly expressed on the plasma membrane regulates Ca^{2+} influx from the external environment. The gating patterns of such channels primarily depend on the activation mechanism. Generally, Ca^{2+} channels consist of; Voltage-operated Ca^{2+} channels (VOCCs) and ligand gated Ca^{2+} channels (Fasolato et al., 1994; Rizzuto and Pozzan, 2006; Cross et al., 2010). In addition, channels belonging to the so-called transient receptor potential (TRP) ion-channel family also play a role (Pedersen et al., 2005; Birnbaumer et al., 2009; Venkatachalam and Montell, 2010). It is worth noting that cells can express more than one type of plasma membrane channel differentially distributed depending on the type of cells. Furthermore, the heterogeneity of plasma membrane channels can be further complicated as new channels can be inserted into the membrane upon activation of specific receptors (Pietrobon et al., 1990; Rizzuto and Pozzan, 2006; Berridge et al., 2003; 2006).

1.5.2.1 Voltage –Operated Ca²⁺ Channels

The VOCCs are a group of transmembrane ion channels activated by changes in membrane potential and primarily found in excitable cells (such as muscle, glial, neuronal cells etc.). This group of channels mediates Ca²⁺ influx into cells in response to membrane depolarization and thus transduces electrical signals into chemical signals. These channels exist in several structurally related multi-unit subtypes consisting of a pore forming and voltage sensing α 1 subunit and several auxiliary subunits including 2δ , β and γ subunits. There are two major categories of VOCCs depending on the activation threshold by depolarization: high voltage-activated (HVA) channels, and low voltage-activated (LVA) channels. The HVA channels can be further subdivided, based on pharmacologic and biophysical characteristics, into L-, N-, P/Q-, and R- type (Dunlap et al., 1995; Jone, 2003; Cross et al., 2010). HVA channels are pharmacologically classified into; the ω -conotoxin-GVIA sensitive channels (N-type), the dihydropyridine (DHP) – sensitive channels (L-type) and the ω -conotoxin-VIA sensitive channels (P/Q-type) (Catterall et al., 2011). Although these channels are primarily permeable to Ca²⁺, they are also slightly permeable to Na⁺, and because of that they are sometimes referred to as Ca²⁺-Na⁺ channels (Hall, 2011). However, under normal physiological conditions the permeability of VOCCs to Ca²⁺ is overwhelmingly high, about 1000-fold greater than to Na⁺ (Hall, 2011). At resting membrane potential, usually most of the VOCCs are closed and only open following a depolarizing stimulus, which is the basis for being "Voltage-operated" channels.

1.5.2.2 Ligand-Gated Ca²⁺ Channels

These Ca²⁺ channels open in response to the binding of a molecule (the ligand). The channels undergo conformational changes following the binding of extracellular ligands to their binding site, thus allowing for the opening of the channel pore. There are four members of this receptor family and include Receptor-Operated Ca²⁺ channels (ROCs), Second Messenger-Operated Ca²⁺ Channels SMOCCs, G-protein Operated Ca²⁺ Channels (GOCCs) and Store-Operated Ca²⁺ Channels (SOCCs).

i) Receptor -Operated Ca²⁺ Channels.

Receptor-Operated Ca²⁺ Channels (ROCCs) comprise of plasma-membrane Ca²⁺ channels opened by the binding of an agonist to its receptor, where the receptor protein is distinct from the channel protein (Pietrobon et al., 1990; Barritt, 1999). The basic structure of ROCCs consists of an agonist recognition site, a transmembrane ion permeation pathway and gating elements that couple agonist-induced conformational changes to the opening or closing of the permeation pore (Traynelis et al., 2010). The binding of the ligand to the receptor allows Ca²⁺ influx and hence transduction of an extracellular signal into the target cell. There are numerous subtypes of ROCCs, differentiated based on their selectivity for cations, mechanisms of channel opening and physiological roles. This group of Ca²⁺ channels includes nicotinic channels activated by acetylcholine (Ach), the channels gated by ATP, and ionotropic glutamatergic receptors channels. The ionotropic glutamate receptors channels include N-methyl-D-aspartic acid (NMDA) receptor, α -amino-3-hydroxy-5-methyl-4-isoxazolepropionic acid (AMPA) receptors and kainate receptors (Stawski et al., 2010; Cross et al., 2010; Kaczor and Matosiuk, 2010; Benarroch et al., 2011).

Glutamate receptors mediate fast excitatory synaptic transmission and thus regulate a broad spectrum of processes in the brain, spinal cord, retina, and peripheral nervous system. AMPA and kainate channels are non-selective Ca²⁺ channels and mediate fast excitatory transmission in the CNS marked by rapid desensitization. Activation of NMDA receptors results in the opening of an ion channel that is non-selective to cations. It has higher permeability to Ca²⁺ than Na⁺ and K⁺. In addition to being non-selective to cations, the NMDA receptors are unique in two ways: Firstly, they are both ligand-gated and voltage-dependent; secondly, they require co-activation by two ligands, glutamate and glycine. Voltage-dependence, occurs as a result of ion channel blockage at resting state by extracellular Mg²⁺ ions (Traynelis et al., 2010; Cull-Candy et al., 2001). Ca²⁺ flux through NMDARs plays critical roles in synaptic plasticity long-term potentiation (LTP) induction, which is a cellular mechanism for learning and memory.

ii) G-protein Operated Ca²⁺ Channels

GOCCs require the interaction directly with G-protein for their activation. These latter exist as heterotrimeric molecules composed of α , β and γ subunits. There are 17 α -subunits, 5 β -subunits and 12 γ -subunits characterized so far (Wettschureck and Offermanns, 2005; Radhika and Dhanasekaran, 2001). G-proteins are activated by a range of signals, from single photons to polypeptide hormones and neurotransmitters (Masseck et al., 2011) and they have a fundamental role in various intracellular signalling pathways that are activated by 7-TMD receptors. Irrespective of the ligand, there are two principal signal transduction pathways involving the G protein-coupled receptors: the 3'-5'-cyclic adenosine monophosphate (cAMP) signal pathway and the phosphatidylinositol signal pathway (Jalink and Moolenaar, 2010). At resting state G-proteins carry, GDP bound to their α -subunit. Therefore, binding of the ligand to the GOCC causes a conformational change leading to the exchange of bound GDP for a GTP. The G-protein α subunit, together with the bound GTP, can then dissociate from the β and γ subunits to further affect intracellular signalling proteins or target functional proteins such as enzymes and ion channels, directly depending on the α subunit type (G_{as} , $G_{ai/o}$, $G_{aq/11}$, $G_{a12/13}$). The role in Ca²⁺ homeostasis is mainly attributes to their ability to activate phospholipase-C β (PLC β). Once activated, PLC β cleaves phosphatidylinositol-4, 5-bisphosphate (PIP₂) present in the membrane producing the second messengers, inositol-1, 4, 5-trisphosphate (IP₃) and diacylglycerol (DAG). IP₃ is the main agonist of the IP₃R expressed on the membrane of intracellular Ca²⁺ stores and induces its opening with a massive release of Ca²⁺ into the cytosol. G-proteins directly act on different Ca²⁺ permeable channels by means of both α and $\beta\gamma$ subunits (Schaefer et al., 2000; Dolphin, 2003).

iii) Second Messenger Operated Ca²⁺ Channels

Second messenger operated Ca²⁺ channels (SMOCCs), require a second messenger produced in the cytosol or in the plasma membrane by any type of signal

transduction pathway. The second messengers are molecules that relay signals received at receptors on the cell surface such as the arrival of protein hormones, growth factors, etc. to target molecules in the cytosol, the nucleus and even in the plasma membrane (channels) (Jalink and Moolenaar, 2010). Apart from serving as relay molecules, second messengers also play a great role in amplifying the strength of the signal. Binding of a ligand to a single receptor at the cell surface may cause massive changes in the biochemical activities within the cell. The most common second messengers include; cAMP, cGMP, IP₃, DAG, arachidonic acid and Ca²⁺ itself (Hardie, 2003; Shuttleworth, 2009; Desch et al, 2010).

iv) Store-Operated Ca²⁺ Channels

SOCCs are present in both excitable and non-excitable cells although are well characterized in non-excitable cells (Putney, 1986; 2011; Lewis, 2011). Depletion of the intracellular Ca²⁺ stores activates these receptors thus allowing Ca²⁺ entry through a phenomenon called store-operated calcium entry (SOCE) also referred to as capacitative calcium entry (CCE). Store depletion usually originates from activation of PLC via G-protein coupled receptors or tyrosine-kinase receptors in the plasma membrane.

PLC is a key enzyme, which hydrolyzes PIP₂ into second messengers, IP₃ and DAG. IP₃ triggers the release of Ca²⁺ from intracellular stores (Fukami et al., 2010) followed by SOCE, which relies on extracellular Ca²⁺ influx through the SOCCs present in the plasma membrane and is tightly regulated by Ca²⁺ concentration in the ER ([Ca²⁺]_{ER}) (Blaustein and Golovina, 2001). Ca²⁺ influx through SOCCs allows refilling of the ER after IP₃-dependent Ca²⁺ release into the cytoplasm. Changes in [Ca²⁺]_{ER} are key factors and linked in reciprocal fashion to the rate at which Ca²⁺ cross the plasma membrane via SOCCs (Lewis, 2010). Searching for the mechanism responsible for the crosstalk between [Ca²⁺]_{ER} and the activation of SOCCs on the plasma membrane has indeed been a subject of great interest.

Two recently identified proteins are responsible for the crosstalk between ER and SOCCs. The first of the two protein families, which functions as sensors of Ca^{2+} levels in the ER, comprises the stromal interacting molecules-(STIM)-1 and -2 (Liou et al., 2005; Putney, 2011). The primary structure of STIM proteins consist of single transmembrane proteins that reside in the ER with their N termini being oriented toward the lumen and contain an EF-hand Ca^{2+} binding motif (Putney, 2010), see also figure 8A. Although there are conflicting data on the role of STIM1 and STIM2 in SOCE, recent reports suggest that STIM1 is the major SOCE signal transmitter, whereas STIM2 has primary responsibility for equilibrating Ca^{2+} homeostasis (Gruszczynska-Biegala et al., 2011).

The second of the two protein families is the Ca^{2+} channel-forming protein Orai in the plasma membrane (Cahalan, 2009; Putney, 2011). Orai channel subunits span the plasma membrane four times, with their C and N termini directed to the cytoplasm as shown in (figure 8B). When there is ER Ca^{2+} depletion, Ca^{2+} dissociates from STIM, resulting in a conformational change that promotes the self-association and migration to closely apposed ER-plasma membrane junctions. It is at these junctions, where STIM oligomers interact with Orai subunits. The interaction between STIMs and Orai1 causes the activation of the Ca^{2+} -Release Activated Ca^{2+} (CRAC) current (Hoth and Penner, 1992) through SOCCs, which consist of the pore-forming Orai subunits (Orai1, -2, or -3) (Putney 2010; 2011). STIM interacts by its C-terminal domain with the N- and C-terminal domains of Orai subunits (figure 8C). Indeed, the interaction between STIM and Orai leads to the formation of complexes, designated as “puncta”, that can be visualized in fluorescent microscopy in cells expressing STIM1-GFP mutants (Cahalan, 2009).

Furthermore, the activity of SOCCs appears to be highly influenced by the pivotal role of mitochondria in intracellular store Ca^{2+} homeostasis. Respiring mitochondria rapidly sequester some of the Ca^{2+} released from the stores, resulting in more extensive store depletion and thus robust activation of CRAC (Parekh, 2008). As SOCCs open, causing rise in cytoplasmic Ca^{2+} this latter feeds back to inactivate the

channels. Since the incoming Ca^{2+} is buffered by mitochondria, the plausible explanation is that the Ca^{2+} dependent inactivation of the SOCCs will be reduced, resulting in more prolonged Ca^{2+} influx (Parekh, 2008). Mitochondria can also release Ca^{2+} close to the ER, accelerating store refilling and thus promoting deactivation of the SOCCs.

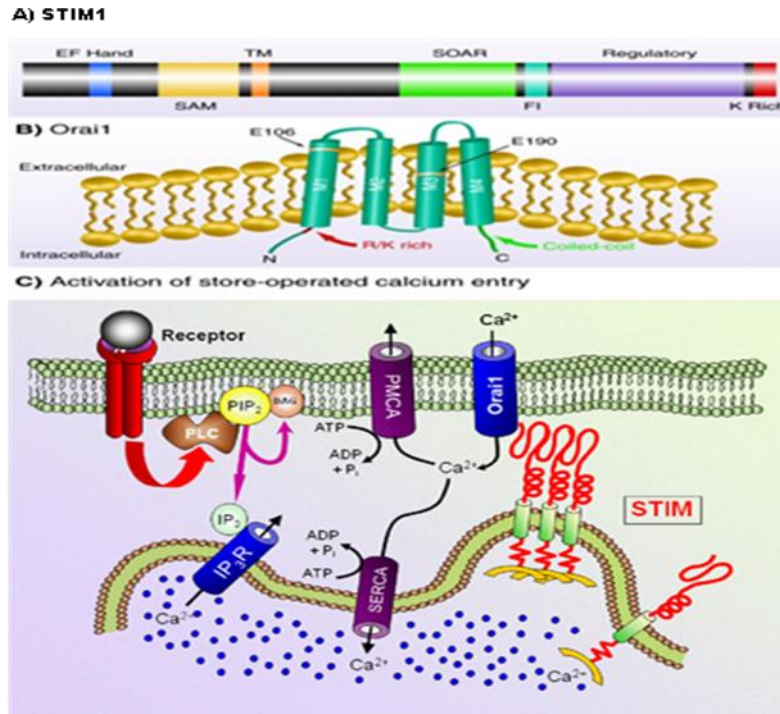


Figure 8: *STIM1 and Orai1 interaction and activation of SOCE.* A) Molecular structure of STIM1, the N terminus that is directed to the lumen of the ER and contains an EF-hand domain that acts as a Ca^{2+} sensor, followed by a sterile α -motif [(SAM); i.e., a protein interaction domain] and the transmembrane (TM) domain. The C terminus is found within a region of coiled-coil domains, a STIM–Orai activating region (SOAR), which is involved in activation of Orai channels and a region enriched in acidic residues that appear to be involved in fast inactivation (FI) by Ca^{2+} . B) Molecular structure of Orai1, Orai1 channel subunits span the plasma membrane four times, with the C and N termini directed to the cytoplasm. C) Activation of SOCE, interaction of STIM1 and Orai1 to activate the SOCC. Adapted and modified from (Putney, 2010).

1.5.3 Calcium release from intracellular stores

1.5.3.1 Endoplasmic reticulum

Endoplasmic reticulum (ER), also known as sarcoplasmic reticulum (SR) in muscle cells, forms a membranous extension from the nuclear envelope. It is a continuous membrane system forming a series of flattened sac-like structures within the cytoplasm of eukaryotic cells and is important in the biosynthesis, processing, and transport of proteins and lipids. The ER usually constitutes more than half of the membranous content of a cell (Berridge, 2002). The ER has two distinct regions. The first, called the rough ER (RER), named for its rough appearance due to the presence of ribosomes attached to its outer cytoplasmic surface (figure 9). The RER forms a region of the ER immediately associated with the nuclear envelope and it synthesizes secretory proteins, phospholipids, and membranes. The second region of the ER, the smooth ER (SER), is not associated with ribosomes (figure 9). The SER is involved in the synthesis of lipids and the detoxification of some toxic chemicals.

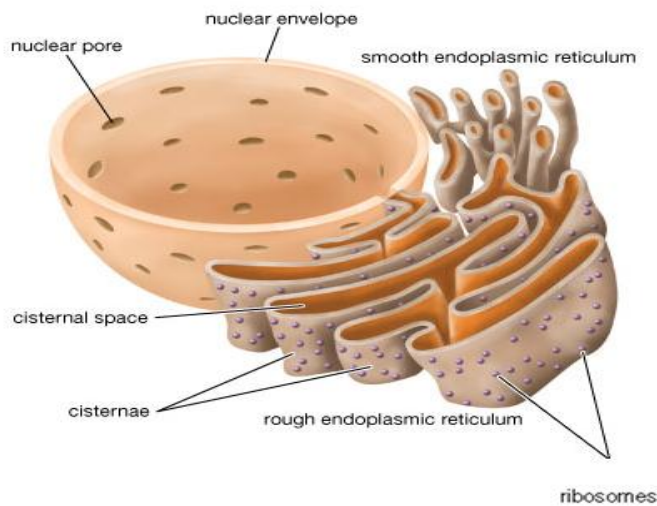


Figure 9: Structure of the ER: The two distinct regions of the ER; the rough ER (RER), named for its rough appearance due to the ribosomes attached to its outer cytoplasmic surface and the smooth ER (SER) that is not associated with ribosomes. Adapted and modified from (www.britannica.com/bps/media-view/114952/0/0/0).

The ER is the major and most important intracellular Ca^{2+} store with a typical $[\text{Ca}^{2+}]_{\text{ER}}$ of about 0.5mM. It forms as a tunnel through which Ca^{2+} moves within the cell. A specialized pump, SERCA (subtype 1-3) found on the ER membrane (Pozzan et al., 1994) pumps Ca^{2+} into the ER. The IP_3Rs and RyRs are the main channels through which Ca^{2+} leaves the ER. Apart from IP_3Rs and RyRs , a small amount of Ca^{2+} leaves the ER also in the absence of any ligand-activated Ca^{2+} efflux through the so-called leak channels, the nature of which is highly debated. Possible candidates include the ribosomal-translocon complex, polycystin-2 (TRPP2), Bcl-2 family members, and pannexins (Guerrero-Hernandez et al. 2010). In addition, activity of RyRs and IP_3Rs at resting Ca^{2+} and IP_3 levels also may contribute to basal ER Ca^{2+} leak. Wt full-length PS1 and PS2 also form Ca^{2+} leak channels in the ER membrane, independently of γ -secretase activities (Tu et al., 2006; Nelson et al., 2007).

Ca^{2+} release from the intracellular stores requires a stimulus capable of generating second messengers, which trigger its release from the ER via IP_3R and RyR channels (Carafoli et al., 2002; Bootman et al., 2002; Berridge et al., 2003). Both IP_3Rs and RyRs exist in multiple isoforms. Accordingly, the precise RyR , IP_3Rs and SERCA isoform composition, and the subcellular localization in the ER, are important factors for shaping and determining the magnitude and kinetics of cell's Ca^{2+} signal.

i) IP_3 -Receptors

The IP_3R is a tetrameric intracellular IP_3 -gated Ca^{2+} release channel that is predominantly located on the membrane of the ER, with a total molecular mass of >200 kDa. The IP_3Rs is present in almost all cell types and plays a crucial role in intracellular Ca^{2+} signaling. So far, there are three mammalian IP_3R isoforms, designated $\text{IP}_3\text{R1}$, $\text{IP}_3\text{R2}$, and $\text{IP}_3\text{R3}$, expressed in different mammalian cell types (Foskett et al., 2007; Zhang et al., 2011). The tissue expression pattern of the three subtypes are distinct but sometimes overlapping, and most tissues express more than one subtype as heterotetrameric receptor complexes (Wojcikiewicz and He, 1995). Furthermore, the

three mammalian IP₃R subtypes share between 65–85% homology (Zhang et al., 2011). The tissue expression pattern of the different IP₃R is as following; IP₃R1 predominates in the CNS particularly in the cerebellum, IP₃R2 in cardiac myocytes and IP₃R3 in kidney and pancreatic cells (Vermassen et al., 2004). Every IP₃R subunit has a single IP₃-binding site, lying towards the N-terminal, and six TMDs, close to the C-terminal; these TMDs anchor the protein to the ER membrane. In fact in all IP₃R regardless of their subunit composition, the N-terminal region consist of; the ligand coupling/suppressor domain, which suppresses IP₃-binding activity and serves as the key determinant for the different of IP₃-binding affinity for each subtype (Iwai et al., 2007) and IP₃-binding core domain that is the minimum region required for specific IP₃-binding (Mikoshiha, 2007). On the other hand the COOH-terminal region bears the 6TMDs and a short cytoplasmic COOH-terminal tail, called the “gatekeeper domain”, which is critical for IP₃R channel opening. In summary, each IP₃R subunit consists of five functional domains: an N-terminal coupling/suppressor domain, an IP₃-binding core domain, an internal coupling domain, a transmembrane/channel-forming domain, and a gatekeeper domain (Furuichi et al., 1989; Mikoshiha, 2007). The pore of the receptor consists of TMD-5 and 6, together with the intervening loop (figure 10). The N-terminal and internal coupling domains transfers the IP₃ binding signal to the gatekeeper domain, which triggers a conformational change in the activation gate formed within the transmembrane/channel-forming domain.

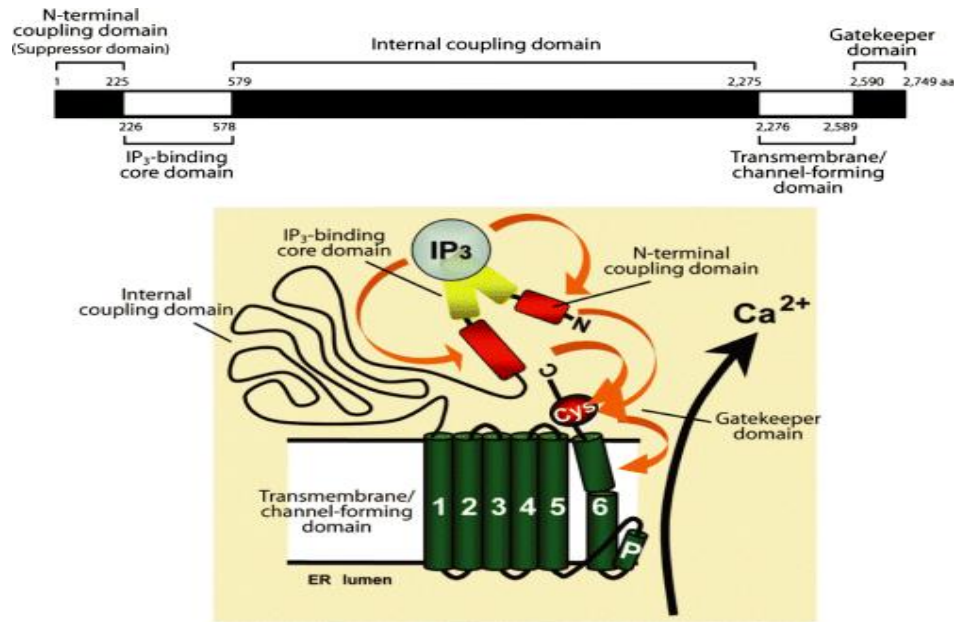


Figure 10: *Structural model of mouse IP₃R1:* IP₃R is tetrameric and each subunit consists of five functional domains: an N-terminal coupling/suppressor domain, an IP₃-binding core domain, an internal coupling domain, a transmembrane/channel-forming domain, and a gatekeeper domain are indicated. The figure is adapted and modified from (Mikoshiba et al., 2007).

The generation and mobilization of IP₃ is crucial for Ca²⁺ release from the ER via IP₃Rs. The generation of IP₃ requires stimuli such as hormones, growth factors, neurotransmitters, neurotrophins, odorants, and light that function through G-protein coupled receptors or tyrosine-kinase coupled receptors to activate PLC (figure 11). As mentioned earlier, PLC is a key enzyme, which hydrolyzes PIP₂ into second messengers, IP₃ and DAG. IP₃ triggers the release of Ca²⁺ from intracellular stores, and DAG mediates the activation of protein kinase C (PKC) (Fukami et al., 2010).

The phosphoinositide-specific PLC family comprises of six different isoforms (namely PLC β, γ, δ, ε, ζ, η). The hydrolysis of PIP₂ by each isoform requires different stimuli (see also figure 11). However, all PLCs require Ca²⁺ for their biological activities and it has been established that PLCη isoform, in particular, has the highest Ca²⁺ sensitivity followed by PLCδ and PLCζ, in fact these isoforms can even be activated by normal cytosolic Ca²⁺ levels (Allen et al., 1997; Cockcroft, 2006; Swann et al., 2006).

Furthermore, PLC β , PLC γ , PLC δ and PLC ϵ can be activated by G-protein coupled-, tyrosine-kinase coupled agonists, elevation in $[Ca^{2+}]_{cyt}$ and through Ras related mechanisms, respectively (Berridge et al., 2003). The PLC ζ , a sperm-specific isoform, is widely considered a physiological stimulus injected by the sperm to trigger intracellular Ca^{2+} oscillations at fertilization (Swann et al., 2006; Nomikos et al., 2011). PLC η is a neuron-specific isoform enriched in the hippocampus, cerebral cortex and the olfactory bulb (Cockcroft, 2006; Nakahara et al., 2005). Under physiological conditions, especially in neurons, PLC η could function as Ca^{2+} -sensor enzymes that are activated by small increases in $[Ca^{2+}]_{cyt}$ (Cockcroft, 2006). These separate receptor mechanisms coupled to energy-requiring transduction mechanisms, which activate PLC to hydrolyse the lipid precursor PIP $_2$ to generate IP $_3$ and DAG. IP $_3$ then binds to IP $_3$ Rs to induce Ca^{2+} release from the ER into the cytosol and to promote Ca^{2+} influx through SOCE mechanisms.

The most important modulators of the the Ca^{2+} release activity of the IP $_3$ R channel in the ER includes intracellular modulators (IP $_3$, Ca^{2+} , ATP, CaM), protein kinases, and IP $_3$ R-binding proteins leading to various spatiotemporal cytosolic Ca^{2+} patterns and consequently diverse cellular responses (Mikoshiha, 2007; Zhang et al., 2011).

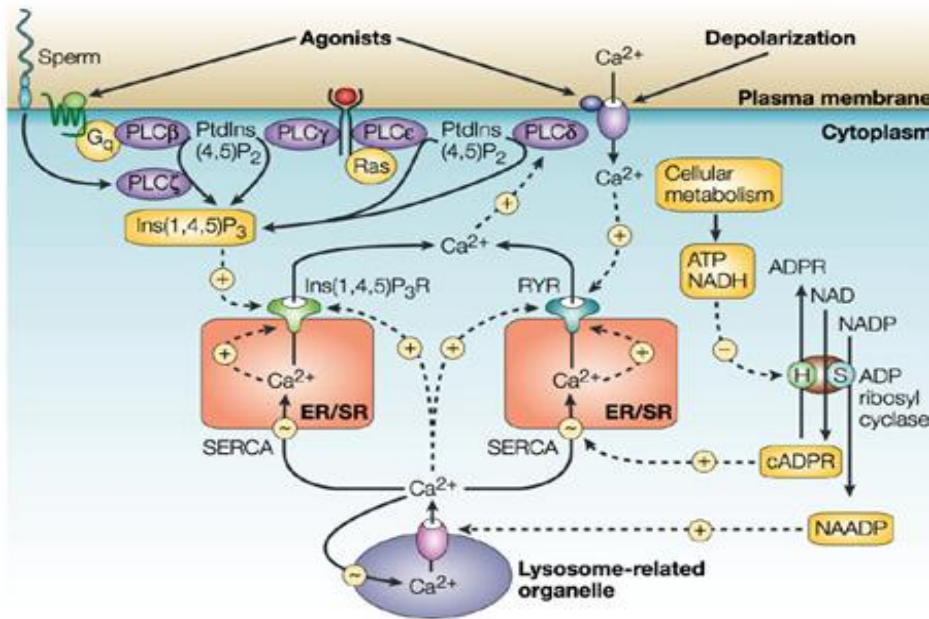


Figure 11: Summary of the plasma membrane receptor-mediated mechanisms for stimulating the formation of IP₃. Many agonists bind to G-protein coupled receptors or tyrosine-kinase coupled receptors, which use a GTP-binding protein to activate appropriate PLC. The activated PLC hydrolyses the lipid precursor PIP₂ to generate IP₃ and DAG. IP₃ then binds to IP₃Rs to induce Ca²⁺ release from the ER into the cytosol and to promote influx of external Ca²⁺ through CCE. Adapted and modified from (Berridge, 2003).

ii) Ryanodine Receptors

RyRs are a family of large, homotetrameric intracellular Ca²⁺ release channels that upon activation, allow rapid release of Ca²⁺ from the ER stores into the cytosol. There are three main isoforms of RyRs (namely; RyR1, RyR2 and RyR3) and exist as homotetramers with a total molecular mass of >2 MDa (each subunit is >550 kDa). The molecular structure is still debated and it remains unclear as to how many TMDs exist in the RyR channels, however the prevailing view favours the six TMD structure for its monomeric form and possibly as many as eight TMD may exist (Kushnir et al., 2010).

In terms of tissue distribution: RyR1 primarily expresses in skeletal muscles, RyR2, in myocardium and RyR3, exhibit more wide expression, but especially in the brain (Lanner et al., 2010). However, all the three isoforms expresses in the mammalian brain. Within the brain RyR1, is enriched in Purkinje cells of the cerebellum, RyR2 is predominantly expressed in the dentate gyrus of the hippocampus and RyR3 has been detected in the hippocampal CA1 pyramidal cell layer, the basal ganglia and olfactory bulbs (reviewed in Kushnir et al., 2010). RyR2 also localize in pancreatic islets whereby RyR1 and RyR3 also localize in leukocytes. Interestingly, smooth muscle cells also express all three isoforms (Kushnir et al., 2010). The three isoforms share about 65% homology (Lanner et al., 2010). RyR also play important role in mediating Ca^{2+} release from the intracellular stores into the cytosol by detecting Ca^{2+} concentration on its cytosolic side, thus establishing a positive feedback mechanism (Lanner et al., 2010; Fill and Copello, 2002).

Certainly, a small amount of Ca^{2+} in the cytosol near RyR will cause it to release even more Ca^{2+} , a phenomenon referred to as a calcium-induced calcium release (CICR), resulting in amplification of Ca^{2+} signals (Ozawa, 2010). Ca^{2+} is the most important activator of RyRs by priming their response, as all three isoforms exhibit a biphasic response to free Ca^{2+} and can participate in CICR in permeabilized systems. Ca^{2+} dependent RyRs activation generally occurs at about 0.3–10 μM Ca^{2+} and inhibited by millimolar Ca^{2+} concentrations. This Ca^{2+} sensitivity is important as it ensures that RyRs remain closed at resting $[\text{Ca}^{2+}]_{\text{cyt}}$ (0.1 to 0.2 μM) and avoids the sustained activation of the receptors at high Ca^{2+} concentrations (Betzenhauser and Marks, 2010). It is worth noting that the effect of higher Ca^{2+} levels on RyRs also varies with different isoforms; for example, Ca^{2+} has stronger inhibitory effects on RyR1 but less so on RyR2 and RyR3.

RyRs can also be activated by the intracellular messenger cyclic ADP ribose (Fill and Copello, 2002), as a physiological gating agent. Pharmacologically, suramin and 4-chloro-m-cresol activate the RyRs by acting as direct agonists. In addition, caffeine and ryanodine are commonly used pharmacological agonists for the activation of RyR

channels. Caffeine increases the receptors sensitivity to CICR. On the other hand at nM and up to 10 μM concentration, ryanodine, locks the RyR in an ‘open state’ whereas, when applied at higher concentrations (above 100 μM) it locks the channel in a ‘closed state’ (Lai et al., 1989; Fill and Copello, 2002; Ozawa, 2010).

Furthermore RyRs can be modulated directly or indirectly by various ion like Mg^{2+} , small molecules and proteins including protein kinase A (PKA), FK506 binding proteins (FKBP12 and 12.6), calmodulin (CaM), Ca^{2+} /calmodulin-dependent protein kinase II (CaMKII), calsequestrin (CSQ) and triadin (Lanner et al 2010). In the skeletal muscle the L-type VOCCs, subtype $\text{Ca}_v1.1/1.2$ modulates RyR1 directly or indirectly. In this case T-tubule depolarization leads to Ca^{2+} entry through $\text{Ca}_v1.2$ and hence through CICR, Ca^{2+} binds to RyR2 leading to activation of the channel and release of SR Ca^{2+} (Kushnir et al., 2010; Betzenhauser and Marks, 2010).

1.5.3.2 Other intracellular Ca^{2+} stores

It is worth noting that the ER is not the only indispensable mobilizable Ca^{2+} store, almost all organelles so far studied have the ability to act as mobilizable Ca^{2+} stores, albeit with very different kinetics. The Golgi apparatus, made up of cisternae stack has four functional regions: the cis-Golgi network, medial-Golgi, endo-Golgi, and trans-Golgi network, which play role in Ca^{2+} homeostasis (Pizzo et al., 2011). Lysosomes, mitochondria and the nucleus are also essential stores with regard to Ca^{2+} transport and Ca^{2+} homeostasis in different cell types (Michelangeli et al., 2005; Davies and Terhzaz, 2008). The role of the Golgi apparatus and other organelles in Ca^{2+} homeostasis has been unraveled in recent years especially with the development of modern tools for Ca^{2+} imaging and detection of localized Ca^{2+} signals. With the application of classical Ca^{2+} dyes and genetically-encoded Ca^{2+} probes, it is now possible to visualize cytoplasmic and organellar Ca^{2+} dynamics as well as Ca^{2+} microdomains in real time and to investigate their role in tissues and cells physiology (Rudolf et al., 2003; Palmer and Tsien, 2006).

1.5.4 The sarco/endoplasmic reticulum Ca^{2+} ATPase pump

The sarco/endoplasmic reticulum Ca^{2+} ATPase (SERCA) pump is a single polypeptide of molecular mass of 110 kDa and localized both in the ER and in SR membrane. The major function of SERCA is to transport Ca^{2+} from the cytosol into the ER. SERCA-dependent Ca^{2+} transport is the only Ca^{2+} uptake mechanism in this organelle (Verkhatsky, 2005; Arbabian et al., 2011). SERCA is classified under a family of P-type ATPases that includes other members such as; plasma membrane Ca^{2+} ATPase (PMCA), Na^+/K^+ ATPase, and H^+ , K^+ ATPase. All P-type ATPases operate by the transfer of terminal phosphate from ATP to an aspartate residue in the catalytic domain, resulting in a reversible conformational change. The hydrolysis of ATP thus couples to the movement of ions across a biological membrane. Under similar mechanism, SERCA pump utilizes the energy derived from ATP hydrolysis to transport Ca^{2+} across the membrane. Two Ca^{2+} ions are transported for each ATP molecule hydrolyzed.

There are three distinct genes encoding SERCA 1, 2, and 3 that can produce more than 10 isoforms, through alternative splicing (Vandecaetsbeek et al., 2011). Interestingly, all SERCA isoforms have a highly conserved primary structure such that all isoforms consist of essentially identical TM topologies and tertiary structures. SERCA-2 is evolutionary the oldest and the most widely expressed isoform in vertebrates. SERCA-2 encodes SERCA-2A and predominantly found in cardiac and slow-twitch skeletal muscle, and SERCA-2B, expressed in all tissues though at low levels (Arbabian et al., 2011). A third and recently reported isoform, SERCA-2C occur in cardiac muscles. SERCA-1 is expressed in fast-twitch skeletal muscle and is alternatively spliced to encode SERCA-1A and SERCA 1B. SERCA-3 isoforms are expressed in several non-muscle tissues, but considered minor form.

1.5.5 Organization of the intracellular Ca^{2+} signal

The cytosolic Ca^{2+} signal, resulting from both Ca^{2+} release and influx, is highly organized in spatial and temporal patterns. Such localization and the integrated free

cytosolic Ca^{2+} concentration over time contain specific information require for different biological processes (Berridge, 2006). Generally, when Ca^{2+} enters the cytosol via different channels on the plasma membrane or from intracellular stores, it forms Ca^{2+} microdomains close to either plasma membrane or internal stores. Ca^{2+} microdomains are defined as localized increase in $[\text{Ca}^{2+}]$ associated with Ca^{2+} release in one part of the cell (hot spots) usually close to Ca^{2+} channel (Berridge et al., 2003; Rizzuto and Pozzan, 2006). Due to their defined spatial and temporal patterns, these microdomains form building blocks of intracellular Ca^{2+} signals. Microdomains occur as local plumes of Ca^{2+} rise, depending on their size and location designated as; ‘Spark’ when formed by the opening of a group of RyRs. ‘Sparklet’; when arise because of brief opening of VOCCs. ‘Puff’; unitary intracellular Ca^{2+} waves that result from release of Ca^{2+} from IP_3Rs . ‘Blink’; formed by fall in level of Ca^{2+} within the lumen of the ER/SR; ‘syntilla’, as elementary events produced by RyR in the hypothalamic neuronal presynaptic endings (Parker et al., 1996; Berridge, 2003; Rizzuto and Pozzan, 2006; Smith et al., 2009).

The organization of Ca^{2+} signals into microdomains is the basis for the versatility of the Ca^{2+} signalling system, allowing cells to regulate different biological processes within localized regions of the cell at the same time. The opening of Ca^{2+} channels just below the plasma membrane results in a rim of Ca^{2+} microdomains at the vicinity of the channel mouth. Furthermore, these microdomains near the plasma membrane originate from Ca^{2+} release from the ER through IP_3R channels, near the vicinity of the plasma membrane. Areas of contact between the ER and the plasma membrane have been established (Berridge, 2003).

The shape and duration of microdomains are primarily regulated by both Ca^{2+} influx and release from intracellular stores and uptake by other organelles like mitochondria (Rizzuto and Pozzan, 2006; Contreras et al., 2010; Zampese et al., 2011), which appear to be the target of most of the Ca^{2+} microdomains. Indeed Ca^{2+} microdomains are crucial for mitochondrial Ca^{2+} uptake by the low affinity, mitochondrial Ca^{2+} uniporter (MCU). The close apposition of ER Ca^{2+} release sources

and mitochondria ensures that the MCU becomes activated through high local $[Ca^{2+}]$ that exceeds the average $[Ca^{2+}]_{\text{cyt}}$ (Pizzo et al., 2007; Giorgi et al., 2009; Drago et al., 2011). Although not all cellular processes and functions require Ca^{2+} microdomains, substantial biological processes primarily require Ca^{2+} microdomains for their activation. Such processes include synaptic vesicle fusion, exocytosis, cAMP response element-binding (CREB) phosphorylation, synaptic protein (syntaxin 1A) activity and mitochondrial Ca^{2+} uptake (Rizzuto and Pozzan, 2006; Giorgi et al., 2009).

1.5.6 Regulation of intracellular Ca^{2+} dynamics

The amount of intracellular Ca^{2+} at any particular moment in time is determined by a state of balance between ‘on’ reactions that introduce Ca^{2+} into the cytoplasm and ‘off’ reactions that remove the signal through a combined action of buffers, pumps and exchangers (Berridge et al., 2003). In summary, the the Ca^{2+} signalling network consist of four functional units (reviewed in Berridge et al., 2000, 2003). The signalling is triggered by a stimulus that generates various Ca^{2+} mobilizing signals, then the latter activate the ‘on’ mechanisms that feed Ca^{2+} into the cytoplasm, thereafter, Ca^{2+} functions as a messenger to stimulate numerous Ca^{2+} -sensitive processes and finally, the ‘off’ mechanisms remove excess Ca^{2+} from the cytoplasm to restore the resting state. Of the accumulated Ca^{2+} from the two principal sources, only a small proportion binds to the effectors to activate various cellular processes that operate over a wide temporal spectrum, while a large amount of it is bound to intracellular buffers (Prins and Michalak, 2011). Ca^{2+} -binding proteins (CaBPs) involved in buffering cytosolic Ca^{2+} levels, include calbindin-D28, calretinins, and parvalbumin (Solovey and Dawson, 2010). Ca^{2+} leaves effectors and buffers, during ‘off’ reactions and removed from the cell by various exchangers and pumps.

The exchangers and pumps that extrude Ca^{2+} include: Na^+ / Ca^{2+} exchanger (NCX) or $Na^+ / Ca^{2+} / K^+$ exchanger (NCKX) (Molinaro et al., 2011) and PMCA (Brini and Carafoli, 2009; Roberts-Thomson et al., 2010), respectively. SERCA pumps Ca^{2+} back into the ER in competition with PMCA (Arbabian et al., 2011).

The mitochondria have also been implicated to play an active role during the recovery process by rapidly sequestering Ca^{2+} , thus shaping the cytosolic Ca^{2+} signals (Pizzo and Pozzan, 2007; Contreras et al., 2010). Mitochondrial Ca^{2+} occur via the MCU, which is an ion channel involved in potent and rapid Ca^{2+} uptake into the mitochondria (Giorgi et al., 2009; Drago et al., 2011). As far as this latter is concerned, after years of intense research, the nature of the so-long sought MCU was finally identified by combining bioinformatics and genomics (Baughman et al. 2011; De Stefani et al., 2011). It is a 40 kDa protein with two hypothetical transmembrane domains that, upon expression in bacteria and incorporation in black lipid films, reconstitutes Ca^{2+} permeable channels with electrophysiological and pharmacological properties compatible with those previously described (Kirichok et al. 2004).

Regulation of Ca^{2+} signalling within the cell occurs through an elaborate and well-established mechanism called “self assessment system” that depends exclusively on the equilibrium between the rates of the efflux mechanisms and the rate of inward Ca^{2+} “leak” across the plasma membrane (Berridge et al., 2003; Rizzuto and Pozzan, 2006). The fine-tuning of the spatial and temporal properties of the Ca^{2+} signals in the cell is made possible by the presence of Ca^{2+} buffers, exchangers and pumps that determine the balance between “on” and “off” reactions. The fact that Ca^{2+} signalling has a direct role in health and disease, any disruption of intracellular Ca^{2+} signalling and homeostasis cascade will trigger mechanisms for the physiopathological events that eventually lead to cell injury and death.

1.6 Neuronal Ca^{2+} signalling and homeostasis

Neuronal Ca^{2+} homeostasis and Ca^{2+} signalling like in other cell types play important role in regulating a large number of neuronal processes ranging from regulation of excitability to neurite outgrowth and synaptogenesis, synaptic transmission and plasticity, cell survival and gene transcription (Wojda et al., 2008; Mattson, 2007; Gleichmann and Mattson, 2011). The main functions of neurons include information

processing and impulse transmission to effector cells responsible for mediating behavioural responses such as learning and memory, emotional responses in response to different environmental cues and body movements. In that context, Ca^{2+} functions as a second messenger to transfer signals both locally and globally within a neuron and helps to adapt to its activity dependent requirements through feedback and feed-forward mechanisms. Since neurons interconnects through synapses, Ca^{2+} also functions as a key regulator of electrochemical signalling even in neuronal networks.

As it is the case for other excitable cells, neuronal Ca^{2+} signalling utilize both extracellular and intracellular Ca^{2+} pools in response to stimulation. For example, Ca^{2+} influx into dendrites and the cell body to a larger extent dependent on presynaptic neurotransmitter release and plasma membrane potential. The neuronal extracellular Ca^{2+} level is usually 10,000-folds higher than the intracellular concentration. It is estimated that the extracellular Ca^{2+} concentration is about 1 - 2mM whereas the typical resting $[\text{Ca}^{2+}]_{\text{cyt}}$ is approximately 100nM (Gleichmann and Mattson, 2011). The high Ca^{2+} concentration gradient between the two sides is the basis for significant increase in $[\text{Ca}^{2+}]_{\text{cyt}}$ after plasma membrane depolarization. Membrane depolarization occurs as result of influx of Na^+ and efflux of K^+ , which significantly affect the membrane potential. Ca^{2+} influx due to plasma membrane depolarization occur as short Ca^{2+} transients. These transients do not cause significant changes in $[\text{Ca}^{2+}]_{\text{cyt}}$ level as large part of it, is quickly extruded by $\text{Na}^+/\text{Ca}^{2+}/\text{K}^+$ exchangers and the PMCA pumps or sequestered by Ca^{2+} binding proteins (buffers) and the intracellular stores (Brini and Carafoli, 2009; Roberts-Thomson et al., 2010; Pizzo and Pozzan, 2007; Molinaro et al., 2011). During such brief Ca^{2+} transients, different Ca^{2+} dependent biochemical and metabolic process utilizing Ca^{2+} signalling as second messengers are thus, activated and executed. Properly and tightly controlled Ca^{2+} fluxes across the plasma membrane and between intracellular compartments are critical for neuronal well-being and functioning.

VOCCs of various types, ROCCs and SMOCCs as explained in previous sections, primarily regulate the entry of Ca^{2+} from the extracellular medium especially during neuronal activities. Activation of VOCCs (L-type, N-type, P/Q-type, and R-type)

or ionotropic glutamate receptors (NMDA, AMPA and Kainate) triggers Ca^{2+} influx, hence increases the neuronal $[\text{Ca}^{2+}]_{\text{cyt}}$ upon neuronal depolarization and stimulation respectively. Activation of metabotropic glutamate receptors of Group I (mGluR1, mGluR5), which are coupled to PLC activation, results into mobilization of IP_3 , ER Ca^{2+} release through IP_3 Rs, possibly involving further Ca^{2+} release through RyRs (CICR) and Ca^{2+} entry through SOCCs. Following these transients, basal Ca^{2+} level is regained mainly through Ca^{2+} extrusion into the extracellular milieu by $\text{Na}^+/\text{Ca}^{2+}$ exchangers and the PMCA) and/or by mitochondrial uptake. Some of the released Ca^{2+} is pumped back into the intracellular stores by the SERCA pump (Berridge et al., 2003; Saris and Carafoli, 2005; Pizzo and Pozzan, 2007).

The extensive neuronal Ca^{2+} signalling also requires energy utilization and hence increases energy demand as all exchangers and pumps required to maintain Ca^{2+} homeostasis are ATP-dependent. In other words, Ca^{2+} signalling and neuronal excitability regulate each other and both depend on energy availability that is in turn determined by metabolic capacity. Tight control of Ca^{2+} signalling and homeostasis is therefore critical, if not well controlled neuronal excitability may change, consequently affecting network activity and energy metabolism. Under such conditions, uncontrolled Ca^{2+} influx may also lead to increased generation of toxic mitochondrial reactive oxygen species (ROS). Reduced mitochondria capacity to buffer Ca^{2+} , decreases with increased oxidative damage. For example, during aging and neurodegenerative diseases, altered or uncontrolled Ca^{2+} signalling and homeostasis is a common phenomenon that, consequently, compromises the ability of neurons to maintain energy levels and increases ROS generation, hence contributing to neurodegenerative processes (Gleichmann and Mattson, 2011). How exactly ROS deranges Ca^{2+} signalling, is still under investigation. However, ROS can cause oxidative modifications that consequently modulate the kinetics of key proteins in the ER and mitochondria Ca^{2+} homeostasis toolkit. Such proteins include; the mPTP, SERCA, IP_3 R and RyR (Csordas and Hajnoczky, 2009, Drago, et al., 2011).

The neuronal ER has a unique structure characterized by an internally interconnected, continuous membrane system of tubules and cisternae, which extends from the nuclear envelope to axons and all the way to presynaptic terminals, as well as to dendrites and dendritic spines (Berridge, 1998; Renvoisé and Blackstone, 2010). Due to this unique structure of the ER, others have considered it as a neuron-within-a-neuron especially due to the formation of a binary membrane system together with the plasma membrane (Verkhratsky, 2005). The uptake of Ca^{2+} into the ER lumen primes the Ca^{2+} release receptors on its membrane by enhancing their Ca^{2+} sensitivity. Because of its participation in a wide variety of processes, from plasma membrane excitability to synaptic plasticity (Verkhratsky, 2005), neuronal Ca^{2+} homeostasis must be tightly regulated in order to prevent disorders.

1.7 Presenilins and intracellular Ca^{2+} homeostasis in AD

PSs interact with different proteins involved in Ca^{2+} regulation. PSs are also involved in physiological regulation of intracellular Ca^{2+} homeostasis (Tu et al., 2006; Cheung et al., 2008). How do PSs play a role in intracellular Ca^{2+} homeostasis is a hot topic under active investigation.

Wt PSs play a physiological role in regulating ER Ca^{2+} homeostasis through an array of mechanisms. Some researchers have suggested that PSs regulate the activity of both ER Ca^{2+} uptake and release machinery through their interaction with SERCA pump activity and, IP_3R and RyR gating activity (Cheung et al., 2008; Green et al., 2008). Emerging evidence also suggests that PSs are likely to play a role in modulating the interaction between ER and mitochondria, which are important partners in intracellular Ca^{2+} homeostasis (Pizzo and Pozzan, 2007; Area-Gomez et al., 2009; Zampese et al., 2011). However, a precise mechanistic explanation on the physiological significance of the interaction between PSs and Ca^{2+} homeostasis is still lacking.

By using artificial planer lipid bi-layer membranes, as well as PS1 and PS2 double knockout mouse embryonic fibroblasts (MEFs), wt PSs formed low conductance Ca^{2+} channels in the ER membrane (Tu et al., 2006). These results suggested that PSs serve as ER Ca^{2+} leak channels independently of γ -secretase activities, since PS1-D257A, a mutant that abolishes the catalytic activity of the γ -secretase complex had similar effects as wt PS1. Furthermore, in experiments involving PS double knockout MEFs, PS accounts for about 80% of passive Ca^{2+} leak from the ER pointing out to a significant contribution of PS in ER Ca^{2+} release (Tu et al., 2006). In the bi-layer membrane, the FAD-linked PS mutations PS1-M146V or PS2-N141I completely abolished the low conductance channel activity and increased ER Ca^{2+} levels upon over-expression in MEFs (Tu et al., 2006). Taken together the findings reported in this study suggested that PSs regulate intracellular Ca^{2+} homeostasis by forming passive Ca^{2+} leak channels on the ER membrane a phenomenon sort to be lost upon expression of PS1 or PS2 mutants. However, these findings came from PS over-expression. Under such conditions, there is a large amount of the holo-presenilin protein (immature) expressed. Thus, the full-length PS conformation seems to be necessary for this role.

Recently data have been generated providing further insights on the understanding of the role of PSs on intracellular Ca^{2+} homeostasis in AD, particularly FAD. Different FAD linked PS mutations have been identified and extensively studied to address this question. As it was mentioned earlier, mutations in both PS1 and PS2 or APP genes are the major cause of early onset FAD (Rogaev et al, 1995; Sherrington et al, 1995; Scheuner et al., 1996). These mutations consistently increase the relative ratio between the amyloid peptides, $\text{A}\beta_{42}/\text{A}\beta_{40}$ (Borchelt et al, 1996; Scheuner et al, 1996). From the phenotypic point of view, PS1 and PS2 seem to result in a gain of toxic function; however, biochemically, they result in a partial loss of function in the γ -secretase (reviewed in De Strooper, 2007; Wolfe, 2007; Hardy, 2007).

Alteration in the consecutive APP processing could provide plausible explanation on how loss-of-function mutations in PS1 and PS2 might result in gain of toxic function as result of decreased $\text{A}\beta_{40}$ generation but increased production of $\text{A}\beta_{42}$

(De Strooper, 2007). The cleavages of APP at the individual sites are heterogeneous and could give rise to roughly two different product lines, A β 49 (ϵ) - A β 46 (ζ) - A β 43 (γ) - A β 40 (γ) and A β 37 (γ), whereas the other product line generates A β 48 (ϵ) - A β 45 (ζ) - A β 42 (γ) - A β 39 (γ) (Wolfe, 2007; Steiner et al., 2008). This cleavage occurs systematically, with secretase cleaving the APP CTF first at the ϵ -site, which is close to the cytoplasmic border of the membrane (figures 12). As result of this cleavage, the AICD detaches from the membrane, leaving a long A β species in the membrane. Subsequent cleavages will then take place roughly every third amino acid down the α -helical transmembrane domain via the ζ - to the γ -site and progressively removing C-terminal residues, until the peptide is short enough for release from the membrane (Wolfe, 2007). Interestingly, the proteolytic activity at these two sites is affected by FAD linked PS1, PS2 or APP mutations, which in turn shift the initial ϵ -cleavage site to produce more A β 48, thus favouring increased production of A β 42 relative to A β 40 along with an increase in a new 51-residue AICD relative to the 50-residue product (Sato et al, 2003). Indeed, the model suggested by Wolfe (2007) and presented here in figure 12, highlights how reduction of proteolytic function owing to PS mutations might lower A β production but at the same time increase the ratio of A β 42 to A β 40. On the other hand, less catalytically efficient γ -secretase complexes would allow more time for the release of longer A β peptides.

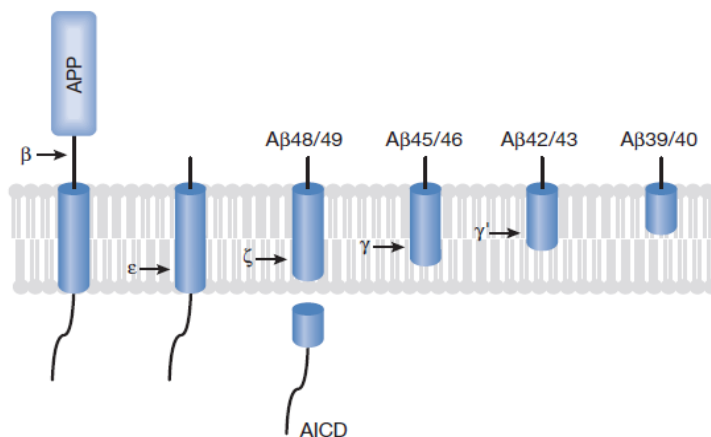


Figure 12: Model of processive proteolysis of the APP transmembrane domain by γ -secretase. The cleavage begins at the ϵ -cleavage site and the AICD detaches from the membrane and leaves a long A β

species in the membrane. Subsequent cleavages will then take place roughly every third amino acid down the α -helical transmembrane domain via the ζ - to the γ -site, progressively removing C-terminal residues until the peptide is short enough for release from the membrane. Adapted and modified from (Wolfe, 2007).

Conversely, complete loss of PS function in the brains of mice results in neurodegeneration in the total absence of A β generation (De Strooper, 2007). These latter findings complicate the possible mechanistic explanation for the role of PSs in FAD and further suggest the possibility of additional mechanisms other than just alteration in A β generation.

Although there are contradictory data on how PSs perturb intracellular Ca²⁺ homeostasis, PS1 mutations cause a more aggressive form of FAD by causing Ca²⁺ overload in the ER. This notion is supported by a wealth of experimental evidence from different studies registering increase in Ca²⁺ release in the cytosolic compartment from ER upon stimulation in cells expressing FAD linked PS1 mutants. The elevated Ca²⁺ release from the ER was due to abnormally increased ER Ca²⁺ content. This phenomenon led to the formulation of the “Ca²⁺ overload” hypothesis for FAD. It is proposed that the reduced ER Ca²⁺ leak due to loss of function of PS (as leaky channels) results in increased [Ca²⁺]_{ER} and consequently exaggerated Ca²⁺ release upon cell stimulation. The formulation of this hypothesis indeed fuelled further research in this area; however, despite its wide acceptance by many research groups, contradictory reports are available for both PS1 and PS2 FAD linked mutations. Exaggerated Ca²⁺ release in the cytosol (LaFerla 2002; Thinakaran and Sisodia, 2006) and reduced Ca²⁺ release (Zatti et al., 2006; Giacomello et al., 2005; Brunello et al., 2009) are attribute to the FAD linked PS1 and PS2 mutants.

Over-expression of FAD-linked PS mutants can enhance Ca²⁺ release even in the absence of ER Ca²⁺ overload (Cheung, et al. 2008; 2010). The latter findings have been associated with increased sensitivity of the ER Ca²⁺ release toolkit (IP₃Rs and RyRs) other than ER Ca²⁺ overload. FAD linked PS mutants modulate ER Ca²⁺ channels gating activity via a mechanism involving the IP₃Rs (Cheung et al., 2008). Recent experimental evidence also suggest that several FAD-linked PS mutants can influence the expression

pattern of IP₃R and RyR proteins in cell lines, neurons, and brain microsomes (Zampese et al., 2009). Furthermore, the SERCA pump is another target of FAD linked PS mutants, being either potentiated (Green et al., 2008) or inhibited (Brunello et al., 2009). Taken together these findings strongly support the notion that PSs are involved in ER Ca²⁺ homeostasis, although they are somehow at odd with the Ca²⁺ overload hypothesis and in fact they even challenge the whole concept of the Ca²⁺ overload.

In the contrary, reduced ER Ca²⁺ concentration occurs in different cell line models and primary cortical neurons over-expressing FAD linked PS2 mutants. Particularly: PS2 wt, PS2-T122R, PS2-D366A, PS2-M239I and PS2-N141I and also some of FAD linked PS1 (PS1-P117L, PS1-M146L, PS1-L286V and PS1-A246E) mutants cause strong reduction in [Ca²⁺]_{ER} (Giacomello et al., 2005; Zatti et al., 2006; Brunello et al. 2009; Zampese et al., 2009). Most of these studies involved direct measurement of the [Ca²⁺]_{ER} by employing ER-targeted Ca²⁺ probes (e.g. ER-targeted aequorin) that allow real time detection of [Ca²⁺]_{ER} dynamics. Studies involving fibroblasts from patients bearing FAD linked PS2 mutations also reported similar findings. The mechanism governing the strong reduction in ER Ca²⁺ concentration as result of expression FAD linked PS mutants remain unclear. However, the reduction in ER Ca²⁺ content might be partly due to the inhibition of the SERCA pump activity by PS mutants and also increased Ca²⁺ leak through the IP₃R and RyR ER Ca²⁺ channels (Cheung et al., 2010; Brunello et al., 2009).

1.8 The soluble Aβ42 oligomers and AD

Since the formulation of the amyloid hypothesis until recently, the neuropathology in AD patients was strongly associated with extracellular Aβ42 plaques (Hardy and Higgins, 1992). However, recently it has become apparent from correlation studies that soluble oligomeric species, rather than monomeric or deposited Aβ42 plaques are associated with onset of the neuropathology and dementia in AD (Walsh and Selkoe, 2007; Shankar and Walsh, 2009). As opposed to the case for Aβ monomers,

found in both health and disease or fibril, there is growing evidence that soluble oligomeric or prefibrillary intermediate species of A β peptide are responsible for neuronal dysfunction and neurodegeneration observed in AD patients (Walsh and Selkoe, 2007). Indeed data from AD human brain (Shankar et al., 2008; Shankar and Walsh, 2009), tg mice (Lesné et al., 2006), and neuronal cultures treated with synthetic A β 42 peptides (Lambert et al., 1998; Resende et al., 2008) suggest that A β 42 oligomers may be responsible for the pathological changes and neuronal dysfunction in AD patients even prior to dementia.

A body of evidence from studies published recently, further support the notion that A β 42 oligomers (for example, dimers) exert detrimental effects on synaptic function (Shankar et al., 2008; Shankar and Walsh, 2009). A β 42 oligomers also impair LTP and LTD, which are the electrophysiological correlate of learning and memory and promote synaptotoxicity (Berridge, 2011). Both free and soluble A β 42 oligomers, either produced within the synapse or entering from outside, may be responsible for the synaptic dysfunction, partly by causing derangement of Ca²⁺ homeostasis (Demuro et al., 2005). Indeed, the soluble oligomeric forms of A β 42 increase Ca²⁺ entry by either functioning as artificial channels (Arispe et al., 2010; Mattson, 2010; Demuro et al., 2011) or by activating different Ca²⁺ channels in the plasma membrane (Alberdi et al., 2010; Berridge, 2011), see also figure 13. Therefore, Ca²⁺ influx induced by A β 42-dependent mechanisms contributes to the intracellular Ca²⁺ elevation frequently reported in AD.

Furthermore, exaggerated amount of Ca²⁺ released from the ER is another frequently reported consequence of the alteration in Ca²⁺ signalling and remodelling, which occur in AD (Berridge, 2010). Exaggerated Ca²⁺ released by InsP₃R and RyR channels occurs in neurons from mice expressing the FAD linked PS mutations, which increase A β 42 generation from APP. However, direct evidence on the relationship between increased A β 42 generation and Ca²⁺ dysregulation observed in PS mutants is still controversial. A β 42 oligomers are likely to destabilize the [Ca²⁺]_{cyt} through a number of mechanisms: enhanced InsP₃R and RyR channels sensitivity and gating, and increase in the expression of the RyRs, which amplify the IP₃-mediated Ca²⁺ release

from intracellular stores (Kelly et al., 1996; Resende et al., 2008; Berridge, 2010; Demuro et al., 2010; Mattson, 2010).

The molecular mechanism(s) through which A β 42 oligomers cause synaptic dysfunction is not understood. However, A β 42 oligomers trigger the internalization of post-synaptic AMPA and NMDA-type glutamate receptors (D'Amelio et al., 2011). Acceleration of this molecular mechanism could lead to a toxic gain of function in the form of an imbalance between LTP and LTD. As result, this may lead to synaptic dysfunction, spine and synaptic losses; consequently, cognitive decline in AD (Hsieh et al., 2006; D'Amelio et al., 2011).

A β 42 oligomers cause elevation of $[Ca^{2+}]_{cyt}$ that leads to activation of caspases (especially caspase-3), and protein phosphatases like calcineurin. Activated calcineurin mediates both LTD and spine loss, causing synaptic dysfunction (D'Amelio et al., 2011). Furthermore, the same Authors reported that the AD tg mice Tg2576 (based on mutant APP) develop memory dysfunction and loss of apical dendritic spines in the CA1 of the hippocampus in early adulthood (3 months of age) prior to the development of extensive amyloid plaques. Such changes are associated with increased calcineurin activity, post-synaptic loss of the AMPAR GluR1 subunit, change in glutamatergic synaptic transmission, and a slight enhancement of LTD in the CA1. It appears that caspase-3 activation occurs upstream of these changes, since a single injection of caspase-3 inhibitor was sufficient to down regulate caspase-3 and calcineurin activity in vivo, thus restoring GluR1 levels at PSD, as well as spine size and memory performance. Indeed these findings indirectly provide additional evidence on the role of the soluble form of A β 42 oligomers in synaptic disruption in AD.

Further insights on the importance of A β 42 oligomers in AD, another study Laurén et al (2009) reported high-affinity binding between A β 42 oligomers and the cellular prion protein (PrP^C) on neurons. Prion proteins constitute high affinity receptors for A β 42 oligomers whereas the monomeric form binds with a lower affinity. The binding of A β 42 oligomers to the PrP^C inhibited LTP suggesting that PrP^C could be an important mediator in A β 42 oligomers-induced synaptic dysfunction. Although the

proposed mechanisms are not strong enough to explain the actual molecular mechanism mediating the interaction between A β 42 oligomers and synaptic components, yet they point out important milestones in AD research.

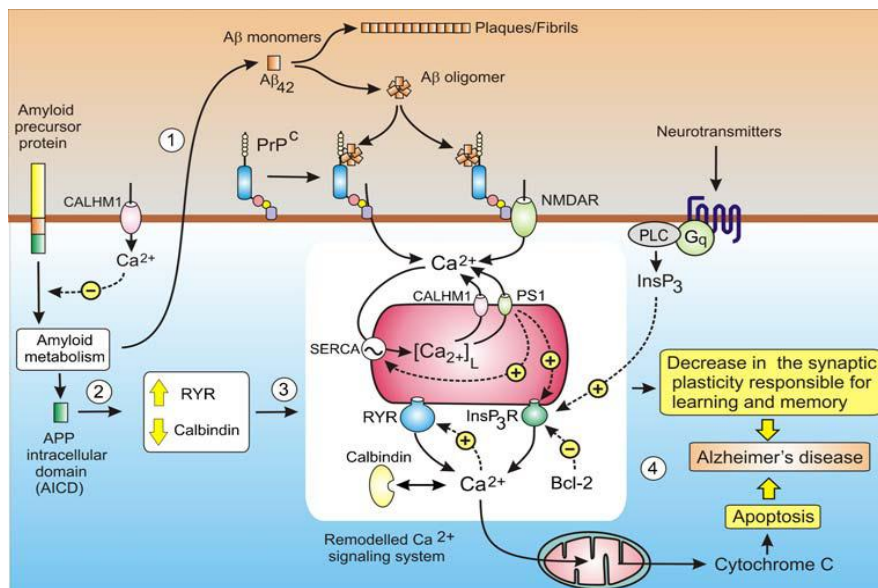


Figure 13: Schematic model for A β monomers in which misfolding triggers self-aggregation into oligomers, fibrils, and fibrillar aggregates or plaques and remodelling of the Ca²⁺ signalling system. Adapted and modified from (Berridge, 2010).

1.8.1 The A β oligomers and neuronal Ca²⁺ dysregulation

The role of A β 42 oligomers in modulating neuronal intracellular Ca²⁺ homeostasis is a complex subject and its understanding requires multidimensional approach. However, a spate of recent studies have suggested that A β 42 oligomers can specifically cause synaptic toxicity in part through Ca²⁺ dysregulation (Demuro et al., 2005). A β 42 oligomers cause a generalized increase in cell membrane permeability to Ca²⁺; interferes with mitochondrial activities by causing overproduction of reactive oxygen species (ROS); inhibits respiration and ATP production and damages the

structure of mitochondria. In fact, A β 42 oligomers interfere with the activities of the mitochondrial protein, cyclophilin D (CypD), a regulator of mitochondrial permeability transition pore (mPTP) (Du and Yan, 2010). In this context, A β 42 increases the CypD expression level and its activity thus decreasing the threshold of mPTP formation. A β aggravate the formation of mPTPs resulting in mitochondrial perturbations including increased ROS generation, Ca²⁺ dysregulation and mitochondrial membrane potential collapse (Du and Yan, 2010). These severe mitochondrial disturbances eventually lead to multiple cellular stresses, neuronal death and finally deficits in learning and memory ability (Du et al., 2008; Sanz-Blasco et al., 2008).

Increased generation of toxic A β 42 and accumulation of both the oligomeric species and plaques causes Ca²⁺ dysregulation (Berridge, 2011). In addition to the artificial channels formed by A β on the plasma membrane as explained above, A β 42 oligomers can also bind directly to the NMDA receptors, inducing massive Ca²⁺ influx (Berridge, 2010; Alberdi et al., 2010) see also figure 13. Such high Ca²⁺ influx through the NMDA receptors increases the vulnerability of neurons to excitotoxicity (Alberdi et al., 2010). Another mechanism through which A β perturbs neuronal Ca²⁺ homeostasis in synaptic terminals is by inducing membrane lipid peroxidation, leading to Ca²⁺ overload, synaptic dysfunction, neuronal degeneration, and cognitive impairment (Mattson, 2010).

1.8.2 Role of Ca²⁺ in learning and memory

The role of Ca²⁺ in learning and memory is a complicated topic. However, Ca²⁺ plays dichotomous role in these processes; it is required for LTP and LTD induction of both the AMPA and NMDA receptor origin. The generation of high levels of Ca²⁺ waves as result of Ca²⁺ influx, activate LTP that is required for learning and memory formation mechanisms. Persistent low Ca²⁺ levels on the other hand are required for LTD induction, a phenomenon implicated in memory erasure (Berridge, 2010). As such, the induction of LTP requires high Ca²⁺ influx through the NMDA receptors, whereas LTD formation occurs as result of Ca²⁺ release from the intracellular stores (Kato et al., 2000). Indeed, both high and low Ca²⁺ waves due to influx and release from the

intracellular stores respectively, further activate the different signalling pathways that are involved in AMPA and NMDA receptors trafficking, insertion and surface redistribution. High Ca^{2+} waves can also activate different protein kinases like: Ca^{2+} /calmodulin-dependent protein kinases II (CAMKII), glycogen synthase kinase 3 β (GSK-3 β), glutamate receptor interacting proteins (GRIP) and translocated actin-recruiting phosphoprotein (TARP), which phosphorylates AMPA receptors and increase their surface expression and sensitivity that is required for induction and maintenance of LTP (Berridge, 2010; 2011).

Conversely, A β oligomers can inhibit the induction of LTP (Shankar and Walsh, 2009). Surprisingly, reduced LTP was reported in the PS double knock out mouse where there appeared to be a selective decrease in presynaptic transmitter release (Zhang, et al., 2010). Furthermore, the remodeling of the intracellular Ca^{2+} signalling system has profound impact on the process of LTD (Hsieh et al., 2006; Kuchibhotla et al., 2008). Since LTD induction requires small elevations in Ca^{2+} , thus any upregulations of Ca^{2+} signalling will selectively enhance LTD and continuously erase any memories formed by LTP.

1.9 Ca^{2+} measurements in living cells

Since the development of Ca^{2+} imaging techniques using fluorescent Ca^{2+} indicators or sensors, it has been possible to study cytoplasmic and organellar Ca^{2+} dynamics as well as domains and their role in tissues and cells physiopathology (Rudolf et al., 2003; Palmer and Tsien, 2006). Fluorescent indicators for Ca^{2+} , coupled with live cell imaging, provide the exceptional ability to follow Ca^{2+} signals in real time. It is therefore possible to define the vast array of Ca^{2+} signals, predict their point of origin and make precise interpretation on how these signals regulate different cellular processes. Ca^{2+} sensors are molecules that can form selective and reversible complexes with Ca^{2+} ions and, most importantly, the physicochemical characteristics of the free and bound form are sufficiently different to enable measurement of the relative concentrations. Ca^{2+} -measuring toolkit comprises of synthetic (or chemical) and protein

(genetic)-based fluorescent probes. The application of individual probes or a combination of chemical probe with genetic targeting based probes has indeed expanded available options for measuring local Ca^{2+} events in living cells.

1.9.1 Synthetic Ca^{2+} probes

A number of synthetic fluorescent probes is available and can be loaded in live cells and follow intracellular Ca^{2+} dynamics in real time. The popular synthetic probes used for Ca^{2+} measurements include; quin-2, fura-2, fluo-3, fluo-4, indo-1, and new generation probes. These probes are polycarboxylate-based indicators, originally introduced by R.Y. Tsien (Tsien, 1980), Nobel prize laureate in Chemistry, and based on EGTA Ca^{2+} -chelator structure. For example in BAPTA, a prototype fluorescent polycarboxylate dye, the two methylene groups of EGTA have been replaced by two benzene rings to enable it to function as a chromophore. The conformational change caused by Ca^{2+} binding to the carboxyl groups is transmitted to the chromophore and results in changes in the excitation and/or emission properties of the dye. BAPTA absorbs light in the ultraviolet (UV) spectrum thus could not directly be used as intracellular Ca^{2+} indicator, but its derivative quin-2 became immediately popular. All synthetic Ca^{2+} probes operate under the principal that binding of Ca^{2+} on the dye induces conformational changes, consequently leading to a change in its spectral emission and/or excitation properties (Rudolf et al., 2003). Synthetic probes are classified as, either ratiometric or non-ratiometric.

The commonly used ratiometric dyes are fura-2 and indo-1. The working principle of ratiometric dyes relies on the fact that their excitation or emission spectrum changes depending on the free Ca^{2+} concentration. The excitation spectrum for a ratiometric dye change depending on whether it is or not bound to Ca^{2+} . The relative approximate Ca^{2+} concentration measured as the ratio between the two fluorescence intensity values obtained at the two different wavelengths. Determining the ratio is advantageous as it allows correction of errors that are likely to be due to unequal dye

loading, bleaching or focal plane shift in the cause of an experiment (Rudolf et al., 2003).

The commonly used non-ratiometric dyes such as fluo dyes and rhod dyes rely on single excitation. It is possible to use them in the visible range. Ca^{2+} concentration is thus determined as relative increase in the fluorescence intensity upon elevation of free Ca^{2+} concentration. The new generation dyes such as Ca^{2+} green, Ca^{2+} orange and Ca^{2+} crimson indicators are also available and have widely been used.

1.9.2 Protein based Ca^{2+} probes

Protein based Ca^{2+} probes also called genetically encoded indicators are a subset of fluorescent indicators that have the advantage of monitoring the dynamics of Ca^{2+} in specific subcellular locations (Tsien, 1999). These probes are generally defined as optical sensors produced by translation of a nucleotide sequence, and they include a fluorescent protein moiety and an element of response to Ca^{2+} . As it is the case for synthetic Ca^{2+} dyes, the binding of Ca^{2+} leads to a change in their optical properties. Depending on these latter, the genetically encoded Ca^{2+} indicators fall in two major groups namely: (i) photoproteins, such as aequorin-based probes, (ii) green fluorescent protein (GFP) based probes.

i) Aequorin based probes

The majority of photoproteins are from the bioluminescent molecule aequorin, a Ca^{2+} -sensitive photoprotein derived from a marine organism, the jellyfish *Aequorea victoria*. The basic molecular structure of aequorin consists of an apoprotein (molecular weight ~ 21 kDa) and a hydrophobic prosthetic group, coelenterazine (molecular weight ~ 400 Da). The sequence of the polypeptide includes three high-affinity binding sites for Ca^{2+} . The binding of Ca^{2+} to aequorin results in the breaking of the covalent bond between the apoprotein and the prosthetic group, a reaction associated with the emission

of a photon. The emitted photons through special calibration extrapolate into absolute $[Ca^{2+}]$ using special optical instruments.

It is worth noting that the intensity and amount of emitted largely depend on $[Ca^{2+}]$ to which the photoprotein is exposed. It is for the same reason that aequorin based probes are mainly used for population studies and not individual cells since the amount of photons emitted by a single cell is very low for detection. Early applications of aequorin for Ca^{2+} imaging in living cells, was carried out by microinjection of purified photoprotein as the only possible and practical approach for introducing it into living cells. However, advances in a rapidly evolving field of molecular biology made it possible for cloning of its cDNA. Indeed the cloning of its cDNA has also allowed its wide application and expression in many cell types and selective targeting to different subcellular compartments such as the cytosol, ER, mitochondria, Golgi apparatus and plasma membrane, by insertion of specific signal sequences (Rizzuto et al., 1994; Rudolf et al., 2003).

ii) GFP based probes

GFP based Ca^{2+} probes use calmodulin (CaM) as a molecular switch, which changes its conformation on the binding of Ca^{2+} . Usually CaM, which is the element of response to Ca^{2+} , inserted into a single fluorescent protein or is sandwiched between two fluorescent proteins, modulates the state of protonation of its chromophore (Romoser et al., 1997). The conformation changes that occur in the GFP based probes due to binding of Ca^{2+} alter the fluorescence properties of the GFP moieties and are used to calculate the dynamics of $[Ca^{2+}]$. The most commonly used GFP based Ca^{2+} probes include cameleons, camgaroos, and pericams (Rudolf et al., 2003).

For the cameleon probes, the CaM and the CaM-binding peptide M13 are fused together between the cyan fluorescence protein (CFP) and the yellow fluorescence protein (YFP). In this regard, a Ca^{2+} -induced interaction between CaM and M13, allows

an increase in the efficiency of energy transfer by resonance fluorescence (FRET) between the two GFP moieties.

FRET is an important tool for investigating a variety of biological phenomena that produce changes in molecular proximity. It is usually defined as non-radiative energy transfer between a donor chromophore and an acceptor chromophore when their emission (for donor) and excitation (for acceptor) spectra overlap. The pre-requisite for FRET to occur is the close proximity between the two molecules, donor and acceptor (2-7 nm) and their ideal relative orientation. With reference to cameleon probes, without FRET (low $[Ca^{2+}]$) the excitation and emission wavelengths for CFP are usually 430 nm and 480 nm respectively, while YFP remains unaffected. Following $[Ca^{2+}]$ increases and the conformational change due to CaM, CFP and YFP are brought together and excited CFP will transfer its energy to YFP that usually emits at 535 nm (figure 14). The conformational change caused by a rise in $[Ca^{2+}]$ can therefore be observed both as an increase in YFP (535 nm) emission and at the same time as a decrease in CFP (480 nm) emission. In order to get a reliable readout, the two signals are compared by obtaining a ratio between F_{535}/F_{480} , a rise in $[Ca^{2+}]$ will lead to a magnified increase in F_{535}/F_{480} ratio and viceversa for a decrease in $[Ca^{2+}]$. Since the discovery of cameleon probes, different recombinant chimera targeted to several cell compartments are available and efficiently used to monitor, Ca^{2+} dynamics at the single cell level (Rudolf et al., 2003).

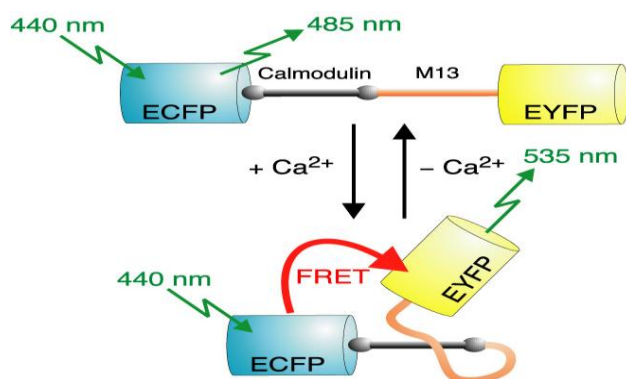


Figure 14: Schematic representation of the "Cameleon YC 2.1" construct and the principle of Ca^{2+} detection by FRET. Adopted and modified from (Fiala and Spall, 2003).

1.10 Fura-2 measurement of cytosolic free Ca^{2+} in living cells

Fura-2 is a ratiometric Ca^{2+} dye whose excitation or emission spectrum changes according to the free $[\text{Ca}^{2+}]$ in the cell (Grynkiewicz et al., 1985; Tsien, 1999) as explained above. Molecular Probes® introduced fura-2 as commercial Ca^{2+} imaging dye in 1985 and since then a number of modifications have taken place to improve the efficiency of this type of Ca^{2+} dyes. Indeed, fura-2 has made a substantial contribution towards the understanding of different aspects of Ca^{2+} signalling. With respect to the molecular structure, fura-2 is a polycarboxylate-based indicator, based on the EGTA Ca^{2+} -chelator structure with four COOH-groups to bind Ca^{2+} (Figure 15 A). This probe operate under the principal that the binding of Ca^{2+} on the dye induces conformational changes, consequently leading to a change in its spectral excitation properties (Rudolf et al., 2003).

Fura-2-acetoxymethyl ester, often abbreviated as fura-2/AM, is a membrane-permeable derivative made from modification of fura-2 by addition of the AM ester moiety. The AM esters have relatively low water solubility, to facilitate the loading of cells with fura-2/AM, pluronic; a mild detergent serves as a dispersing agent. It is worth noting that fura-2/AM complex itself does not bind free Ca^{2+} , but endogenous esterase hydrolyzed it to fura-2 once the dye is inside the cells. The use of appropriate amount of AM esters minimizes accumulation of the lipophilic AM esters in the cytoplasm, and therefore reduces the amount of formaldehyde generated as one of the by-product from their hydrolysis. Furthermore, the rate of hydrolysis of the AM esters varies in different cell types. Some cells hydrolyze the AM esters very slowly or show variable loading. Therefore, use of excessive dye as a means to maximize the loading is not always advisable as it may cause harm than good to the cells due to the difficulties in the clearance of unhydrolyzed AM esters as well as formaldehyde. Formaldehyde trapped in the cell cause glycolytic block through functional blockade of the glyceraldehyde-3-phosphate dehydrogenase by NAD depletion and thus leading to irreversible reduction in ATP production (García-Sancho, 1985). Furthermore, given that fura-2 is accumulated within the cells (up to 100 times) and works as a Ca^{2+} buffer, it is always advisable to

use the minimum concentration of fura-2/AM whenever possible to obtain an adequate signal: typically as low as 0.5 μM and rarely above 5 μM .

The excitation spectrum of fura-2 changes depending on concentration of free Ca^{2+} . Fura-2/AM has an emission peak at 510 nm and changes its excitation peak from 340 nm to 380 nm in response to Ca^{2+} binding (see figure 15B). The excitation peak usually shifts from 380 nm for Ca^{2+} free condition to 340 nm for the Ca^{2+} saturated form. When there is a Ca^{2+} free dependent change in the wavelength of maximal emission or excitation, the Ca^{2+} concentration can be determined from a ratio of the fluorescence intensities acquired at the two distinct wavelengths (Rudolf et al., 2003).

The K_d of Fura-2 for Ca^{2+} is approximately 135 nM (in Mg^{2+} -free medium) and ~224 nM (in 1mM Mg^{2+} medium) and is highly dependent on pH, temperature, ionic strength and viscosity of the cytosol, thus great care should be taken when non-standard conditions are used (Grynkiewicz et al., 1985). This K_d value highly correlates with the free $[\text{Ca}^{2+}]_{\text{cyt}}$ of different cells, which is also in the nanomolar range, mostly between 100 to 200 nM in the resting state (Pozzan et al., 1994; Berridge et al., 2000). At low concentrations of the indicator, the 340/380 nm excitation ratio for fura-2 allows accurate measurements of the intracellular Ca^{2+} dynamics. However, the accuracy of measurements of the $[\text{Ca}^{2+}]_{\text{cyt}}$ tend to be reduced as it rises above 1 μM .

Determining the intracellular Ca^{2+} dynamics by computing the ratio between the excitation peak at 340 nm and 380 nm in response to Ca^{2+} binding, considerably minimizes measurement errors. In most cases, errors in fluorescence measurement are likely to occur due to the effects of uneven dye loading, leakage and photo bleaching, problems associated with changes in cells thickness during the experiment, as well as certain changes in the detector sensitivity. Another advantage of using fura-2/AM is that it often allows long imaging acquisitions (up to one-two hours) without a significant loss of fluorescence resulting from either dye leakage or bleaching. Furthermore, because fura-2 is brighter than quin-2, the prototype of these dyes, it allows to carry out measurements at intracellular concentrations of the dye low enough and unlikely to cause dramatic Ca^{2+} buffering or damping of Ca^{2+} transients. However, it is worthy note

that the Ca^{2+} buffering is still a relevant aspect and high if compared to the genetically encoded probes.

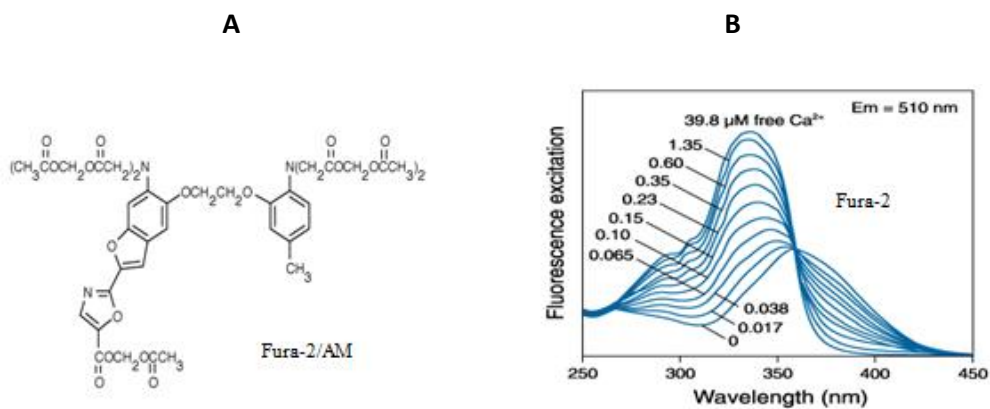


Figure 15: *Fura-2/AM*: **(A)** Chemical structure of fura-2/AM (note the four COOH-groups typical of the EGTA Ca^{2+} -chelator structure important for Ca^{2+} -binding. **(B)** Fluorescence excitation spectrum of Fura-2 (recorded at 510 nm emission wavelength) in solutions containing zero to 39.8 μM free Ca^{2+} . Adopted and modified from (<http://probes.invitrogen.com/media/pis/mp01200.pdf>).

AIMS OF THE PROJECT

The present work started from a previous project in the laboratory showing a strong reduction in intracellular Ca^{2+} store content. The observations were made in different model systems; ranging from fibroblasts from patients bearing FAD linked PS2 mutations, different cell lines (SH-SY5Y cells, HeLa, wt and double knock-out mouse embryonic fibroblasts) and rat cortical neurons transiently-expressing FAD linked PS2 mutants, employing both fura-2 and ER-targeted aequorin Ca^{2+} probes (Giacomello et al., 2005; Zatti et al., 2006; Brunello et al., 2009). Generally, transient transfection of mutated proteins or stably expressing cell clones are the most commonly used approaches for defining the molecular mechanism of disease-associated proteins.

In this work, we took advantage of two lines of tg mice expressing FAD linked PS2 alone or together with APP mutant, in order to investigate in a more physiological environment the functional effects of PS2 mutations on Ca^{2+} homeostasis. We focused our attention on Ca^{2+} dysregulation in cortical neurons from tg AD mouse models based on mutant PS2, i.e. the line PS2.30H homozygous for human PS2-N141I and the line B6.152H double homozygous for human PS2-N141I and human APP_{swe} K670N, M671L both in the background strain C57BL/6J (Richards et al., 2003; Ozmen et al., 2009).

The second part of this study focused on the role of A β 42 oligomers in intracellular Ca^{2+} dynamics. Recent data from both AD mouse models and in human subjects, suggest a strong correlation between levels of A β oligomers and functional impairment as compared to either A β plaque deposition or total A β monomer concentration. Although the underlying mechanism through which A β 42 oligomers cause neurotoxicity is still vague, a body of evidence suggests that, they also cause Ca^{2+} dysregulation (Demuro et al., 2005; Du et al., 2008; Sanz-Blasco et al., 2008). The consequence of Ca^{2+} dysregulation by A β oligomers include; synaptic dysfunction and impaired memory function. In this study, we also investigated the role of soluble A β 42

oligomers in AD and their effect on intracellular Ca^{2+} homeostasis in wt cortical neurons.

The aims of the work described here were:

- A) To characterize the Ca^{2+} dynamics of cortical neurons obtained as primary cultures from wt, single (PS2-N141I) and double (APP/PS2-N141I) tg mouse models of AD, with respect to:
 - i) various depolarizing stimuli
 - ii) Ca^{2+} release from IP3 sensitive stores, as assayed by IP3 generating agonists
 - iii) Ca^{2+} release from ryanodine sensitive stores, as assayed by caffeine
 - iv) the total store Ca^{2+} content, as assayed by Ca^{2+} ionophores

- B) To investigate on the possible mechanism(s) by which PS2-N141I mutations affect the intracellular Ca^{2+} dynamics in the cortical neurons

- C) To investigate on the possible patho-physiological implication of the alteration in intracellular stores Ca^{2+} dynamics in tg neurons.

- D) To carry out assays for $\text{A}\beta_{40/42}$ production in the tg cortical neurons and their implication on intracellular Ca^{2+} store content.

- E) To study the role of $\text{A}\beta_{42}$ oligomers on intracellular Ca^{2+} store dynamics. Do they affect ER Ca^{2+} content and/or release?

MATERIALS AND METHODS

3.1 Chemicals and reagents

Neurobasal medium (No.21103), Minimum Essential Medium 32360-026 1x (Gibco® MEM), DMEM-Dulbecco's Modified Eagle Medium 12491-015 (Gibco® DMEM), RPMI 1640, N2, B27 supplement, trypsin, L-glutamine, penicilin, streptomycin, neomycin, fura-2/AM, pluronics, sera, lipofectamine™2000, and hoechst (33342, trihydrochloride, trihydrate) were purchased from Invitrogen (Carlsbad CA, USA). Ionomycin was from Calbiochem (Merck KGaA; Darmstadt, Germany). The synthetic Aβ1-42 peptide was from AnaSpec, Inc. (Fremont, USA). Poly-L-lysine (P-2676), cytosine arabinoside (AraC), trypsin, trypsin inhibitor type-II-soybean, deoxyribonuclease I (DNase I), bovine serum albumin (BSA, A9418), carbachol (carbamylcholine chloride), S-3, 5-dihydroxyphenylglycine (DHPG), caffeine (1, 3, 7-trimethylxanthine), 1, 1, 1, 3, 3, 3-hexafluoro-2-isopropanol (HFIP), and other reagents were purchased from Sigma Chemical Co. (St. Louis, MO, USA), unless otherwise stated.

3.2 Animals

3.2.1 Tg mouse lines

The tg AD mouse models used were: the line PS2.30H homozygous for human PS2-N141I and the line B6.152H, double homozygous for human PS2-N141I and human APP swedish Generation and characterization of both lines, here by referred simply as PS2 (or single tg) and PS2APP (or double tg) respectively, have been described previously (Richard et al., 2003; Ozmen et al., 2009). Both tg mouse lines were kindly donated by Dr. Lawrence Ozmen (La ROCHE, Basel, Switzerland). The C57BL/6J mice used as control background strain were from Charles River Lion. The mice were fed on a standard laboratory chow diet and clean tap water ad libitum. The

Interdepartmental Centre of Experimental Research on Laboratory Animals (CEASA), of the University of Padova, approved all experimental procedures (Prot.N. 56880). Handling of animals was in accordance to the directive 2010/63/EU of the European parliament on the protection of animals used for scientific purposes.

3.3 Primary neuronal culture

3.3.1 Coating of glass coverslips

Poly-L-lysine was dissolved in phosphate buffered saline (PBS), to a final concentration of 100 µg /ml. The filter-sterilized poly-L-lysine solution was applied on glass coverslips of 15 mm diameter on 12-well cell culture multiwell plates or 13 mm glass coverslips in 24-well cell culture multiwall plates (BD Falcon™). The coverslips were incubated in a CO₂ (5%, 37°C) incubator for two to three hours and then were washed four times with sterile PBS solution.

3.3.2 Preparation of primary mouse neuronal cultures

A single newborn mouse (postnatal day zero to one), was killed by decapitation with a scissor. The skull was opened and the brain removed. After the removal of the olfactory bulbs, then the two cerebral hemispheres separated by making an incision along the midline and then cortices from the rest of brain and cleaned by removing all the meninges. The cells from the neonatal cortices were dissociated in trypsin (0.8mg/ml) for 10 minutes at 37°C while stirring but avoiding bubbles and aggregates formation. Trypsin inhibitor (6.3µg/ml) plus DNase I (40µg/ml) stopped typsin digestion. The cortical tissues were gently triturated eight fold with a polished Pasteur pipette with a wide opening to dissociate larger aggregates. After allowing the aggregates, which were still present in the suspension to sediment for 10 minutes, then supernatants collected in solution with sterile Krebs solution 10X, 3% BSA, 0.62mM MgSO₄ and 100µM CaCl₂.

3.3.4 Seeding of cortical neurons

Well-resuspended cells were seeded on poly-L-lysine coated coverslips glass coverslips at a density of 0.6×10^6 cells per well on 15mm diameter coverslips in 12 wells, cell culture multiwell plate or 0.3×10^6 per well on 13mm diameter coverslips in 24 wells cell culture multiwell plate. The growth medium consisted of MEM Gibco 32360-026 supplemented with: glucose (20mM), L-glutamate (0.5mM), N2 supplement (1%), B27 supplement (0.5%), biotin (0.875mg/L), pyruvic acid (1mM), penicillin (25 μ g/ml), streptomycin (25 μ g/ml), neomycin (50 μ g/ml) and 10% horse serum (HS). After 24hrs of plating, the growth medium was replaced with serum free Neurobasal[®] medium 1X, supplemented with: 2% (v/v) B-27 and 2mM L-glutamine. Every after 4 days of culture, 200 μ l of fresh medium were added in every well. The cultures were maintained in incubator at 37°C in a humidified atmosphere of 5% CO₂/ 95% air for 10-12 days. Under these conditions, glial growth is less than 10%.

3.4 Cell lines

SH-SY5Y cells were maintained in DMEM supplemented with 10% fetal calf serum (FCS) containing 0.1% penicillin (100 U/ml) and streptomycin (100 μ g/ml), and 1% L-glutamine. PC12 cells were maintained in RPMI 1640 medium supplemented with 10% HS, 5% FCS, 0.1% penicillin (100 U/ml) and streptomycin (100 μ g/ml), and 2 mM L-glutamine. Both cell types were maintained in the incubator at 37°C and 5% CO₂/ 95% air.

3.5 Cell line and neuron transfection

For aequorin (AEQ) experiments, SH-SY5Y cells were seeded on 13 mm diameter coverslips and allowed to grow to 50% confluence. The cells were transfected by means of Lipofectamine[™]2000 using 1.5 μ g of DNA (1 μ g PS2-cDNA or void vector plus 0.5 μ g Aeq cDNA). Briefly, the cDNA to Lipofectamine mixture ratio 1:2.

i.e. 1.5 μg of DNA mixed with 3 μl of lipofectamine was used. Intracellular Ca^{2+} measurements were carried out 24 hours after transfection by means of the Aeq technique as previously described (Brini et al., 1995).

3.6 Preparation of amyloid- β ($\text{A}\beta$) peptide solutions and treatment protocols

3.6.1 Fresh and $\text{A}\beta_{42}$ oligomers

PREPARATION: 1.0 mg of synthetic $\text{A}\beta$ 1-42 peptide (Anaspec) was dissolved in 400 μl of 1, 1, 1, 3, 3, 3-hexafluoro-2-isopropanol (HFIP) at RT for 10-20 minutes to a final concentration of 200 μM , and stored as 10-20 μl aliquots at -80°C until use. To prepare $\text{A}\beta_{42}$ monomers and oligomers, the HFIP was carefully removed by air pipeting several times on the wall of the tube. The dried HFIP film was then dissolved in double distilled water to the final concentration of 50 μM . The solution used immediately contains only monomers whereas when left at RT for 24-48 hrs it contained soluble oligomers of different molecular weights, as checked by SDS-PAGE (see figure 15A). Samples of these preparations were loaded without boiling (2 $\mu\text{g}/\text{lane}$) on a 10-18% Tris-Tricine polyacrylamide gel and visualized by silver staining.

USE: monomers or oligomers were used at 0.5 μM final concentration either acutely or during the loading period with fura-2 (40 min at 37°C plus 20 min at RT).

3.7 $\text{A}\beta_{42}$ and $\text{A}\beta_{40}$ assay.

The human/rat β -amyloid (40) ELISA kit Wako II and the human/rat β -amyloid (42) ELISA kit high sensitive (WAKO, Germany) were used. The total soluble and insoluble fractions of $\text{A}\beta$ were extracted by the formic acid procedure as described (Borchelt et al. 1996). Brain cortices from 2 week wt and tg mice were individually removed from one hemisphere (about 100 mg), quickly transferred in pre-weighed round bottom eppendorf tubes, snap-frozen in liquid nitrogen and stored at -80°C until use. Upon thawing, each eppendorf was weighed immediately to determine the weight of

each hemi-brain. The tissue was cut with scissors and homogenized with a pipette tip and 1 ml syringe in ice-cold Homogenizing Buffer (Tris HCl 50 mM, NaCl 150 mM, DTT 1 mM, NaF 10 mM with protease and phosphatase inhibitors at 4 ul/mg of wet tissue). Equal volumes were spun at 175000xg for 30 min at 4°C = 50000 rpm. The supernatants containing the salt soluble A β were stocked at -80°C.

Formic acid (70% in water) was added to pellets in an amount corresponding to half of the volume used in the first centrifugation; after mixing, the solution was incubated for 30 min at 4°C, bath sonicated at 4 °C for 20 min; rotated 2h at 4°C and finally centrifuged as above. Aliquots were frozen -80 °C until assayed. Before the ELISA measurement, each aliquot was buffered by dilution (1:20) in Tris Base 1M/NaOH 0.1M pH 7-8 containing 0.025% phenol red.

3.8 Ca²⁺ imaging by fura-2

For Ca²⁺ imaging, cells were loaded with fura-2/AM, which diffuses across the cell membrane and is de-esterified by cellular esterase to yield fura-2 free acid. Neuronal cultures, seeded on coverslips, were loaded in the growth medium whereas the cultured cells were loaded in modified Krebs–Ringer buffer (mKRB, in mM: 140 NaCl, 2.8 KCl, 1 MgCl₂, 2 CaCl₂, 10 HEPES, 11 glucose, pH 7.4 at 37°C). Pluronic 0.02% (F-127, Sigma No. P2443) and sulfinpyrazone (200 μ M) were used to facilitate the loading of cells with fura-2/AM and prevent dye leakage, respectively. The final concentrations of fura-2/AM were 1 μ M and 4 μ M for primary cortical neurons and cell lines respectively.

The cells were incubated for 40 minutes at 37°C and 20 minutes at RT. Each coverslip was then washed and maintained in modified Krebs–Ringer buffer (mKRB, in mM: 140 NaCl, 2.8 KCl, 1 MgCl₂, 2 CaCl₂, 10 HEPES, 11 glucose, pH 7.4 at RT) and finally mounted in the perfusion chamber RC-20H, (Warner Instruments) that forms a sandwich with a plastic open round bath recording chamber (76 \times 1 volume). To secure the coverslip on the imaging chamber we used vacuum grease. The two tubes at both ends of the chamber allowed for perfusion of solutions through out the coverslip. The

input line consists of a narrow tube connected to a syringe with perfusion solution (driven by gravity), while a suction line connected to a vacuum trap empties the output line. The cells were then processed for Ca^{2+} imaging analysis with a 20xUV permeable objective (Olympus Biosystems GmbH, Planegg, Germany) mounted on an Axiovert 100TV microscope (Zeiss, Germany). Alternating excitation wavelengths of 340 and 380 nm were obtained by a monochromator (Polychrome II) controlled by TILLvision software (TILL Photonics, Martinsried, Germany). A neutral density filter, UVND 0.6 (Chroma, US) was used in the excitation pathway to avoid sample damage. The emitted fluorescence was measured at 500-530 nm. Images were acquired every 5 seconds, with 150-300 ms exposure time unless stated otherwise at each wavelength, by a TILL-Imago camera controlled by the same software. The region of interest (ROI) adapted for image analysis corresponded to the entire soma; some 25-60 ROIs were selected for Ca^{2+} imaging. After background subtraction, the intensities of the emitted fluorescence were off-line ratioed (F340/F380) and averaged. Cytosolic Ca^{2+} changes were inferred by ratio changes, normalized to the resting values.

Unless otherwise stated, following 2 minutes perfusion in Ca^{2+} -containing mKRB, the neurons were exposed for 6 minutes to KCl (30mM) by equimolar substitution in the same medium. Intracellular Ca^{2+} stores were subsequently assayed in Ca^{2+} free mKRB containing EGTA (0.5mM). The size of intracellular Ca^{2+} pools was estimated by integrating the normalized ratio peaks above resting level. Data were analyzed by Origin7.5 SR5 (OriginLab Corporation, Northampton/Wellesley Hills, MA, USA). Traces are representative of 20-36 independent experiments. Averages are expressed as mean \pm S.E.M. (n= number of independent experiments; * $P < 0.05$, ** $P < 0.01$, *** $P < 0.001$, unpaired Student's t-test). Analysis of the differences between the categories was carried out by one-way ANOVA followed by Tukey HSD (Honestly Significantly Different) multiple comparison tests.

3.9 Ca²⁺ measurements by aequorin

SH-SY5Y cells seeded on 13 mm diameter coverslips were transfected with the cDNA coding for cyt- Aeq and mutant PS2, as described above (3.5). 24h upon transfection, the cells were incubated at 37°C with coelenterazine (5 μM) for 1-2 hr in a modified mKRB, in mM: 140 NaCl, 2.8 KCl, 2 MgCl₂, 1 CaCl₂, 10 HEPES, 11 glucose, pH 7.4) and then transferred to the recording apparatus. Briefly, the medium was carefully removed by aspiration and then the cells were washed twice in mKRB solution and transferred into the new plate containing 200 μl of mKRB solution containing 1 mM Ca²⁺ in each well. The experiments were carried out in mKRB medium containing in mM: 143 NaCl, 1 MgCl₂, 10 HEPES, pH 7.4 at 37°C). To determine the total amount of Ca²⁺ released from intracellular stores, bradykinin (100 nM) and cyclopiazonic acid (CPA, 20 μM) were added together with agonists after 2 minutes of perfusion in a Ca²⁺ free, EGTA (0.5 mM) containing mKRB medium. All the experiments were terminated by lysing the cells with 100 μM digitonin in hypotonic Ca²⁺ rich solution (10 mM CaCl₂ in water) to discharge the remaining unused Aeq pool. The photons emitted were collected by a low noise photomultiplier with an inbuilt amplifier –discriminator (Thorn-EMI photon board), stored on an IBM-compatible computer and offline calibrated into Ca²⁺ concentration values as described by Brini et al. (1995).

3.10 Protein extracts preparation and western blot analysis

Proteins were extracted in RIPA buffer (Sigma-Aldrich) from 10-12 DIV primary neuronal cultures from the three genotypes. Briefly, the neuronal cultures were washed twice with ice-cold phosphate-buffered saline (PBS) and harvested with RIPA buffer supplemented with protease inhibitors (Complete Mini™, Roche). Samples were analyzed in SDS-PAGE gel electrophoresis, electrophoretic transfer and western blotting; immunodetection was carried out with antibodies to APP (Zymed Laboratories Inc., USA); PS2 (Ab-2, Calbiochem, Merck, Darmstadt, Germany); PS2 (Epitomics, Inc., California, USA); IP₃R-1 (PA3-901A, ABR-Affinity BioReagents, Inc.); IP₃R-3

(610312, BD Biosciences Pharmingen); RyR-1 and -2 (Thermo Scientific, Meredian Road, Rockford IL 61105, USA); actin (A4700, Sigma-Aldrich). Incubation with appropriate secondary antibodies conjugated to HRP allowed band detection by ECL. The chemiluminescence reagent ECL (Amersham, GE Healthcare, UK Ltd Amersham Place Little Chalfont Buckinghamshire HP7 9NA England) was used to visualize the proteins. Densitometry was performed with ImageJ. Data presented as mean \pm S.E.M. of three independent samples ratioed against actin or total proteins (ponceau).

3.11 Neuronal survival assay

Primary cortical neurons were plated at the density of 0.3×10^6 per well on 13mm diameter coverslips in 24 well plate, as explained above. To improve loading of the intracellular Ca^{2+} stores at 10 DIV, we preloaded the stores by supplementing the culture medium with KCl and CaCl_2 to 10mM and 2mM final concentration respectively for 24 hours prior to survival assay. We employed a stimulus that mediates toxicity through Ca^{2+} release from ER, H_2O_2 (Pinton et al., 2001). The neurons were treated with H_2O_2 (10 and 20 μM) final concentration in presence or absence of DHPG (10 μM) for 24 hours.

We carried out Survival assay in primary neuronal cultures by terminal dUTP nick end labelling (TUNEL) assay (In Situ Death Detection kit, Fluorescein, Roche Diagnostics). After TUNEL labelling procedure, the coverslips were then mounted on microscope glass slides with mowiol, left to dry and apoptotic cells were observed by using an oil immersion 63X PlanApo 1.40 NA objective on a Leica DMIRE3 wide field inverted microscope equipped with a DC 500 digital camera (Leica). The acquisition software was FW4000 (Leica). Apoptotic nuclei identified according to manufacturer's instructions. At least 10 fields counted for each condition done in triplicate for at least three independent cultures.

3.12 Statistical analysis

Data were analysed Origin 7.5 SR5 (OriginLab Corporation, Northampton/Wellesley Hills, MA, USA). Averages are expressed as mean \pm S.E.M. (n= number of independent experiments; * P<0.05, ** P< 0.01, *** P<0.001, unpaired Student's t-test) or analysis of the differences between the categories carried out by one-way ANOVA followed by Tukey HSD (Honestly Significantly Different) multiple comparisons tests with a confidence interval of 95%.

RESULTS

The main part of this work focused at unraveling the functional effect of a FAD-linked PS2 mutation on intracellular Ca^{2+} homeostasis (**Result I**). For this purpose, we selected PS2-N141I as reference mutation since it is the only available AD mouse model based on mutant PS2. For this purpose, we investigated Ca^{2+} homeostasis in the model more relevant for AD patho-physiology, i.e. in cortical neurons from two lines of tg mice expressing PS2-N141I alone or together with the Swedish mutant APP (from here on simply referred as PS2 and PS2APP respectively). In this model, we used fura-2/AM technique for Ca^{2+} measurements, whereas the aequorin-based probe for Ca^{2+} imaging was employed for the initial part of the study involving the neuroblastoma cell line (SH-SY5Y). For cell death assay in primary neuronal cultures, terminal deoxynucleotidyl transferase dUTP nick end labelling (TUNEL) assay was carried out.

The second part of this study focused on investigating the effects of $\text{A}\beta_{42}$ oligomers on intracellular Ca^{2+} homeostasis in cell lines (the rat pheochromcytoma PC12) and wt cortical neurons (**Result II**).

Result I

4.1 Ca^{2+} Homeostasis in Primary Cortical Neuronal Cultures from Tg Mice

4.1.1 Ca^{2+} release induced by IP_3 -generating agonists in cells transiently transfected with the FAD linked PS2-N141I mutant

Previous studies have suggested that transient expression of FAD-linked PS2 mutants (M239I and T122R) reduces Ca^{2+} content of the intracellular stores (Giacomello et al., 2005; Zatti et al., 2006). These mutants can inhibit SERCA pump activity,

increase IP₃R and RyR activity, and modulate capacitative Ca²⁺ entry (Brunello et al., 2009). Before carrying out our analysis with tg mouse model based on the FAD-linked PS2-N141I, we first checked whether this PS2 mutation also exerts the same effect on Ca²⁺ homeostasis in a cell line model. We thus transiently over-expressed the PS2 mutants in the human neuroblastoma cell line SH-SY5Y and assessed Ca²⁺ release from the intracellular stores to confirm the previous findings. We analyzed the size of intracellular Ca²⁺ stores by the AEQ technique (see also material and method). In brief, the cells were transfected by means of LipofectamineTM2000 using 1.5 µg of DNA (1 µg PS2-cDNA or PcDNA3 (void vector) plus 0.5 µg of cytosolic targeted AEQ cDNA for 24 hours. Ca²⁺ release from intracellular stores was estimated by challenging the cells with the IP₃-generating agonist bradykinin (BK) (100 nM) plus cyclopiazonic acid (CPA) (20 µM) in Ca²⁺ free-EGTA (600 µM) containing mKRB medium.

The average delta peak and area under the curve for cytosolic Ca²⁺ in response to BK plus CPA were 2.17±0.15 µM and 62.30±4.98 (a.u.) (mean Δ±SEM, n = 11) respectively, in the SH-SY5Y cells transfected with void vector. Cells transiently expressing PS2 mutants (PS2-N141I or PS2-T122R) had significantly reduced Ca²⁺ release from the BK responsive intracellular stores as seen from reduced delta peak and delta peak area as compared to the control cells. The delta peak and area under the curve for cytosolic Ca²⁺ rise in response to BK plus CPA for the cells overexpressing PS2-N141I were 1.29±0.04 µM (p<0.0001) and 31.82±2.69 (a.u.) (p<0.0001) (mean Δ±SEM, n = 10) respectively, corresponding to 40.36% and 48.93% reduction respectively (figure 1A, B). For the cells over-expressing PS2-T122R, another FAD-linked mutant, the average delta peak and area under the curve for cytosolic Ca²⁺ rise in response to BK were 1.40±0.07 µM (p<0.0001) and 34.07±2.88 (a.u.) (p<0.0001) (mean Δ±SEM, n = 11) corresponding to 35.27% and 45.32% reduction respectively (figure 1A, B).

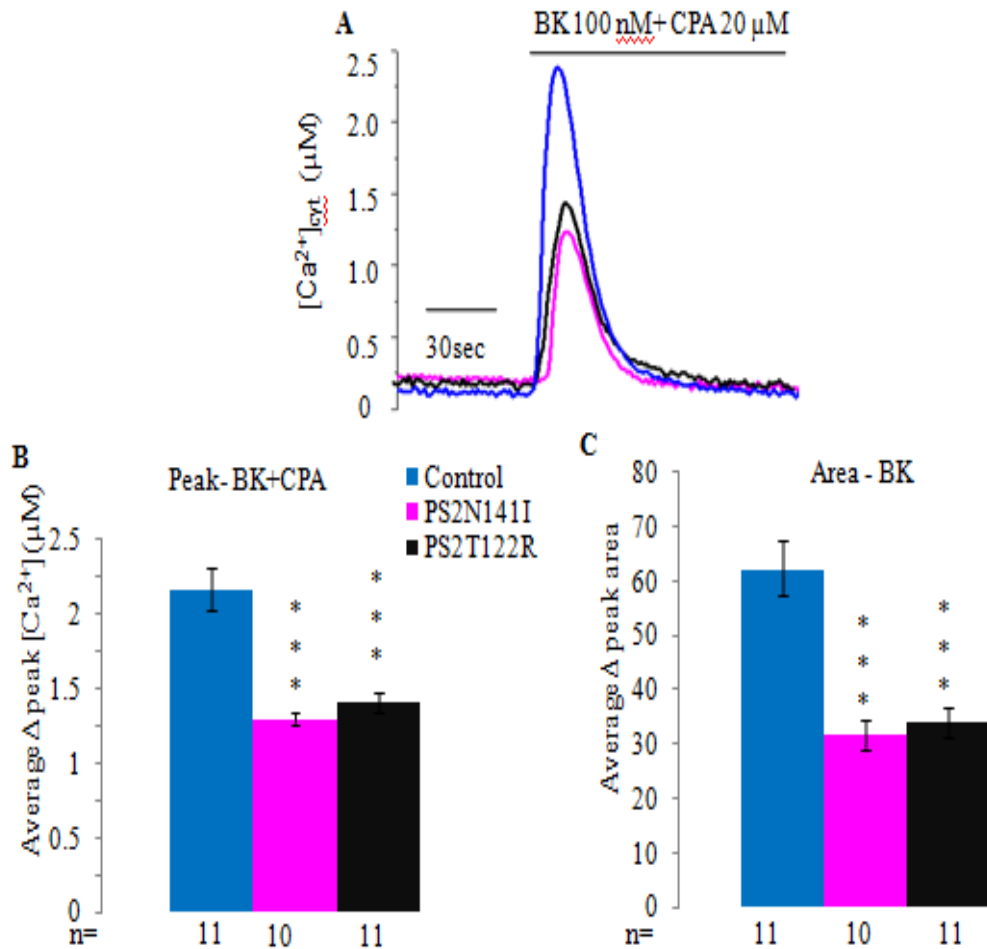


Figure 1: Reduced Ca²⁺ release in response to IP₃-generating agonist bradykinin (BK) plus cyclopiazonic acid (CPA) in cells overexpressing PS2 mutants. SH-SY5Y cells were transfected with the mutant PS2 (or the void vector) and cytosolic targeted AEQ cDNA for 24 hours. Ca²⁺ release from ER was estimated by challenging the cells with the IP₃ generating BK (100 nM) plus CPA (20 μM) in Ca²⁺ free-EGTA (600 μM) containing mKRB medium. (A) Representative trace of AEQ measurements for cytosolic Ca²⁺ rise in response to BK plus CPA in Ca²⁺ free, EGTA-containing medium, to discharge the intracellular Ca²⁺ stores. (B, C) Average peak and peak area respectively, measured above the baseline in response to BK plus CPA for control cells overexpressing void vector (blue bars) or PS2-N141I (magenta bars) or PS2-T122R (black bars). Data presented on bars are expressed as mean±S.E.M (n=number of independent experiments; Δ peak: F_{2, 29} =23.19; P<0.0001; Δ peak area: F_{2, 29} =21.04; P<0.0001, one-way ANOVA followed by Tukey HSD; * P< 0.05; ** P< 0.01; *** P< 0.001.

4.1.2 Expression levels of PS2 in wt and tg mice

Transient transfection of mutated proteins or stably transfected cell clones are the most commonly used approaches to start defining the molecular mechanism of disease-associated proteins. Both approaches however face two major criticisms: in the first case, the level of overexpression is usually very high (even 50-100 fold increase in protein levels). Secondly, the specificity of each clone (and/or adaptation phenomena to the over-expressed protein) may lead to erroneous interpretations of the results.

In the study presented here, we have taken advantage of the two available lines of tg mice expressing the FAD linked PS2-N141I alone or together with mutant APP, in order to investigate its effects on Ca^{2+} homeostasis in a more suitable environment. In particular we employed the single tg mouse line PS2.30H, homozygous for human PS2-N141I (referred as PS2), and the double tg mouse line B6.152H (also known as PS2APP), double homozygous for human PS2-N141I and the human Swedish mutant APP K670N, M671L (APP^{swe}), both in the background strain C57BL/6J. While PS2-N141I is ubiquitously expressed, being under the control of the prion protein promoter, the APP^{swe} mutant is expressed only by neurons and T lymphocytes, being under the control of the Thy1 promoter (Richards et al., 2003; Page et al., 2008; Ozmen et al., 2009).

The expression level of both PS2 was analyzed by Western blot analysis using cell extracts from primary neuronal cultures at 12 DIVs from wt, single or double tg mice (see Fig. 2). Proteins were extracted in RIPA buffer (Sigma-Aldrich) from 10-12 DIV primary neuronal cultures from the three genotypes. Samples were analyzed in 12 % SDS-PAGE gel electrophoresis. Compared to control (i.e wt mice), the amount of PS2 increased by about 50% in the two genotypes when considering both the C-terminal fragment and the full-length protein (FL) as detected by the same antibody.

Primary cortical neuron 10 DIV

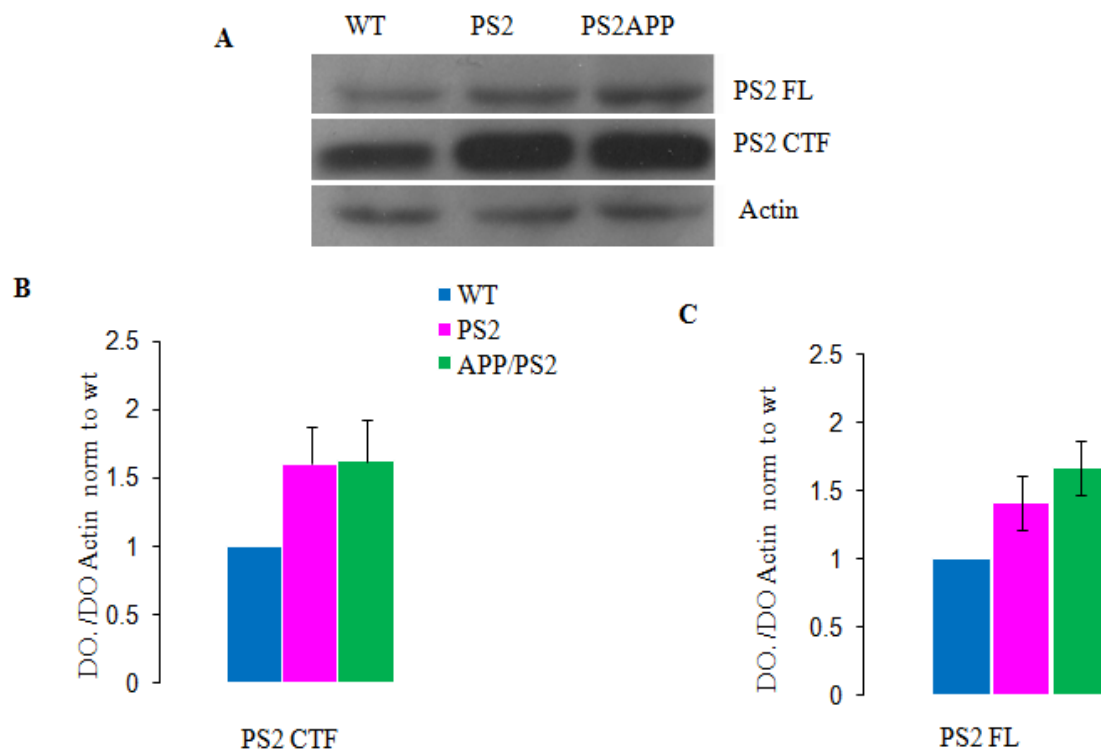


Figure 2: Western blot analysis for PS2 in primary neuronal cultures. Proteins were extracted in RIPA buffer (Sigma-Aldrich) from 10-12 DIV primary neuronal cultures from the three genotypes. Samples were analyzed in 12% SDS-PAGE gel electrophoresis. Immunodetection was carried out with the rabbit polyclonal anti-PS2 (Epitomics, Inc., California, USA) recognizing both human and mouse proteins. Incubation with appropriate secondary antibodies conjugated to HRP allowed band detection by ECL. (A), western blot analysis of PS2 levels expressed in primary neuronal culture extracts. (B), corresponding histogram of the densitometric analysis for CTF-PS2 expression in primary neuronal culture extracts. (C), corresponding histogram of the densitometric analysis for FL- PS2 expression in primary neuronal culture extracts. The bands were first normalized by actin levels, and then to wt values, Data are presented as mean±S.E.M of samples from three independent cultures, * P< 0.05, ** P<0.001, *** P<0001 (Student's t test).

4.1.3 Ca²⁺ release induced by IP₃-generating agonists is reduced in neurons from tg mice carrying PS2-N141I.

Since transient expression of different FAD-linked PS2 mutants as well as of the wt form reduces the Ca²⁺ content of intracellular stores (Giacomello et al., 2005; Zatti et al., 2006), we investigated this phenomenon in a more physio-pathological environment, a model closer and relevant to the disease. The functional effects of PS2 mutations in Ca²⁺ homeostasis were studied in neurons from wt, PS2 (line PS2.30H) and PS2APP (line B6.152H) mice, respectively single and double tg mice homozygous for huPS2-N141I and huAPP^{swe} K670N, M671L (Richard et al., 2003; Ozmen et al., 2009). Cytosolic Ca²⁺ changes were then investigated in cultured cortical neurons using the trappable fluorescent Ca²⁺ indicator fura-2.

Primary cortical neuronal cultures were prepared from postnatal day zero to one-day-old pups. The neuronal cultures were prepared and maintained in vitro for 24 hours with MEM gibco 32360-026 containing: glucose (20 mM), L-glutamate (0.5 mM), N2 supplement (1%), B27 supplement (0.5%), biotin (0.875 mg/L), pyruvic acid (1mM), penicillin (25 µg/ml), streptomycin (25 µg/ml), neomycin (50 µg/ml) and horse serum (10%) and then maintained in neurobasal medium supplemented with B27 (2%) and glutamine (2 mM) for the rest of the time (usually 11-12 DIV) (see also material and method for detailed protocol). When primary neuronal cultures were bathed at RT in a mKRB containing CaCl₂, (2mM), the [Ca²⁺]_{cyt} rises caused by Ca²⁺ release from intracellular stores were modest but were substantially augmented by filling them by a short exposure to high potassium chloride (KCl) (Smith et al, 2005; Zatti et al., 2006; Zhang et al., 2010) (figure 3A, B). The intracellular stores were thus loaded with Ca²⁺ by a 6 minutes exposure to KCl (30 mM) in the same isosmotic buffer. The resulting depolarization induces opening of VOCCs and rapid Ca²⁺ influx into the cortical neurons and filling of the ER Ca²⁺ stores.

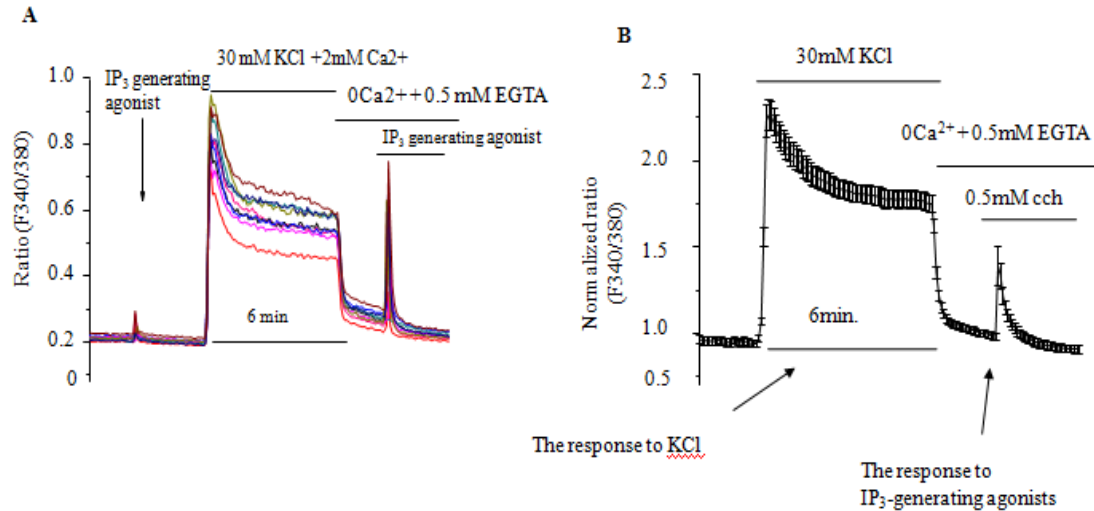


Figure 3: Loading of the intracellular Ca^{2+} stores by a short exposure to high potassium chloride (KCl). (A), Neurons (10-12 DIV) were perfused with Ca^{2+} (2 mM) in mKRB for 2 minutes, then exposed to carbachol (CCH, 0.5 mM) in a Ca^{2+} free, EGTA (0.5 mM)-containing medium to fully discharge the intracellular Ca^{2+} stores. Note a small number of cells responding to CCH. The same neurons subsequently exposed to KCl (30 mM) in Ca^{2+} in mKRB for 6 minutes and the exposed to CCH in a Ca^{2+} free, EGTA (0.5 mM)-containing medium to fully discharge the intracellular Ca^{2+} stores (F340/380 ratio representative traces). (B), Typical intracellular stores Ca^{2+} loading procedure used in all experiments.

Prior to accessing the store Ca^{2+} content, the neurons were perfused with Ca^{2+} free mKRB containing EGTA (0.5 mM) for 2 minutes to remove extracellular Ca^{2+} . Immediately, Ca^{2+} release from intracellular stores was estimated by challenging the neurons with carbachol (CCH, 0.5 mM) or (RS)-3, 5-dihydroxyphenylglycine (DHPG, 10 μM). Both CCH and DHPG activate G-protein coupled receptors leading to generation of IP_3 , which in turn binds to IP_3R and triggers Ca^{2+} release from intracellular stores into the cytosol. For presentation and statistical analysis, the ratios (F340/F380) were off-line averaged (30–60 cells) and normalized to the basal resting value (Normalized Ratio). Traces are representative of about 20-36 number of independent experiments (coverslips), corresponding to 3-12 cultures. The average delta peak (expressed as mean $\Delta \pm \text{SEM}$), was calculated as the difference between the peak height from its basal Ca^{2+} level.

Fig. 4A shows representative traces of the typical behaviour of neurons, at rest, upon depolarization with KCl and after challenging, in EGTA-containing medium, with the IP₃-generating agonist CCH. In most neurons, the resting Ca²⁺ concentration was stable with rare spontaneous Ca²⁺ spikes of short duration. The latter were completely abolished by removal of Ca²⁺ from the medium. Upon addition of KCl (30 mM) a rapid increase in [Ca²⁺]_{cyt} was observed that remained elevated well above the pre-stimulatory level until Ca²⁺ in the medium was removed by EGTA. No significant difference was observed between neurons from wt, PS2 or PS2APP mice in terms of the KCl induced peak and subsequent plateau, consistent with data present in (Zhang et al., 2010; Smith et al., 2005 (figure 4B,C)). Of note, no difference was also found in the absolute ratio values measured at resting, suggesting that up to 10-12 DIVs, tg cortical neurons fully control their resting Ca²⁺ values (see table 1).

Table 1: Average resting absolute ratio values

	WT	PS2	PS2APP
Ratio at rest			
(F340/F380)	0.17±0.01	0.17±0.003	0.16±0.003
N	20	20	20

Neurons (10-12 DIV) were perfused with mKRB containing Ca²⁺ (2 mM) for 2 minutes. No difference was found between wt and tg mice in the absolute ratio values measured in neurons at rest. Data are expressed as mean $\Delta \pm$ SEM (n=number of independent experiments).

The average delta peak and area under the curve for cytosolic Ca²⁺ in response to CCH were 0.37±0.02 and 7.68±0.45 (mean $\Delta \pm$ SEM, n = 36) respectively, in the wt cortical neurons (control). Interestingly, cortical neurons from both PS2 and PS2APP mice had significantly reduced Ca²⁺ release from the CCH responsive intracellular stores

as seen from reduced delta peak and delta peak area compared to the controls (figure 4D, E). For the neurons from mutant PS2 tg mice, the average delta peak and area under the curve for cytosolic Ca^{2+} rise were 0.18 ± 0.02 ($P < 0.0001$) and 5.24 ± 0.55 ($P < 0.0001$) (mean $\Delta \pm$ SEM, $n = 20$) respectively, corresponding to a 52.26% and 31.78% reduction in peak and area, respectively. On the other hand in the cortical neurons from PS2APP, the average delta peak and delta peak area for cytosolic Ca^{2+} were 0.19 ± 0.02 ($P < 0.0001$) and 3.93 ± 0.52 ($P < 0.0001$) (mean $\Delta \pm$ SEM, $n = 25$) respectively, corresponding to 48.03% and 48.81% respectively. Noteworthy only neurons responding to KCl and CCH were included in the calculation. In particular, the number of CCH responding cells was higher in wt neurons (89.40%) than in the PS2 and PS2APP neuronal cultures, being 68.82% and 67.83% respectively (figure 4F).

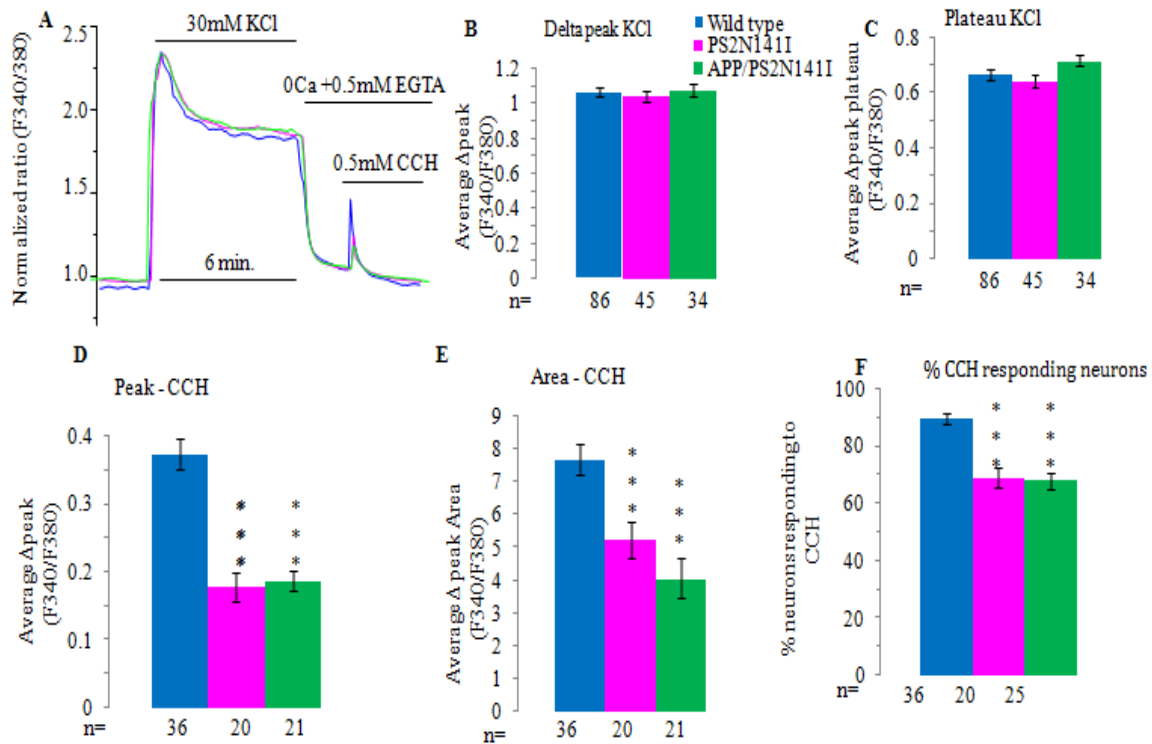


Figure 4: Reduced Ca^{2+} release in response to IP_3 -generating agonists in tg mice. Neurons (10-12 DIV) were perfused with mKRB containing Ca^{2+} (2 mM) for 2 minutes, then exposed to KCl (30 mM) in Ca^{2+} containing KRB in for 6 minutes and subsequently exposed to CCH (0.5 mM) in a Ca^{2+} free, EGTA (0.5

mM)-containing mKRB to discharge intracellular Ca^{2+} stores in neurons from wt and tg mice. **(A)**, Representative trace of average normalized ratio of fura-2 fluorescence for wt (blue) and PS2 (magenta) neurons. **(B, C)**, Bars represent the average peak and plateau measured after KCl addition, expressed as mean $\Delta \pm \text{SEM}$ (n=number of independent experiments). **(D, E)**, Average peak and peak area, in response to CCH (0.5 mM), expressed as mean $\Delta \pm \text{SEM}$ (n= number of independent experiments; Δ peak: $F_{2,74}=28.09$, $P<0.0001$; Δ peak area: $F_{2,74}=13.78$, $P<0.0001$, one-way ANOVA followed by Tukey HSD). **(F)** Percentage number of cells responding to CCH (expressed as % of KCl responding cells). * $P<0.05$, ** $P<0.01$, *** $P<0.001$.

Similar results were obtained when DHPG was used as a stimulus. The average delta peak and area under the curve for cytosolic Ca^{2+} were 0.31 ± 0.02 and 5.21 ± 0.64 (mean $\Delta \pm \text{SEM}$, n = 9) respectively, in the wt cortical neurons (control). Cortical neurons from both PS2 and PS2APP mice had significantly reduced Ca^{2+} release from the DHPG responsive intracellular stores as seen from reduced delta peak and delta peak area as compared to the wt neurons (figure 5B, C, D). For the neurons from PS2 mice, the average delta peak and area under the curve for cytosolic Ca^{2+} rise were 0.20 ± 0.01 ($P<0.0001$) and 3.30 ± 0.38 ($P<0.01$) (mean $\Delta \pm \text{SEM}$, n = 8) respectively, corresponding to a 34.1 % and 36.8% reduction in peak and area, respectively. In cortical neurons from PS2APP, the average delta peak and delta peak area for cytosolic Ca^{2+} rises were 0.16 ± 0.02 ($P<0.0001$) and 3.06 ± 0.43 ($P<0.01$) (mean $\Delta \pm \text{SEM}$, n = 12) respectively, corresponding to 49.5% and 41.2% respectively.

In contrast, addition of CCH (0.5 mM) or DHPG (10 μM) in Ca^{2+} free, EGTA-containing medium under resting, unstimulated conditions, was almost ineffective: in most neurons and resulted in much smaller changes in $[\text{Ca}^{2+}]_{\text{cyt}}$ (figure 5A).

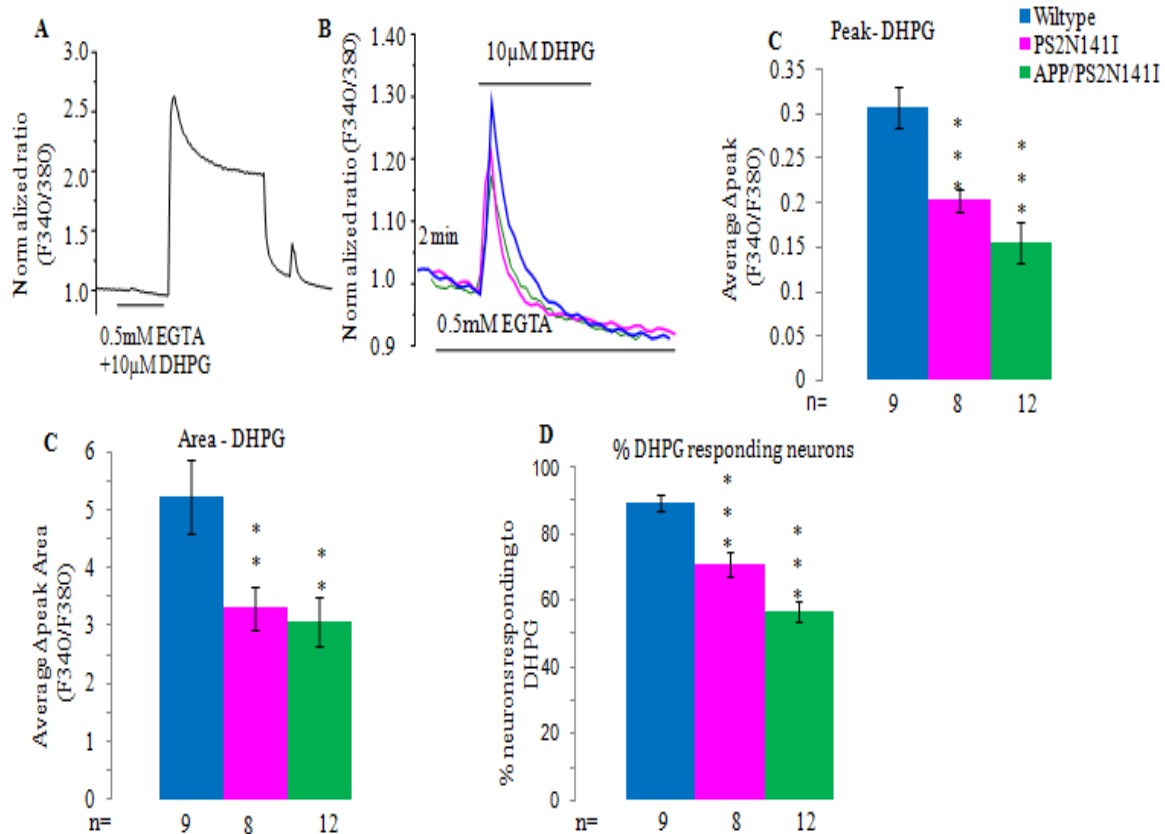


Figure 5: Reduced Ca^{2+} release in response to the IP_3 -generating agonist, DHPG, in tg mice. Cortical neurons (10-12 DIV) were perfused with mKRB containing Ca^{2+} (2 mM) for 2 minutes, then, the neurons were exposed to KCl (30 mM) in Ca^{2+} in mKRB for 6 minutes, before stimulation with DHPG (10 μ M) in a Ca^{2+} free, EGTA (0.5 mM)-containing mKRB to fully discharge the intracellular Ca^{2+} stores in both wt and tg mice. (A), Representative trace of fura-2 fluorescence ratio for cytosolic Ca^{2+} rise in response to DHPG (10 μ M) in a Ca^{2+} free, EGTA (0.5 mM)-containing medium, then KCl (30 mM), followed by DHPG (10 μ M) in Ca^{2+} free, EGTA (0.5 mM)-containing medium to fully discharge the intracellular Ca^{2+} stores (B), Representative traces (blue – wt; magenta-PS2; green – PS2APP) of fura-2 fluorescence ratio for cytosolic Ca^{2+} rise in response to DHPG (10 μ M). (C, D), Average peak and peak area respectively, measured above the baseline in response to DHPG (10 μ M) and expressed as mean \pm S.E.M (n=number of independent experiments; Δ peak: $F_{2,26} = 12.57$, $P < 0.0001$; Δ peak area: $F_{2,26} = 5.55$, $P < 0.01$, one-way ANOVA followed by Tukey HSD. (E), Percentage number of cells responding to DHPG (expressed as % out of KCl responding cells).

4.1.4 The total intracellular store Ca²⁺ content assayed by ionomycin is reduced in cortical neurons from tg mice

The reduced response to IP₃ generating agonists in tg mouse neurons can be explained as due to different plausible possibilities: It could be due to reduced IP₃ generation upon application of the agonists. Alternatively there could be reduced IP₃ receptor density/sensitivity or reduced Ca²⁺ content in the stores (or a combination of these mechanisms) (Zatti et al., 2004; Brunello et al., 2009; Cheung et al., 2008; 2010; Foskett, 2010). To evaluate the total content of intracellular Ca²⁺ stores, we measured the size of the ionomycin-sensitive Ca²⁺ pool in both wt and tg neurons. Ionomycin is a Ca²⁺ ionophore that facilitates Ca²⁺ transport across the majority of the the membranes and not only across ER membranes; the ionomycin-sensitive Ca²⁺ pool may come from neutral and mild acidic intracellular compartments, such as the Golgi apparatus, mitochondria and part of the constitutive vesicles (Fasolato et al. 1991). Therefore, the size of this pool was estimated from the cytosolic peak and the area under the curve obtained from fura-2 signal after exposing the neurons to ionomycin (1 μM) in Ca²⁺ free, EGTA-containing medium. The average delta peak and area under the curve for cytosolic Ca²⁺ rise in response to ionomycin were 0.65±0.03 and 23.0±1.35 (mean Δ±SEM, n = 16) respectively, in the wt cortical neurons. Interestingly, cortical neurons from PS2 and PS2APP mice had significantly reduced Ca²⁺ release from the stores (as shown in figure 6A-C). For the neurons from PS2 tg mice, the average delta peak and area under the curve for cytosolic Ca²⁺ were 0.42±0.02 (P<0.0001) and 16.53±91 (P<0.0001) (mean Δ±SEM, n = 14) respectively. On the other hand in the cortical neurons from PS2APP mice, the average delta peak and area under the curve for cytosolic Ca²⁺ were 0.47±0.03 (P<0.0001) and 17.86±0.90 (P<0.0001) (mean Δ±SEM, n = 12) respectively.

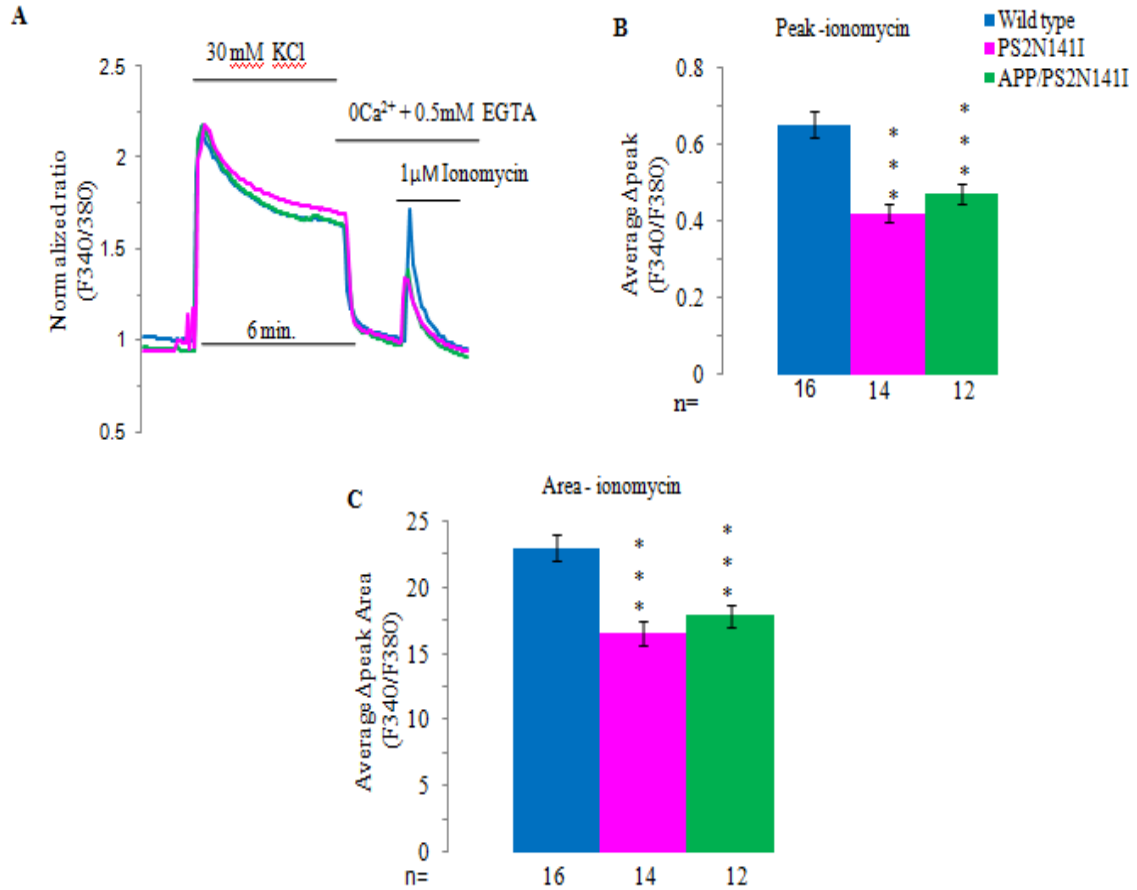


Figure 6: Reduced total Ca^{2+} content intracellular store in cortical neurons from *tg* mice. Cortical neurons (10-12 DIV) were perfused with mKRB containing Ca^{2+} (2 mM) in for 2 minutes, then exposed to KCl (30 mM) in the same medium for 6 minutes and then exposed to ionomycin (1 μ M) in a Ca^{2+} free, EGTA (0.5 mM)-containing mKRB to fully discharge intracellular Ca^{2+} stores in both wt and *tg* mice. (A), Representative traces (blue – wt; magenta-PS2; green – PS2APP) of fura-2 fluorescence ratio for cytosolic Ca^{2+} rise in response to KCl (30 mM), followed by ionomycin (1 μ M) in Ca^{2+} free, EGTA (0.5 mM)-containing medium to fully discharge the intracellular Ca^{2+} stores. (B, C), Average delta peak and area under the curve respectively, measured above the baseline in response to ionomycin and expressed as mean $\Delta \pm$ SEM (n= number of independent experiments; Δ peak: $F_{2, 34} = 12.10$; $P < 0.0001$; Δ peak area: $F_{2, 34} = 11.39$; $P < 0.0001$, one-way ANOVA followed by Tukey HSD.

4.1.5 Ca²⁺ release from the ryanodine-sensitive intracellular Ca²⁺ stores is increased in neurons from both tg mice

Ca²⁺ release from intracellular stores in neurons not only depends on IP₃R channels, but also on RyR channels. Certainly, a small amount of Ca²⁺ in the cytosol near RyR will cause it to release even more Ca²⁺, through CICR, resulting in even greater amplification of Ca²⁺ signals (Zucchi and Ronca-Testoni, 1997). Caffeine and ryanodine are commonly used pharmacological agonists for activating of RyR channels. Caffeine increases the receptors Ca²⁺ sensitivity of CICR. We therefore analyzed caffeine induced Ca²⁺ release from intracellular stores in both wt and tg mice neuronal cultures.

Figure 7 shows the response of both wt and tg neurons to caffeine (20mM). The average delta peak and area under the curve for cytosolic Ca²⁺ rise in response to caffeine were 0.14±0.01 and 1.90±0.23 (mean Δ±SEM, n = 15) respectively, in wt cortical neurons (control). The cortical neurons from both PS2 and PS2APP tg mice had modest but significant increased Ca²⁺ release (figure 7C, D). For the neurons from PS2, the average delta peak and area under the curve for cytosolic Ca²⁺ were 0.20±0.02 (P<0.01) and 3.72±0.55 (P<0.001) (mean Δ±SEM, n = 19) respectively. On the other hand in the cortical neurons from PS2APP, the average delta peak and delta peak area for cytosolic Ca²⁺ were 0.20±0.02 (p<0.01) and 3.34±0.30 (P<0.001) (mean Δ±SEM, n = 16) respectively. Of note, the caffeine-induced Ca²⁺ release was completely inhibited by pre-incubation with ryanodine 20 μM (figure 7A, B).

When a comparison of pool sizes released by different stimuli used in this study was made, both the IP₃- and caffeine-sensitive Ca²⁺ pools were smaller than the total pool released by ionomycin and, between these latter, the pool released by caffeine was the smallest (figure 8).

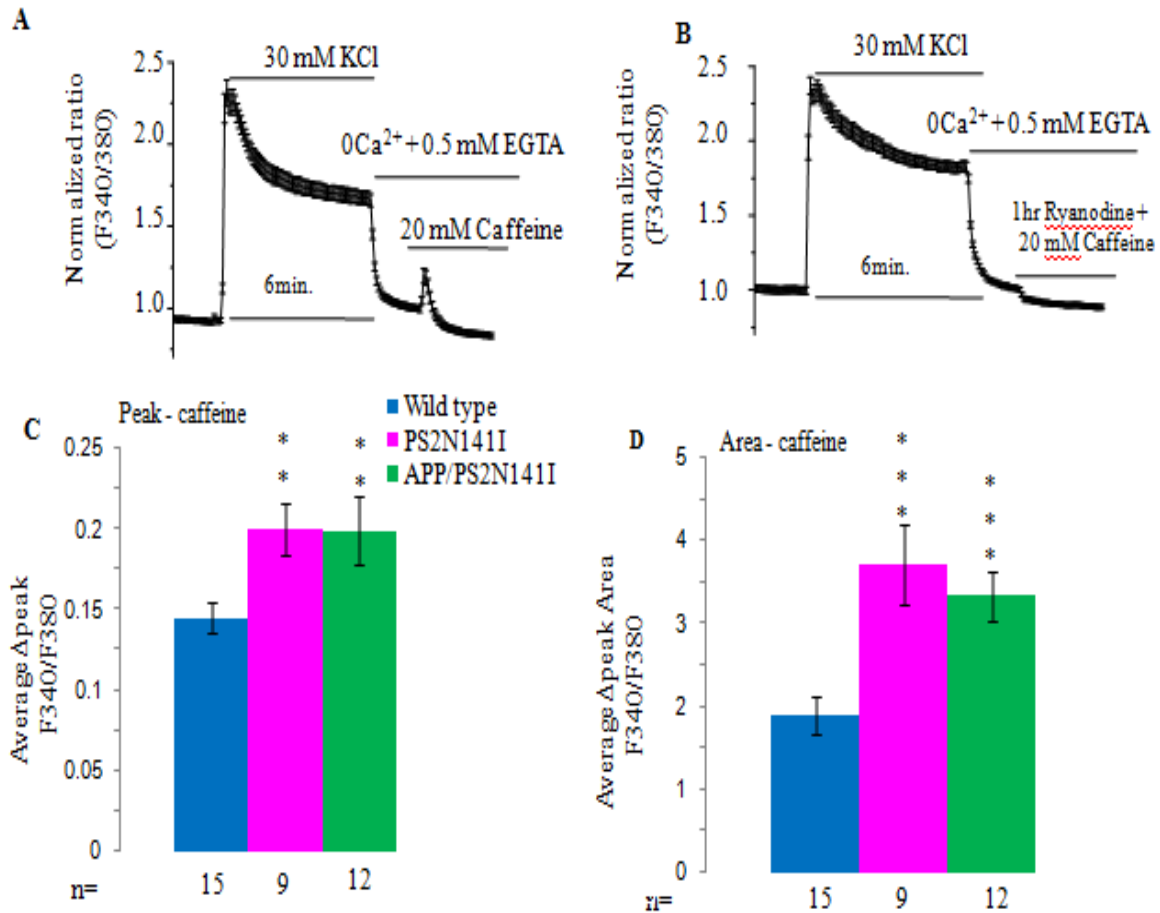


Figure 7: Ca^{2+} release induced by caffeine is increased in cortical neurons from *tg* mice. Cortical neurons (10-12 DIV) were perfused with mKRB containing Ca^{2+} (2 mM) for 2 minutes, exposed to KCl (30 mM) in the same medium for 6 minutes and then exposed to caffeine (20 mM) in a Ca^{2+} free, EGTA (0.5 mM)-containing medium to discharge the intracellular Ca^{2+} stores in wt and *tg* neurons. (**A**, **B**) Representative trace of fura-2 fluorescence ratio showing inhibition of caffeine induced Ca^{2+} release from intracellular stores by 1hr incubation with ryanodine (20 μ M). (**C**, **D**) Average delta peak and area under the curve respectively, measured above the baseline in response to caffeine and expressed as mean $\Delta \pm$ SEM (n=number of independent experiments; Δ peak: $F_{2, 27}=6.08$; $P<0.01$; Δ peak area: $F_{2, 27} = 9.30$; $P<0.001$, one-way ANOVA followed by Tukey HSD; * $P< 0.05$; ** $P< 0.01$; *** $P< 0.001$).

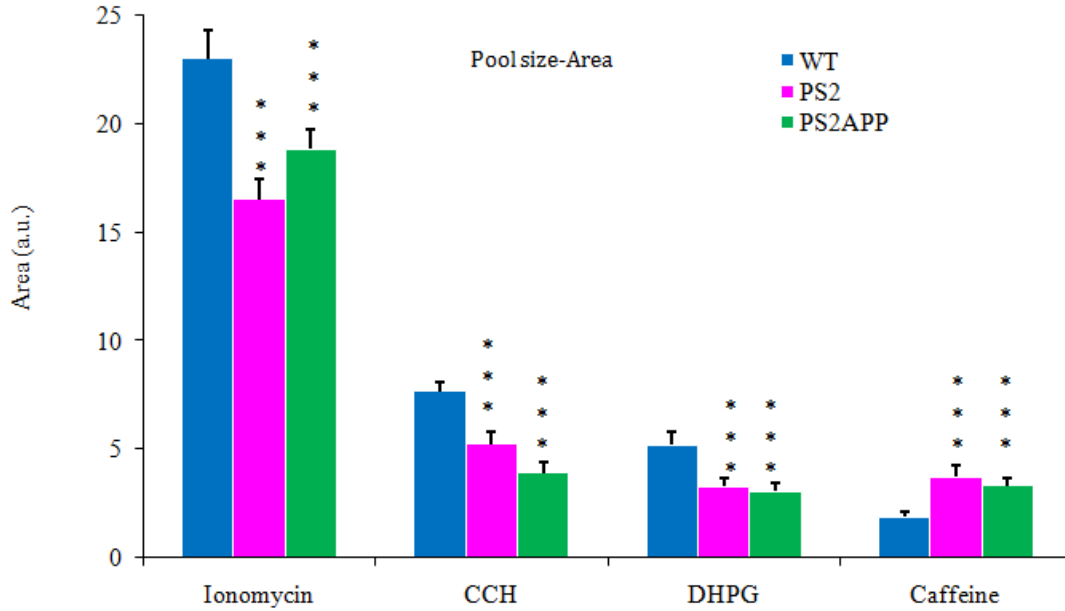


Figure 8: Summary of all intracellular stores ER Ca^{2+} pool sizes induced by different stimuli. A comparison of pool sizes (area) released by ionomycin, IP_3 -generating agonists and caffeine. Note: the pool sizes of both IP_3 -generating agonists and caffeine were smaller than ionomycin pool.

4.1.6 *PS2-N141I does not alter SERCA-2B and IP_3R protein levels but upregulates RyR protein levels in the tg neurons*

PSs are known to physiologically regulate the activity of both ER Ca^{2+} uptake and release machinery through their interaction with SERCA pump activity and IP_3R and RyR gating activity (Cheung et al., 2008; Green et al., 2008). Similar PS2 mutants are likely to affect the expression and functions of these proteins. To test the hypothesis that PS2-N141I could directly affect the expression levels of different proteins constituting the ER Ca^{2+} uptake and release machinery: We carried out western blot analysis in primary neuronal cultures cell pellets at 10-12DIV and total brain homogenates from P12 mice to determine the protein expression levels for SERCA-2B, IP_3R s, and RyRs. The protein expression levels for SERCA-2B and IP_3R were unaltered in PS2 mice and were comparable to the levels in wt (figure 9A, B, C, D).

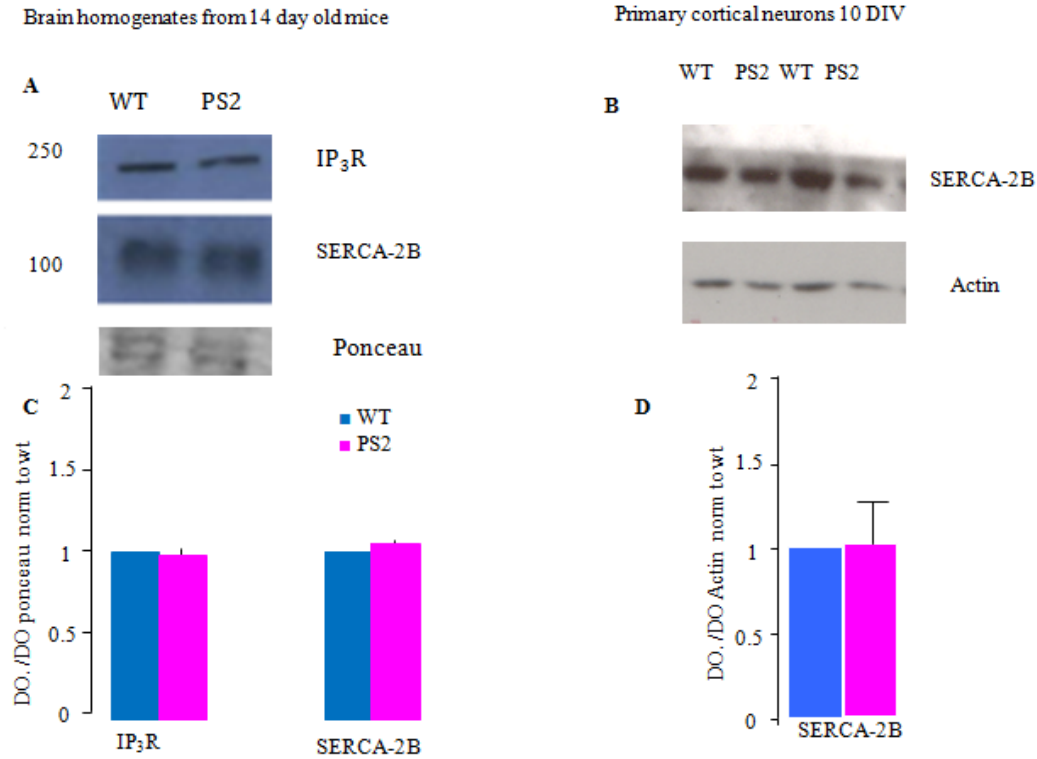


Figure 9: *PS2-N141I* does not alter *SERCA-2B* and *IP₃R* protein levels. **(A)**, Western blot analysis of *IP₃R* and *SERCA-2B* levels expressed in the whole brain homogenate. **(B)**, Western blot analysis of *IP₃R* and *SERCA-2B* levels expressed in primary neuronal culture extracts. **(C)**, Corresponding histogram of the densitometric analysis for *IP₃R* and *SERCA-2B* expression in whole brain homogenated blots. **(D)**, corresponding histogram of the densitometric analysis for *SERCA-2B* expression in primary neuronal culture extracts. For brain homogenates the bands were first normalized to ponceau levels, and then normalized to wt values, whereas for primary neuronal cultures, the bands were first normalized by actin levels, and then to wt values, Data are presented as mean±S.E.M of 9 independent samples, * $P < 0.05$, ** $P < 0.005$ (Student's t test).

Interestingly, the protein expression level for RyR was significantly increased in both primary neuronal cultures (figure 10B, D) and total brain homogenates (figure 10A, C) from tg mice in comparison to similar samples from wt.

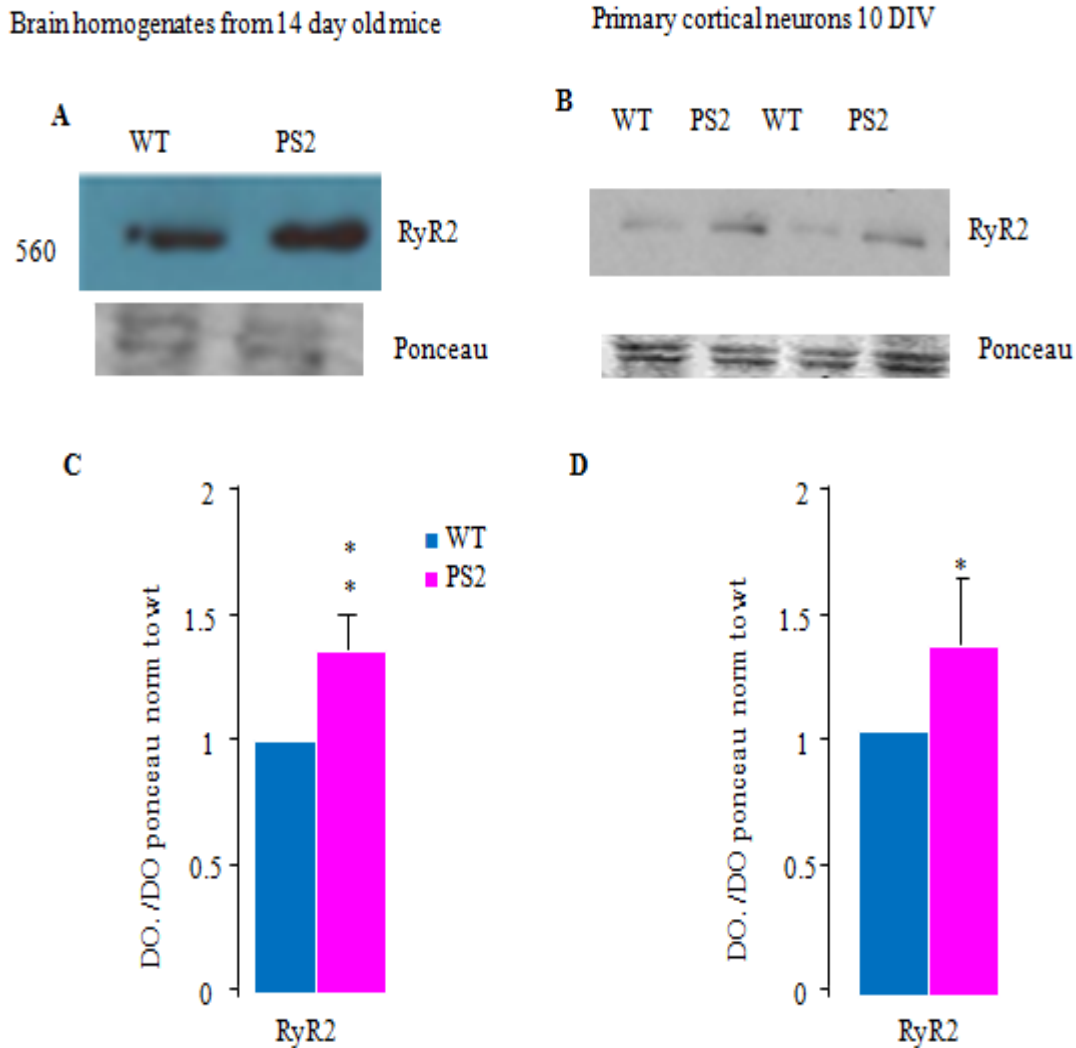


Figure 10: *PS2-N141I* upregulates RyR2 protein levels in the tg neurons. (A), Western blot analysis of RyR2 levels expressed in the whole brain homogenate. (B), Western blot analysis of RyR2 levels expressed in primary neuronal culture extracts. (C), Corresponding histogram of the densitometric analysis for RyR2 expression in whole brain homogenate blots. (D), Corresponding histogram of the densitometric analysis for RyR2 expression in primary neuronal culture extracts. For brain homogenates the bands were first normalized by ponceau levels and then to wt values. Data are presented as mean±S.E.M * P< 0.05, ** P<0.005 (Student's t test).

4.1.7 Intracellular store Ca²⁺ leak is increased in tg neurons

The results obtained in CCH, DHPG and ionomycin experiments of this study are consistent with the hypothesis that PS2 mutants partially deplete the intracellular stores (Brunello et al., 2009). We asked whether increased Ca²⁺ leak in tg neurons would have a contribution in reducing the Ca²⁺ levels of intracellular stores of our model. To measure the rate of passive intracellular Ca²⁺ leak in these neurons more directly, we compared the sizes of ionomycin induced Ca²⁺ responses after 60 and 180-seconds of incubation in Ca²⁺ -free medium containing 0.5 mM EGTA (the respective ionomycin pools are hereby referred to as IO₆₀ and IO₁₈₀). We thus used the IO₁₈₀/ IO₆₀ ratio as a quantitative measure of Ca²⁺ leak within 120-second time period of incubation with EGTA (Zhang et al., 2010).

Both wt and tg cortical neurons (10-12 DIV) were perfused with mKRB containing Ca²⁺ (2 mM) for 2 minutes, exposed to KCl (30 mM) in the same medium for 6 minutes, the neurons were then exposed to a Ca²⁺ free, EGTA (0.5 mM)-containing medium for 2 minutes and immediately exposed to ionomycin (1μM) in a Ca²⁺ free, EGTA (0.5 mM)-containing medium to fully discharge intracellular Ca²⁺ stores. The average delta peak IO₁₈₀/IO₆₀ ratio was equal to 0.76 for the wt neurons. Considering the area, IO₁₈₀/IO₆₀ ratio was 0.79. For the PS2 tg neurons, the average delta peak IO₁₈₀/IO₆₀ ratio was equal to 0.45. Whereas the area under the curve, IO₁₈₀/IO₆₀ ratio was 0.55 for the tg neurons.

The interpretation of these data is that tg neurons lost 56% of accumulated intracellular store Ca²⁺ content after 120 seconds of incubation in Ca²⁺ free medium by considering the average delta peak IO₁₈₀/IO₆₀ ratio (figure 11A, B). In contrast, wt neurons only lost 24% of accumulated Ca²⁺ during the same time period suggesting that tg neurons have much more passive Ca²⁺ leak. A similar trend was also observed by comparing delta peak area ratios (see also table 2).

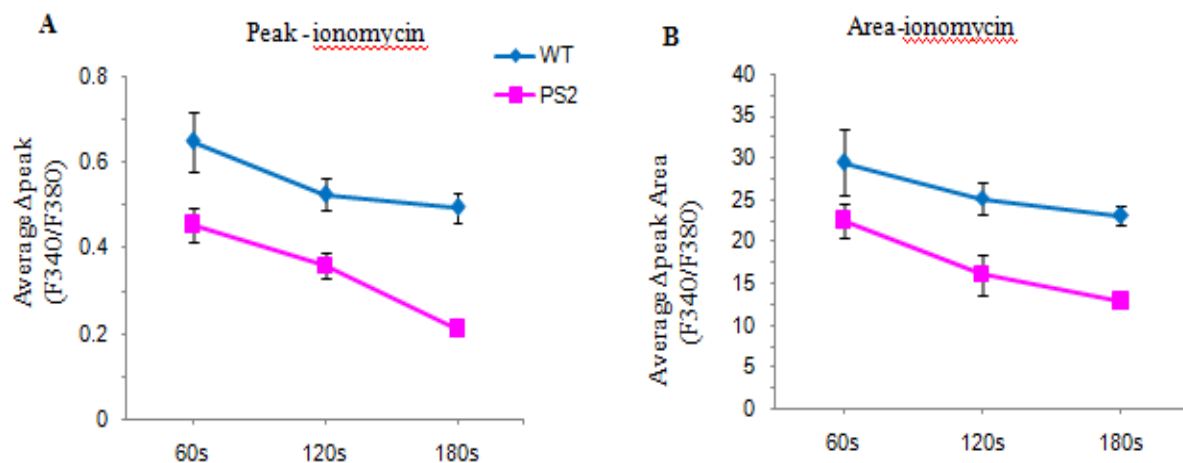


Figure 11: Intracellular stores Ca^{2+} leak is increased in tg cortical neurons. Cortical neurons (10-12 DIV) were perfused with mKRB containing Ca^{2+} (2 mM) for 2 minutes, exposed to KCl (30 mM) in the same medium for 6 minutes and then incubated in a Ca^{2+} free, EGTA (0.5 mM)-containing medium to estimate the intracellular stores with ionomycin (1 μ M) after 60, 120 and 180 seconds to fully discharge the intracellular Ca^{2+} stores in both wt and tg neurons. (A, B) Graphs of the delta peak response and area under the curve for wt (blue) and tg (magenta). Data presented as mean \pm S.E.M.

Table 2: Passive Ca^{2+} leak

Genotype	Delta Peak	%change	Area	%change
	IO_{180}/IO_{60}		IO_{180}/IO_{60}	
WT	0.76	24	0.79	21
PS2	0.45	56	0.55	45

IO_{180}/IO_{60} as quantitative measure of passive Ca^{2+} loss from intracellular stores in 2 minutes of incubation in mKRB containing EGTA (0.5 mM).

4.1.8 Do primary cultures of cortical neurons from tg mice produce enough A β 42 to affect Ca²⁺ homeostasis?

Double tg mice carrying hAPP^{swe} and hPS2-N141I produce elevated amounts of both A β 40 and A β 42 peptides and form senile plaques at old age, showing behavioural changes that begin when A β deposits and inflammation start to appear in the subiculum and frontolateral cortex (Richard et al., 2003, Ozmen et al, 2009). Furthermore, age-related cognitive deficits and amyloid deposits with inflammation become very remarkable in neo-and limbic cortices at about 8 months of age (Richard et al., 2003). As far as single tg mice is concerned, no published data are available yet. Nonetheless, it is conceivable that the PS2 mutant increases the amount of A β 42 peptides by hydrolyzing the endogenous APP substrate. Indeed, we estimated the total A β 42 levels from two weeks mouse brain homogenates by an ELISA kit (WAKO) detecting both mouse and human A β 42 with high sensitivity. Whereas in double tg mice A β 42 levels reach 40 times the endogenous amount present in wt mice, the level in single tg mice was much less but still greater (4 times). The A β 42/A β 40 in the double tg was 16 times the wt ratio and the ratio in the single tg was 4 times higher compared to wt (figure 12A, B).

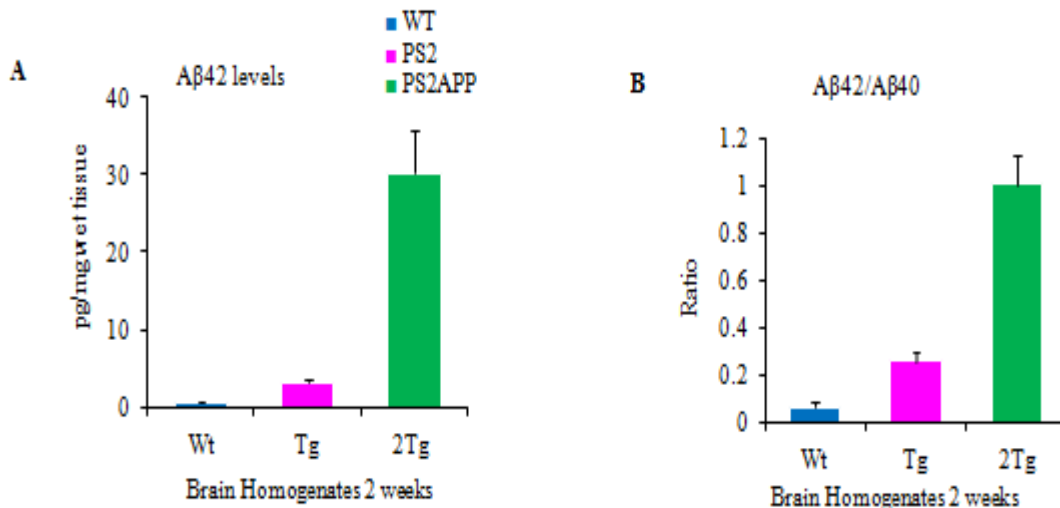


Figure 12: Both $A\beta_{42}$ levels and $A\beta_{42}/A\beta_{40}$ ratio are high in tg mice brain as early as 2weeks. (A), $A\beta_{42}$ level assay in wt (blue), single tg (magenta) and double tg (green) brain homogenates quantified by ELISA kit (WAKO). (B), $A\beta_{42}/A\beta_{40}$ ration for brain homogenate from wt, single and double tg. Data presented as mean \pm S.E.M.

4.1.9 Tg neurons have higher synchronous Ca^{2+} oscillations induced by picrotoxin

Synchronous neuronal Ca^{2+} oscillations are key indicator of interneuronal communication, required for different physiological functions (Bacci et al., 1999). They usually present a burst of synchronous neuronal activities with a well-defined temporal pattern. In primary neuronal cultures, they occur as synchronous burst of activities of a group of neurons. Both spontaneous and induced oscillations occur in primary neuronal cultures, especially when exposed to high extracellular Ca^{2+} milieu (Bacci et al., 1999; Pratt et al., 2011). Picrotoxin also called “*cocculin*” is a commonly used tool for induction of synchronous neuronal Ca^{2+} oscillations both in situ and in primary cultures. This drug acts as a noncompetitive antagonist for the $GABA_A$ receptor chloride channels, by directly antagonizing the $GABA_A$ receptor channel, which is a ligand-gated ion channel concerned chiefly with the passing of chloride ions (Cl^-) across the cell membrane. Therefore, picrotoxin reduces the channel conductance by reducing not only the opening frequency but also the mean open time. The overall outcome is the removal of GABAergic inhibition and thus allows synchronous Ca^{2+} oscillations.

To examine neuronal Ca^{2+} excitability (synchronous oscillations) in this study we have taken advantage of the antagonizing effect of picrotoxin on the GABAergic inhibition thus allowing the neurons to spike synchronously. Synchronous oscillations were recorded for a fixed duration (10 minutes) at 17DIV when neurons are mature enough to be easily excited. During the recording period (10 minutes), the average number of synchronous Ca^{2+} oscillations and the delta peak amplitude in response to picrotoxin (50 μ M) in $CaCl_2$ (2 mM) containing mKRB medium were 18.95 ± 1.48 and 0.59 ± 0.2 (mean $\Delta\pm$ SEM, n=19) respectively (figure 13A, D). When similar analysis was carried out in tg neurons, both PS2 and PS2APP tg mice neurons had significantly

increased synchronous Ca^{2+} oscillations in response to picrotoxin (figure 13B, C, D). It is worthy note that the delta peak amplitudes were not significantly different (figure 13E). For the PS2 tg mice the average number of synchronous Ca^{2+} oscillations and delta peak amplitude in response to picrotoxin (50 μM) in CaCl_2 (2 mM) containing mKRB medium were 30.76 ± 2.08 ($p < 0.0001$) and 0.59 ± 0.02 ($p > 0.5$) (mean $\Delta \pm \text{SEM}$, $n = 21$) respectively corresponding to 62.35% increase in the number of oscillations. For neurons from PS2APP mice, the average number of synchronous Ca^{2+} oscillations and delta peak amplitude were 30.67 ± 1.50 ($p < 0.0001$) and 0.55 ± 0.01 ($p > 0.5$) (mean $\Delta \pm \text{SEM}$, $n = 18$) respectively, corresponding to 61.85% increase in the number of oscillations.

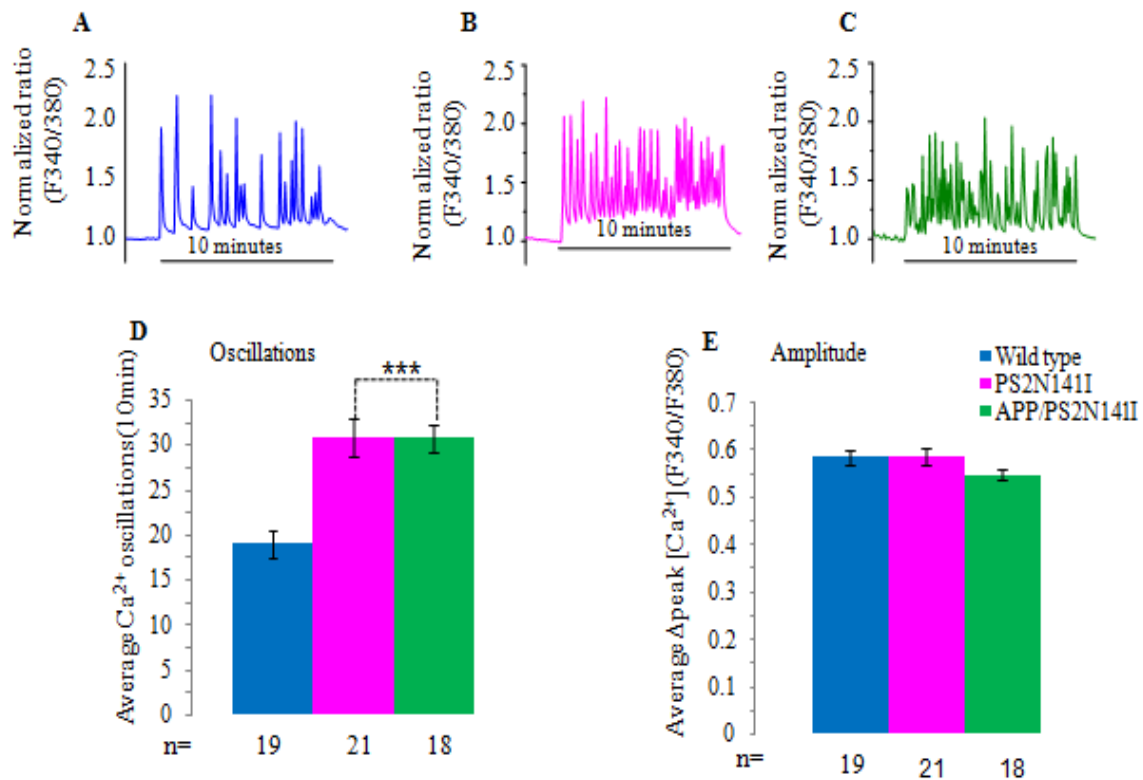


Figure 13: PS2 and PS2APP neurons exhibit significantly higher frequency of picrotoxin-induced synchronous Ca^{2+} oscillations than wt neurons. Cortical neurons (17 DIV) were perfused with Ca^{2+} (2 mM) in mKRB for 2 minutes, then exposed to picrotoxin (50 μM) in mKRB with Ca^{2+} (2 mM) and synchronous Ca^{2+} oscillations were recorded for 10 minutes before exposure to Ca^{2+} free, EGTA (0.5

mM)-containing medium to terminate the oscillations. **(A, B, C)** Representative traces of normalized fura-2 fluorescence ratio for synchronous Ca^{2+} oscillations recorded for 10 minutes in wt **(A)**, PS2 **(B)** and PS2APP **(C)** cortical neurons, note the high number of synchronous Ca^{2+} oscillations in neurons from tg mice, error bars have been omitted for clarity of traces. **(D)** Average number of oscillations recorded in wt (blue), PS2 (magenta) and PS2APP (green) cortical neurons recorded for a period of 10 minutes; $F_{2,55}=18$; $P<0.0001$, one-way ANOVA followed by Tukey HSD; * $P<0.05$; ** $P<0.01$; *** $P<0.001$. **(E)** Average delta peak amplitude for cytosolic Ca^{2+} rise measured above the baseline Ca^{2+} in response to picrotoxin and expressed as mean $\Delta\pm\text{SEM}$ (n=number of independent experiments, blue-wt; magenta-PS2; green-PS2APP).

Presenilins are known to play a role in modulating Ca^{2+} release from the intracellular stores particularly the ER and their mutants cause Ca^{2+} dysregulation (LaFerla 2002; Giacomello et al., 2005; Thinakaran and Sisodia, 2006; Zatti et al., 2006; Brunello et al., 2009). This prompted us to ask whether the increase in number of synchronous Ca^{2+} oscillations observed in PS2 mutant neurons could be as result of dysregulation of intracellular Ca^{2+} stores. To test this hypothesis, we recorded Ca^{2+} oscillations in neurons with pre-depleted internal stores by pre-treating the neurons with thapsigargin (1 μM) for one hour during fura-2/AM loading. Thapsigargin is a SERCA pump inhibitor that blocks the uptake of Ca^{2+} from the cytosol into the ER, thereby leading to ER Ca^{2+} depletion. If internal stores are the source of synchronous Ca^{2+} oscillations it would be expected that depleting the intracellular Ca^{2+} stores should reduce the frequency of synchronous oscillations in tg mice neurons.

Pre-treatment with thapsigargin (1 μM) did not significantly affect the high frequency of synchronous Ca^{2+} oscillations in neurons from tg mice (figure 14). The average number of synchronous Ca^{2+} oscillations in control (not treated with thapsigargin), wt, PS2 and PS2APP neurons were; 21.10 ± 1.23 (mean $\Delta\pm\text{SEM}$, n=15), 34.73 ± 2.15 (mean $\Delta\pm\text{SEM}$, n=11) and 33.20 ± 1.34 (mean $\Delta\pm\text{SEM}$, n=6) respectively (figure 14B, C, D). For the wt, PS2 and PS2APP neurons pretreated with thapsigargin, the average number of synchronous Ca^{2+} oscillations were; 28.0 ± 4.62 (mean $\Delta\pm\text{SEM}$,

n=6), 34.25 ± 1.53 (mean $\Delta \pm$ SEM, n = 8) and 33.20 ± 1.46 (mean $\Delta \pm$ SEM, n = 8) respectively.

Since RyRs also mediate Ca^{2+} efflux from the ER and further amplify the IP_3R response through CICR, we analyzed the contribution of RyRs to synchronous Ca^{2+} oscillations in the neurons. The neurons from both wt and tg mice were pre-incubated with ryanodine ($50 \mu\text{M}$) for one hour during fura-2/AM loading and picrotoxin induced synchronous Ca^{2+} oscillations were measured as described above. It is worth noting that ryanodine at low concentration, locks the RyR channel to an ‘open state’ but to a ‘closed state’ when applied at higher concentrations above $100 \mu\text{M}$ (Lai et al., 1989; Buck et al., 1992; Fill and Copello, 2002; Ozawa, 2010). Emptying the ER by ryanodine did not significantly decrease the high frequency of synchronous Ca^{2+} oscillations in neurons from the tg mice (figure 14D, E, F). The average number of synchronous Ca^{2+} oscillations of control (not treated with ryanodine) wt, PS2 and PS2APP neurons were; 21.10 ± 1.23 (mean $\Delta \pm$ SEM, n=15), 34.73 ± 2.15 (mean $\Delta \pm$ SEM, n=11) and 33.20 ± 1.34 (mean $\Delta \pm$ SEM, n = 6) respectively. For wt, PS2 and PS2APP neurons, pretreated with ryanodine, the average number of synchronous Ca^{2+} oscillations were 24.4 ± 1.91 (mean $\Delta \pm$ SEM, n=9), 36.0 ± 2.02 (mean $\Delta \pm$ SEM, n=9) and 33.24 ± 1.03 (mean $\Delta \pm$ SEM, n=6) respectively.

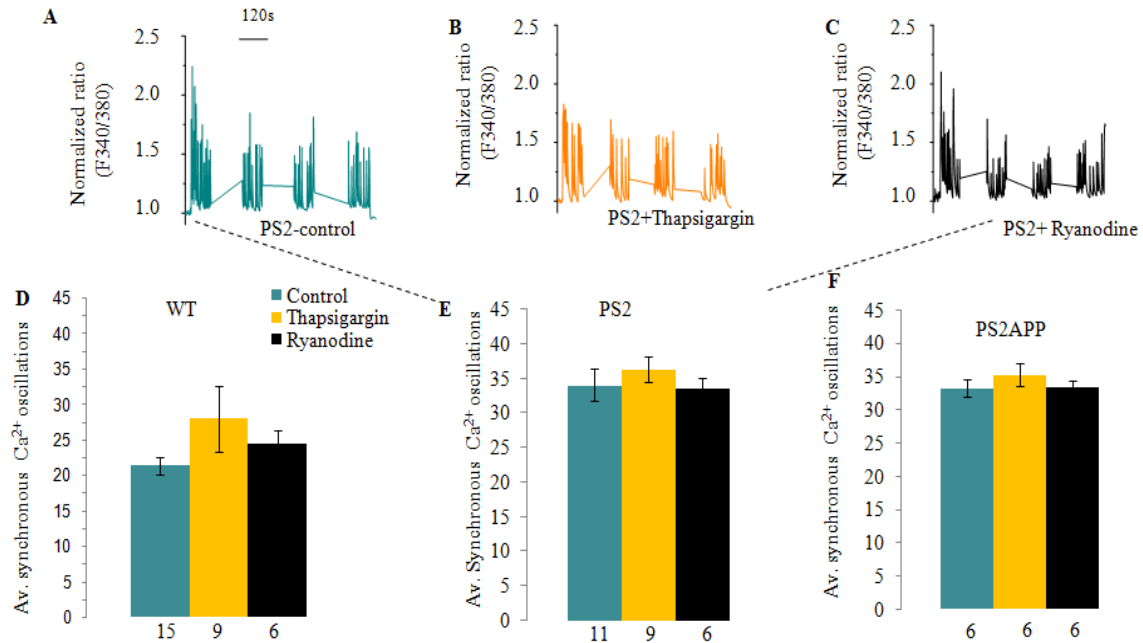


Figure 14: Blocking Ca^{2+} release from internal stores does not significantly reduce the high frequency of synchronous Ca^{2+} oscillations of cortical neurons induced by Picrotoxin ($50\mu M$). Cortical neurons (17 DIV) were perfused with Ca^{2+} (2 mM) in mKRB for 2 minutes, then exposed to picrotoxin ($50\mu M$) in mKRB with 2 mM Ca^{2+} and synchronous Ca^{2+} oscillations were recorded every second for 8 minutes and then exposed to a Ca^{2+} free, EGTA (0.5 mM)-containing medium to attenuate the oscillations. (A,B and C), Representative traces of average normalized fura-2 fluorescence ratio synchronous for Ca^{2+} oscillations recorded for 8 minutes in PS2N141I. (A), PS2N141I, control (not treated). (B), PS2N141I neuron, pretreated with thapsigargin ($1\mu M$) for one hour during fura-2/AM loading. (C), PS2N141I neuron, pretreated with ryanodine ($50\mu M$) for one hour during fura-2/AM loading. Note that error bars have been omitted for clarity of traces. (D), Average number of oscillations recorded in the wt neurons (light blue bar, wt control; orange bar, wt plus thapsigargin ($1\mu M$) for one hour; black bar, wt plus ryanodine ($50\mu M$) for one hour. (E), Average number of oscillations recorded in the PS2-N141I neurons (light blue bar, PS2-N141I control; orange bar, PS2-N141I plus thapsigargin ($1\mu M$) for one hour; black, PS2-N141I plus ryanodine ($50\mu M$) for one hour (F), Average number of oscillations recorded in the PS2APP neurons (light blue bar, control; orange bar, PS2APP plus thapsigargin ($1\mu M$) one hour; black, PS2APP plus ryanodine ($50\mu M$) for one hour. Notice that the number of synchronous Ca^{2+} oscillations in neurons pre-treated with either ryanodine or thapsigargin in both PS2-N141I and PS2APP are not significantly different from control neurons. Bar graphs show mean $\Delta \pm$ SEM; n= number of independent experiments.

Interestingly, picROTOXIN evoked Ca^{2+} oscillations were significantly inhibited in the presence of Lanthanum Chloride (LaCl_3) ($1\mu\text{M}$) in both in wt and tg neurons (figure 15B, C). LaCl_3 is a non-specific Ca^{2+} channel blocker frequently used to study SOCCs, suggesting that Ca^{2+} entry could be possibly via this type of Ca^{2+} permeable channels.

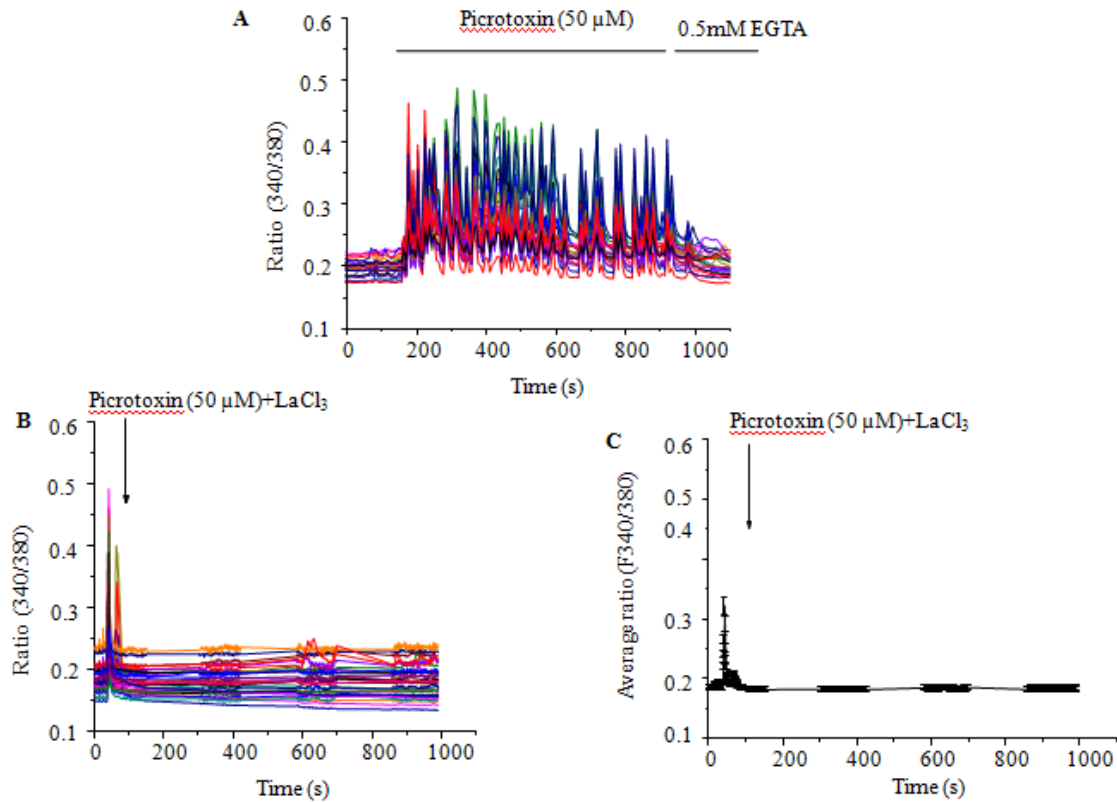


Figure 15: Lanthanum Chloride (LaCl_3) inhibits picROTOXIN induced synchronous Ca^{2+} oscillations of cortical neurons in tg. Cortical neurons (17 DIV) were perfused with Ca^{2+} (2 mM) in mKRB for 2 minutes, then exposed to picROTOXIN (50 μM) with or without LaCl_3 (1 μM) in mKRB with 2 mM Ca^{2+} and synchronous Ca^{2+} oscillations were recorded every second for 10 minutes and then exposed to a Ca^{2+} free, EGTA (0.5 mM)-containing medium to stop Ca^{2+} oscillations. (A, B), Representative traces for fura-2/AM F340/380 ratio (absolute values) from PS2 tg neuron. Note lack of synchronous Ca^{2+} oscillations after LaCl_3 application (B). (C), Representative trace for average ratio (F340/380) from trace B.

4.1.10 In the tg neurons reduction in ER Ca²⁺ content does not affect the sensitivity to ER mediated death stimuli

The [Ca²⁺]_{ER} is critical for intracellular signal transduction and cell survival. Both genetic and pharmacological studies have suggested that varying the Ca²⁺ concentration in the ER can have both beneficial and detrimental effects on cell survival (Pinton et al., 2001; Scorrano et al., 2003). Decreased [Ca²⁺]_{ER} have been linked to increased resistance to certain death stimuli, such as c₂-ceramide and H₂O₂. FAD linked PS2 reduce Ca²⁺ release from ER in different cell lines and rat primary cortical neurons over-expressing mutations (Giacomello et al., 2005; Zatti et al., 2006; Brunello et al., 2009). Although the mechanisms underlying the reduction in the ER and other intracellular Ca²⁺ stores start to reveal, the physiological relevance of this phenomenon in AD remains unclear. Like other PS2 mutants, the PS2-N141I mutation leads to a reduced [Ca²⁺]_{ER} (see above). We hypothesized that this would be beneficial in the event of death stimuli that involved the ER- Ca²⁺ pathway.

Survival assays were carried out in primary cortical neurons from both wt and tg mice, seeded as for Ca²⁺ measurements. As stated earlier on, cultured neurons have modest amount of mobilizable Ca²⁺ in their intracellular stores (Smith et al, 2005; Zatti et al. 2006; Zhang et al., 2010 and figure 3A). Since our focus was to test the response to death stimuli that require Ca²⁺ release from the ER, we firstly preloaded the stores by supplementing the culture medium with KCl and CaCl₂ to 10mM and 2mM final concentration respectively. This protocol significantly improved the loading of the intracellular stores and indeed increased the number of neurons with loaded stores for both PS2 and wt neurons. For the survival assay, we employed as a stimulus, H₂O₂ that mediates its toxicity through ER Ca²⁺ release (Pinton et al., 2001). Although treatment with H₂O₂ (10 and 20 μM) for 24 hours increased the number of apoptotic neurons compared to basal condition, no significant synergy with the addition of DHPG (10 μM) was observed. Furthermore, although there seemed to be a tendency of PS2 cultures to be more susceptible to H₂O₂ in some experiments (figure 16, B), the differences were not statistically significant.

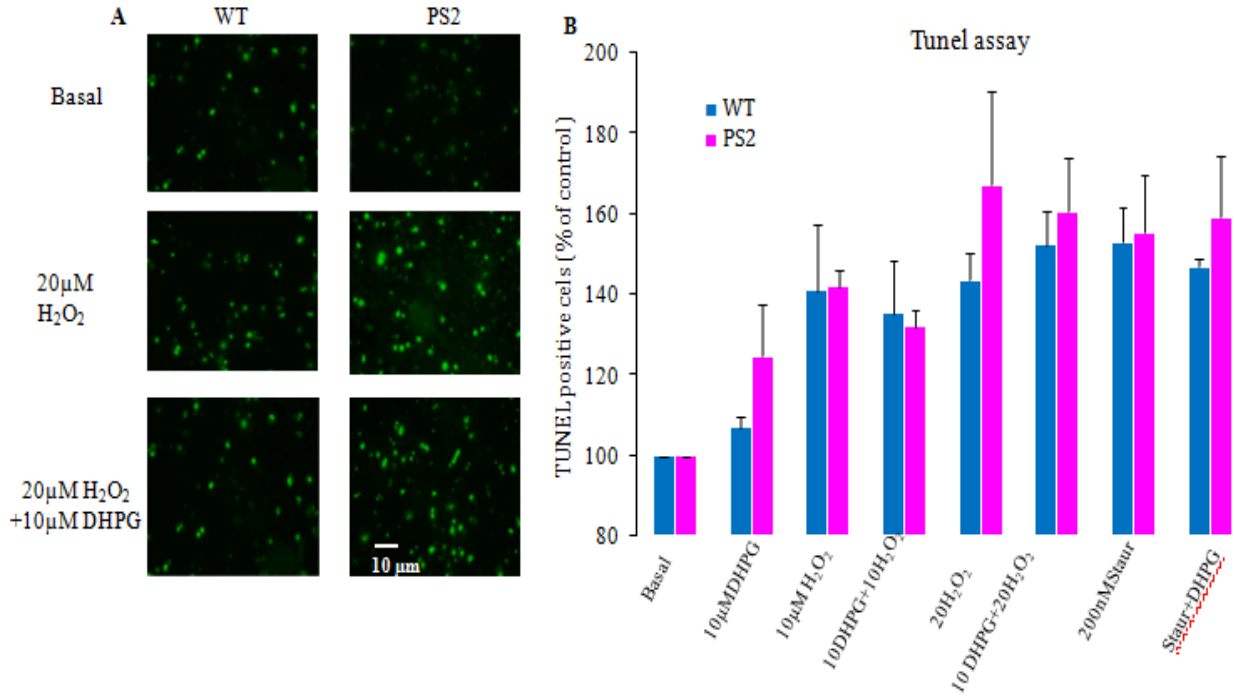


Figure 16: Effects of H₂O₂ on primary culture neuron viability. Wt and tg primary neuronal cultures at 10DIV were treated with H₂O₂ (10 and 20 μM) or staurosporin (200 μM) in presence or absence of DHPG (10 μM) for 24 hours and then apoptotic cells were measured by TUNEL assay kit. (A), Representative photos for both wt and PS2 tg neurons (apoptotic cells marked green). (B), Quantification of TUNEL positive cells, wt (blue) and PS2 tg (magenta). Bar graphs show mean $\Delta \pm$ SEM of average survival normalized to control (basal survival levels) for each genotype. Note: Differences between wt and PS2 cultures are not statistically significant.

Result II

4.2 Functional effects of synthetic A β 42 oligomers on Ca²⁺ homeostasis.

4.2.1 *Ca²⁺ release induced by IP₃-generating agonists is reduced in mouse cortical neurons treated with A β 42 oligomers*

Soluble A β 42 oligomers, rather than deposited amyloid plaques, have recently been associated with the onset of cognitive decline in AD (Walsh and Selkoe, 2007; Shankar and Walsh, 2009). The A β 42 oligomers, produced within neurons or entering from outside, can specifically cause synaptic toxicity in part through Ca²⁺ dysregulation (Lambert et al., 1998; Demuro et al., 2010; Mattson, 2010; Berridge, 2010; 2011). A mechanistic explanation for this effect is still lacking, however there are suggestions that A β 42 oligomers can elevate the [Ca²⁺]_{cyt} by forming artificial channels or activating Ca²⁺ channels on plasma membrane and/or intracellular organelles (Kelly et al., 1996; Demuro et al., 2010; 2011). Our investigation focused on the effect of A β 42 oligomers on intracellular Ca²⁺ stores of primary neuronal cultures obtained from newborn wt C57B6J mice (see material and methods). Neurons were either acutely treated or pre-incubated with A β 42 (0.5 μ M) during the fura-2 loading procedure (40 min at 37°C plus 20 min at RT). To prepare A β 42 monomers and oligomers, aliquots of synthetic A β 1-42 dissolved in HFIP, were carefully evaporated by air pipetting several times on the wall of the tube. The dried HFIP film was then dissolved in double distilled water to the final concentration of 50 μ M (Giliberto et al., 2009). The solution, when used immediately, contains mainly monomers (~4 kDa) whereas, when left at RT for 24-48 hours, it contains soluble oligomers of higher molecular weight (~25 kDa), as checked by SDS-PAGE (figure 17A). Upon fura-2 loading, cells were washed and imaged at RT, as previously described (see section 3.9). Neuronal Ca²⁺ stores were assayed by stimulation with the IP₃ generating agonist CCH (0.5 mM) or DHPG (10 μ M) after depolarization with KCl (30 mM) to allow pre-loading of the intracellular Ca²⁺ stores. Pre-treatment

with A β 42 oligomers did affect neither the resting Ca²⁺ level (figure 17B) nor the peak and long lasting Ca²⁺ plateaus caused by KCl-induced depolarization (figure 17C, D).

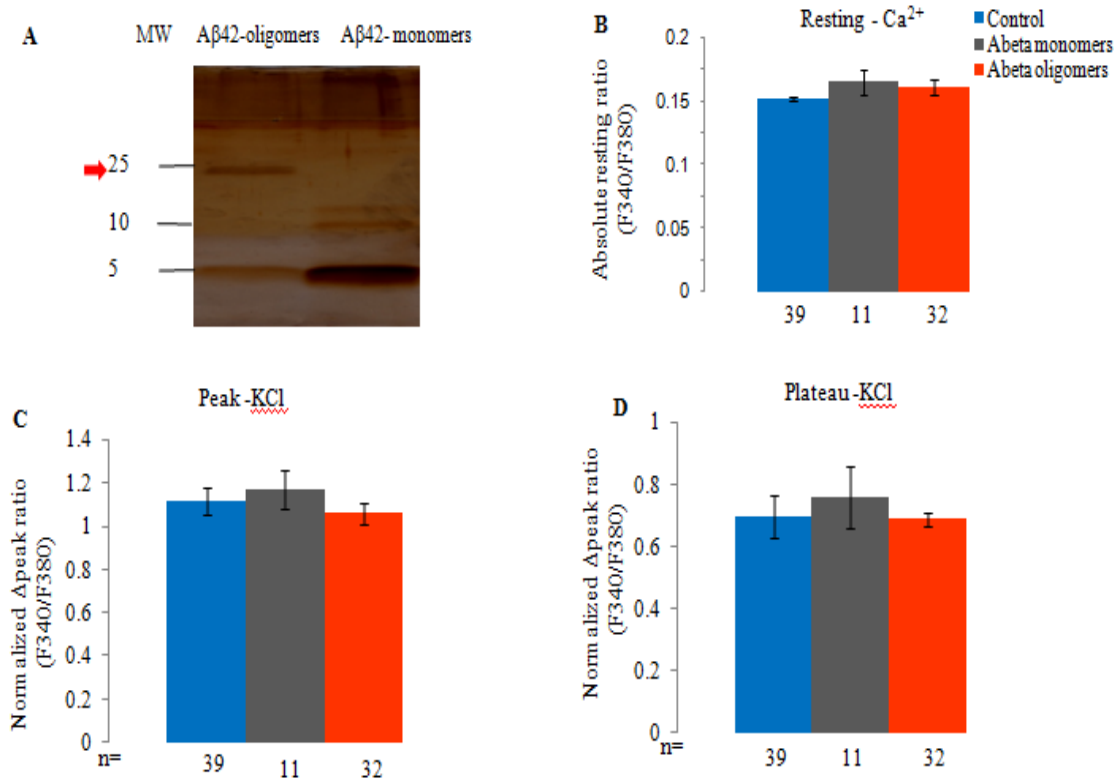


Figure 17: A β 42 oligomers do not affect the resting Ca²⁺ levels and influx caused by KCl-induced depolarization. Wt neurons (10-12 DIV) were perfused with mKRB containing CaCl₂ (2 mM) for 2 minutes, then exposed in the same medium to KCl (30 mM) for 6 minutes and then to a Ca²⁺ free, EGTA (0.5mM)-containing medium to remove extracellular Ca²⁺. (A) Silver staining of A β 42 preparation of monomers and oligomers loaded without boiling (2 μ g/lane) on 18% Tris-Tricine polyacrylamide gel; note, A β 42 oligomers (arrow). (B), Bars represent absolute ratio (F340/380) levels measured at resting in control and A β 42 oligomer treated neurons. (C, D) Bars represent the average delta peak and plateau response to KCl, respectively normalized to the resting level and presented as mean Δ \pm SEM; n= number of independent experiments.

The average delta peak and area under the curve for cytosolic Ca^{2+} rises in response to CCH were 0.36 ± 0.03 and 6.44 ± 0.71 (mean $\Delta \pm \text{SEM}$, $n=7$) respectively, in the control (not treated with $\text{A}\beta 42$) neurons. In neurons pre-treated with $\text{A}\beta 42$ oligomers ($0.5 \mu\text{M}$), Ca^{2+} release from the CCH responsive intracellular stores was significantly reduced (figure 18). For the neurons treated with $\text{A}\beta 42$ oligomers for one hour during the fura-2 loading, the normalized delta peak and delta peak area under the curve for cytosolic Ca^{2+} rises in response to CCH were 0.26 ± 0.02 ($p < 0.01$) and 4.44 ± 0.47 ($p < 0.05$) (mean $\Delta \pm \text{SEM}$, $n=10$) respectively, corresponding to a 28.2% and 31.0% reduction in peak and area, respectively. In contrast, $\text{A}\beta 42$ monomers did not significantly affect Ca^{2+} release from the CCH responsive intracellular stores of cortical neurons (figure 18A, B, C). The average delta peak and area were 0.37 ± 0.04 and 5.52 ± 0.53 (mean $\Delta \pm \text{SEM}$, $n=8$) respectively. Noteworthy only responding neurons were included in this calculation. In particular, the number of responding cells was higher in untreated neurons than in those treated with $\text{A}\beta 42$ oligomers, corresponding to 91.01% and 70.47%, respectively.

We then carried out similar analysis in cortical neurons by acute application of $\text{A}\beta 42$ ($0.5 \mu\text{M}$). $\text{A}\beta 42$ oligomers applied in complete medium did not induce Ca^{2+} release or entry, neither modified the response to KCl (30mM). Conversely, acute treatment significantly reduced Ca^{2+} release from the CCH responsive intracellular stores (figure 18D, E). The average delta peak and area under the curve for cytosolic Ca^{2+} rises in response to CCH were 0.21 ± 0.01 and 3.91 ± 0.24 (mean $\Delta \pm \text{SEM}$, $n=7$) respectively, in the control neurons. Note that these values are lower than the ones above, because fura-2 was ratioed at 360/380 nm instead of 340/380 nm. Since the signal at 340 nm is very small and become even smaller with a reduction in $[\text{Ca}^{2+}]_{\text{cyt}}$ release (as expected upon $\text{A}\beta 42$ treatment), it was chosen to use for ratioing the signal at 360nm where the fluorescence is higher (due to better permeation through microscopy optics) but it is practically insensitive to Ca^{2+} changes (in fact it is the fura-2 isosbetic point). Under this condition, only the F380 nm is monitoring the Ca^{2+} changes. This was applied only for this particular set of experiments, as a further control to verify whether the estimated reduction was effectively due to $\text{A}\beta 42$ oligomers.

For the neurons acutely treated with A β 42 oligomers (0.5 μ M) for 5 minutes, the delta peak and delta peak area under the curve for cytosolic Ca²⁺ rises in response to CCH were, 0.15 \pm 0.02 (p<0.01) and 2.31 \pm 0.20 (p<0.05) (mean Δ \pm SEM, n=8) respectively. This corresponded to a 27.9% and 40.9% reduction in peak and area, respectively, percentages rather similar to those reported above during chronic treatment. As it was the case with chronic treatment with A β 42 monomers, Ca²⁺ release following acute application of the monomers was not significantly different from untreated control neurons, the average delta peak and area were 0.22 \pm 0.01 and 3.15 \pm 0.28 (mean Δ \pm SEM, n = 8) respectively.

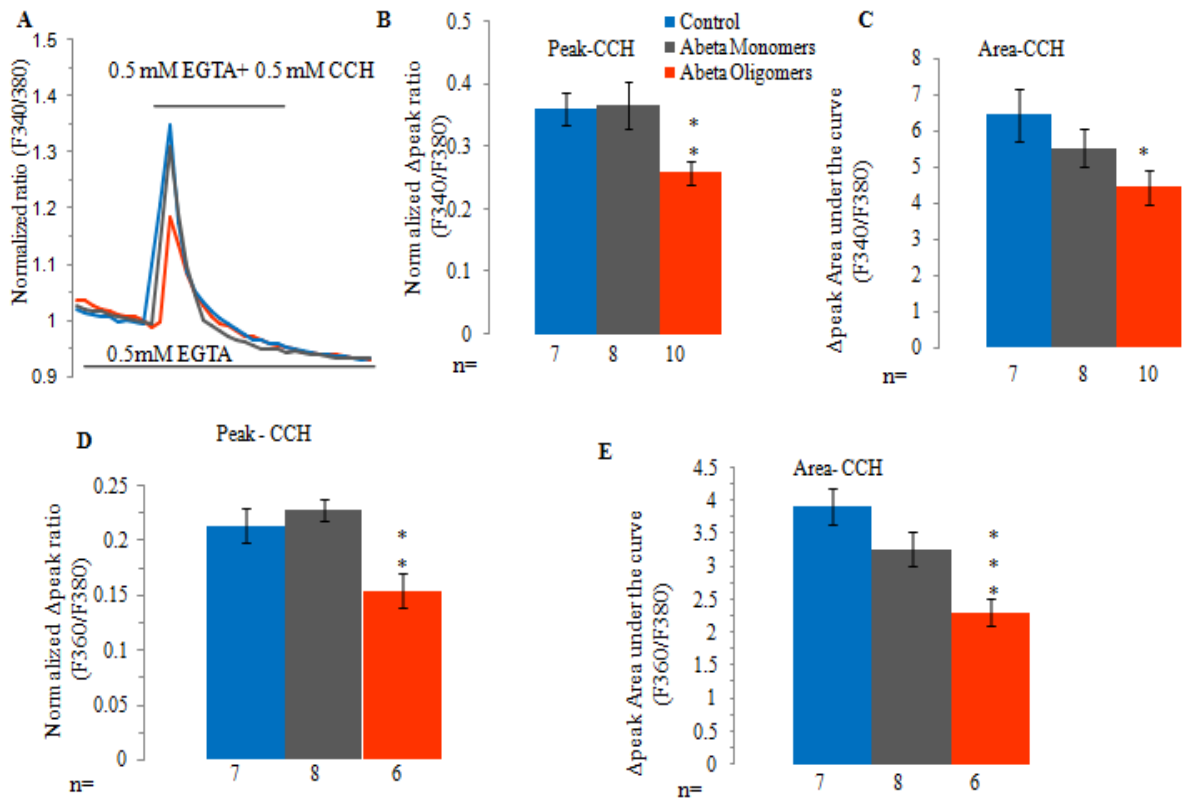


Figure 18: Both acute and prolonged treatment of cortical neurons with A β 42 oligomers reduce Ca²⁺ release induced by the IP₃ generating agonist CCH. Cortical neurons (10-12 DIV) were perfused with mKRB containing CaCl₂ (2 mM) for 2 minutes, exposed to KCl (30 mM) for 6 minutes and then to CCH (0.5 mM) in a Ca²⁺ free, EGTA (0.5 mM)-containing medium to discharge the IP₃ sensitive intracellular Ca²⁺ stores of control or A β 42 treated cortical neurons. (A), Representative traces of fura-2 ratio changes

in response to CCH in control (blue), monomer-treated (grey), oligomer-treated (red) neurons. A β 42 oligomers or monomers (0.5 μ M) were present during the loading period with fura-2. **(B,C)**, Average normalized delta peak and area under the curve, in response to CCH (0.5 mM) in control (blue bars), monomer-treated (grey bars) or oligomer-treated (red bars) neurons as described in **A**. Data are expressed as mean \pm S.E.M. (n=number of independent experiments; Δ peak: $F_{2, 18}=6.42$; $P<0.01$; Δ peak area: $F_{2, 18}=3.36$; $P<0.05$, one-way ANOVA followed by Tukey HSD. **(D, E)** Average delta peak and delta peak area respectively, in response to CCH (0.5 mM) without or with A β 42 (0.5 μ M) added acutely for 5 minutes; control (blue bars), monomer-treated (grey bars), oligomer-treated (red bars) neurons. Note the change in fura-2 wavelengths (360/380). Data presented on bars are expressed as mean \pm S.E.M (n = number of independent experiments; Δ peak: $F_{2,17}= 6.$, $P<0.01$; Δ peak area: $F_{2,17}= 11,54$ $P<0.001$, one-way ANOVA followed by Tukey HSD ; * $P< 0.05$; ** $P< 0.01$; *** $P< 0.001$.

Similar findings were also obtained when DHPG was used. The average delta peak and area under the curve for cytosolic Ca²⁺ rises in response to DHPG were 0.29 ± 0.02 and 4.70 ± 0.43 (mean $\Delta\pm$ SEM, n = 8) respectively, in the wt control neurons. Interestingly, treatment of wt cortical neurons with A β 42 oligomers for one hour during fura-2 loading significantly reduced Ca²⁺ release from the DHPG responsive intracellular stores (figure 19A, B). The average delta peak and area were 0.18 ± 0.02 and 2.59 ± 0.17 (mean $\Delta\pm$ SEM, n = 7) respectively, corresponding to a 37.50% and 44.98% reduction in peak and area, respectively.

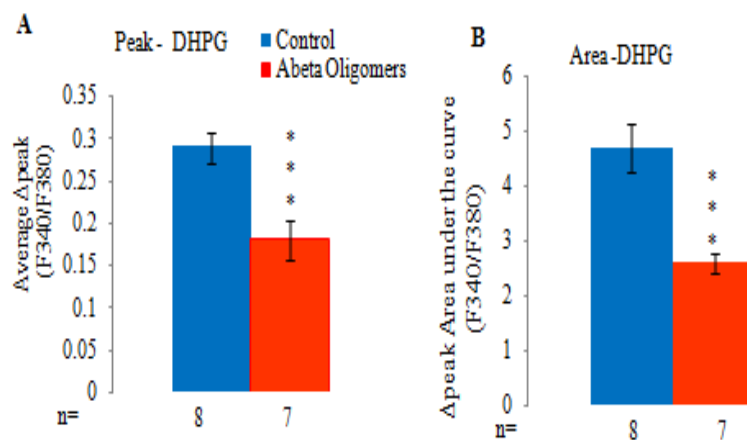


Figure 19: *Aβ42 oligomers reduce Ca²⁺ release induced by the IP₃ generating agonist DHPG.* Cortical neurons (10-12 DIV) were treated as described in Figure 18 but exposed in Ca²⁺ free, EGTA (0.5 mM)-containing medium with DHPG (10 μM), to fully discharge intracellular Ca²⁺ stores in control neurons or neurons pretreated with Aβ42 peptides. (A, B) Average delta peak and area under the curve, respectively measured above the baseline in response to the IP₃ generating agonist, DHPG in control (blue bars) and oligomer pretreated (red bars) neurons. Oligomers were used at 0.5 μM final concentration during the loading period with fura-2 (40 min at 37°C plus 20 min at RT). Data presented on bars are expressed as mean ±S.E.M (n=number of independent experiments. * P< 0.05; ** P< 0.01; *** P< 0.001, unpaired Student's t-test.

4.2.2 Ca²⁺ release induced by IP₃-generating agonists is reduced in cell lines treated with Aβ42 oligomers

The functional effect of Aβ42 oligomers in intracellular Ca²⁺ homeostasis is not only restricted to primary neuronal cultures. Similar results were also obtained with the rat pheochromocytoma PC12 cell line. Although the average delta peak for the cells treated with Aβ42 oligomers for one hour was not significantly reduced (but there was a tendency towards reduction), the area under the curve was significantly different from the control cells (figure 20A, B). The average delta peak and area under the curve for the cytosolic Ca²⁺ rises in response to BK (100 nM) were 0.50±0.06 and 17.27±1.45 (mean Δ±SEM, n = 10) respectively in control cells. For the cells treated with Aβ42 oligomers, the average delta peak and area under the curve for cytosolic Ca²⁺ rises in response to BK (100 nM) were 0.37±0.06 04 (p>0.05) and 10.46±0.87 (p<0.01) (mean Δ±SEM, n = 8) respectively.

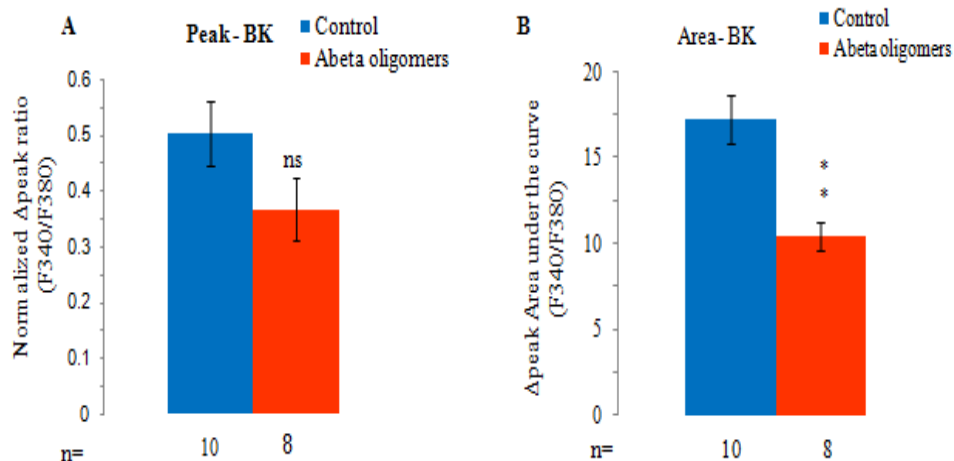


Figure 20: Aβ42 oligomers reduce Ca²⁺ release from the intracellular stores in PC12 cells. Cells were perfused with Ca²⁺ (2 mM) in mKRB for 2 minutes, exposed to Ca²⁺ free, EGTA (0.5 mM)-containing medium then challenged with respective stimuli in Ca²⁺ free, EGTA (0.5 mM)-containing medium to discharge intracellular Ca²⁺ stores in control cells or cells pretreated with Aβ42 oligomers. **(A)**, average delta peak measured above the baseline in response to BK (100 nM) in PC12 cells: control (blue bars) or PC12 cells pre-treated with Aβ42 oligomers (red bars) for 1hour. **(B)**, Average delta peak area under the curve in response to BK in PC12 control cells (blue bars) or PC12 cells pre-treated with Aβ42 oligomers (red bars) for 1hour. Data are expressed as mean ± S.E.M (n=number of independent experiments; * P< 0.05; ** P< 0.01; *** P< 0.001, unpaired Student's t-test.

4.2.3 *The total intracellular store Ca²⁺ content is not affected in cells treated with Aβ42 oligomers.*

The reduced response to IP₃ generating agonists in wt mouse neurons and PC12 cells treated with Aβ42 oligomers could be because of reduced IP₃ generation by the agonists, reduced IP₃ receptor density/sensitivity or reduced Ca²⁺ content in the stores, increased Ca²⁺ extrusion or even a combination of these mechanisms. To evaluate the total Ca²⁺ content of intracellular stores, we measured the size of the ionomycin-sensitive Ca²⁺ pool in both control and cells pre-treated with Aβ42 oligomers. As stated earlier ionomycin is a Ca²⁺ ionophore that facilitates Ca²⁺ transport across all intracellular membranes and not only across ER membranes but also from other intracellular compartments endowed with a neutral or mildly acidic pH.

The size of the ionomycin-sensitive Ca^{2+} pool was estimated from the cytosolic peak and the area under the curve obtained from the fura-2 signal after exposure to ionomycin (1 μM) in a Ca^{2+} free-EGTA containing medium. The average delta peak and area under the curve were 0.66 ± 0.04 and 18.97 ± 1.50 (mean $\Delta\pm\text{SEM}$, $n=6$) respectively, in control cortical neurons. Pre-treatment of the neurons with either $\text{A}\beta 42$ (0.5 μM) oligomers or monomers did not significantly change the intracellular store Ca^{2+} content released by stimulation with ionomycin. For neurons pre-treated with $\text{A}\beta 42$ oligomers, the average delta peak and area under the curve for cytosolic Ca^{2+} rises in response to ionomycin were 0.75 ± 0.04 ($p>0.05$) and 18.88 ± 1.54 ($p>0.05$) (mean $\Delta\pm\text{SEM}$, $n = 6$) respectively (figure 21A, B). In addition, no significant differences were observed in neurons pre-treated with $\text{A}\beta 42$ monomers. The average delta peak and area under the curve were 0.80 ± 0.05 ($P>0.05$) and 22.97 ± 2.33 ($p>0.05$) (mean $\Delta\pm\text{SEM}$, $n=7$) respectively (figure 21A, B). Similar results were obtained when monensin was used to enable ionomycin to release Ca^{2+} also from the acidic pool (figure 21C, D).

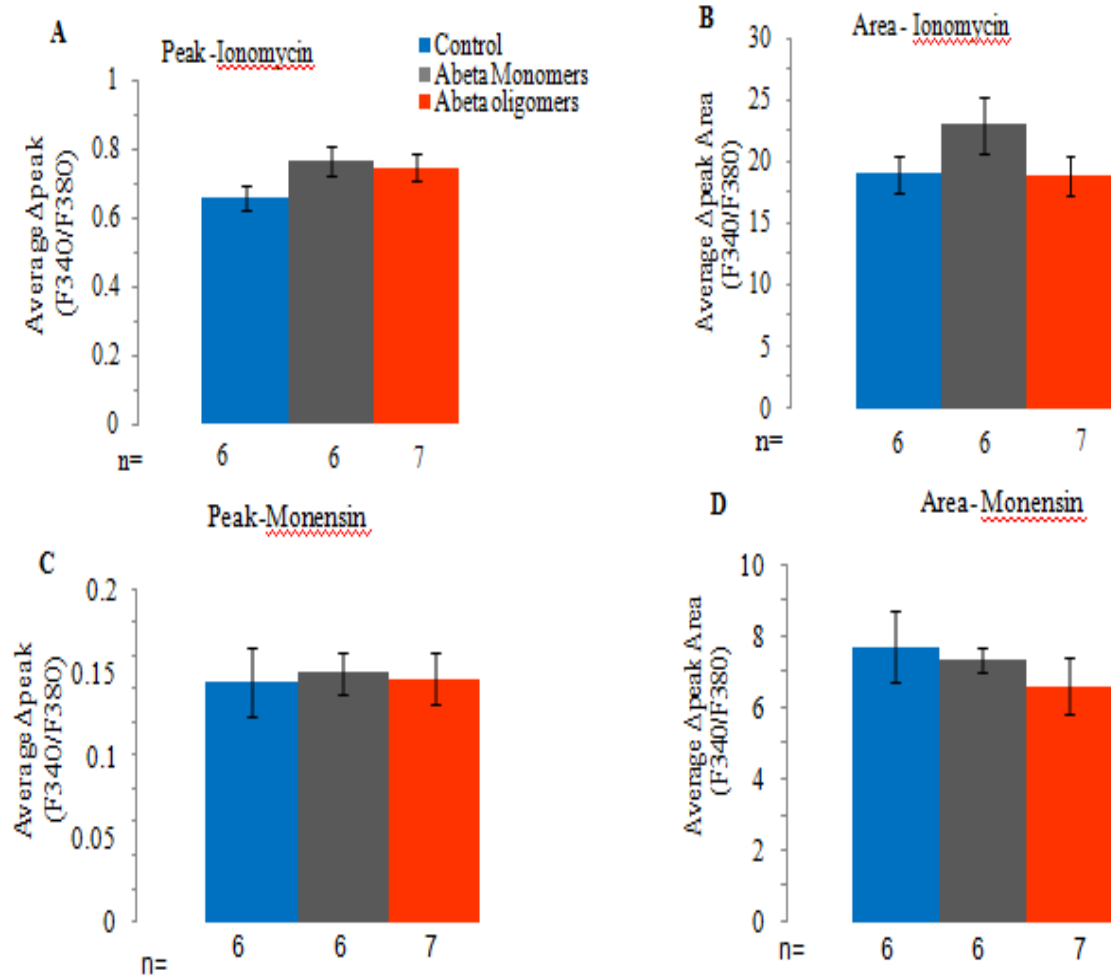


Figure 21: $\text{A}\beta$ -42 oligomers do not affect the total intracellular store Ca^{2+} content. Cortical neurons (10-12 DIV) were perfused with mKRB containing CaCl_2 (2 mM) for 2 minutes, exposed to KCl (30 mM) in the same medium for 6 minutes and then to a Ca^{2+} free, EGTA (0.5 mM)-containing medium to remove extracellular Ca^{2+} . Ionomycin (1 μM) was added in Ca^{2+} free, EGTA (0.5 mM)-containing medium to fully discharge the intracellular Ca^{2+} stores and then monensin (10 μM) in Ca^{2+} free, EGTA (0.5 mM)-containing medium to discharge Ca^{2+} from acidic compartment. (A, B), Average delta peak and area under the curve, respectively measured above the baseline in response to ionomycin (1 μM) in control (blue bars), monomer-treated (grey bars) or oligomer-treated (red bars) neurons. $\text{A}\beta$ 42 oligomers or monomers were used at 0.5 μM final concentration during loading period with Fura-2 (40 min at 37°C plus 20 min at RT). (C, D), Average delta peak and area under the curve respectively, measured above the baseline in response to ionomycin (1 μM) in presence of monensin (10 μM). Data are expressed as mean \pm S.E.M (n= number of independent experiments).

4.2.4 Ca²⁺ release from the ryanodine-sensitive intracellular Ca²⁺ stores is increased in cells treated with A β 42 oligomers

As pointed out earlier, Ca²⁺ release from stores in neurons depends not only from IP₃R channels, but also from RyRs. How A β 42 oligomers regulate the expression and function of the machinery that mediates disruption of Ca²⁺ homeostasis in AD remains unclear. However it has been suggested that A β 42 peptides can selectively elevated RyR mRNA and protein levels in vitro and in vivo (Supnet et al., 2006), thus suggesting a possible role for RyRs in AD pathology. Caffeine at high concentrations (mM) is a widely used pharmacological tool to activate Ca²⁺ release from RyR channels. To study the functional effect of A β 42 oligomers on cortical neurons, we depolarized the neurons for six minutes with KCl (30 mM) to allow loading of intracellular stores, then RyR-sensitive stores were assayed by challenging the cells with caffeine (20 mM) in Ca²⁺ free, EGTA (0.5 mM) containing mKRB. The average delta peak and area under the curve for cytosolic Ca²⁺ rises in response to caffeine were 0.14 \pm 0.02 and 1.15 \pm 0.23 (mean Δ \pm SEM, n=7) respectively, in control neurons). Notably, in neurons treated with A β 42 oligomers, Ca²⁺ release from caffeine-responsive intracellular stores was significantly increased (figure 22A, B). The average delta peak and area under the curve for cytosolic Ca²⁺ rises in response to caffeine were 0.24 \pm 0.02 (p<0.01) and 3.35 \pm 0.19 (p<0.0001) (mean Δ \pm SEM, n=6) respectively, corresponding to 1.72 and 2.93 fold increase respectively. Of note, 1 hour pre-incubation with ryanodine (20 μ M) completely inhibited the caffeine-induced Ca²⁺ release.

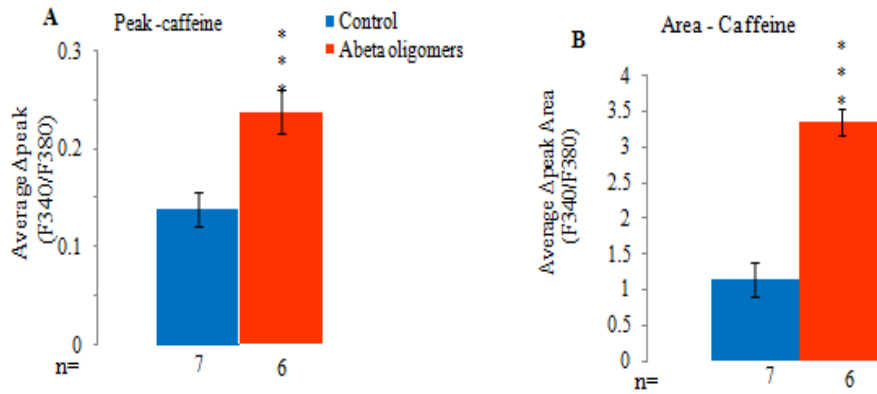


Figure 22: *Aβ42 oligomers increase Ca^{2+} release from RyRs.* Cortical neurons (10-12 DIV) were perfused with mKRB containing $CaCl_2$ (2 mM) for 2 minutes, exposed to KCl (30 mM) in the same medium for 6 minutes and then exposed to a Ca^{2+} free, EGTA (0.5 mM)-containing medium to remove extracellular Ca^{2+} and finally exposed to caffeine in Ca^{2+} free, EGTA (0.5 mM)-containing medium. (**A**, **B**), Average delta peak and delta peak area respectively, measured above the baseline in response to caffeine (20 mM) in control (blue bars) or oligomer-treated neurons (red bars). Aβ42 oligomers were used at 0.5 μM final concentration during loading period with fura-2 (40 min at 37°C plus 20 min at RT). Data presented on bars are expressed as mean ±S.E.M (n= number of independent experiments; * P< 0.05; ** P< 0.01; *** P< 0.001, unpaired Student's t-test).

DISCUSSION

AD is one of the most common neurodegenerative diseases, characterized clinically by progressive impairments in cognition and memory. Both sporadic AD and FAD cases present similar pathological features, showing at the cellular level a massive neuron loss, associated with the presence of extracellular aggregates of β -amyloid (senile plaques) and intracellular deposits of fibrillary tangles due to hyperphosphorylated tau (Goedert & Spillantini, 2006; Selkoe, 2001; Querfurth and LaFerla, 2010). Majority of reported AD cases are sporadic, yet the major breakthroughs in the disease study are based on a small percentage of FAD cases linked to autosomal dominant mutations in three genes related to $A\beta$ production: APP, PS1, and PS2.

The role of neuronal Ca^{2+} homeostasis dysregulation in aging and several other neurological disorders including AD has been underscored and extensively studied in recent years (Khachaturian, 1994; Verkhratsky, 2005; Bezprozvanny and Mattson, 2008). Neurons utilize Ca^{2+} signalling to control a variety of functions, including membrane excitability, neurotransmitter release, gene expression, cell growth and differentiation, free radical species formation and cell death (Berridge, 1998).

Particularly, FAD-linked mutations in PS1 and PS2 are causally implicated in neurodegeneration because they are linked with neuron death due to amyloid toxicity and perturbation of intracellular Ca^{2+} homeostasis. Evidence accumulated for many years since PSs were discovered (Sherrington et al., 1995; Scheuner et al., 1996) have established a strong link between PS FAD mutants and dysregulation of intracellular Ca^{2+} homeostasis both in the mouse models of AD and human patients. However the precision on when and how Ca^{2+} dysregulation occurs is still lacking; and it is not yet clear whether alterations of Ca^{2+} signalling anticipated are concomitant or follow the other pathological signs such as increase in $A\beta$ load, synapse dysfunction, neurite distortion and formation of senile plaques. As far as PS2 mutations are concerned, previous studies show that at least in human fibroblasts from FAD patients carrying

PS2-T122R, Ca^{2+} dysregulation occurs well before the onset of cognitive impairment and memory decline (Zatti et al., 2006).

PSs play a relevant role in physiological Ca^{2+} signalling. Both PS1 and PS2 have been found to regulate Ca^{2+} release from the ER through interactions with IP_3Rs (Cheung et al., 2008; 2010) and/or RyRs (Rybalchenko et al., 2008; Hayrapetyan et al., 2008), form Ca^{2+} leak channels in the ER membrane (Tu et al., 2006) and modulate SERCA pump activity (Green et al., 2008, Brunello et al., 2009). PSs affect intracellular Ca^{2+} levels by mediating Ca^{2+} influx through VOCCs (Cook et al., 2005). Thus, any alteration of both PS1 and PS2 in the form of genetic deletion or expression of mutants, results in ER Ca^{2+} dysregulation.

The results presented in this work, show the functional effects of a FAD-linked PS2 mutation (PS2-N141I) on Ca^{2+} homeostasis in a more relevant environment, closer to the disease pathology. We employed cortical neurons from two tg mouse lines, PS2.30H and B6.152H, the first is based on the PS2 mutant alone, while the second is based on the same PS2 mutant and the APP^{swe} mutant. We studied Ca^{2+} dysregulation in primary cultures cortical neurons at 10 DIV, when A β levels are still very low and no plaques are present yet, i.e well before the appearance of the first cognitive deficit (usually 8 months for the double mutant, as reported by Richards et al., 2003).

Previous studies in our laboratory have shown transient expression of FAD-linked PS2 mutants causes a strong reduction in $[\text{Ca}^{2+}]_{\text{ER}}$ in different cell lines and fibroblasts from FAD patients (Giacomello et al., 2005; Zatti et al., 2006; Brunello et al., 2009). As it was pointed out earlier, transient transfection and overexpression of mutated proteins or stably transfected cell clones succumb to two major criticisms: firstly, the level of overexpression is usually very high and secondly, the specificity of each clone may lead to erroneous interpretations of the results. By the use of western blot analysis, we observed that PS2 expression in both tg mice retained levels only slightly higher than the endogenous levels in wt control mice, unlike the case of transient expression where the expression levels of the protein studied may be as high as 50-100 times the endogenous level (Ye et al., 2009). Thus, the models used in this study would be of

physiological relevance to the in vivo situation as the aforementioned complications are minimized. However, we noted that the level of full length PS2 was slightly higher in the PS2APP tg mice. It is possible that the slight increase in PS2 expression to the enhancing effect of APP on the expression of other genes (Ohkawara et al., 2011).

In primary neuronal cultures at rest, $[Ca^{2+}]_{cyt}$ increases caused by intracellular Ca^{2+} release are highly variable, but can be substantially augmented by filling them with a brief exposure to KCl as previously reported (Smith et al, 2005; Zatti et al. 2006; Zhang et al., 2010; Supnet et al., 2010). The resulting depolarization by KCl induces opening of VOCCs, rapid Ca^{2+} influx into cortical neurons and filling of the ER stores hence allowing measurement of their Ca^{2+} content. When Ca^{2+} influx was measured in response to high concentrations of KCl, by monitoring the $[Ca^{2+}]_{cyt}$, we did not find any difference in KCl-induced Ca^{2+} peaks and plateaus between wt and tg neurons suggesting that PS2-N141I (but also mutant APP) does not affect neuronal global Ca^{2+} handling at this early stage.

The ER is the major and most important intracellular Ca^{2+} store endowed with Ca^{2+} pumps (SERCA) and release receptor channels (IP₃R and RyRs) on its membrane. Both Ca^{2+} pumps and release receptor channels play a key role of modulating intracellular Ca^{2+} dynamics. Given that transfection of primary neuronal cultures (and acute brain slices as well) is extremely inefficient with the available ER-targeted Ca^{2+} probe, we chose to employ trappable cytosolic fluorescent Ca^{2+} probes like fura 2/AM. We estimated the amount of Ca^{2+} stored in the ER lumen from the size of the Ca^{2+} released into the cytosol by stimulation of IP₃R and RyR channels in a Ca^{2+} free extracellular medium with receptor specific agonists.

Results from this study show that cortical neurons from the two tg mouse models of AD based on PS2-N141I have a similar reduction of cytosolic Ca^{2+} release in response to IP₃ generating agonists (CCH and DHPG) as compared to wt neurons. Whereas CCH binds to muscarinic receptors, DHPG binds to metabotropic receptors to activate specific PLC isoforms. Interestingly reduction in Ca^{2+} release from intracellular

stores was observed regardless of the IP₃ generating agonist employed, reflecting a reduction of the [Ca²⁺]_{ER} in the tg neurons.

The reduction in the ER Ca²⁺ content in both tg cortical neurons suggests that PS2-N141I has an inherent capacity to modulate the dynamic release and storage of Ca²⁺ by the ER also at the level of tg neurons. Although we can not exclude a defect in agonist-receptor coupling in tg neurons, the most plausible explanation for that reduction is the possibility of a functional defect in the Ca²⁺ entry/exit pathways of the ER, as previously reported in cell lines expressing PS2 mutants (Giacomello et al., 2005; Zatti et al., 2006; Brunello et al., 2009). In line with a previous study using PS1 mutants (Leissring et al., 2001), comparable expression levels of IP₃Rs and SERCA-2B were detected in primary culture neurons as well as in brain homogenates (14days) from wt and tg mice expressing PS2-N141I.

Moreover, our results show that the total Ca²⁺ content of intracellular stores, as assayed by ionomycin, is also compromised in the tg neurons. As explained earlier, ionomycin is a Ca²⁺ ionophore that facilitates Ca²⁺ transport across the majority of the membranes: the ionomycin-sensitive Ca²⁺ pool may come from neutral and mild acidic intracellular compartments, such as the Golgi apparatus and part of the constitutive vesicles (Fasolato et al. 1991). We observed strong reduction in the size of the pool mobilizable by ionomycin in both PS2 and PS2-APP neurons. Taken together, our data suggest that cortical neurons in primary cultures from both tg mice show altered Ca²⁺ dynamics marked by reduced total Ca²⁺ content of intracellular stores and, consequently, reduced response to IP₃-generating agonists.

In addition to IP₃Rs, RyRs widely distributed on the ER membrane also mediate ER Ca²⁺ release. Particularly, RyRs play a crucial role in mediating Ca²⁺ release from the intracellular stores into the cytosol by sensing Ca²⁺ concentration on its cytosolic side, thus establishing a positive feedback mechanism (Lanner et al., 2010; Fill and Copello, 2002). In fact, a small amount of Ca²⁺ in the cytosolic compartment near RyR will cause it to release even more Ca²⁺, by activation of CICR, resulting in amplification of the Ca²⁺ signal (Stutzmann et al., 2007).

A novel unexpected finding emerged with tg mice (not previously assayed in the cell lines because of lack of sensitivity) is the increase in Ca^{2+} release upon stimulation with caffeine. Increased Ca^{2+} release by RyRs is a finding also common to other AD mouse models based on PS-FAD mutants (Chan et al., 2000; Smith et al., 2005; Lee et al., 2006; Stutzmann et al., 2006; Chakroborty et al., 2009; Zhang et al., 2010; Supnet et al., 2010). It is worthy note that both the IP_3 - and caffeine-sensitive Ca^{2+} pools are smaller than the total pool released by ionomycin and, between these latter, the pool released by caffeine is the smallest. Therefore, the exaggerated Ca^{2+} release observed with caffeine does not contradict the overall reduction in the store Ca^{2+} content.

Consistently, we also found a modest but significant increase in the level of RyR2 in primary neuronal cultures and brain homogenates from tg mice as compared to wt. The fact that there is upregulation of RyRs expression and likewise the related increase in ER Ca^{2+} release via RyRs, one may anticipate that even the overall Ca^{2+} signal should also be amplified as result of excessive activation of CICR. However, this was not the case since the massive Ca^{2+} response induced by depolarization with high KCl was similar in both tg and wt neurons as previously reported (Smith et al., 2005; Zhang et al., 2010; Supnet et al., 2010). Given the small size of caffeine-sensitive stores, it is also possible that their contribution was masked. It is possible that, the upregulation of RyRs could be due to either an adaptation phenomenon to compensate the reduction in Ca^{2+} release via IP_3 Rs or a direct effect of mutant PS2 itself on RyR activity (Lee et al., 2006; Hayrapetyan et al., 2008; Brunello et al., 2009). Since IP_3 generating agonists can also activate RyRs (Mellentin et al., 2007), it is also conceivable that the reduction in ER Ca^{2+} release through IP_3 Rs reported in this study and measured as $[\text{Ca}^{2+}]_{\text{cyt}}$ rises may have been underestimated due to concomitant stimulation of CICR.

PSs interact with both the ER Ca^{2+} uptake and release machinery through their interaction with SERCA pump activity and IP_3 R and RyR gating activity (Cheung et al., 2008; Green et al., 2008). Indeed compelling evidence indicate that the reduction in ER Ca^{2+} content, observed in different FAD-linked PS2 mutants, mainly occurs because of SERCA pump inhibition and partially due to increased Ca^{2+} leak through IP_3 R and RyR

Ca²⁺ channels (Brunello et al., 2009). The overall outcome of these effects is partially depleted Ca²⁺ stores and consequently less Ca²⁺ available for cytosolic release upon stimulation. We confirm this finding showing that in primary cortical neurons from both tg mice, IP₃-sensitive stores have a reduced Ca²⁺ content (as assayed by CCH and/or DHPG), a reduced capability to restore/maintain their Ca²⁺ content and increased passive Ca²⁺ leak.

Our results provide novel and specific aspects of Ca²⁺ signalling in tg mice based on FAD-mutant PS2. Firstly, the reduction of the store Ca²⁺ content, as assayed by both ionomycin and IP₃ generating agonists, is of an entity similar to that previously estimated in cell lines transiently over-expressing the same PS2 mutant at high levels (Zampese et al., 2009). Therefore, the observed reduction cannot be considered an artifact of PS2 over-expression, but it is rather due to the mutant itself. In addition, the relevant role of PS2-N141I on cellular Ca²⁺ handling is further strengthened by the findings from this study: Ca²⁺ dysregulation described in our models appears to occur at a very early stage prior to the formation of amyloid plaques. Furthermore, Ca²⁺ dysregulation appears similar both qualitatively and quantitatively in the two tg mouse lines, suggesting that overexpression of mutant APP in double tg mice has no primary effect on the store Ca²⁺ content at this early stage. Indeed, the direct role of FAD-linked APP mutation in perturbing Ca²⁺ homeostasis has not yet been demonstrated (Stieren et al., 2010).

Although PSs play other physiological functions, which have recently been unravelled, they primarily represent the catalytic core of the multiprotein γ -secretase complex required for A β production. Both FAD-linked PS1 and PS2 mutations have been associated with altered A β peptide generation, resulting in increased ratios between the amyloid peptides A β 42/A β 40 (Borchelt et al, 1996; Scheuner et al, 1996; Citron et al., 1997; Tomita et al., 1997). The PS2-APP line has been reported to produce high levels of both peptides with plaque deposition starting between five and six months (Richard et al., 2003; Ozmen et al., 2009); conversely the PS2.30H line that expresses only the mutant PS2 is expected to have a much reduced A β load.

We tested this aspect and observed that, at two weeks in brain homogenates of single tg mice the amount of total (soluble and insoluble) A β 42 load is about four times that found in wt, whereas, in double tg mice, it exceeds this value by a factor of 40 times. Within such differences in levels of A β 42 load between single and double tg mice and yet similar ER Ca²⁺ dynamics, it is therefore rather unlikely that the reduction in ER Ca²⁺ release upon stimulation can be attributed to intra- and/or extracellular A β peptides. The interpretation of these results is that PS2 mutation might be responsible for the ER Ca²⁺ dysregulation observed in our model.

Nevertheless, the results described here are at odd, in respect to Ca²⁺ release from intracellular stores in cells expressing most of the PS1 and some PS2 mutants (Zampese et al., 2009). Exaggerated Ca²⁺ release from intracellular stores in cells over-expressing PS1 (Leissring et al., 1999a; Chan et al., 2000; Schneider et al., 2001; Stutzmann et al., 2004) and PS2 mutants (Leissring et al., 1999b) has been reported. Data from these groups suggested that the elevated Ca²⁺ release from the ER was due to abnormal increase in ER Ca²⁺ content, leading to “Ca²⁺ overload” (Leissring et al., 2000). The Ca²⁺ overload hypothesis proposes that reduced ER Ca²⁺ leak due to loss of function of PS (as ER leak channels) results in a build up of [Ca²⁺]_{ER} and consequently to an exaggerated Ca²⁺ release upon cell stimulation (Tu et al., 2006, Nelson, 2007, Zhang et al., 2010).

The validity of the Ca²⁺ overload hypothesis has recently been questioned, since over-expression of FAD-linked PS mutants enhanced Ca²⁺ release even in the absence of ER Ca²⁺ overload (Cheung et al., 2008; 2010). In fact, these latter findings suggested that exaggerated ER Ca²⁺ release could occur because of increased sensitivity of the ER Ca²⁺ release channels rather than to ER Ca²⁺ overload (Cheung et al., 2008). So far, it remains unresolved as to why there should be divergent results in respect to the functional effects of these PS mutants on Ca²⁺ homeostasis. Among the possible explanations is the fact that studies sustaining the Ca²⁺ overload hypothesis mainly focused on PS1 mutants and primarily based on cytosolic Ca²⁺ measurements (Leissring et al., 1999; LaFerla 2002; Stutzmann et al., 2004; Thinakaran and Sisodia, 2006;

Zampese et al., 2009). Indeed discrepancies arose when the focus shifted from PS1 to PS2 mutations and when organelle-targeted Ca^{2+} probes were employed (Zampese et al. 2009).

Another possible reason for the inconsistency of results regarding the functional effects of FAD-linked PS mutations on Ca^{2+} homeostasis could arise from the differences in methodologies and cell types used by different researchers to measure ER Ca^{2+} release. Most of the previous studies that reported elevated ER Ca^{2+} release used caged IP_3 to induce Ca^{2+} release through IP_3Rs , on the contrary, in our study we used IP_3 generating agonists. IP_3 is known to sensitize the receptors leading to exaggerated response (Leissring et al., 1999a) as might be the case in experiments carried out by using caged IP_3 .

Despite the contradictory results available in literature, it remains undisputable that FAD-linked PS2 mutants cause an imbalance of intracellular Ca^{2+} homeostasis. Changes in ER Ca^{2+} dynamics due to FAD-linked mutations should not be underestimated when considering the pathophysiology of FAD. Particularly, intracellular Ca^{2+} dysregulation has a tangible contribution in neurodegeneration and memory impairment by affecting synaptic stability, plasticity, and neurotransmission. Neural events such as LTP and LTD, which are the electrophysiological correlate of learning and memory, are highly dependent on both extracellular and intracellular Ca^{2+} dynamics. Such activity dependent synaptic events are impaired in cortical and hippocampal neurons of AD patients and tg mice expressing FAD-linked PS1 or PS2 mutants (Parent et al., 1999; Schneider et al., 2001; Richards et al., 2003; Berridge, 2011).

Furthermore, studies in both in vivo and in vitro models suggest that FAD-linked PS1 and PS2 mutations perturb intracellular Ca^{2+} homeostasis in a manner that sensitizes neurons to apoptosis and excitotoxicity and hence neurodegeneration (Bezprozvanny and Mattson, 2008). The FAD-linked PS2 mutants, in particular affect Ca^{2+} regulation by causing partial ER Ca^{2+} depletion and thus lowering its level in the intracellular stores. Data on the pathophysiological relevance and implication of a partially depleted ER as far as FAD is concerned lacks. Previous studies employing both genetic and

pharmacological approaches have suggested that varying the Ca^{2+} concentration inside the ER can have detrimental effects on cell survival (Scorrano et al., 2003). Reduced ER Ca^{2+} is protective against stimuli like ceramide, H_2O_2 and arachidonic acid, which act through the mitochondrial death pathway (Pinton et al., 2000; 2001; Scorrano et al., 2003; Oake et al., 2003; Ferrari et al., 2010) involving ER Ca^{2+} release.

Our data show similar neuronal death in PS2 tg neurons as compared to wt neurons when exposed to a death stimulus linked to ER Ca^{2+} release, H_2O_2 in presence or absence of IP_3 generating agonist to induce ER Ca^{2+} release. Under such conditions, the mitochondria accumulate Ca^{2+} asynchronously with slow kinetics and may suffer changes in the morphology associated with PTP opening. Using genetically encoded Ca^{2+} indicators specifically targeted to mitochondria (aequorin- and GFP-based probes) in SH-SY5Y cells and rat primary neuronal cultures, we have previously shown that overexpression or down-regulation of PS2, but not PS1, modulates the Ca^{2+} shuttling between ER and mitochondria (Zampese et al., 2011; see appendix 1 for details).

Mitochondria take up Ca^{2+} through a low affinity electrogenic uniporter, the recently identified MCU (Drago et al., 2011; De Stefani et al., 2011) because they are located at privileged locations where they sense microdomains of high $[\text{Ca}^{2+}]$ (Rizzuto and Pozzan, 2006; Ferrari et al., 2010; Pinton et al., 2008; Giorgi et al., 2009). In fact, IP_3 producing agonists increase mitochondrial matrix Ca^{2+} , and if the uptake is too high, it may turn to apoptosis via the PTP opening (Szalai et al., 1999). In this regards, H_2O_2 used here, has been shown to activate apoptotic programmes by triggering a progressive Ca^{2+} flux from intracellular stores, leading to increased mitochondria Ca^{2+} uptake. When the Ca^{2+} signal is sufficiently high, it will triggers apoptosis because of mitochondria Ca^{2+} overload, characterized by mitochondria morphological alterations and loss of membrane potential. Such changes are likely to trigger the opening of the PTP and eventually cytochrome c release into the cytosol and therefore activation of caspases, the final executioners of the death program.

The FAD-linked PS2 mutants strongly favour Ca^{2+} transfer between ER and mitochondria by increasing the interaction between the two organelles that augments the

frequency of Ca^{2+} hot spots generated at the cytoplasmic surface of the outer mitochondrial membrane upon stimulation (Zampese et al., 2011). In line with our previous work and as far as FAD is concerned, a favoured interaction between the ER and mitochondria might result either in chronic mitochondrial Ca^{2+} overload. Such overload may lead to metabolic dysfunction and ultimately to neuronal death or, it may have a pro-survival effect by improving the functional coupling between ER and mitochondria under conditions of reduced ER Ca^{2+} content. The survival assay, carried out in primary neuronal cultures, excludes an increased toxicity linked to the PS2 mutant when the apoptotic stimulus was coupled with ER Ca^{2+} release.

Neuronal excitability has a strong link with intracellular Ca^{2+} dynamics. Ca^{2+} released from the ER modulates neuronal excitability by altering the plasma membrane potential (Bacci et al., 1999). To a large extent the interplay between the ER and the plasma membrane operating as binary membrane systems controls neuronal Ca^{2+} signalling (Cahalan, 2009). Synchronous neuronal Ca^{2+} oscillations or spikes are a key indicator of interneuronal communication, required for different physiological functions (Bacci et al., 1999). Such Ca^{2+} spikes usually occur as burst of synchronous neuronal activities with a well-defined spatial and temporal pattern. In primary neuronal cultures, groups of neurons show synchronous activities that occur in bursts, especially upon plasma membrane depolarization (Bacci et al., 1999; Pratt et al., 2011).

During normal aging and in AD patients, defective neuronal excitability and their ability to maintain tight regulation of Ca^{2+} gradients across the plasma membrane and ER membrane is a commonly reported feature. This is a common feature because neurons encounter increased oxidative stress and inefficient energy metabolism. The overall outcome for such changes in Ca^{2+} handling finally compromises the function of proteins that control membrane excitability and subcellular Ca^{2+} dynamics. Indeed a growing body of evidence points out toward a dysfunction of neuronal networks during AD pathology as result of defective intrinsic neuronal excitability mainly attributed to dysregulation of Ca^{2+} homeostasis (Santos et al., 2010). Alteration in neuronal

excitability is likely to affect neuronal communication and plasticity, both being essential for learning and memory.

To understand the effect of PS2-N141I on Ca^{2+} -dependent neuronal excitability and indirectly on synaptic transmission, we examined the synchronous neuronal activity induced by picrotoxin (a GABA receptor inhibitor). Our results show significantly elevated picrotoxin evoked Ca^{2+} spikes in the tg neurons as compared to wt controls. In the tg neurons, the number of synchronous Ca^{2+} spikes, during a fixed time, was almost twice that found in wt neurons, without significant changes in amplitudes. These high levels of synchronous Ca^{2+} spikes required influx of extracellular Ca^{2+} , as removal of Ca^{2+} from the medium abolished the spikes. Furthermore, these synchronous Ca^{2+} spikes did not require Ca^{2+} release from the ER, because pre-emptying of the ER by using either thapsigargin or ryanodine had no effect in both wt and tg neurons. Interestingly, wt neurons treated with thapsigargin had a tendency towards increased amplitude of synchronous spikes possibly due to activation of SOCCE. It remains to demonstrate whether the chronic reduction in ER Ca^{2+} release due to the PS2 mutant, has any role in determining the increased number of synchronous Ca^{2+} spikes observed in the tg neurons.

It is possible that partial depletion of the intracellular Ca^{2+} stores in the PS2 tg neuron serves as a trigger for activation of the synchronous Ca^{2+} spikes. Although we do not have strong evidence to support this hypothesis, a culprit candidate would be the SOCC. In a context where most of the key actors remain to be identified, our results show that Ca^{2+} oscillations required a Ca^{2+} influx that was completely inhibited by LaCl_3 at low concentrations (μM) range, suggesting that Ca^{2+} entry could be possibly via a Ca^{2+} permeable channel. It remains to be determined the protein expression levels of the most relevant actors in SOCCE, i.e. STIM-1/2 and Orai1/2. Further investigation is required to reveal the actual mechanism behind this fact. An alternative explanation is that this phenomenon is unrelated and due to different mechanisms other than the functional effects of the PS2 mutant on Ca^{2+} homeostasis.

Conversely, increased rate of spontaneous synchronous Ca^{2+} oscillations has previously been reported in PS1 knockout neurons (Pratt et al., 2011) and was reduced by lentivirus mediated-expression of wt PS1 or FAD-linked PS1-M146V but not PS1-D257A that does not support γ -secretase activity. In this particular study, the authors postulate that these effects are due to a novel and selective role of the γ -secretase in the regulation of low-level tonic Ca^{2+} influx into presynaptic axon terminals that selectively influences spontaneous release. Whether a similar mechanism applies also to the PS2 mutant is a subject of further investigation. The PS2 mutant may also function at multiple levels to regulate and stabilize the $[\text{Ca}^{2+}]_{\text{cyt}}$ that ultimately controls the neuronal firing behaviour and influences synaptic transmission. How exactly this phenomenon manifests itself and its relevance to FAD pathology, is unclear

Nevertheless, compelling evidence suggests that FAD-linked PS1 mutations are strongly associated with intractable epileptic seizures much more than sporadic AD, further pointing out that these mutations might have a profound effect on overall network excitability (Supnet and Bezprozvanny, 2010). Apart from causing intracellular Ca^{2+} dysregulation such FAD-linked PS1 mutants have also been implicated to cause neuronal hyperexcitability, epileptiform activity and consequently functional disruption of neuronal networks in tg mouse models of AD (Del Vecchio et al., 2004; Kuchibhotla et al., 2008). Alterations in ER Ca^{2+} handling are also part of early adaptation strategies utilized by neurons to combat and depress increased membrane excitability during AD pathology and thus prevent excitotoxicity (Supnet and Bezprozvanny, 2010).

Interestingly, $\text{A}\beta_{42}$ particularly the oligomeric form, can also alter neuronal excitability. Intraneuronal $\text{A}\beta_{42}$ tends to increase with time in AD tg neuronal cultures and synaptic activities have been shown to reduce $\text{A}\beta_{42}$ load (Tampellini et al., 2011). It is therefore possible that increase in excitability is an adaptive phenomenon to deal with intraneuronal $\text{A}\beta_{42}$ load. Alternatively, the alteration in neuronal excitability is likely to be a multifaceted event that could arise as result of altered PS activity and/or secondary effects due to $\text{A}\beta_{42}$.

As pointed out earlier PS2 and PS2-APP mice produce both extra- and intra-neuronal A β 42 peptides (Richard et al., 2003; Ozmen et al., 2009), though PS2-APP tg mouse produces a larger quantity. Compelling evidence indicates that A β 42 can also perturb intracellular Ca²⁺ homeostasis through destabilization of cytosolic Ca²⁺ levels (Demuro et al., 2005). Precisely, how A β 42 causes intracellular Ca²⁺ dysregulation is still controversial. There are suggestions that A β 42 oligomers can elevate the [Ca²⁺]_{cyt} by either functioning as artificial channels or by activating plasma membrane Ca²⁺ channels (Arispe et al., 2010; Demuro et al., 2011). However, considering our results on single and double tg neurons it is very unlikely that the reduction in ER Ca²⁺ release described was due to the effect of A β 42. This observation also strengthens the hypothesis that the reduced [Ca²⁺]_{ER} observed in our model is attributable to the PS2 mutation.

Conversely, treating wt neurons with synthetic A β 42 oligomers for a brief period ranging from five minutes to an hour causes significant alteration of intracellular Ca²⁺ dynamics (Kelly et al., 2006; Resende et al., 2008). Results from our study show that wt cortical neurons from C57B6J mice, when pre-treated with A β 42 oligomers, exhibit reduced Ca²⁺ release in response to IP₃ generating agonists when compared with untreated controls. Our results also suggest that A β 42 oligomers do not affect the total ER Ca²⁺ content (as assayed by ionomycin) instead affect activation of IP₃Rs by IP₃ generating agonists.

These findings are in agreement with previous data showing that exposure of rodent cortical neurons to other A β species, such as A β 25-35 and A β 1-40, resulted in a concentration and time-dependent manner, reduction of ER Ca²⁺ release induced by CCH (Kelly et al., 2006). These authors associate the reduction in ER Ca²⁺ release to the attenuation of CCH-induced GTPase activity by the A β peptides. A β peptides drastically decreased the CCH-induced accumulation of inositol phosphates (IP, IP₂, IP₃, and IP₄), suggesting that their generation and accumulation is critically affected in the presence of A β 25-35 and A β 40.

It is possible that A β peptides in general interfere with both metabotropic and muscarinic receptor coupling to the G-proteins that are required for IP₃ generation and

subsequently affect downstream events including IP₃-induced Ca²⁺ release from the ER. Furthermore, saturation-binding assays like [³H] quinuclidinyl benzilate (QNB) (Kelly et al., 1996), suggests that Aβ does not affect the ligand binding affinity to the receptors. A plausible explanation for this effect is that Aβ peptides have a specific effect on the efficiency of G-protein coupling to metabotropic and muscarinic receptors. However, the question on how Aβ affects G-protein coupling to muscarinic receptors remains unanswered. Reduction in muscarinic receptors has previously been reported in studies involving postmortem brain tissues from AD patients and yet the mechanism underlying such changes are still unknown (Mulugeta et al., 2003; Tsang et al., 2007, Querfurth and LaFerla, 2010). Taken together our data and also by others suggest that Aβ₄₂ affects IP₃ production and hence causes reduced Ca²⁺ release from the ER while the total store Ca²⁺ content is spared.

The results described here are at odd with previous reports, as far as the total Ca²⁺ released from intracellular stores is concerned. Recent evidence shows that exposure of neurons to Aβ depletes the ER Ca²⁺ content (Resende et al., 2008). Aβ can directly activate IP₃R and raise the cytosolic Ca²⁺ by making the IP₃R channels leaky. The latter suggestion implies that acute Aβ application on neurons would render exaggerated cytosolic Ca²⁺, a phenomenon we did not observe in our model. Although we do not have a clear explanation for the differences between our results and those described by Resende et al (2008), methodological differences could be accounted for the discrepancies. It is important to note that we measured Ca²⁺ release from the intracellular stores in mouse primary cortical neurons, whereas Resende and colleagues measured Ca²⁺ release from intracellular stores from primary rat embryonic cortical neurons. However, to clear out this controversy it would be necessary to apply permeable caged-IP₃ to study directly the effect of Aβ₄₂ oligomers on intracellular Ca²⁺ stores.

In line with previous studies, we observed an increase in ER Ca²⁺ release via RyRs in neurons pretreated with Aβ₄₂ oligomers (Supnet et al., 2006; 2010; Resende et al., 2008) upon stimulation by a pharmacological agonist. The mechanism through

which A β 42 regulates the expression and function of the machinery that mediates dysregulation of intracellular Ca²⁺ homeostasis in AD, is still blurred and a subject of further investigation. However emerging evidence from recent studies suggests that high levels of A β 42 can selectively elevate RyR mRNA and protein levels and function both *in vitro* and *in vivo* (Supnet et al., 2006; Chakroborty et al., 2009).

The hypersensitivity of RyR receptors in AD, especially in this neuronal pathway, could be an additional mechanism that contributes to synaptic failure and memory dysfunction in AD. However this argument does not always hold true because knockdown of RyR3 with small interfering RNA (siRNA) in cortical neuronal cultures from APP tg mice (Supnet et al., 2010), which produce abundant A β 42, increases their susceptibility to exogenous stressors like glutamate and H₂O₂. In the same study Supnet and colleagues (2010) suggest that upregulation of RyRs protects against rather than contributing to neuronal death. Nevertheless, the increased neuronal RyR response due to A β 42 oligomers may serve as an adaptive phenomenon to deal with impaired IP₃Rs activity and protect neurons; however, for the time being, it remains an open question for further investigation.

CONCLUSIONS

Neuronal Ca^{2+} dysregulation is a key and frequently report phenomenon in the pathogenesis of both sporadic AD and FAD. In the study described here we took advantage of the two available lines of tg mouse models of AD, homozygous for human PS2-N141I and double homozygous for human PS2-N141I and human APP^{swe} mutations to investigate in a more physiological and relevant environment the functional effects of PS2 mutant on Ca^{2+} homeostasis. By employing classical Ca^{2+} imaging techniques we particularly focused our attention on Ca^{2+} dysregulation in primary cortical neuronal cultures.

The results from this study give an insight on the functional effects of FAD-linked PS2 mutants on neuronal Ca^{2+} homeostasis. This study highlights the role of PS2-N141I in modulating Ca^{2+} homeostasis of cortical neurons. We have demonstrated that, irrespective of the presence of mutant APP, modest expression of PS2-N141I altered the Ca^{2+} dynamics of intracellular stores. The total Ca^{2+} content of intracellular stores is partially depleted, as demonstrated by reduced Ca^{2+} release upon ionomycin stimulation. Consequently, the tg neurons have reduced Ca^{2+} release in response to IP_3 -generating agonists. However, the PS2 mutant does not affect the protein expression levels for both SERCA pump and IP_3 Rs. Our results suggest that the PS2-N141I FAD mutant causes a functional defect in ER Ca^{2+} entry/exit pathways. We also show that both tg neurons express very low levels of the mutant protein but show Ca^{2+} dysregulation, similar quantitatively and qualitatively to that previously reported in cell lines upon transient over-expression of the same mutant protein.

Conversely, measurements of Ca^{2+} release via RyRs revealed a novel and unexpected finding in PS2 mutant tg mice i.e. increased Ca^{2+} release in response to caffeine. In addition, RyR2 protein expression level was elevated in tg neurons. Upregulation of RyRs function and protein levels could save as an adaptation

phenomenon to compensate the reduction in Ca^{2+} release via IP_3Rs or a direct effect of mutant PS2 on RyR or a secondary effect.

Furthermore, PS2-N141I causes alteration in neuronal Ca^{2+} excitability. The tg neurons had significantly elevated number of picrotoxin-evoked synchronous Ca^{2+} oscillations, which required extracellular Ca^{2+} influx but not Ca^{2+} release from intracellular stores. Interestingly, while Ca^{2+} dysregulation appeared to be similar qualitatively and quantitatively in both single and double tg mouse models, the total amount of brain A β 42 and A β 40 peptides (ELISA) as well as their ratios were strikingly different between the two tg lines. These results strongly suggest that in tg mice the expression of mutant APP and/or A β levels have no primary effect on the store Ca^{2+} content at this early stage and provide evidence that the quite similar effects on Ca^{2+} dynamics observed in both tg mice are due to the mutant PS2.

Finally, results presented in this work suggest that although Ca^{2+} dysregulation is an early event in FAD, it does not affect neuronal response and vulnerability to cytotoxic stimuli at this early stage.

The second part of this study focused on the role of A β 42 oligomers in cellular Ca^{2+} dynamics. Synthetic A β 42 oligomers reduced Ca^{2+} release in response to IP_3 generating agonists in wt neurons but did not affect the total Ca^{2+} content as monitored by ionomycin. Conversely, A β 42 oligomers increased the Ca^{2+} release induced by caffeine. It is likely that A β 42 oligomers exert their effect on the activation pathway from IP_3 generating agonists to IP_3Rs . However, the mechanisms through which A β 42 deranges intracellular Ca^{2+} homeostasis require further investigation.

Nonetheless, it is conceivable that in addition to A β 42 oligomers, also intracellular Ca^{2+} stores could become likely therapeutic targets in FAD and AD in general.

PERSPECTIVES AND FURTHER STUDIES

The results described in this study highlight the role of PS2-N141I in modulating Ca^{2+} homeostasis of cortical neurons. Certainly, further investigation of FAD-PS2 induced alterations in Ca^{2+} dynamics of intracellular stores by using the model employed in this study is inevitable. In-depth analysis of such dynamics by employing available probes targeted to various cellular compartments (organelles) is necessary and will cast new light on the role of intracellular store Ca^{2+} alteration in PS2 based AD mouse models.

Despite the methodological difficulties faced with, the use of both synthetic and genetically encoded Ca^{2+} probes have allowed to study and understand the complex interactions between different Ca^{2+} sources and their ability to produce spatial and temporal specificity of signalling in living cells. This has enabled the understanding of the role of Ca^{2+} signalling in the basic functioning of the body and even predicting the ultimate effects in cases of dysregulation. However, the major methodological challenges have always been how to elucidate Ca^{2+} signalling, handling and processing in different organelles and linking it with the downstream effectors.

In order to address these ambiguities, research focus in this discipline should be to re-examine the role and the complex mechanisms of Ca^{2+} signalling and link them to the physio-pathological changes observed in different diseases particularly AD. To study accurately the role of Ca^{2+} in physiopathology, a methodology that allows constant monitoring of Ca^{2+} dynamics in living cells with both spatial and temporal occurrence is essential. Furthermore, this may require development of new methodological approaches or refine available techniques. The use of in vivo animal models is also inevitable in order to extend and translate some of the interesting Ca^{2+} signalling observations in cell and tissue cultures into the true biological systems.

Particularly, the use of genetically encoded Ca^{2+} sensors targeted to different cellular organelles like: the ER, mitochondria, the Golgi apparatus, lysosomes and

vesicles will allow direct measurement and analysis of Ca^{2+} steady state and dynamics in neurons. The use of viral vectors will be mandatory to reach high transfection efficiency in primary neuronal cultures and in vivo too.

The mechanisms through which PS2-N141I upregulates RyR receptor expression and function and its relevance, as far as FAD is concerned, require further investigation. Whether this phenomenon has beneficial or detrimental effects requires further studies. Furthermore, PS2-N141I alters neuronal Ca^{2+} excitability. Nevertheless, the exact mechanisms are open questions for further investigation. In the context where most of the key actors remain to be identified, data presented here show that Ca^{2+} oscillations required Ca^{2+} influx (but not Ca^{2+} release) that was completely inhibited by LaCl_3 at low concentrations, suggesting that Ca^{2+} entry could be possibly via a Ca^{2+} permeable channel of the SOCC type. Further investigations are required to reveal the actual mechanism behind this fact.

The final part of my work opens new perspectives about the possible implication of the role of $\text{A}\beta_{42}$ oligomers in ER Ca^{2+} dynamics. However, the mechanisms through which $\text{A}\beta_{42}$ deranges ER Ca^{2+} homeostasis require further investigation. It is likely that $\text{A}\beta_{42}$ oligomers exert their effect on the activation pathway from IP_3 generating agonists to IP_3Rs . Determining IP_3 production in neurons pretreated with $\text{A}\beta_{42}$ oligomers or stimulation of IP_3Rs in such neurons by using caged IP_3 will be useful in addressing some of these questions.

REFERENCES

- Abner, E. L., Kryscio, R. J., Schmitt, F. A., Santacruz, K. S., Jicha, G. A., Lin, Y., Neltner, J. M., Smith, C. D., Van Eldik, L. J. and Nelson, P. T. (2011). "End-stage" neurofibrillary tangle pathology in preclinical Alzheimer's disease: fact or fiction? *J Alzheimers Dis.* **25**(3):445-53.
- Addis, D. R. and Tippett, L. J. (2004). Memory of myself: autobiographical memory and identity in Alzheimer's disease. *Memory.* **12**(1):56-74.
- Ahn, K., Shelton, C. C., Tian, Y., Zhang, X., Gilchrist, M. L., Sisodia, S. S. and Li, Y. M. (2010). Activation and intrinsic gamma-secretase activity of presenilin 1. *Proc Natl Acad Sci U S A.* **107**(50):21435-40.
- Alberdi, E., Sánchez-Gómez, M.V., Cavaliere, F., Pérez-Samartín, A., Zugaza, J. L., Trullas, R., Domercq, M. and Matute, C. (2010). Amyloid beta oligomers induce Ca²⁺ dysregulation and neuronal death through activation of ionotropic glutamate receptors. *Cell Calcium.* **47**(3):264-72.
- Albert, M. S., DeKosky, S. T., Dickson, D., Dubois, B., Feldman, H. H., Fox, N. C., Gamst, A., Holtzman, D. M., Jagust, W. J., Petersen, R. C., Snyder, P. J., Carrillo, M. C., Thies, B. and Phelps, C. H. (2011). The diagnosis of mild cognitive impairment due to Alzheimer's disease: recommendations from the National Institute on Aging-Alzheimer's Association workgroups on diagnostic guidelines for Alzheimer's disease. *Alzheimers Dement.* **7**(3):270-9.
- Allen, V., Swigart, P., Cheung, R., Cockcroft, S. and Katan, M. (1997). Regulation of inositol lipid-specific phospholipase c delta by changes in Ca²⁺ ion concentrations. *Biochem J.* **327** (Pt 2):545-52.
- Ankarcrona, M. and Hultenby, K. (2002). Presenilin-1 is located in rat mitochondria. *Biochem Biophys Res Commun.* **295**(3):766-70.
- Annaert, W. G., Levesque, L., Craessaerts, K., Dierinck, I., Snellings, G., Westaway, D., George-Hyslop, P. S., Cordell, B., Fraser, P. and De Strooper, B. (1999). Presenilin 1 controls gamma-secretase processing of amyloid precursor protein in pre-golgi compartments of hippocampal neurons. *J Cell Biol.* **147**(2):277-94.
- Arbabian, A., Brouland, J. P., Gélébart, P., Kovács, T., Bobe, R., Enouf, J. and Papp, B. (2011). Endoplasmic reticulum calcium pumps and cancer. *Biofactors.* **37**(3):139-49.
- Area-Gomez, E., de Groof, A. J., Boldogh, I., Bird, T. D., Gibson, G. E., Koehler, C. M., Yu, W. H., Duff, K. E., Yaffe, M. P., Pon, L. A. and Schon, E. A. (2009). Presenilins are enriched in endoplasmic reticulum membranes associated with mitochondria. *Am J Pathol.* **175** (5): 1810-6.
- Arispe, N., Diaz, J., Durell, S. R., Shafirir, Y. and Guy, H. R. (2010). Polyhistidine peptide inhibitor of the Abeta calcium channel potently blocks the Abeta-induced calcium

- response in cells. Theoretical modeling suggests a cooperative binding process. *Biochemistry*. **49**(36):7847-53.
- Asai, M, Hattori, C., Szabó, B., Sasagawa, N., Maruyama, K., Tanuma, S. and Ishiura, S. (2003). Putative function of ADAM9, ADAM10, and ADAM17 as APP alpha-secretase. *Biochem Biophys Res Commun*. **301**(1):231-5.
- Bacci, A., Verderio, C., Pravettoni, E. and Matteoli, M. (1999). Synaptic and intrinsic mechanisms shape synchronous oscillations in hippocampal neurons in culture. *Eur J Neurosci*. **11**(2):389-97.
- Bao, J., Wolpowitz, D., Role, L. W. and Talmage, D. A. (2003). Back signaling by the Nrg-1 intracellular domain. *J Cell Biol*. **161**(6):1133-41.
- Barritt, G. J. (1999). Receptor-activated Ca²⁺ inflow in animal cells: a variety of pathways tailored to meet different intracellular Ca²⁺ signalling requirements. *Biochem J*. **337** (Pt 2):153-69.
- Baughman, J. M., Perocchi, F., Girgis, H. S., Plovanich, M., Belcher-Timme, C. A., Sancak, Y., Bao, X. R., Strittmatter, L., Goldberger, O., Bogorad, R. L., Kotliansky, V., Mootha, V. K. (2011). Integrative genomics identifies MCU as an essential component of the mitochondrial calcium uniporter. *Nature*. **476**(7360):341-5.
- Belyaev, N. D, Kellett, K. A., Beckett, C., Makova, N. Z., Revett, T. J., Nalivaeva, N. N., Hooper, N. M. and Turner, A. J. (2010). The transcriptionally active amyloid precursor protein (APP) intracellular domain is preferentially produced from the 695 isoform of APP in a {beta}-secretase-dependent pathway. *J Biol Chem*. **285**(53):41443-54.
- Benarroch, E. E. (2011). NMDA receptors: recent insights and clinical correlations. *Neurology*. **76**(20):1750-7
- Berridge, M. J. (1998). Neuronal calcium signalling. *Neuron*. **21** (1): 13-26.
- Berridge, M. J. (2002). The endoplasmic reticulum: a multifunctional signaling organelle. *Cell Calcium*. **32** (5-6): 235-49.
- Berridge, M. J. (2006). Calcium microdomains: organization and function. *Cell Calcium*. **40** (5-6): 405-12.
- Berridge, M. J. (2010). Calcium hypothesis of Alzheimer's disease. *Pflugers Arch*. **459**(3):441-9.
- Berridge, M. J. (2011). Calcium signalling and Alzheimer's disease. *Neurochem Res*. **36**(7):1149-56.
- Berridge, M. J., Lipp, P., Bootman, M. D. (2000). The versatility and universality of calcium signalling. *Nat Rev Mol Cell Biol*. **1**(1):11-21.
- Berridge, M.J., Bootman, M. D. and Roderick, H. L. (2003). Calcium signalling: dynamics, homeostasis and remodelling. *Nat Rev Mol Cell Biol*. **4**:517-29.
- Betzenhauser, M. J. and Marks, A. R. (2010). Ryanodine receptor channelopathies. *Pflugers Arch*. **460**(2):467-80.

- Bezprozvanny, I. (2009). Calcium signaling and neurodegenerative diseases. *Trends Mol Med.* **15**:89-100.
- Bezprozvanny, I. and Mattson, M. P. (2008). Neuronal calcium mishandling and the pathogenesis of Alzheimer's disease. *Trends Neurosci.* **31**:454-63.
- Birnbaumer L. (2009). The TRPC class of ion channels: a critical review of their roles in slow, sustained increases in intracellular Ca^{2+} concentrations. *Annu Rev Pharmacol Toxicol.* **49**:395-426.
- Blaustein, M. P. and Golovina, V. A. (2001). Structural complexity and functional diversity of endoplasmic reticulum Ca^{2+} stores. *Trends Neurosci.* **24**(10):602-8.
- Bonsignore, M., Barkow, K. and Heun, R. (2002). Possible influence of selection bias on gender differences in the risk of Alzheimer's disease. *Arch Womens Ment Health.* **5**(2):73-7.
- Bootman, M. D, Berridge, M. J. and Roderick, H. L. (2002). Activating calcium release through inositol 1,4,5-trisphosphate receptors without inositol 1,4,5-trisphosphate. *Proc Natl Acad Sci U S A.* **99**(11):7320-2.
- Borchelt, D. R. (1998). Metabolism of presenilin 1: influence of presenilin 1 on amyloid precursor protein processing. *Neurobiol Aging.* **19**(1 Suppl):S15-8.
- Borchelt, D. R., Thinakaran, G., Eckman, C.B., Lee, M. K., Davenport, F., Ratovitsky, T., Prada, C. M., Kim, G., Seekins, S., Yager, D., Slunt, H. H., Wang, R., Seeger, M., Levey, A. I., Gandy, S. E., Copeland, N. G., Jenkins, N. A., Price, D. L., Younkin, S. G. and Sisodia, S. S. (1996). Familial Alzheimer's disease-linked presenilin 1 variants elevate A β 1-42/1-40 ratio in vitro and in vivo. *Neuron*, **17**:1005-1013.
- Brini, M. and Carafoli, E. (2009). Calcium pumps in health and disease. *Physiol Rev.* **89**(4):1341-78.
- Brookmeyer, R., Johnson, E., Ziegler-Graham, K., Arrighi, H. M. (2007). Forecasting the global burden of Alzheimer's disease. *Alzheimers Dement.* **3** (3):186-91.
- Brunello, L., Zampese, E., Florean, C., Pozzan, T., Pizzo P. and Fasolato, C. (2009). Presenilin-2 dampens intracellular Ca^{2+} stores by increasing Ca^{2+} leakage and reducing Ca^{2+} uptake. *J Cell Mol Med.* **13**:3358-69.
- Buck, E., Zimanyi, I., Abramson, J. J. and Pessah, I. N. (1992). Ryanodine stabilizes multiple conformational states of the skeletal muscle calcium release channel. *J. Biol. Chem.* **267**, 23560-23567.
- Buxbaum, J. D., Thinakaran, G., Koliatsos, V., O'Callahan, J., Slunt, H. H., Price, D. L., Sisodia, S. S. (1998). Alzheimer amyloid protein precursor in the rat hippocampus: transport and processing through the perforant path. *J Neurosci.* **18**(23):9629-37.
- Caamaño-Isorna, F., Corral, M., Montes-Martínez, A. and Takkouche, B. (2006). Education and dementia: a meta-analytic study. *Neuroepidemiology.* **26**(4):226-32.
- Cahalan, M. D. (2009). STIMulating store-operated Ca^{2+} entry. *Nat Cell Biol.* **11**(6):669-77.

- Cai, W., Hisatsune, C., Nakamura, K., Nakamura, T., Inoue, T. and Mikoshiba, K. (2004). Activity-dependent expression of inositol 1,4,5-trisphosphate receptor type 1 in hippocampal neurons. *J Biol Chem.* **279**(22):23691-8.
- Campbell, A., Kumar, A., La Rosa, F. G., Prasad, K. N. and Bondy, S. C. (2000). Aluminum increases levels of beta-amyloid and ubiquitin in neuroblastoma but not in glioma cells. *Proc Soc Exp Biol Med.* **223**(4):397-402.
- Carafoli, E. (2002). Calcium signaling: a tale for all seasons. *Proc Natl Acad Sci U S A.* **99**:1115-22.
- Carafoli, E., Genazzani, A. and Guerini, D. (1999). Calcium controls the transcription of its own transporters and channels in developing neurons. *Biochem Biophys Res Commun.* **266**(3):624-32
- Casserly, I. P. and Topol, E. (2004). Convergence of atherosclerosis and alzheimer's disease: Cholesterol, inflammation, and misfolded proteins. *J Discov Med.* **4**(22):149-56.
- Catterall, W. A. (2011). Voltage-gated calcium channels. *Cold Spring Harb Perspect Biol.* **3**(8):a003947.
- Chakroborty, S., Goussakov, I., Miller, M. B. and Stutzmann, G. E. (2009). Deviant ryanodine receptor-mediated calcium release resets synaptic homeostasis in presymptomatic 3xTg-AD mice. *J Neurosci.* **29**:9458-70.
- Chan, S. L., Mayne, M., Holden, C. P., Geiger, J. D. and Mattson, M. P. (2000). Presenilin-1 mutations increase levels of ryanodine receptors and calcium release in PC12 cells and cortical neurons. *J Biol Chem.* **275**(24):18195-200.
- Chasseigneaux, S., Dinc, L., Rose, C., Chabret, C., Couplier, F., Topilko, P., Mauger, G. and Allinquant, B. (2011). Secreted amyloid precursor protein β and secreted amyloid precursor protein α induce axon outgrowth in vitro through Egr1 signaling pathway. *PLoS One.* **6**(1):e16301.
- Chen, F., Tandon, A., Sanjo, N., Gu, Y. J., Hasegawa, H., Arawaka, S., Lee, F. J., Ruan, X., Mastrangelo, P., Erdebil, S., Wang, L., Westaway, D., Mount, H. T., Yankner, B., Fraser, P. E. and St George-Hyslop, P. (2003). Presenilin 1 and presenilin 2 have differential effects on the stability and maturation of nicastrin in Mammalian brain. *J Biol Chem.* **278**(22):19974-9.
- Chen, F., Yu, G., Arawaka, S., Nishimura, M., Kawarai, T., Yu, H., Tandon, A., Supala, A., Song, Y. Q., Rogaeva, E., Milman, P., Sato, C., Yu, C., Janus, C., Lee, J., Song, L., Zhang, L., Fraser, P. E. and St George-Hyslop, P. H. (2001). Nicastrin binds to membrane-tethered Notch. *Nat Cell Biol.* **3**(8):751-4.
- Chen, Q. and Schubert, D. (2002). Presenilin-interacting proteins. *Expert Rev Mol Med.* **4**(19):1-18.
- Cheung, K. H., Mei, L., Mak, D. O., Hayashi, I., Iwatsubo, T., Kang, D. E. and Foscett, J. K. (2010). Gain-of-function enhancement of IP3 receptor modal gating by familial Alzheimer's disease-linked presenilin mutants in human cells and mouse neurons. *Science Signaling.* **3**:ra22.

- Cheung, K. H., Shineman, D., Muller, M., Cardenas, C., Mei, L., Yang, J., Tomita, T., Iwatsubo, T., Lee, V. M. and Foskett, J. K. (2008). Mechanism of Ca²⁺ disruption in Alzheimer's disease by presenilin regulation of InsP₃ receptor channel gating. *Neuron*. **58**:871-83.
- Chow, V. W., Mattson, M. P., Wong, P. C. and Gleichmann, M. (2010). An overview of APP processing enzymes and products. *Neuromolecular Med*. **12**(1):1-12.
- Cobb, J. L., Wolf, P. A., Au, R., White, R. and D'Agostino, R. B. (1995). The effect of education on the incidence of dementia and Alzheimer's disease in the Framingham Study. *Neurology*. **45**(9):1707-12.
- Cockcroft, S. (2006). The latest phospholipase C, PLCeta, is implicated in neuronal function. *Trends Biochem Sci*. **31**(1):4-7.
- Colciaghi, F., Marcello, E., Borroni, B., Zimmermann, M., Caltagirone, C., Cattabeni, F., Padovani, A. and Di Luca, M. (2004). Platelet APP, ADAM 10 and BACE alterations in the early stages of Alzheimer disease. *Neurology*. **62**(3):498-501.
- Contreras, L., Drago, I., Zampese, E. and Pozzan, T. (2010). Mitochondria: the calcium connection. *Biochim Biophys Acta*. **1797**(6-7):607-18.
- Cook, D. G., Li, X., Cherry, S. D. and Cantrell, A. R. (2005). Presenilin 1 deficiency alters the activity of voltage-gated Ca²⁺ channels in cultured cortical neurons. *J Neurophysiol*. **94**(6):4421-9.
- Coulson, E. J., Paliga, K., Beyreuther, K. and Masters, C. L. (2000). What the evolution of the amyloid protein precursor supergene family tells us about its function. *Neurochem Int*. **36**(3):175-84.
- Cross, J. L., Meloni, B. P., Bakker, A. J., Lee, S. and Knuckey, N. W. (2010). Modes of Neuronal Calcium Entry and Homeostasis following Cerebral Ischemia. *Stroke Res Treat*. **2010**:316862.
- Cruts, M. and Van Broeckhoven, C. (1998). Molecular genetics of Alzheimer's disease. *Ann Med*. **30**(6):560-5.
- Csordás, G. and Hajnóczky, G. (2009). SR/ER-mitochondrial local communication: calcium and ROS. *Biochim Biophys Acta*. **1787**(11):1352-62.
- Cull-Candy, S., Brickley, S. and Farrant, M. (2001). NMDA receptor subunits: diversity, development and disease. *Curr Opin Neurobiol*. **11**(3):327-35.
- D'Amelio, M., Cavallucci, V., Middei, S., Marchetti, C., Pacioni, S., Ferri, A., Diamantini, A., De Zio, D., Carrara, P., Battistini, L., Moreno, S., Bacci, A., Ammassari-Teule, M., Marie, H. and Cecconi, F. (2011). Caspase-3 triggers early synaptic dysfunction in a mouse model of Alzheimer's disease. *Nat Neurosci*. **14**(1):69-76.
- Dartigues, J. F. and Féart, C. (2011). Risk factors for Alzheimer disease: aging beyond age? *Neurology*. **77**(3):206-7
- Davies, S. A and Terhzaz, S. (2009). Organellar calcium signalling mechanisms in Drosophila epithelial function. *J Exp Biol*. **212**(Pt 3):387-400.

- Davis, J. A., Naruse, S., Chen, H., Eckman, C., Younkin, S., Price, D. L., Borchelt, D. R., Sisodia, S. S. and Wong, P. C. (1998). An Alzheimer's disease-linked PS1 variant rescues the developmental abnormalities of PS1-deficient embryos. *Neuron*. **20**(3):603-9.
- De Deyn, P. P., Goeman, J., Vervaet, A., Dourcy-Belle-Rose, B., Van Dam, D. and Geerts, E. (2011). Prevalence and incidence of dementia among 75-80-year-old community-dwelling elderly in different districts of Antwerp, Belgium: The Antwerp Cognition (ANCOG) Study. *Clin Neurol Neurosurg*. **113**(9):736-45.
- De Stefani, D., Raffaello, A., Teardo, E., Szabò, I. and Rizzuto, R. (2011). A forty-kilodalton protein of the inner membrane is the mitochondrial calcium uniporter. *Nature*. **476**(7360):336-40.
- De Strooper, B. (2005). Nicastrin: gatekeeper of the gamma-secretase complex. *Cell*. **122**(3):318-20.
- De Strooper, B. (2007) Loss-of-function presenilin mutations in Alzheimer disease *EMBO Rep*. **8**, 141–146.
- De Strooper, B. and Annaert, W. (2010) Novel research horizons for presenilins and γ -secretases in cell biology and disease. *Annu Rev Cell Dev Biol*. **26**:235-60.
- De Strooper, B., Annaert, W., Cupers, P., Saftig, P., Craessaerts, K., Mumm, J. S., Schroeter, E. H., Schrijvers, V., Wolfe, M. S., Ray, W. J., Goate, A. and Kopan, R. (1999). A presenilin-1-dependent gamma-secretase-like protease mediates release of Notch intracellular domain. *Nature*. **398**(6727):518-22.
- Del Vecchio, R. A., Gold, L. H., Novick, S. J., Wong, G. and Hyde, L. A. (2004). Increased seizure threshold and severity in young transgenic CRND8 mice. *Neurosci Lett*. **367**:164–7.
- Demuro, A., Mina, E., Kaye, R., Milton, S. C., Parker, I. and Glabe, C. G. (2005). Calcium dysregulation and membrane disruption as a ubiquitous neurotoxic mechanism of soluble amyloid oligomers. *J Biol Chem*. **280**(17):17294-300.
- Demuro, A., Parker, I. and Stutzmann, G. E. (2010). Calcium signaling and amyloid toxicity in Alzheimer's disease. *J Biol Chem* **285**:12463–12468.
- Demuro, A., Smith, M. and Parker, I. (2011). Single-channel Ca²⁺ imaging implicates A β 1-42 amyloid pores in Alzheimer's disease pathology. *J Cell Biol*. **195**:515-524
- Desch, M., Schinner, E., Kees, F., Hofmann, F., Seifert, R. and Schlossmann, J. (2010). Cyclic cytidine 3',5'-monophosphate (cCMP) signals via cGMP kinase I. *FEBS Lett*. **584**(18):3979-84.
- Devenny, D. A., Krinsky-McHale, S. J., Sersen, G. and Silverman, W. P. (2000). Sequence of cognitive decline in dementia in adults with Down's syndrome. *J Intellect Disabil Res*. **44** (Pt 6):654-65.
- Dolphin, A. C. (2003). G protein modulation of voltage-gated calcium channels. *Pharmacol Rev*. **55**(4):607-27.

- Drago, I., Pizzo, P. and Pozzan, T. (2011). After half a century mitochondrial calcium in- and efflux machineries reveal themselves. *EMBO J.* **30**(20):4119-25.
- Du, H. and Yan, S. S. (2010). Mitochondrial permeability transition pore in Alzheimer's disease: cyclophilin D and amyloid beta. *Biochim Biophys Acta.* **1802**(1):198-204
- Du, H., Guo, L., Fang, F., Chen, D., Sosunov, A. A., McKhann, G. M., Yan, Y., Wang, C., Zhang, H., Molkentin, J. D., Gunn-Moore, F. J., Vonsattel, J. P, Arancio, O., Chen, J. X. and Yan, S. D. (2008). Cyclophilin D deficiency attenuates mitochondrial and neuronal perturbation and ameliorates learning and memory in Alzheimer's disease. *Nat Med.* **14**(10):1097-105.
- Dunlap, K., Luebke, J. I and Turner, T. J. (1995). Exocytotic Ca²⁺ channels in mammalian central neurons. *Trends Neurosci.* **18**(2):89-98.
- Duyckaerts, C., Delatour, B. and Potier, M. C. (2009). Classification and basic pathology of Alzheimer disease. *Acta Neuropathol.* **118**(1):5-36.
- Esselens, C., Oorschot, V., Baert, V., Raemaekers, T., Spittaels, K., Serneels, L., Zheng, H., Saftig, P., De Strooper, B., Klumperman, J. and Annaert, W. (2004). Presenilin 1 mediates the turnover of telencephalin in hippocampal neurons via an autophagic degradative pathway. *J Cell Biol.* **166**(7):1041-54.
- Fahrenholz, F., Gilbert, S., Kojro, E., Lammich, S. and Postina R. (2000). Alpha-secretase activity of the disintegrin metalloprotease ADAM 10. Influences of domain structure. *Ann NY Acad Sci.* **920**:215-22.
- Farlow, M. R. (1998). Etiology and pathogenesis of Alzheimer's disease. *Am J Health Syst Pharm.* 55 Suppl 2:S5-10.
- Fasolato, C., Innocenti, B. and Pozzan, T. (1994). Receptor-activated Ca²⁺ influx: how many mechanisms for how many channels? *Trends Pharmacol Sci.* **15**(3):77-83.
- Fasolato, C., Zottini, M., Clementi, E., Zacchetti, D., Meldolesi, J. and Pozzan, T. (1991). Intracellular Ca²⁺ pools in PC12 cells. Three intracellular pools are distinguished by their turnover and mechanisms of Ca²⁺ accumulation, storage, and release. *J Biol Chem.* **266**(30):20159-67.
- Fedrizzi, L., Lim, D., Carafoli, E. (2008). Calcium and signal transduction. *Biochem Mol Biol Educ.* **36**(3):175-80.
- Fellin, T., Pascual, O., Gobbo, S., Pozzan, T., Haydon, P.G. and Carmignoto, G. (2004). Neuronal synchrony mediated by astrocytic glutamate through activation of extrasynaptic NMDA receptors. *Neuron.* **43**:729-43.
- Ferrari, D., Pinton, P., Campanella, M., Callegari, M. G., Pizzirani, C., Rimessi, A., Di Virgilio, F., Pozzan, T. and Rizzuto R. (2010). Functional and structural alterations in the endoplasmic reticulum and mitochondria during apoptosis triggered by C2-ceramide and CD95/APO-1/FAS receptor stimulation. *Biochem Biophys Res Commun.* **391**(1):575-81.
- Ferreira, P. C., Piai Kde, A., Takayanagui, A. M. and Segura-Muñoz, S. I. (2008). Aluminum as a risk factor for Alzheimer's disease. *Rev Lat Am Enfermagem.* **16**(1):151-7.

- Fiala, A. and Spall, T. (2003). In vivo calcium imaging of brain activity in *Drosophila* by transgenic cameleon expression. *Sci STKE*. **2003**(174):PL6.
- Fill, M. and Copello, J. A. (2002). Ryanodine receptor calcium release channels. *Physiol Rev*. **82**(4):893-922.
- Fluhrer, R., Kamp, F., Grammer, G., Nuscher, B., Steiner, H., Beyer, K. and Haass, C. (2011). The Nicastrin ectodomain adopts a highly thermostable structure. *Biol Chem*. **392**(11):995-1001.
- Flynn, A. (2003). The role of dietary calcium in bone health. *Proc Nutr Soc*. **62**(4):851-8.
- Förstl, H. and Kurz, A. (1999). Clinical features of Alzheimer's disease. *Eur Arch Psychiatry Clin Neurosci*. **249** (6): 288-90.
- Fortna, R. R., Crystal, A. S., Morais, V. A., Pijak, D. S., Lee, V. M. and Doms, R. W. (2004). Membrane topology and nicastrin-enhanced endoproteolysis of APH-1, a component of the gamma-secretase complex. *J Biol Chem*. **279**(5):3685-93.
- Foskett, J. K. (2010). Inositol trisphosphate receptor Ca²⁺ release channels in neurological diseases. *Pflügers Archiv*. **460**:481-94.
- Foskett, J. K., White, C., Cheung, K. H. and Mak, D. O. (2007). Inositol trisphosphate receptor Ca²⁺ release channels. *Physiol Rev*. **87**(2):593-658.
- Francis, R., McGrath, G., Zhang, J., Ruddy, D. A., Sym, M., Apfeld, J., Nicoll, M., Maxwell, M., Hai, B., Ellis, M. C., Parks, A. L., Xu, W., Li, J., Gurney, M., Myers, R. L., Himes, C. S., Hiesch, R., Ruble, C., Nye, J. S. and Curtis, D. (2002). aph-1 and pen-2 are required for Notch pathway signaling, gamma-secretase cleavage of betaAPP, and presenilin protein accumulation. *Dev Cell*. **3**(1):85-97.
- Frank, A. R. and Petersen, R. C. (2008). Mild cognitive impairment. *Handb Clin Neurol*. **89**:217-21.
- Fukami, K., Inanobe, S., Kanemaru, K. and Nakamura, Y. (2010). Phospholipase C is a key enzyme regulating intracellular calcium and modulating the phosphoinositide balance. *Prog Lipid Res*. **49**(4):429-37.
- Furuichi, T., Yoshikawa, S., Miyawaki, A., Wada, K., Maeda, N. and Mikoshiba, K. (1989). Primary structure and functional expression of the inositol 1,4,5-trisphosphate-binding protein P400. *Nature*. **342**(6245):32-8
- Furukawa, K., Sopher, B. L., Rydel, R. E., Begley, J. G., Pham, D. G., Martin, G. M., Fox, M. and Mattson, M. P. (1996). Increased activity-regulating and neuroprotective efficacy of alpha-secretase-derived secreted amyloid precursor protein conferred by a C-terminal heparin-binding domain. *J Neurochem*. **67**(5):1882-96.
- Gakhar-Koppole, N., Hundeshagen, P., Mandl, C., Weyer, S. W., Allinquant, B., Müller, U. and Ciccolini, F. (2008). Activity requires soluble amyloid precursor protein alpha to promote neurite outgrowth in neural stem cell-derived neurons via activation of the MAPK pathway. *Eur J Neurosci*. **28**(5):871-82.

- García-Sancho, J. (1985). Pyruvate prevents the ATP depletion caused by formaldehyde or calcium-chelator esters in the human red cell. *Biochim Biophys Acta*. **813**(1):148-50.
- Giacomello, M., Barbiero, L., Zatti, G., Squitti, R., Binetti, G., Pozzan, T., Fasolato, C., Ghidoni, R. and Pizzo, P. (2005). Reduction of Ca²⁺ stores and capacitative Ca²⁺ entry is associated with the familial Alzheimer's disease presenilin-2 T122R mutation and anticipates the onset of dementia. *Neurobiol. Dis.* **18**, 638–648.
- Giliberto L, Matsuda S, Vidal R, D'Adamio L. (2009). Generation and initial characterization of FDD knock in mice. *PLoS One*. **4**(11):e7900.
- Giorgi, C., De Stefani, D., Bononi, A., Rizzuto, R. and Pinton P. (2009). Structural and functional link between the mitochondrial network and the endoplasmic reticulum. *Int J Biochem Cell Biol*. **41**(10):1 817-27.
- Gleichmann, M. and Mattson, M. P. (2011). Neuronal calcium homeostasis and dysregulation. *Antioxid Redox Signal*. **14**(7):1261-73.
- Goate, A., Chartier-Harlin, M. C., Mullan, M., Brown, J., Crawford, F., Fidani, L., Giuffra, L., Haynes, A., Irving, N., James, L., Mant, R., Newton, P., Rooke K., Roques P., Talbot, C., Pericak-Vance, C., Roses, A., Williamson, R, Rossor, M., Owen, M. and Hardy, J. (1991). Segregation of a missense mutation in the amyloid precursor protein gene with familial Alzheimer's disease". *Nature*. **349** (6311): 704-6.
- Goedert, M. and Spillantini, M. G. (2006). A century of Alzheimer's disease. *Science*. **314**(5800):777-81.
- Grand, J. H., Caspar, S. and Macdonald, S. W. (2011). Clinical features and multidisciplinary approaches to dementia care. *J Multidiscip Healthc*. **4**:125-47.
- Green, K. N., Demuro, A., Akbari, Y., Hitt, B. D., Smith, I. F., Parker, I. and LaFerla, F. M. (2008). SERCA pump activity is physiologically regulated by presenilin and regulates amyloid beta production. *J Cell Biol*. **181**:1107-16.
- Gruszczynska-Biegala, J., Pomorski, P., Wisniewska, M.B. and Kuznicki, J. (2011). Differential roles for STIM1 and STIM2 in store-operated calcium entry in rat neurons. *PLoS One*. **6**(4):e19285.
- Grynkiewicz, G., Poenie, M. and Tsien, R. Y. (1985). A new generation of Ca²⁺ indicators with greatly improved fluorescence properties. *J Biol Chem*. **260**(6):3440-50.
- Guerrero-Hernandez, A., Dagnino-Acosta, A., Verkhratsky, A. (2010). An intelligent sarco-endoplasmic reticulum Ca²⁺ store: release and leak channels have differential access to a concealed Ca²⁺ pool. *Cell Calcium*. **48**(2-3):143-9.
- Guo, Z., Cupples, L. A., Kurz, A., Auerbach, S. H., Volicer, L., Chui, H., Green, R. C., Sadovnick, A. D., Duara, R., DeCarli, C., Johnson, K., Go, R. C., Growdon, J. H., Haines, J. L., Kukull, W. A. and Farrer, L. A. (2000). Head injury and the risk of AD in the MIRAGE study. *Neurology*. **54**(6):1316-23
- Haass, C. (2004). Take five--BACE and the *gamma-secretase* quartet conduct Alzheimer's amyloid beta-peptide generation. *EMBO J*. **23**(3):483-8.

- Hall, J. E. (2011). In *Guyton and Hall Textbook of Medical Physiology with Student Consult Online Access* (12th Ed.). Philadelphia: Elsevier Saunders. p. 64. ISBN 978-1-4160-4574-8.
<http://asia.elsevierhealth.com/media/us/samplechapters/9781416045748/Guyton%20&%20Hall%20Sample%20Chapter.pdf>. Retrieved 22-09- 2011.
- Hardie, R. C. TRP channels in *Drosophila* photoreceptors: the lipid connection. *Cell Calcium*. **33**(5-6):385-93.
- Hardy, J. (2009). The amyloid hypothesis for Alzheimer's disease: a critical reappraisal. *J Neurochem*. **110** (4): 1129-34.
- Hardy, J. A. (2007). Putting presenilins centre stage. *EMBO Rep*. **8**, 134–135.
- Hardy, J. A. and Higgins, G. A. (1992). Alzheimer's disease: the amyloid cascade hypothesis. *Science*. **256**(5054):184-5.
- Hardy, J. and Selkoe, D. J. (2002). The amyloid hypothesis of Alzheimer's disease: Progress and problems on the road to therapeutics. *Science*. **297**:353–356
- Haroutunian, V., Perl, D. P., Purohit, D. P., Marin, D., Khan, K., Lantz, M., Davis, K. L. and Mohs, R. C. (1998). Regional distribution of neuritic plaques in the nondemented elderly and subjects with very mild Alzheimer disease. *Arch Neurol*. **55**(9):1185-91.
- Hasegawa, H., Sanjo, N., Chen, F., Gu, Y. J., Shier, C., Petit, A., Kawarai, T., Katayama, T., Schmidt, S. D., Mathews, P. M., Schmitt-Ulms, G., Fraser, P. E., and St George-Hyslop, P. (2004). Both the sequence and length of the C terminus of PEN-2 are critical for intermolecular interactions and function of presenilin complexes. *J Biol Chem*. **279**(45):46455-63.
- Hass, M. R., Sato, C., Kopan, R. and Zhao, G. (2009). Presenilin: RIP and beyond. *Semin Cell Dev Biol*. **20**(2):201-10.
- Hayrapetyan, V., Rybalchenko, V., Rybalchenko, N. and Koulen, P. (2008). The N-terminus of presenilin-2 increases single channel activity of brain ryanodine receptors through direct protein-protein interaction. *Cell Calcium*. **44**:507–518.
- Hebert, L. E., Scherr, P. A., McCann, J. J., Beckett, L. A. and Evans, D. A. (2001). Is the risk of developing Alzheimer's disease greater for women than for men? *Am J Epidemiol*. **153**(2):132-6.
- Herms, J., Schneider, I., Dewachter, I., Caluwaerts, N., Kretzschmar, H., and Van Leuven, F. (2003). Capacitive calcium entry is directly attenuated by mutant presenilin-1, independent of the expression of the amyloid precursor protein. *J Biol Chem*. **278**:2484-9.
- Herreman, A., Hartmann, D., Annaert, W., Saftig, P., Craessaerts, K., Serneels, L., Umans, L., Schrijvers, V., Checler, F., Vanderstichele, H., Baekelandt, V., Dressel, R., Cupers, P., Huylebroeck, D., Zwijsen, A., Van Leuven, F. and De Strooper, B. (1999). Presenilin 2 deficiency causes a mild pulmonary phenotype and no changes in amyloid precursor protein processing but enhances the embryonic lethal phenotype of presenilin 1 deficiency. *Proc Natl Acad Sci U S A*. **96** (21): 11872-7.

- Hof, P. R., Vogt, B. A., Bouras, C. and Morrison, J. H. (1997). Atypical form of Alzheimer's disease with prominent posterior cortical atrophy: a review of lesion distribution and circuit disconnection in cortical visual pathways. *Vision Res.* **37**(24):3609-25.
- Horsburgh, K., McCarron, M. O., White, F. and Nicoll, J. A. (2000). The role of apolipoprotein E in Alzheimer's disease, acute brain injury and cerebrovascular disease: evidence of common mechanisms and utility of animal models. *Neurobiol Aging.* **21**(2):245-55.
- Hoth, M. and Penner, R. (1992). Depletion of intracellular calcium stores activates a calcium current in mast cells. *Nature.* **355**(6358):353-6.
- Hoyert, D. L. and Rosenberg, H. M. (1997). Alzheimer's disease as a cause of death in the United States. *Public Health Rep.* **112**(6):497-505.
- Hsieh, H., Boehm, J., Sato, C., Iwatsubo, T., Tomita, T., Sisodia, S. and Malinow, R. (2006). AMPAR removal underlies Abeta-induced synaptic depression and dendritic spine loss. *Neuron.* **52**(5):831-43.
- Iwai, M., Michikawa, T., Bosanac, I., Ikura, M. and Mikoshiba, K. (2007). Molecular basis of the isoform-specific ligand-binding affinity of inositol 1,4,5-trisphosphate receptors. *J Biol Chem.* **282**(17):12755-64.
- Jalink, K. and Moolenaar, W. H. (2010). G protein-coupled receptors: the inside story. *Bioessays.* **32**(1):13-6.
- Jankowsky, J. L., Fadale, D. J., Anderson, J., Xu, G. M., Gonzales, V., Jenkins, N. A., Copeland, N. G., Lee, M. K., Younkin, L. H., Wagner, S. L., Younkin, S. G. and Borchelt, D. R. (2003). Mutant presenilins specifically elevate the levels of the 42 residue beta-amyloid peptide in vivo: evidence for augmentation of a 42-specific gamma secretase. *Hum Mol Genet.* **13**(2):159-70.
- Jayadev, S., Leverenz, J. B., Steinbart, E., Stahl, J., Klunk, W., Yu, C. E. and Bird, T. D. (2010). Alzheimer's disease phenotypes and genotypes associated with mutations in presenilin 2. *Brain.* **133**(Pt 4):1143-54
- Jellinger, K. A., Paulus, W., Wrocklage, C. and Litvan, I. (2001). Effects of closed traumatic brain injury and genetic factors on the development of Alzheimer's disease. *Eur J Neurol.* **8**(6):707-10.
- Johnson, G. V. and Stoothoff, W. H. (2004). Tau phosphorylation in neuronal cell function and dysfunction. *J Cell Sci.* **117**(Pt 24):5721-9.
- Jones, S. W. (2003). Calcium channels: unanswered questions. *J Bioenerg Biomembr.* **35**(6):461-75.
- Kaczor A. A. and Matusiuk, D. (2010). Molecular structure of ionotropic glutamate receptors. *Curr Med Chem.* **17**(24):2608-35.
- Kaether, C., Haass, C. and Steiner, H. (2006). Assembly, trafficking and function of gamma-secretase. *Neurodegener Dis.* **3**(4-5):275-83.

- Kang, D. E., Soriano, S., Xia, X., Eberhart, C. G., De Strooper, B., Zheng, H. and Koo, E. H. (2002). Presenilin couples the paired phosphorylation of beta-catenin independent of axin: implications for beta-catenin activation in tumorigenesis. *Cell*. **110**(6):751-62.
- Katan, M. (2005). New insights into the families of PLC enzymes: looking back and going forward. *Biochem J*. **391**(Pt 3):e7-9.
- Kato, N., Isomura, Y. and Tanaka, T. (2000). Intracellular calcium releases facilitate induction of long-term depression. *Neuropharmacology*. **39**(6):1107-10.
- Kawahara, M., Kato, M. and Kuroda, Y. (2001). Effects of aluminum on the neurotoxicity of primary cultured neurons and on the aggregation of beta-amyloid protein. *Brain Res Bull*. **55**(2):211-7.
- Kelly, J. F., Furukawa, K., Barger, S. W., Rengen, M. R., Mark, R. J., Blanc, E. M., Roth, G. S. and Mattson, M. P. (1996). Amyloid beta-peptide disrupts carbachol-induced muscarinic cholinergic signal transduction in cortical neurons. *Proc Natl Acad Sci U S A*. **93**(13):6753-8.
- Khachaturian, Z. S. (1994). Calcium hypothesis of Alzheimer's disease and brain aging. *Ann N Y Acad Sci*. **15**:747:1-11.
- Kimberly, W.T., LaVoie, M. J., Ostaszewski, B. L., Ye, W., Wolfe, M. S. and Selkoe, D. J. (2003). Gamma-secretase is a membrane protein complex comprised of presenilin, nicastrin, Aph-1, and Pen-2. *Proc Natl Acad Sci U S A*. **100**(11):6382-7.
- Kimura, N., Nakamura, S., Honda, T., Takashima, A., Nakayama, H., Ono, F., Sakakibara, I., Doi, K., Kawamura, S. and Yoshikawa, Y. (2001). Age-related changes in the localization of presenilin-1 in cynomolgus monkey brain. *Brain Res*. **922**:30-41.
- Kirichok Y, Krapivinsky G, Clapham DE. (2004). The mitochondrial calcium uniporter is a highly selective ion channel. *Nature*. **427**(6972):360-4.
- Koo, E. H. and Kopan, R. (2004). Potential role of presenilin-regulated signaling pathways in sporadic neurodegeneration. *Nat Med. Suppl*: **S26**-33.
- Kuchibhotla, K. V., Goldman, S. T., Lattarulo, C. R., Wu, H. Y., Hyman, B. T. and Bacskai, B. J. (2008). Abeta plaques lead to aberrant regulation of calcium homeostasis in vivo resulting in structural and functional disruption of neuronal networks. *Neuron*. **59**(2):214-25.
- Kuchibhotla, K.V., Goldman, S.T., Lattarulo, C.R., Wu, H.Y., Hyman, B.T. and Bacskai, B. J. (2008). Abeta plaques lead to aberrant regulation of calcium homeostasis in vivo resulting in structural and functional disruption of neuronal networks. *Neuron*. **59**:214-25. 89.
- Kushnir, A., Betzenhauser, M. J. and Marks, A. R. (2010). Ryanodine receptor studies using genetically engineered mice. *FEBS Lett*. **584**(10):1956-65.
- Ladeira, R. B., Diniz, B. S., Nunes, P. V. and Forlenza, O. V. (2009). Combining cognitive screening tests for the evaluation of mild cognitive impairment in the elderly. *Clinics (Sao Paulo)*. **64**(10):967-73.

- LaFerla, F. M. (2002). Calcium dyshomeostasis and intracellular signalling in Alzheimer's disease. *Nat Rev Neurosci.* **3**:862-72.
- Lai, F. A., Misra, M., Xu, L., Smith, H. A. and Meissner, G. (1989). The ryanodine receptor-Ca²⁺ release channel complex of skeletal muscle sarcoplasmic reticulum. Evidence for a cooperatively coupled, negatively charged homotetramer. *J Biol Chem.* **264**(28):16776-85.
- Lai, M. T., Chen, E., Crouthamel, M. C., DiMuzio-Mower, J., Xu, M., Huang, Q., Price, E., Register, R. B., Shi, X. P., Donoviel, D. B., Bernstein, A., Hazuda, D., Gardell, S. J. and Li, Y. M. (2003). Presenilin-1 and presenilin-2 exhibit distinct yet overlapping gamma-secretase activities. *J Biol Chem.* **278**(25):22475-81.
- Lambert, M. P., Barlow, A. K., Chromy, B. A., Edwards, C., Freed, R., Liosatos, M., Morgan, T. E., Rozovsky, I., Trommer, B., Viola, K. L., Wals, P., Zhang, C., Finch, C. E., Krafft, G. A. and Klein, W. (1998). Diffusible, nonfibrillar ligands derived from Abeta1-42 are potent central nervous system neurotoxins. *Proc Natl Acad Sci U S A.* **95**:6448-6453.
- Lanner, J. T., Georgiou, D. K., Joshi, A. D. and Hamilton, S. L. (2010). Ryanodine receptors: structure, expression, molecular details, and function in calcium release. *Cold Spring Harb Perspect Biol.* **2**(11):a003996.
- Laudon, H., Hansson, E. M., Melén, K., Bergman, A., Farmery, M. R., Winblad, B., Lendahl, U., von Heijne, G. and Näslund, J. (2005). A nine-transmembrane domain topology for presenilin 1. *J Biol Chem.* **280** (42): 35352-60.
- Laurén, J., Gimbel, D. A., Nygaard, H. B., Gilbert, J. W. and Strittmatter, S. M. (2009). Cellular prion protein mediates impairment of synaptic plasticity by amyloid-beta oligomers. *Nature.* **457**:1128-1132.
- Lee, M. K., Slunt, H. H., Martin, L. J., Thinakaran, G., Kim, G., Gandy, S. E., Seeger, M., Koo, E., Price, D. L. and Sisodia, S. S. (1996). Expression of presenilin 1 and 2 (PS1 and PS2) in human and murine tissues. *J Neurosci.* **16**(23):7513-25.
- Lee, S. F., Shah, S., Yu, C., Wigley, W. C., Li, H., Lim, M., Pedersen, K., Han, W., Thomas, P., Lundkvist, J., Hao, Y. H. and Yu, G. (2004). A conserved GXXXG motif in APh-1 is critical for assembly and activity of the gamma-secretase complex. *J Biol Chem.* **279**(6):4144-52.
- Lee, S. Y., Hwang, D. Y., Kim, Y. K., Lee, J. W., Shin, I. C., Oh, K. W., Lee, M. K., Lim, J. S., Yoon, D. Y., Hwang, S. J. and Hong, J. T. (2006) PS2 mutation increases neuronal cell vulnerability to neurotoxicants through activation of caspase-3 by enhancing of ryanodine receptor-mediated calcium release. *FASEB J.* **20**, 151-153.
- Leissring, M. A., Akbari, Y., Fanger, C. M., Cahalan, M. D., Mattson, M. P. and LaFerla, F. M. (2000). Capacitative calcium entry deficits and elevated luminal calcium content in mutant presenilin-1 knockin mice. *J Cell Biol.* **149**:793-8.
- Leissring, M. A., LaFerla, F. M., Callamaras, N., Parker, I. (2001). Subcellular mechanisms of presenilin-mediated enhancement of calcium signaling. *Neurobiol Dis.* **8**(3):469-78.

- Leissring, M. A., Parker, I. and LaFerla, F. M. (1999b). Presenilin-2 mutations modulate amplitude and kinetics of inositol 1, 4,5-trisphosphate-mediated calcium signals. *J Biol Chem.* **274**(46):32535-8.
- Leissring, M. A., Paul, B.A., Parker, I., Cotman, C. W. and LaFerla, F. M. (1999a). Alzheimer's presenilin-1 mutation potentiates inositol 1,4,5-trisphosphate-mediated calcium signaling in *Xenopus* oocytes. *J Neurochem* **72**:1061–1068
- Lemaire, H G., Salbaum J. M., Multhaup, G., Kang, J., Bayney, R. M., Unterbeck, A., Beyreuther, K. and Müller-Hill, B. (1989). The PreA4 (695) precursor protein of Alzheimer's disease A4 amyloid is encoded by 16 exons. *Nucleic Acids Res.* **17**(2):517–522.
- Lesné, S., Koh, M. T., Kotilinek, L., Kaye, R., Glabe, C. G, Yang, A., Gallagher, M. and Ashe, K. H. (2006). A specific amyloid-beta protein assembly in the brain impairs memory. *Nature.* **440**(7082):352-7.
- Letenneur, L., Gilleron, V., Commenges, D., Helmer, C., Orgogozo, J. M. and Dartigues, J. F. (1999). Are sex and educational level independent predictors of dementia and Alzheimer's disease? Incidence data from the PAQUID project. *J Neurol Neurosurg Psychiatry.* **66**(2):177-83.
- Lewis, R. S. (2011). Store-Operated Calcium Channels: New Perspectives on Mechanism and Function. *Cold Spring Harb Perspect Biol.* cshperspect.a003970v1. doi: 10.1101/cshperspect.a003970.
- Li, H., Wolfe, M. S. and Selkoe, D. J. (2009). Toward structural elucidation of the gamma-secretase complex. *Structure.* **17**(3):326-34
- Li, J., Xu, M., Zhou, H., Ma, J. and Potter, H. (1997). Alzheimer presenilins in the nuclear membrane, interphase kinetochores, and centrosomes suggest a role in chromosome segregation. *Cell.* **90**(5):917-27.
- Liou, J., Kim, M. L., Heo, W. D., Jones, J. T., Myers, J. W., Ferrell, J. E Jr. and Meyer, T. (2005). STIM is a Ca²⁺ sensor essential for Ca²⁺-store-depletion-triggered Ca²⁺ influx. *Curr Biol.* **15** (13): 1235-41.
- Lleó A. (2008). Activity of gamma-secretase on substrates other than APP. *Curr Top Med Chem.* **8**(1):9-16.
- Lovati, C., Galimberti, D., Albani, D., Bertora, P., Venturelli, E., Cislighi, G., Guidi, I., Fenoglio, C., Cortini, F., Clerici, F., Finazzi, D., Forloni, G., Scarpini, E. and Mariani, C. (2010). APOE ε2 and ε4 influence the susceptibility for Alzheimer's disease but not other dementias. *Int J Mol Epidemiol Genet.* **1**(3):193-200.
- Lu, T., Pan, Y., Kao, S. Y., Li, C., Kohane, I., Chan, J. and Yankner, B. A. (2004). Gene regulation and DNA damage in the ageing human brain. *Nature.* **429** (6994):883-91.
- Luo, W. J., Wang, H., Li, H., Kim, B. S., Shah, S., Lee, H. J., Thinakaran, G., Kim, T. W., Yu, G. and Xu, H. (2003). PEN-2 and APH-1 coordinately regulate proteolytic processing of presenilin 1. *J Biol Chem.* **278**(10):7850-4.

- Ma, G., Li, T., Price, D. L. and Wong, P. C. (2005). APH-1a is the principal mammalian APH-1 isoform present in gamma-secretase complexes during embryonic development. *J Neurosci.* **25**(1):192-8.
- Martinez, M., Campion, D., Brice, A., Hannequin, D., Dubois, B., Didierjean, O., Michon, A., Thomas-Anterion, C., Puel, M., Frebourg, T., Agid, Y. and Clerget-Darpoux, F. (1998). Apolipoprotein E epsilon4 allele and familial aggregation of Alzheimer disease. *Arch Neurol.* **55**(6):810-6.
- Maruyama, K., Tomita, T., Shinozaki, K., Kume, H., Asada, H., Saido, T. C., Ishiura, S., Iwatsubo, T. and Obata, K. (1996). Familial Alzheimer's disease-linked mutations at Val717 of amyloid precursor protein are specific for the increased secretion of Abeta 42(43). *Biochem Biophys Res Commun.* **227**(3):730-5.
- Marx, J. (2007). Alzheimer's disease. Fresh evidence points to an old suspect: calcium. *Science.* **318**(5849):384-5.
- Masseck, O. A., Rubelowski, J. M., Spoida, K. and Herlitze, S. (2011). Light- and drug-activated G-protein-coupled receptors to control intracellular signalling. *Exp Physiol.* **96**(1):51-6.
- Masters, C. L. (1984). Etiology and pathogenesis of Alzheimer's disease. *Pathology.* **16**(3):233-4.
- Mastrangelo, P., Mathews, P. M., Chishti, M. A., Schmidt, S. D., Gu, Y., Yang, J., Mazzella, M. J., Coomaraswamy, J., Horne, P., Strome, B., Pelly, H., Levesque, G., Ebeling, C., Jiang, Y., Nixon, R. A., Rozmahel, R., Fraser, P. E, St George-Hyslop, P., Carlson, G. A. and Westaway, D. (2005). Dissociated phenotypes in presenilin transgenic mice define functionally distinct gamma-secretases. *Proc Natl Acad Sci U S A.* **102**(25):8972-7.
- Mattson, M. P. (1997). Cellular actions of beta-amyloid precursor protein and its soluble and fibrillogenic derivatives. *Physiol Rev.* **77**(4):1081-132.
- Mattson, M. P. (2003) Neurobiology: Ballads of a protein quartet. *Nature* **422**, 385-387
- Mattson, M. P. (2007). Calcium and neurodegeneration. *Aging Cell.* **6**:337-50.
- Mattson, M. P. (2010). ER calcium and Alzheimer's disease: in a state of flux. *Sci Signal.* **3**(114):pe10.
- Mayeux, R. (2003). Epidemiology of neurodegeneration. *Annu Rev Neurosci.* **26**:81-104.
- McCarthy, J. V., Twomey, C. and Wujek, P. (2009). Presenilin-dependent regulated intramembrane proteolysis and *gamma-secretase* activity. *Cell Mol Life Sci.* **66**(9):1534-55.
- McEvoy, L. K., Fennema-Notestine, C., Roddey, J. C., Hagler, D. J Jr., Holland, D., Karow, D. S., Pung, C. J., Brewer, J. B. and Dale, A. M. (2009). Alzheimer disease: quantitative structural neuroimaging for detection and prediction of clinical and structural changes in mild cognitive impairment. *Radiology.* **251**(1):195-205.

- Mellentin, C., Jahnsen, H. and Abraham, W. C. (2007). Priming of long-term potentiation mediated by ryanodine receptor activation in rat hippocampal slices. *Neuropharmacology*. **52**(1):118-25.
- Michelangeli, F., Ogunbayo, O. A. and Wootton, L. L. (2005). A plethora of interacting organellar Ca²⁺ stores. *Curr Opin Cell Biol*. **17**(2):135-40.
- Mikoshiba, K. (2007). IP3 receptor/Ca²⁺ channel: from discovery to new signaling concepts. *J Neurochem*. **102**(5):1426-46.
- Miravalle, L., Calero, M., Takao, M., Roher, A. E, Ghetti, B. and Vidal, R. (2005). Amino-terminally truncated Abeta peptide species are the main component of cotton wool plaques. *Biochemistry*. **44**(32):10810-21.
- Molinaro, P., Viggiano, D., Nisticò, R., Sirabella, R., Secondo, A., Boscia, F., Pannaccione, A., Scorziello, A., Mehdawy, B., Sokolow, S., Herchuelz, A., Di Renzo, G. F. and Annunziato, L. (2011). Na⁺-Ca²⁺ exchanger (NCX3) knock-out mice display an impairment in hippocampal long-term potentiation and spatial learning and memory. *J Neurosci*. **31**(20):7312-21.
- Morris, J. C. (2005). Early-stage and preclinical Alzheimer disease. *Alzheimer Dis Assoc Disord*. **19**(3):163-5.
- Morris, J. C. (2006). Mild cognitive impairment is early-stage Alzheimer disease: time to revise diagnostic criteria. *Arch Neurol*. **63**(1):15-6.
- Morrison, J. H. and Hof, P. R. (1997). Life and death of neurons in the aging brain. *Science*. **278**(5337):412-9.
- Morrisette, D. A., Parachikova, A., Green, K. N. and LaFerla, F. M. (2009). Relevance of transgenic mouse models to human Alzheimer disease. *J Biol Chem*. **284**(10):6033-7
- Mulugeta, E., Karlsson, E., Islam, A., Kalaria, R., Mangat, H., Winblad, B. and Adem, A. (2003). Loss of muscarinic M4 receptors in hippocampus of Alzheimer patients. *Brain Res*. **960**(1-2):259-62.
- Mumm, J. S. and Kopan, R. (2000). Notch signaling: from the outside in. *Dev Biol*. **228**(2):151-65.
- Myers, R. H., Schaefer, E. J., Wilson, P. W., D'Agostino, R., Ordovas, J. M., Espino, A., Au, R., White, R. F., Knoefel, J. E., Cobb, J. L., McNulty, K. A., Beiser, A. and Wolf, P. A. (1996). Apolipoprotein E epsilon4 association with dementia in a population-based study: The Framingham study. *Neurology*. **46**(3):673-7.
- Nakahara, M., Shimozaawa, M., Nakamura, Y., Irino, Y., Morita, M., Kudo, Y. and Fukami, K. (2005). A novel phospholipase C, PLC(eta)2, is a neuron-specific isozyme. *J Biol Chem*. **280**(32):29128-34.
- Neely, K. M., Green, K. N. and LaFerla, F. M. (2011). Presenilin is necessary for efficient proteolysis through the autophagy-lysosome system in a γ -secretase-independent manner. *J Neurosci*. **31**(8):2781-91.

- Nelson, O., Tu, H., Lei, T., Bentahir, M., de Strooper, B. and Bezprozvany, I. (2007). Familial Alzheimer disease-linked mutations specifically disrupt Ca²⁺ leak function of presenilin 1. *J Clin Invest* **117**:1230–1239.
- Nelson, P. T., Braak, H. and Markesbery, W. R. (2009). Neuropathology and cognitive impairment in Alzheimer disease: a complex but coherent relationship. *J Neuropathol Exp Neurol*. **68**(1):1-14.
- Nelson, P. T., Head, E., Schmitt, F.A., Davis, P. R., Neltner, J. H., Jicha, G. A., Abner, E. L., Smith, C. D., Van Eldik, L. J., Kryscio, R. J. and Scheff, S. W. (2011). Alzheimer's disease is not "brain aging": neuropathological, genetic, and epidemiological human studies. *Acta Neuropathol*. **121**(5):571-87.
- Nelson, P. T., Kukull, W. A. and Frosch, M. P. (2010). Thinking outside the box: Alzheimer-type neuropathology that does not map directly onto current consensus recommendations. *J Neuropathol Exp Neurol*. **69**(5):449-54.
- Ni, C. Y., Murphy, M. P., Golde, T. E. and Carpenter, G. (2001). gamma -Secretase cleavage and nuclear localization of ErbB-4 receptor tyrosine kinase. *Science*. **294**(5549):2179-81.
- Nikolaev, A., McLaughlin, T., O'Leary, D. D. and Tessier-Lavigne, M. (2009). APP binds DR6 to trigger axon pruning and neuron death via distinct caspases. *Nature*. **457**(7232):981-9.
- Nixon, R. A. and Yang, D. S. (2011). Autophagy failure in Alzheimer's disease-locating the primary defect. *Neurobiol Dis*. **43**(1):38-45.
- Nomikos, M., Elgmati, K., Theodoridou, M., Calver, B. L., Nounesis, G., Swann, K. and Lai, F. A. (2011). Phospholipase C ζ binding to PtdIns(4,5)P₂ requires the XY-linker region. *J Cell Sci*. **124**(Pt 15):2582-90.
- not amyloid load, predict cognitive status in Alzheimer's disease. *Neurology*
- Oakes, S. A., Opferman, J. T., Pozzan, T., Korsmeyer, S.J. and Scorrano, L. (2003). Regulation of endoplasmic reticulum Ca²⁺ dynamics by proapoptotic BCL-2 family members. *Biochem Pharmacol*. **66**(8):1335-40.
- Ohkawara, T., Nagase, H., Koh, C. S. and Nakayama, K. (2011). The amyloid precursor protein intracellular domain alters gene expression and induces neuron-specific apoptosis. *Gene*. **475**(1):1-9.
- Ozawa T. (2010). Modulation of ryanodine receptor Ca²⁺ channels. *Mol Med Report*. **3**(2):199-204.
- Ozmen, L., Albientz, A., Czech, C. and Jacobsen, H. (2009). Expression of transgenic APP mRNA is the key determinant for beta-amyloid deposition in PS2APP transgenic mice. *Neurodegener Dis*. **6**:29-36.
- Page, R. M., Baumann, K., Tomioka, M., Perez-Revuelta, B. I., Fukumori, A., Jacobsen, H., Flohr, A., Luebbers, T., Ozmen, L., Steiner, H. and Haass, C. (2008). Generation of A β 38 and A β 42 Is Independently and Differentially Affected by Familial Alzheimer

- Disease-associated Presenilin Mutations and γ -Secretase Modulation. *J Biol Chem.* **283**:677-683.
- Palmer, A. E. and Tsien, R. Y. (2006). Measuring calcium signaling using genetically targetable fluorescent indicators. *Nat Protoc.* **1**(3):1057-65.
- Pardossi-Piquard, R., Böhm, C., Chen, F., Kanemoto, S., Checler, F., Schmitt-Ulms, G., St George-Hyslop, P. and Fraser, P.E. (2009). TMP21 transmembrane domain regulates gamma-secretase cleavage. *J Biol Chem.* **284**(42):28634-41.
- Parekh, A. B. (2008). Store-operated channels: mechanisms and function. *J Physiol.* **586**(13):3033.
- Parent, A., Linden, D. J., Sisodia, S. S. and Borchelt, D. R. (1999). Synaptic transmission and hippocampal long-term potentiation in transgenic mice expressing FAD-linked presenilin 1. *Neurobiol Dis.* **6**(1):56-62.
- Parker, I., Zang, W. J. and Wier, W. G. (1996). Ca^{2+} sparks involving multiple Ca^{2+} release sites along Z-lines in rat heart cells. *J Physiol.* **497** (Pt 1):31-8.
- Pasternak, S. H., Bagshaw, R. D, Guiral, M., Zhang, S., Ackerley, C. A., Pak, B. J., Callahan, J. W. and Mahuran, D. J. (2003). Presenilin-1, nicastrin, amyloid precursor protein, and gamma-secretase activity are co-localized in the lysosomal membrane. *J Biol Chem.* **278**(29):26687-94.
- Pedersen, S. F., Owsianik, G. and Nilius, B. (2005). **TRP** channels: an overview. *Cell Calcium.* **38**(3-4):233-52.
- Perl, D. P. (2010). Neuropathology of Alzheimer's disease. *Mt Sinai J Med.* **77**(1):32-42.
- Petersen, R. C. (2009). Early Diagnosis of Alzheimer's Disease: Is MCI Too. *Curr Alzheimer Res.* **6**(4): 324–330.
- Pietrobon, D., Di Virgilio, F. and Pozzan, T. (1990). Structural and functional aspects of calcium homeostasis in eukaryotic cells. *Eur J Biochem.* **193**(3):599-622.
- Pinton, P., Ferrari, D., Magalhães, P., Schulze-Osthoff, K., Di Virgilio, F., Pozzan, T. and Rizzuto, R. (2000). Reduced loading of intracellular Ca^{2+} stores and downregulation of capacitative Ca^{2+} influx in Bcl-2-overexpressing cells. *J Cell Biol.* **148** (5): 857-62.
- Pinton, P., Ferrari, D., Rapizzi, E., Di Virgilio, F., Pozzan, T. and Rizzuto, R. (2001). The Ca^{2+} concentration of the endoplasmic reticulum is a key determinant of ceramide-induced apoptosis: significance for the molecular mechanism of Bcl-2 action. *EMBO J.* **20**(11):2690-701.
- Pinton, P., Giorgi, C., Siviero, R., Zecchini, E., Rizzuto, R. (2008). Calcium and apoptosis: ER-mitochondria Ca^{2+} transfer in the control of apoptosis. *Oncogene.* **27**(50):6407-18.
- Pizzo P, Lissandron V, Capitanio P, Pozzan T. (2011). Ca^{2+} signalling in the Golgi apparatus. *Cell Calcium.* **50**(2):184-92.
- Pizzo, P. and Pozzan, T. (2007). Mitochondria-endoplasmic reticulum choreography: structure and signaling dynamics. *Trends Cell Biol.* **17**(10):511-7.

- Plassman, B. L., Havlik, R. J., Steffens, D. C., Helms, M. J., Newman, T. N., Drosdick, D., Phillips, C., Gau, B. A., Welsh-Bohmer, K. A., Burke, J. R., Guralnik, J. M. and Breitner, J. C. (2000). Documented head injury in early adulthood and risk of Alzheimer's disease and other dementias. *Neurology*. **55**(8):1158-66
- Pozzan, T., Rizzuto, R., Volpe, P. and Meldolesi, J. (1994). Molecular and cellular physiology of intracellular calcium stores. *Physiol Rev*. **74**(3):595-636.
- Pratt, K. G., Zhu, P., Watari, H., Cook, D. G. and Sullivan, J. M. (2011). A novel role for γ -secretase: selective regulation of spontaneous neurotransmitter release from hippocampal neurons. *J Neurosci*. **31**(3):899-906.
- Price, D.L., Walker, L. C., Martin, L. J. and Sisodia, S. S. (1992). Amyloidosis in aging and Alzheimer's disease. *Am J Pathol*. **141**(4):767-72.
- Price, J. L., McKeel, D. W Jr., Buckles, V.D., Roe, C. M., Xiong, C., Grundman, M., Hansen, L. A., Petersen, R. C., Parisi, J. E., Dickson, D. W., Smith, C. D., Davis, D. G., Schmitt, F. A., Markesbery, W. R., Kaye, J., Kurlan, R., Hulette, C., Kurland, B. F., Higdon, R., Kukull, W. and Morris. (2009). Neuropathology of nondemented aging: presumptive evidence for preclinical Alzheimer disease. *J CNeurobiol Aging*. **30**(7):1026-36.
- Prins, D. and Michalak, M. (2011). Organellar calcium buffers. *Cold Spring Harb Perspect Biol*. **3**(3). pii: a004069. doi: 10.1101/cshperspect.a004069.
- Prohovnik, I., Perl, D. P., Davis, K. L., Libow, L., Lesser, G. and Haroutunian, V. (2006). Dissociation of neuropathology from severity of dementia in late-onset Alzheimer disease. *Neurology*. **66**(1):49-55.
- Prokop, S., Shirotani, K., Edbauer, D., Haass, C. and Steiner, H. (2004). Requirement of **PEN-2** for stabilization of the presenilin N-/C-terminal fragment heterodimer within the gamma-secretase complex. *J Biol Chem*. **279**(22):23255-61.
- Putney, J W. Jr. (1986). A model for receptor-regulated calcium entry. *Cell Calcium*. **7**(1):1-12.
- Putney, J. W. (2011). The physiological function of store-operated calcium entry. *Neurochem Res*. 1157-65.
- Putney, J.W. (2010). Pharmacology of store-operated calcium channels. *Mol Interv*. **10**(4):209-18.
- Querfurth, H. W. and LaFerla, F. M. (2010). Alzheimer's disease. *N Engl J Med*. **362**(4):329-44.
- Radhika, V. and Dhanasekaran, N. (2001).Transforming G proteins. *Oncogene*. **20**(13):1607-14.
- Raurell, I., Codina, M., Casagolda, D., Del Valle, B., Baulida, J., de Herreros, A. G. and Duñach, M. (2008). Gamma-secretase-dependent and -independent effects of presenilin1 on beta-catenin.Tcf-4 transcriptional activity. *PLoS One*. **3**(12):e4080.
- Renvoisé, B. and Blackstone, C. (2010). Emerging themes of ER organization in the development and maintenance of axons. *Curr Opin Neurobiol*. **20**(5):531-7.
- Resende, R., Ferreira, E., Pereira, C. and Resende de Oliveira, C. (2008). Neurotoxic effect of oligomeric and fibrillar species of amyloid-beta peptide 1-42: involvement of

- endoplasmic reticulum calcium release in oligomer-induced cell death. *Neuroscience*. **155**(3):725-37.
- Richards, J. G., Higgins, G. A., Ouagazzal, A. M., Ozmen, L., Kew, J. N., Bohrmann, B., Malherbe, P., Brockhaus, M., Loetscher, H., Czech, C., Huber, G., Bluethmann, H., Jacobsen, H. and Kemp, J. A. (2003). PS2APP transgenic mice, coexpressing hPS2mut and hAPP^{sw}, show age-related cognitive deficits associated with discrete brain amyloid deposition and inflammation. *J Neurosci*. **23**:8989-9003.
- Rigby, J. E. and Dorling, D. (2007). Mortality in relation to sex in the affluent world. *J Epidemiol Community Health*. **61**(2):159-64.
- Rizzuto, R. and Pozzan, T. (2006). Microdomains of intracellular Ca²⁺: molecular determinants and functional consequences. *Physiol Rev*. **86** (1): 369-408.
- Rizzuto, R., Brini, M. and Pozzan, T. (1994). Targeting recombinant aequorin to specific intracellular organelles. *Methods Cell Biol*. **40**:339-58.
- Roberts-Thomson, S. J., Curry, M. C. and Monteith, G. R. (2010). Plasma membrane calcium pumps and their emerging roles in cancer. *World J Biol Chem*. **1**(8):248-53.
- Rogaev, E. I., Sherrington, R., Rogaeva, E. A., Levesque, G., Ikeda, M., Liang, Y., Chi, H., Lin, C., Holman, K., Tsuda, T., Mar, L., Sorbi, S., Nacmias, B., Piacentini, S., Amaducci, L., Chumakov, I., Cohen, D., Lannfelt, L., Fraser, P. E., Rommens, J. M. and . St George-Hyslop P. H. (1995). Familial Alzheimer's disease in kindreds with missense mutations in a gene on chromosome 1 related to the Alzheimer's disease type 3 gene. *Nature*. **376** (6543): 775-8.
- Rohan de Silva, H. A., Jen, A., Wickenden, C., Jen, L.S, Wilkinson, S.L. and Patel, A. J. (1997). Cell-specific expression of beta-amyloid precursor protein isoform mRNAs and proteins in neurons and astrocytes. *Brain Res Mol Brain Res*. **47**(1-2):147-56.
- Romoser, V. A., Hinkle, P. M. and Persechini A. (1997). Detection in living cells of Ca²⁺-dependent changes in the fluorescence emission of an indicator composed of two green fluorescent protein variants linked by a calmodulin-binding sequence. A new class of fluorescent indicators. *J Biol Chem*. **272**(20):13270-4.
- Roussel, C., Erneux, T., Schiffmann, S. N. and Gall, D. (2006). Modulation of neuronal excitability by intracellular calcium buffering: from spiking to bursting. *Cell Calcium*. **39**(5):455-66.
- Rozzini, L., Chilovi, B. V., Conti, M., Bertolotti, E., Delrio, I., Trabucchi, M. and Padovani, A. (2007). Conversion of amnesic Mild Cognitive Impairment to dementia of Alzheimer type is independent to memory deterioration. *Int J Geriatr Psychiatry*. **22**(12):1217-22.
- Rudolf R, Mongillo M, Rizzuto R and Pozzan T. (2003). Looking forward to seeing calcium. *Nat Rev Mol Cell Biol*. **4** (7): 579-86
- Rybalchenko, V., Hwang, S. Y., Rybalchenko, N. and Koulen . P. (2008). The cytosolic N-terminus of presenilin-1 potentiates mouse ryanodine receptor single channel activity. *Int J Biochem Cell Biol*. **40**(1):84-97.

- Saito, T., Suemoto, T., Brouwers, N., Slegers, K., Funamoto, S., Mihira, N., Matsuba, Y., Yamada, K., Nilsson, P., Takano, J., Nishimura, M., Iwata, N., Van Broeckhoven, C., Ihara, Y. and Saido, T. C. (2011). Potent amyloidogenicity and pathogenicity of A β 43. *Nat Neurosci.* **14**(8):1023-32.
- Santos, S. F., Pierrot, N., Octave, J. N. (2010). Network excitability dysfunction in Alzheimer's disease: insights from in vitro and in vivo models. *Rev Neurosci.* **21**(3):153-71.
- Sanz-Blasco, S., Valero, R. A., Rodríguez-Crespo, I., Villalobos, C. and Núñez, L. (2008). Mitochondrial Ca²⁺ overload underlies Abeta oligomers neurotoxicity providing an unexpected mechanism of neuroprotection by NSAIDs. *PLoS ONE.* **3**(7):e2718
- Sanz-Blasco, S., Valero, R. A., Rodríguez-Crespo, I., Villalobos, C. and Núñez, L. (2008). Mitochondrial Ca²⁺ overload underlies Abeta oligomers neurotoxicity providing an unexpected mechanism of neuroprotection by NSAIDs. *PLoS One.* **3**(7):e2718.
- Saris, N. E., and Carafoli. E. (2005). A historical review of cellular calcium handling, with emphasis on mitochondria. *Biochemistry (Mosc).* **70**:187-94.
- Sastre, M., Steiner, H., Fuchs, K., Capell, A., Multhaup, G., Condron, M. M., Teplow, D. B. and Haass, C. (2001). Presenilin-dependent gamma-secretase processing of beta-amyloid precursor protein at a site corresponding to the S3 cleavage of Notch. *EMBO Rep.* **2**(9):835-41.
- Sato, T., Dohmae, N., Qi, Y., Kakuda, N., Misonou, H., Mitsumori, R., Maruyama, H., Koo, E. H., Haass, C., Takio, K., Morishima-Kawashima, M., Ishiura, S. and Ihara, Y. (2003). Potential link between amyloid beta-protein 42 and C-terminal fragment gamma 49-99 of beta-amyloid precursor protein. *J Biol Chem.* **278**(27):24294-301.
- Schaefer, M., Plant, T. D., Obukhov, A. G., Hofmann, T., Gudermann, T. and Schultz, G. (2000). Receptor-mediated regulation of the nonselective cation channels TRPC4 and TRPC5. *J Biol Chem.* **275**(23):17517-26.
- Scheuner, D., Eckman, C., Jensen, M., Song, X., Citron, M., Suzuki, N., Bird, T. D., Hardy, J., Hutton, M., Kukull, W., Larson, E., Levy-Lahad, E., Viitanen, M., Peskind, E., Poorkaj, P., Schellenberg, G., Tanzi, R., Wasco, W., Lannfelt, L., Selkoe, D. and Younkin, S. (1996). Secreted amyloid beta-protein similar to that in the senile plaques of Alzheimer's disease is increased in vivo by the presenilin 1 and 2 and APP mutations linked to familial Alzheimer's disease. *Nat Med.* **2** (8): 864-70.
- Schmand, B., Smit, J. H., Geerlings, M. I. and Lindeboom, J. (1997). The effects of intelligence and education on the development of dementia. A test of the brain reserve hypothesis. *Psychol Med.* **27**(6):1337-44.
- Schneider, I., Reverse, D., Dewachter, I., Ris, L., Caluwaerts, N., Kuiperi, C., Gilis, M., Geerts, H., Kretschmar, H., Godaux, E., Moechars, D., Van Leuven, F. and Herms, J. (2001). Mutant presenilins disturb neuronal calcium homeostasis in the brain of transgenic mice, decreasing the threshold for excitotoxicity and facilitating long-term potentiation. *J Biol Chem* **276**:11539 –11544.

- Schupf, N., Kapell, D., Nightingale, B., Lee, J. H., Mohlenhoff, J., Bewley, S., Ottman, R. and Mayeux, R. (2001). Specificity of the fivefold increase in AD in mothers of adults with Down syndrome. *Neurology*. **57**(6):979-84.
- Scorrano, L., Oakes, S. A., Opferman, J. T., Cheng, E. H., Sorcinelli, M. D., Pozzan, T. and Korsmeyer, S. J. (2003). BAX and BAK regulation of endoplasmic reticulum Ca²⁺: a control point for apoptosis. *Science*. **300**(5616):135-9.
- Seals, D. F. and Courtneidge, S. A. The ADAMs family of metalloproteases: multidomain proteins with multiple functions. *Genes Dev*. **17**(1):7-30.
- Selkoe D. J. and Wolfe M. S. (2007). Presenilin: running with scissors in the membrane. *Cell* **131**: 215–221.
- Selkoe, D. J. (1998). The cell biology of beta-amyloid precursor protein and presenilin in Alzheimer's disease. *Trends Cell Biol*. **8**(11):447-53.
- Selkoe, D. J. (2001). Alzheimer's disease: genes, proteins, and therapy. *Physiol Rev*. **81** (2): 741-66.
- Shah, S., Lee, S. F., Tabuchi, K., Hao, Y .H., Yu, C., LaPlant, Q., Ball, H., Dann, C. E. 3rd., Südhof, T. and Yu, G. (2005). Nicastrin functions as a gamma-secretase-substrate receptor. *Cell*. **122**(3):435-47.
- Shankar, G. M. and Walsh, D. M. (2009). Alzheimer's disease: synaptic dysfunction and Abeta. *Mol Neurodegener*. **4**:48.
- Shankar, G. M., Li S, Mehta, T. H., Garcia-Munoz, A., Shepardson, N .E, Smith, I., Brett, F. M., Farrell, M. A., Rowan, M. J., Lemere, C. A., Regan, C. M., Walsh, D. M., Sabatini, B. L. and Selkoe, D. J. (2008). Amyloid-beta protein dimers isolated directly from Alzheimer's brains impair synaptic plasticity and memory. *Nat Med*. **14**(8):837-42.
- Shen, J. and Kelleher, R. J 3rd. (2007). The presenilin hypothesis of Alzheimer's disease: evidence for a loss-of-function pathogenic mechanism". *Proc Natl Acad Sci U S A*. **104** (2): 403-9.
- Shen, J., Bronson, R.T., Chen, D. F., Xia, W., Selkoe, D. J. and Tonegawa, S. (1997). Skeletal and CNS defects in Presenilin-1-deficient mice. *Cell*. **89** (4): 629-39.
- Sherrington, R., Rogaev, E. I., Liang, Y., Rogaeva, E. A., Levesque, G., Ikeda, M., Chi, H., Lin, C., Li, G., Holman, K., Tsuda,T., Mar, L., Foncin, J. F., Bruni, A. C., Montesi, M. P., Sorbi, S., Rainero, I., Pinessi, L., Nee, L., Chumakov. I., Pollen, D., Brookes, A., Sanseau, P., Polinsky, R. J., Wasco, W., Da Silva, H, A., Haines, J, L., Pericak-Vance M, A., Tanzi, R. E., Roses, A. D., Fraser, P. E., Rommens, J. M. and St George-Hyslop P. H. (1995). Cloning of a gene bearing missense mutations in early-onset familial Alzheimer's disease. *Nature*. **375** (6534): 754-60.
- Shirotani, K., Edbauer, D., Kostka, M., Steiner, H. and Haass, C. (2004). Immature nicastrin stabilizes APH-1 independent of PEN-2 and presenilin: identification of nicastrin mutants that selectively interact with APH-1. *J Neurochem*. **89**(6):1520-7.

- Shuttleworth, T. J. (2009). Arachidonic acid, ARC channels, and Orai proteins. *Cell Calcium*. **45**(6):602-10.
- Siman, R. and Velji, J. (2003). Localization of presenilin-nicastrin complexes and gamma-secretase activity to the trans-Golgi network. *J Neurochem*. **84**(5):1143-53.
- Singer, D., Lehmann, J., Hanisch, K., Härtig, W. and Hoffmann, R. (2006). Neighbored phosphorylation sites as PHF-tau specific markers in Alzheimer's disease. *Biochem Biophys Res Commun*. **346**(3):819-28.
- Sisodia, S. S. and St. George-Hyslop, P. H. (2002). γ -Secretase, Notch, A β and Alzheimer's where do the presenilins fit in? *Nat Rev Neurosci*. **3**(4):281-90.
- Slooter, A.J., Cruts, M., Kalmijn, S., Hofman, A., Breteler, M. M., Van Broeckhoven, C. and van Duijn, C. M. (1998). Risk estimates of dementia by apolipoprotein E genotypes from a population-based incidence study: the Rotterdam Study. *Arch Neurol*. **55**(7):964-8
- Small, D. H., Gasperini, R., Vincent, A. J., Hung, A. C. and Foa, L. (2009). The role of Abeta-induced calcium dysregulation in the pathogenesis of Alzheimer's disease. *J Alzheimers* **16**:225-233.
- Small, D. H., Klaver, D. W. and Foa, L. (2010). Presenilins and the g-secretase: still a complex problem. *Mol Brain*. **5**;3:7.
- Small, S.A. and Gandy, S. (2006). Sorting through the cell biology of Alzheimer's disease: intracellular pathways to pathogenesis. *Neuron*. **52**(1):15-31.
- Smith, I. F., Hitt, B., Green, K. N., Oddo, S. and LaFerla, F. M. (2005). Enhanced caffeine-induced Ca²⁺ release in the 3xTg-AD mouse model of Alzheimer's disease. *J Neurochem*. **94** (6): 1711-8.
- Smith, I. F., Wiltgen, S. M., Shuai, J. and Parker, I. (2009). Ca²⁺ puffs originate from preestablished stable clusters of inositol trisphosphate receptors. *Sci Signal*. **2**(98):ra77.
- Solovey, G. and Dawson, S. (2010). Observable effects of Ca²⁺ buffers on local Ca²⁺ signals. *Philos Transact A Math Phys Eng Sci*. **368**(1933):5597-603.
- Spasic, D., Tolia, A., Dillen, K., Baert, V., De Strooper, B., Vrijens, S. and Annaert, W. (2006). Presenilin-1 maintains a nine-transmembrane topology throughout the secretory pathway. *J Biol Chem*. **281** (36): 26569-77.
- Sperling, R. A., Aisen, P. S., Beckett, L. A., Bennettm, D. A., Craft, S., Fagan, A. M., Iwatsubo, T., Jack, C. R Jr., Kaye, J., Montine, T. J., Park, D. C., Reiman, E. M., Rowe, C. C., Siemers, E., Stern, Y., Yaffe, K., Carrillo, M. C., Thies, B., Morrison-Bogorad, M., Wagster, M. V. and Phelps, C. H. (2011). Toward defining the preclinical stages of Alzheimer's disease: recommendations from the National Institute on Aging-Alzheimer's Association workgroups on diagnostic guidelines for Alzheimer's disease. *Alzheimers Dement*. **7**(3):280-92.
- St George-Hyslop, P. H. (2000). Genetic factors in the genesis of Alzheimer's disease. *Ann N Y Acad Sci*. **924**:1-7

- Stawski, P., Janovjak, H. and Trauner, D. (2010). Pharmacology of ionotropic glutamate receptors: A structural perspective. *Bioorg Med Chem.* **18**(22):7759-72.
- Steiner, H., Fluhner, R. and Haass, C. (2008). Intramembrane proteolysis by gamma-secretase. *J Biol Chem.* **283**(44):29627-31.
- Steiner, H., Winkler, E., Edbauer, D., Prokop, S., Basset, G., Yamasaki, A., Kostka, M. and Haass, C. (2002). PEN-2 is an integral component of the gamma-secretase complex required for coordinated expression of presenilin and nicastrin. *J Biol Chem.* **277**(42):39062-5.
- Stieren, E., Werchan, W.P., El Ayadi, A., Li, F. and Boehning, D. (2010). FAD mutations in amyloid precursor protein do not directly perturb intracellular calcium homeostasis. *PLoS One.* **5**:e11992.
- Stutzmann, G. E., Caccamo, A., LaFerla, F. M. and Parker, I. (2004). *Dysregulated IP₃ signaling in cortical neurons of knock-in mice expressing an Alzheimer's-linked mutation in presenilin1 results in exaggerated Ca²⁺ signals and altered membrane excitability.* *J Neurosci* **24**:508–513.
- Stutzmann, G. E., Smith, I., Caccamo, A., Oddo, S., Laferla, F. M., Parker, I. (2006). Enhanced ryanodine receptor recruitment contributes to Ca²⁺ disruptions in young, adult, and aged Alzheimer's disease mice. *J Neurosci.* **26**(19):5180-9.
- Stutzmann, G. E., Smith, I., Caccamo, A., Oddo, S., Parker, I. and Laferla, F. (2007). Enhanced ryanodine-mediated calcium release in mutant PS1-expressing Alzheimer's mouse models. *Ann N Y Acad Sci.* **1097**:265-77.
- Suga, K., Tomiyama, T., Mori, H. and Akagawa, K. (2011). Syntaxin 5 interacts with presenilin holoproteins, but not with their N- or C-terminal fragments, and affects beta-amyloid peptide production. *Biochem J.* **381**(Pt 3):619-28.
- Supnet C, Bezprozvanny I. (2010). The dysregulation of intracellular calcium in Alzheimer disease. *Cell Calcium.* **47**(2):183-9.
- Supnet, C., Grant, J., Kong, H., Westaway, D. and Mayne, M. (2006). Amyloid-beta- (1– 42) increases ryanodine receptor-3 expression and function in neurons of TgCRND8 mice. *J Biol Chem* **281**:38440 –38447.
- Supnet, C., Noonan, C., Richard, K., Bradley, J. and Mayne, M. (2010) Up-regulation of the type 3 ryanodine receptor is neuroprotective in the TgCRND8 mouse model of Alzheimer's disease. *J Neurochem.* **112**:356 –365.
- Swann, K., Saunders, C. M. , Rogers, N. T. and Lai, F. A. (2006). PLCzeta (zeta): a sperm protein that triggers Ca²⁺ oscillations and egg activation in mammals. *Semin Cell Dev Biol.* **17**(2):264-73.
- Szalai, G., Krishnamurthy, R. and Hajnóczky, G. (1999). Apoptosis driven by IP(3)-linked mitochondrial calcium signals. *EMBO J.* **18**(22):6349-61.

- Takeuchi, H., Sekiguchi, A., Taki, Y., Yokoyama, S., Yomogida, Y., Komuro, N., Yamanouchi, T., Suzuki, S. and Kawashima, R. (2010). Training of working memory impacts structural connectivity. *J Neurosci.* **30**(9):3297-303.
- Tanabe, C., Hotoda, N., Sasagawa, N., Sehara-Fujisawa, A., Maruyama, K. and Ishiura, S. (2007). ADAM19 is tightly associated with constitutive Alzheimer's disease APP alpha-secretase in A172 cells. *Biochem Biophys Res Commun.* **352**(1):111-7.
- Tanino, H., Shimohama, S., Sasaki, Y., Sumida, Y. and Fujimoto, S. (2000). Increase in phospholipase C-delta1 protein levels in aluminum-treated rat brains. *Biochem Biophys Res Commun.* **271**(3):620-5.
- Tanzi, R. E. and Bertram, L. (2005). Twenty years of the Alzheimer's disease amyloid hypothesis: a genetic perspective. *Cell.* **120**(4):545-55.
- Temple, V. and Konstantareas, M. M. (2005). A comparison of the behavioural and emotional characteristics of Alzheimer's dementia in individuals with and without Down syndrome. *Can J Aging.* **24**(2):179-89.
- Temple, V., Jozsvai, E., Konstantareas, M. M. and Hewitt, T. A. (2001). Alzheimer dementia in Down's syndrome: the relevance of cognitive ability. *J Intellect Disabil Res.* **45**(Pt 1):47-55.
- Thinakaran, G. and Koo, E. H. (2008). Amyloid precursor protein trafficking, processing, and function. *J Biol Chem.* **283**(44):29615-9.
- Thinakaran, G. and Parent, A. T. (2004). Identification of the role of presenilins beyond Alzheimer's disease. *Pharmacol Res.* **50**:411-418
- Thinakaran, G. and Sisodia, S. S. (2006). Presenilins and Alzheimer disease: the calcium conspiracy. *Nat Neurosci.* **9**(11):1354-5
- Thinakaran, G., Borchelt, D. R., Lee, M. K., Slunt, H. H., Spitzer, L., Kim, G., Ratovitsky, T., Davenport, F., Nordstedt, C., Seeger, M., Hardy, J., Levey, A. I., Gandy, S. E., Jenkins, N. A., Copeland, N. G., Price, D. L. and Sisodia, S. S. (1996). Endoproteolysis of presenilin 1 and accumulation of processed derivatives in vivo. *Neuron.* **17**(1):181-90.
- Toescu, E. C. and Vreugdenhil, M. (2010). Calcium and normal brain ageing. *Cell Calcium.* **47**(2):158-64
- Tomita, T., Maruyama, K., Saido, T.C., Kume, H., Shinozaki, K., Tokuhira, S., Capell, A., Walter, J., Grünberg, J., Haass, C., Iwatsubo, T. and Obata, K. (1997). The presenilin 2 mutation (N141I) linked to familial Alzheimer disease (Volga German families) increases the secretion of amyloid beta protein ending at the 42nd (or 43rd) residue. *Proc Natl Acad Sci U S A.* **94**(5):2025-30.
- Tousseyn, T., Thathiah, A., Jorissen, E., Raemaekers, T., Konietzko, U., Reiss, K., Maes, E., Snellinx, A., Serneels, L., Nyabi, O., Annaert, W., Saftig, P., Hartmann, D. and De Strooper, B. (2009). ADAM10, the rate-limiting protease of regulated intramembrane proteolysis of Notch and other proteins, is processed by ADAMS-9, ADAMS-15, and the gamma-secretase. *J Biol Chem.* **284**(17):11738-47.

- Traynelis, S. F., Wollmuth, L. P., McBain, C. J., Menniti, F. S., Vance, K. M., Ogden, K. K., Hansen, K. B., Yuan, H., Myers, S. J. and Dingledine, R. (2010). Glutamate receptor ion channels: structure, regulation, and function. *Pharmacol Rev.* **62**(3):405-96
- Tsang, S. W., Pomakian, J., Marshall, G. A., Vinters, H. V., Cummings, J. L., Chen, C. P., Wong, P.T. and Lai, M. K. Disrupted muscarinic M1 receptor signaling correlates with loss of protein kinase C activity and glutamatergic deficit in Alzheimer's disease. *Neurobiol Aging.* **28**(9):1381-7.
- Tsien, R. Y. (1980). New calcium indicators and buffers with high selectivity against magnesium and protons: design, synthesis, and properties of prototype structures". *Biochemistry.* **19** (11): 2396-404.
- Tsien, R. Y. (1999). Rosy dawn for fluorescent proteins. *Nat Biotechnol.* **17**(10):956-7.
- Tu, H., Nelson, O., Bezprozvanny, A., Wang, Z., Lee, S F., Hao, Y. H., Serneels, L., De Strooper B., Yu, G. and Bezprozvanny, I. (2006). Presenilins form ER calcium leak channels, a function disrupted by mutations linked to familial Alzheimer's disease. *Cell* **126**:981-993.
- Tunnard, C., Whitehead, D., Hurt, C., Wahlund, L. O., Mecocci, P., Tsolaki, M., Vellas, B., Spenger, C., Kłoszewska, I., Soininen, H., Lovestone, S. and Simmons, A. (2011). Apathy and cortical atrophy in Alzheimer's disease. *Int J Geriatr Psychiatry.* **26**(7):741-8.
- Uryu, K., Laurer, H., McIntosh, T., Praticò, D., Martinez, D., Leight, S., Lee, V. M. and Trojanowski, J. Q. (2002). Repetitive mild brain trauma accelerates Abeta deposition, lipid peroxidation, and cognitive impairment in a transgenic mouse model of Alzheimer amyloidosis. *J Neurosci.* **22**(2):446-54.
- Van Vickle, G. D., Esh, C. L., Kalback, W. M., Patton, R. L., Luehrs, D. C., Kokjohn, T. A., Fifield, F. G., Fraser, P. E., Westaway, D., McLaurin, J., Lopez, J., Brune, D., Newel, A. J., Poston, M., Beach, T. G. and Roher, A. E. (2007). TgCRND8 amyloid precursor protein transgenic mice exhibit an altered gamma-secretase processing and an aggressive, additive amyloid pathology subject to immunotherapeutic modulation. *Biochemistry.* **46**(36):10317-27.
- Vandecaetsbeek, I., Vangheluwe, P., Raeymaekers, L., Wuytack, F., Vanoevelen, J. (2011). The Ca²⁺ pumps of the endoplasmic reticulum and Golgi apparatus. *Cold Spring Harb Perspect Biol.* **1**;3(5). pii: a004184. doi: 10.1101/cshperspect.a004184.
- Vassar, R. (2004). BACE1: the beta-secretase enzyme in Alzheimer's disease. *J Mol Neurosci.* **23**(1-2):105-14.
- Venkatachalam, K. and Montell, C. (2010). TRP channels. *Annu Rev Biochem.* **76**:387-417.
- Verkhatsky, A. (2005). Physiology and pathophysiology of the calcium store in the endoplasmic reticulum of neurons. *Physiol Rev.* **85**(1):201-79.
- Vermassen, E., Parys, J .B. and Mauger, J. P. (2004). Subcellular distribution of the inositol 1,4,5-trisphosphate receptors: functional relevance and molecular determinants. *Biol Cell.* **96**(1):3-17.

- Vetrivel K.S., Zhang, Y. W., Xu, H. and Thinakaran, G. (2006). Pathological and physiological functions of presenilins. *Mol Neurodegener.* **1**:4.
- Vetrivel, K. S., Cheng, H., Lin, W., Sakurai, T., Li, T., Nukina, N., Wong, P.C., Xu, H. and Thinakaran, G. (2004). Association of gamma-secretase with lipid rafts in post-Golgi and endosome membranes. *J Biol Chem.* **279**(43):44945-54.
- Vetrivel, K. S., Gong, P., Bowen, J. W., Cheng, H., Chen, Y., Carter, M., Nguyen, P. D., Placanica, L., Wieland, F. T., Li, Y. M., Kounnas, M. Z. and Thinakaran, G. (2007). Dual roles of the transmembrane protein p23/TMP21 in the modulation of amyloid precursor protein metabolism. *Mol Neurodegener.* **8**;2:4.
- Vito, P., Wolozin, B., Ganjei, J. K., Iwasaki, K., Lacanà, E. and D'Adamio, L. (1996). Requirement of the familial Alzheimer's disease gene PS2 for apoptosis. Opposing effect of ALG-3. *J Biol Chem.* **271**(49):31025-8.
- Wakabayashi, T. and De Strooper, B. (2008). Presenilins: members of the gamma-secretase quartets, but part-time soloists too. *Physiology (Bethesda).* **23**:194-204.
- Walsh, D. M. and Selkoe, D. J. (2007). Abeta oligomers - a decade of discovery. *J Neurochem.* **101**(5):1172-84.
- Walsh, D. M., Minogue, A. M., Sala Frigerio, C., Fadeeva, J. V., Wasco, W. and Selkoe, D. J. (2007). The APP family of proteins: similarities and differences. *Biochem Soc Trans.* **35**(Pt 2):416-20.
- Ward, R.V., Davis, J. B., Gray, C. W., Barton, A. J., Bresciani, L. G., Caivano, M., Murphy, V. F., Duff, K., Hutton, M., Hardy, J., Roberts, G. W. and Karran, E. H. (1996). Presenilin-1 is processed into two major cleavage products in neuronal cell lines. *Neurodegeneration.* **5**(4):293-8.
- Wasco, W., Bupp, K., Magendantz, M., Gusella, J. F., Tanzi, R. E. and Solomon, F. (1992). Identification of a mouse brain cDNA that encodes a protein related to the Alzheimer disease-associated amyloid beta protein precursor. *Proc Natl Acad Sci U S A.* **89**(22):10758-62.
- Watanabe, N., Tomita, T., Sato, C., Kitamura, T., Morohashi, Y. and Iwatsubo, T. (2005). Pen-2 is incorporated into the gamma-secretase complex through binding to transmembrane domain 4 of presenilin 1. *J Biol Chem.* **280**(51):41967-75.
- Weber, M. M. (1997). Aloys Alzheimer, a coworker of Emil Kraepelin. *J Psychiatr Res.* **31**(6):635-43.
- Weidemann, A., Eggert, S., Reinhard, F. B., Vogel, M., Paliga, K., Baier, G., Masters, C. L., Beyreuther, K. and Evin, G. (2002). A novel epsilon-cleavage within the transmembrane domain of the Alzheimer amyloid precursor protein demonstrates homology with Notch processing. *Biochemistry.* **41**(8):2825-35.
- Wenk, G. L. (2003). Neuropathologic changes in Alzheimer's disease. *J Clin Psychiatry.* **64** Suppl 9:7-10.

- Wettschureck, N. and Offermanns, S. (2005). Mammalian G proteins and their cell type specific functions. *Physiol Rev.* **85**(4):1159-204.
- Wilson, R. S., Barnes, L. L., Aggarwal, N. T., Boyle, P. A., Hebert, L. E., Mendes de Leon, C. F. and Evans, D. A. (2010). Cognitive activity and the cognitive morbidity of Alzheimer disease. *Neurology.* **75** (11):990-6.
- Wojcikiewicz, R. J. and He, Y. (1995). Type I, II and III inositol 1,4,5-trisphosphate receptor co-immunoprecipitation as evidence for the existence of heterotetrameric receptor complexes. *Biochem Biophys Res Commun.* **213**(1):334-41.
- Wojda, U., Salinska, E. and Kuznicki, J. (2008). Calcium ions in neuronal degeneration. *IUBMB Life.* **60**:575-90.
- Wolfe, M. (2007). When loss is gain: reduced presenilin proteolytic function leads to increased A β 42/A β 40. *EMBO Rep.* **8**, 136–140.
- Wolfe, M. S. (2009). Gamma-Secretase in biology and medicine. *Semin Cell Dev Biol.* **20**(2):219-24.
- Xu, X. (2009). Gamma-secretase catalyzes sequential cleavages of the AbetaPP transmembrane domain. *J Alzheimers Dis.* **16**(2):211-24.
- Yamasaki, A., Eimer, S., Okochi, M., Smialowska, A., Kaether, C., Baumeister, R., Haass, C. and Steiner, H. (2006). The GxGD motif of presenilin contributes to catalytic function and substrate identification of gamma-secretase. *J Neurosci.* **26**(14):3821-8.
- Ye, Y., Kober, V., Tellers, M., Naji, Z., Salmon, P., Julia F. Markusen, J. F. (2009). High-Level Protein Expression in Scalable CHO Transient Transfection. *Biotechnology and Bioengineering.* **103**(3): 542-551.
- Yu, G., Nishimura, M., Arawaka, S., Levitan, D., Zhang, L., Tandon, A., Song, Y. Q., Rogaeva, E., Chen, F., Kawarai, T., Supala, A., Levesque, L., Yu, H., Yang, D. S., Holmes, E., Milman, P., Liang, Y., Zhang, D. M., Xu, D. H., Sato, C., Rogaev, E., Smith, M., Janus, C., Zhang, Y., Aebersold, R., Farrer, L.S., Sorbi, S., Bruni, A., Fraser, P. and St George-Hyslop, P. (2000). Nicastrin modulates presenilin-mediated notch/glp-1 signal transduction and betaAPP processing. *Nature.* **407**(6800):48-54.
- Zampese, E., Brunello, L., Fasolato, C., and Pizzo, P. (2009). Ca²⁺ dysregulation mediated by presenilins in Familial Alzheimer's Disease: causing or modulating factor? *Curr. Trends Neurol.* **3**:1-14.
- Zampese, E., Fasolato, C., Kipanyula, M. J, Bortolozzi, M., Pozzan, T. and Pizzo, P. (2011). Presenilin 2 modulates endoplasmic reticulum (ER)-mitochondria interactions and Ca²⁺ cross-talk. *Proc Natl Acad Sci U S A.* **108**(7):2777-82.
- Zatti, G., Burgo, A., Giacomello, M., Barbiero, L., Ghidoni, R., Sinigaglia, G., Florean C., Bagnoli, S., Binetti, G., Sorbi, S., Pizzo P., and Fasolato, C. (2006). Presenilin mutations linked to familial Alzheimer's disease reduce endoplasmic reticulum and Golgi apparatus calcium levels. *Cell Calcium.* **39**:539-50.

- Zatti, G., Ghidoni, R., Barbiero, L., Binetti, G., Pozzan, T., Fasolato, C., and Pizzo, P. (2004). The presenilin 2 M239I mutation associated with familial Alzheimer's disease reduces Ca²⁺ release from intracellular stores. *Neurobiol Dis.* **15**:269-78.
- Zhang, D., Zhang, C., Ho, A., Kirkwood, A., Südhof, T. C. and Shen, J. (2010). Inactivation of presenilins causes pre-synaptic impairment prior to post-synaptic dysfunction. *J Neurochem.* **115**(5):1215-21.
- Zhang, H., Sun, S., Herreman, A., De Strooper, B. and Bezprozvanny, I. (2010). Role of presenilins in neuronal calcium homeostasis. *J Neurosci.* **30**(25):8566–8580.
- Zhang, S., Fritz, N., Ibarra, C. and Uhle'n, P. (2011). Inositol 1,4,5-Trisphosphate Receptor Subtype-Specific Regulation of Calcium Oscillations. *Neurochem Res.* **36**:1175–1185.
- Zhang, Y. W., Luo, W. J., Wang, H., Lin, P., Vetrivel, K. S., Liao, F., Li, F., Wong, P. C., Farquhar, M. G., Thinakaran, G. and Xu, H. (2005). Nicastrin is critical for stability and trafficking but not association of other presenilin/gamma-secretase components. *J Biol Chem.* **280**(17):17020-6.
- Zhang, Y. W., Thompson, R., Zhang, H. and Xu, H. (2011). APP processing in Alzheimer's disease. *Mol Brain.* **4**:3.
- Zhao, G., Liu, Z., Ilagan, M. X. and Kopan, R. (2010). Gamma-secretase composed of PS1/Pen2/Aph1a can cleave notch and amyloid precursor protein in the absence of nicastrin. *J Neurosci.* **30**(5):1648-56.
- Zhou, S., Zhou, H., Walian, P. J. and Jap, B. K. (2005). CD147 is a regulatory subunit of the gamma-secretase complex in Alzheimer's disease amyloid beta-peptide production. *Proc Natl Acad Sci U S A.* **102**(21):7499-504.
- Zucchi, R. and Ronca-Testoni, S. (1997). The sarcoplasmic reticulum Ca²⁺ channel/ryanodine receptor: modulation by endogenous effectors, drugs and disease states. *Pharmacol Rev.* **49**(1):1-51.

APPENDIX